

MOTION AND RIGIDITY OF THE CARIBBEAN PLATE  
AND GEODETIC OBSERVATIONS OF  
DOMINICA, LESSER ANTILLES

by

JAMIE MILLER

Presented to the Faculty of the Graduate School of  
The University of Texas at Arlington in Partial Fulfillment  
of the Requirements  
for the Degree of

DOCTOR OF PHILOSOPHY

THE UNIVERSITY OF TEXAS AT ARLINGTON

December 2013

Copyright © by Jamie Miller 2013

All Rights Reserved



Dedication

For Paul

## Acknowledgements

I would like to express the deepest appreciation to my committee chair, Glen Mattioli for accepting a non-traditional student, introducing me to geodesy, and providing me with great opportunities for science and adventure. I would like to thank my committee members for their input and guidance. I thank my parents, Jim and Annette Tomlin for their support over these many years and for taking me to my first volcano at the age of three. I still remember the smell and have ever since been intrigued with how the Earth works. My entire family has always provided me with the love and support needed to achieve goals, my house is back open for pool parties! Thanks go to my sons, Harrison and Houston, who both served as outstanding field hands in Dominica. And most of all, I thank my husband, Paul, without whom, this literally would not have been possible. His expertise in all things technical, as well as his ability to “hold down the fort” has afforded me the luxury of doing the things I love.

November 22, 2013

Abstract

MOTION AND RIGIDITY OF THE CARIBBEAN PLATE,  
AND GEODETIC OBSERVATIONS OF  
DOMINICA, LESSER ANTILLES

Jamie Miller, PhD

The University of Texas at Arlington, 2013

Supervising Professor: Glen S. Mattioli

The currently accepted kinematic model of the Caribbean plate presented by DeMets et al. (2007), is based on velocities from 6 continuous and 14 campaign GPS sites. This work attempts to refine the current plate model by evaluating data from an expanded number of stations with an improved spatial distribution. As a measure to better constrain the eastern margin, a study has been conducted on the island of Dominica, which includes campaign GPS data collected over the last decade. The analysis of data from 117 sites includes campaign data in addition to the data from the continuous GPS stations that comprise COCONet. An updated velocity field for the Caribbean plate is presented and an inversion of the velocities for 24 sites yields a plate angular velocity that differs from previously published models. It is determined that a 2-plate model for the Caribbean is a more suitable fit of the data, which suggests that the Caribbean is undergoing deformation within its interior. Analyses for possible east-west deformation across the Lower Nicaraguan Rise and Beata Ridge are presented.

## Table of Contents

Acknowledgements .....	iv
Abstract .....	v
List of Figures .....	viii
List of Tables .....	xi
Chapter 1 Tectonic Setting .....	1
1.1 The Caribbean Plate .....	1
2.2 Dominica and the Central Lesser Antilles .....	6
Chapter 2 GPS Data .....	11
2.1 Campaign GPS Data Acquisition .....	11
2.2 Continuous GPS Data Acquisition .....	12
2.3 GPS Data Processing .....	12
2.4 GOAll - 6.1.2 vs. 6.2 .....	14
Chapter 3 Geodetic Observations of Dominica, Lesser Antilles .....	18
3.1 Introduction .....	18
3.2 Volcanic History of Dominica .....	19
3.3 Results .....	24
3.4 Data Analysis and Discussion .....	37
3.5 Conclusion .....	46
Chapter 4 The Caribbean Plate .....	48
4.1 Introduction .....	48
4.2 The 1-plate model .....	52
4.3 The 2-plate model .....	58
4.4 The rigidity of the Caribbean plate .....	65
4-5 Kinematic versus dynamic model of the Caribbean .....	74

4-6 Conclusion .....	76
Appendix A Dominica Campaign Site Descriptions .....	77
Appendix B COCONet Time Series .....	103
Appendix C Dominica site equipment history .....	153
Appendix D Inversion Input Files .....	155
Appendix E Inversion Results .....	166
References .....	179
Biographical Information .....	184

## List of Figures

Figure 1-1 Reconstructions of the Caribbean at 165 Ma and 144 Ma.....	2
Figure 1-2 Reconstructions of the Caribbean at 120 Ma and 90 Ma.....	3
Figure 1-3 Reconstructions of the Caribbean at 72 Ma and 49 Ma.....	4
Figure 1-4 Reconstructions of the Caribbean at 22 Ma and today.....	5
Figure 1-5 Tectonic setting of the Caribbean plate.....	6
Figure 1-6 Lesser Antilles Arc regional seismicity.....	8
Figure 1-7 Map of Lesser Antilles.....	9
Figure 1-8 Location of Dominica within the Lesser Antilles.....	10
Figure 2-1 Comparative time series for site CRO1.....	16
Figure 2-2 Comparative time series for site CN07.....	17
Figure 3-1 Location of Dominica.....	18
Figure 3-2 Geologic map of Dominica from Smith et al. (2013).....	22
Figure 3-3 A petrogenic model for the geologic evolution of Dominica.....	23
Figure 3-4 Dominica campaign GPS site location map.....	25
Figure 3-5 Time series for site ATRU.....	26
Figure 3-6 Time series for site BELV.....	26
Figure 3-7 Time series for site BOTG.....	27
Figure 3-8 Time series for site BRDX.....	27
Figure 3-9 Time series for site CNCD.....	28
Figure 3-10 Time series for site COHT.....	28
Figure 3-11 Time series for site CONN.....	29
Figure 3-12 Time series for site FRSH.....	29
Figure 3-13 Time series for site GOMM.....	30
Figure 3-14 Time series for site GSAV.....	30



Figure 3-15 Time series for site MHAM .....	31
Figure 3-16 Time series for site MTNV .....	31
Figure 3-17 Time series for site NEWF.....	32
Figure 3-18 Time series for site NVEN .....	32
Figure 3-19 Time series for site SCTT .....	33
Figure 3-20 Time series for site SOIE.....	33
Figure 3-21 Time series for site SPAG .....	34
Figure 3-22 Time series for site SPNG .....	34
Figure 3-23 Time series for site TETE .....	35
Figure 3-24 Time series for site WOTT.....	35
Figure 3-25 Dominica horizontal velocities reported by James (2008).....	39
Figure 3-26 Dominica horizontal velocities (2001-2007). .....	40
Figure 3-27 Dominica residual horizontal site velocities (2001-2012). .....	41
Figure 3-28 Dominica surface deformation.....	43
Figure 3-29 Dominica vertical site velocities (2001-2012) .....	45
Figure 4-1 Caribbean GPS station site map .....	49
Figure 4-2 Demets et al. (2007) velocity vectors and updated values.....	53
Figure 4-3 Caribbean horizontal site velocities.....	57
Figure 4-4 Horizontal velocities for sites on the Caribbean plate. ....	59
Figure 4-5 Data importance .....	63
Figure 4-6 Euler pole locations. ....	64
Figure 4-7 Faults and earthquakes of the Caribbean .....	65
Figure 4-8 Motion along Lower Nicaraguan Rise with respect to a fixed east plate.....	67
Figure 4-9 Motion along Lower Nicaraguan Rise with respect to a fixed west plate. ....	68
Figure 4-10 Motion along the Beata Ridge with respect to fixed east plate. ....	69

Figure 4-11 Motion along the Beata Ridge with respect to fixed west plate.....	70
Figure 4-12 Dominica residual velocities, 1-plate model versus 2-plate model.....	72
Figure 4-13 Western site residual velocities, 1-plate model versus 2-plate model.....	73
Figure 4-14 Caribbean principle stress directions (van Benthem, 2013).....	74
Figure 4-15 Caribbean effective strain rate (van Benthem, 2013).....	75

## List of Tables

Table 2-1 Velocity summary for sites CRO1 and CN07 .....	15
Table 3-1 Dominica site velocity summary .....	36
Table 4-1 Caribbean velocity summary, sorted by site ID. ....	50
Table 4-2 Caribbean velocity summary, sorted by site occupation length .....	51
Table 4-3 Best-fitting Caribbean plate velocity vector information .....	55
Table 4-4 Occupation history and velocities .....	58
Table 4-5 Site data importance values .....	62
Table 4-6 Best fitting Caribbean angular velocity vectors.....	64

## Chapter 1

### Tectonic Setting

#### 1.1 The Caribbean Plate

The Caribbean began to develop less than 200 Ma ago with the breakup of Pangaea (Burke, 1988). Following the opening of the Gulf of Mexico in the mid-late Jurassic, the proto-Caribbean ocean formed as North and South America moved away from each other in Early Cretaceous (Ross and Scotese, 1988). A subduction zone was created as the eastward motion of the Caribbean plate met the rifting of the Atlantic. Reconstructions by Mann et al. (2007), from 165 Ma to the present, provide an overview of the tectonic history of this region (Figure 1-1, Figure 1-2, Figure 1-3, Figure 1-4). The late Jurassic (165 Ma) reconstruction shows the landmasses prior to the separation of North and South America and the rotation of the Maya block southward. At this time, an eastward dipping subduction zone formed the western margin of the Americas. In the early Cretaceous, the proto-Caribbean seaway was beginning to form as extension between North and South America progressed. As the Cretaceous period continued, much of the proto-Caribbean crust was consumed by the advancement of the Guerrero-Caribbean arc from the west (Figure 1-2). During the late Cretaceous, the Caribbean large igneous province (CLIP) was formed by volcanism associated with the Galapagos hotspot (Figure 1-2). The province is characterized by a number of volcanic plateaus separated by deep basins of thinner crust with volcanic under-plating (Mauffret and Leroy, 1997).  $^{40}\text{Ar}/^{39}\text{Ar}$  age determinations place the main pulse of flood-basalt magmatism at 89 Ma, followed by a second pulse at ca. 75 Ma (Hoernle et al., 2004). As the Cretaceous period ended, the Caribbean arc was situated next to the thick buoyant CLIP and the two continued to migrate northeastward until part of the arc collided with the Bahaman carbonate platform in the Eocene.

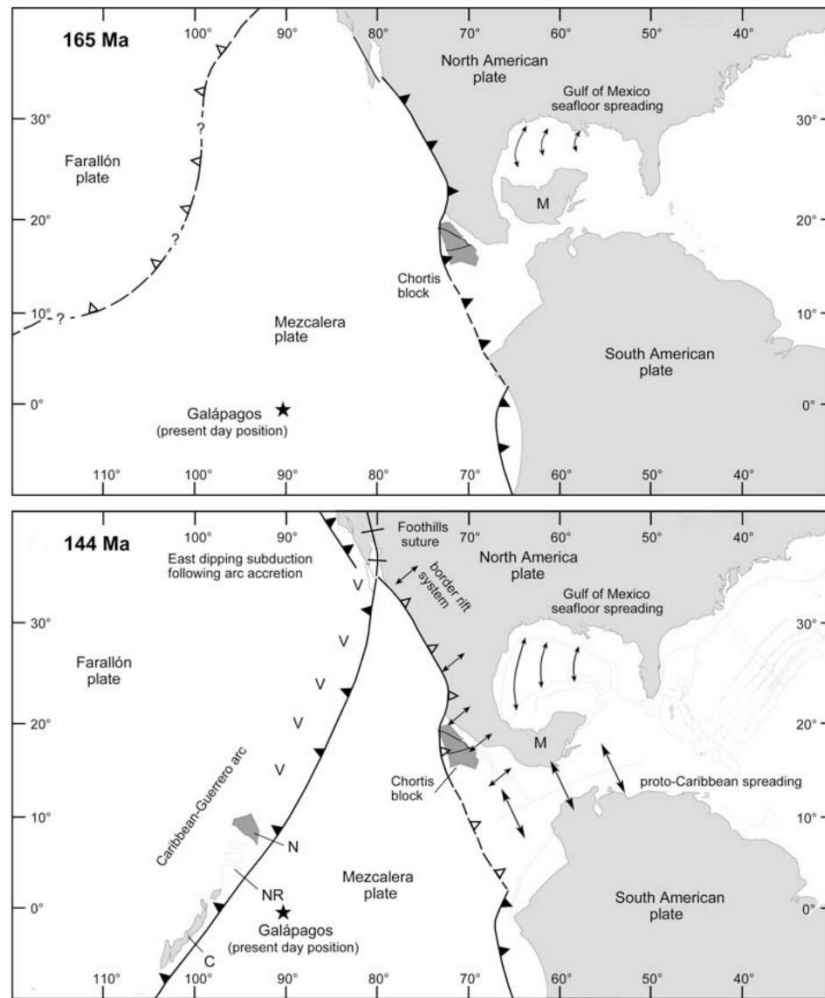


Figure 1-1 Reconstructions of the Caribbean at 165 Ma and 144 Ma  
 Key to abbreviations: N=Nicaragua, NR=Nicaraguan rise, C=Cuba, M=Maya block,  
 G=Guerrero terrane, CLIP=Caribbean large igneous province, Y=Yucatán basin,  
 CT=Cayman trough, and LA=Lesser Antilles. Countries of Costa Rica and Panama  
 correspond to approximate area of Chorotega block; countries of Honduras, Nicaragua,  
 and Guatemala correspond to Chortis block. (Mann et al., 2007)

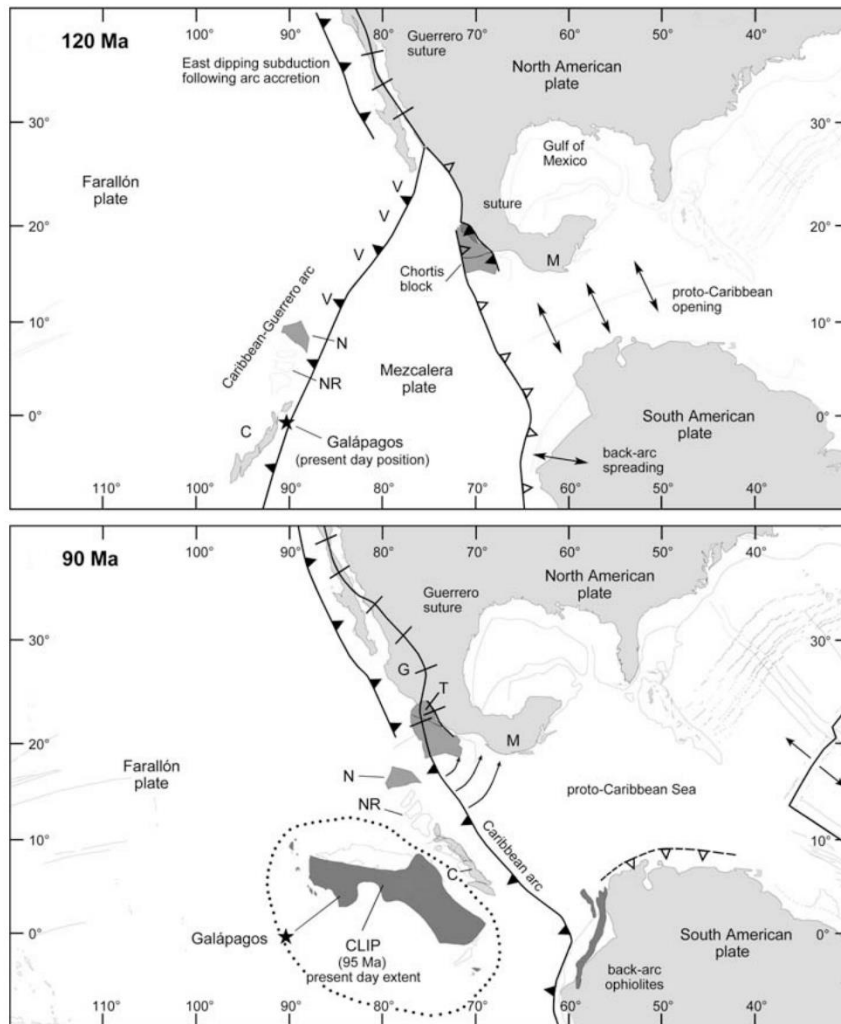


Figure 1-2 Reconstructions of the Caribbean at 120 Ma and 90 Ma  
 Key to abbreviations: N=Nicaragua, NR=Nicaraguan rise, C=Cuba, M=Maya block, G=Guerrero terrane, CLIP=Caribbean large igneous province, Y=Yucatán basin, CT=Cayman trough, and LA=Lesser Antilles. Countries of Costa Rica and Panama correspond to approximate area of Chorotega block; countries of Honduras, Nicaragua, and Guatemala correspond to Chortis block. (Mann et al., 2007)

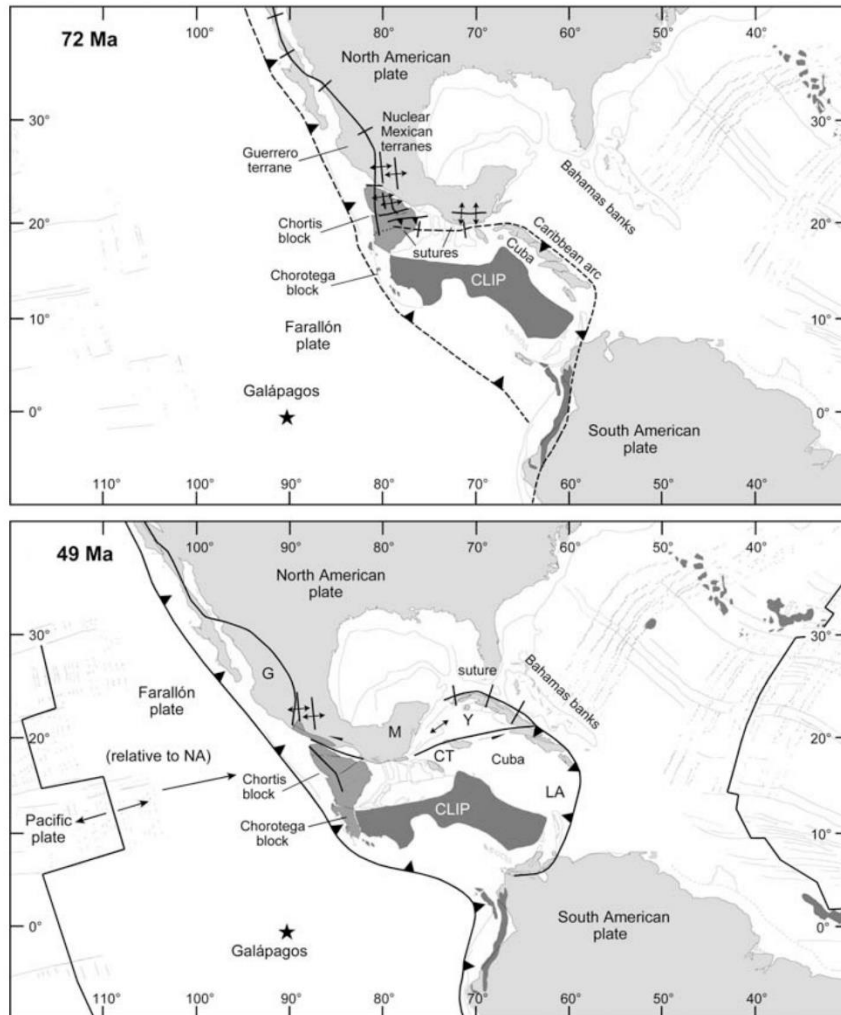


Figure 1-3 Reconstructions of the Caribbean at 72 Ma and 49 Ma  
 Key to abbreviations: N=Nicaragua, NR=Nicaraguan rise, C=Cuba, M=Maya block,  
 G=Guerrero terrane, CLIP=Caribbean large igneous province, Y=Yucatán basin,  
 CT=Cayman trough, and LA=Lesser Antilles. Countries of Costa Rica and Panama  
 correspond to approximate area of Chorotega block; countries of Honduras, Nicaragua,  
 and Guatemala correspond to Chortis block. (Mann et al., 2007)

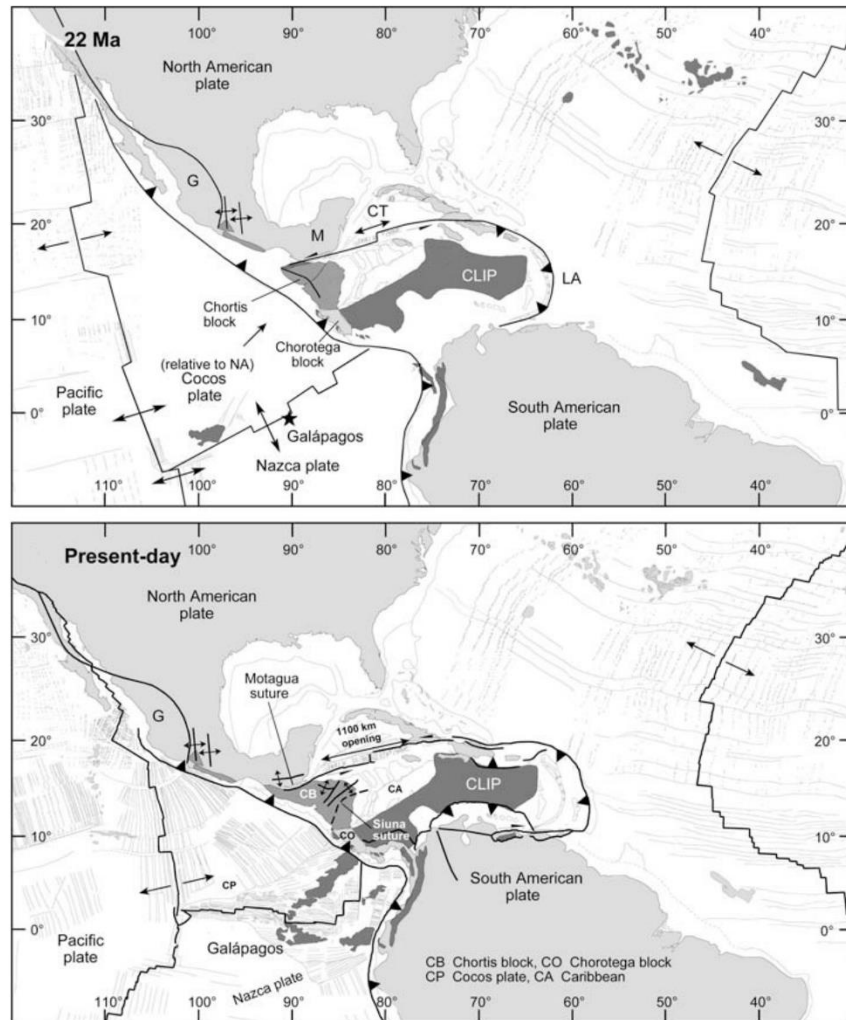


Figure 1-4 Reconstructions of the Caribbean at 22 Ma and today  
 Key to abbreviations: N=Nicaragua, NR=Nicaraguan rise, C=Cuba, M=Maya block,  
 G=Guerrero terrane, CLIP=Caribbean large igneous province, Y=Yucatán basin,  
 CT=Cayman trough, and LA=Lesser Antilles. Countries of Costa Rica and Panama  
 correspond to approximate area of Chorotega block; countries of Honduras, Nicaragua,  
 and Guatemala correspond to Chortis block. (Mann et al., 2007)



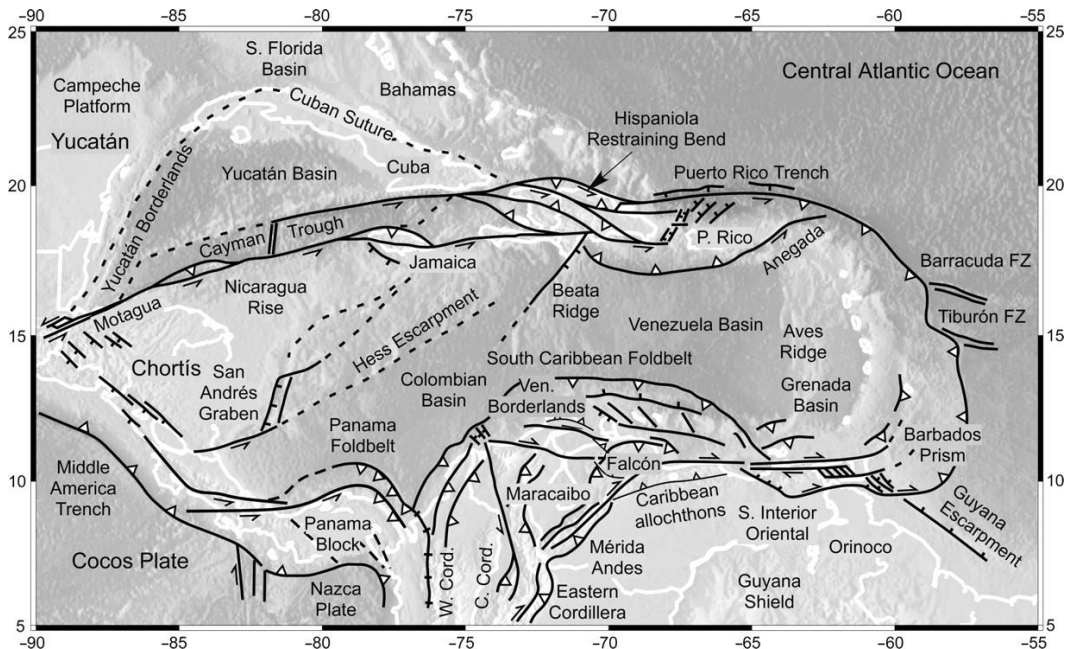


Figure 1-5 Tectonic setting of the Caribbean plate.  
(Giunta and Orioli, 2011)

Today, the eastern edge of the Caribbean plate is marked by a westward dipping subduction zone that has produced the Lesser Antilles (LA) island arc, an approximately 850 km long volcanic island arc that trends north-south and extends from Venezuela in the south to the Greater Antilles (Puerto Rico-Virgin Islands platform) in the north. The LA arc is a result of the North and South American plates being subducted beneath the Caribbean plate. The Greater and Lesser Antilles are separated by the Anegada Passage, a probable Neogene graben complex (Bouysse et al., 1990). To the west of the Lesser Antilles Arc lies the Grenada Basin, which is bordered on its western side by the Aves Ridge.

## 2.2 Dominica and the Central Lesser Antilles

The Lesser Antilles Island arc has a complex history, and has probably been active since the Early Cretaceous (Bouysse, 1988). With the onset of the early Eocene, the volcanic landscape began to develop. Its trace can be identified from Grenada, in the

south, to Anguilla, in the north; however, the arc does not display uniform morphology along its entire length. The Dominica Passage, a deep (1200 m) structure that cuts through the arc serves as a marker between the distinct morphologies of the northern and southern portions of the arc (Bouysse et al., 1990). The current arc is considered to be composed of two segments, each with unique characteristics. The section north of Martinique experiences high seismicity (Smith et al., 2013) (Figure 1-6), has a history of large magnitude earthquakes (Wadge and Shepard, 1984), and a subduction rate of ~2cm/yr (DeMets et al., 2000; 2007) along a slab that dips 50°- 60°. The segment that extends south of St. Lucia has not had large historical earthquakes, nor does it experience the seismic activity that the north does (Figure 1-6). The subduction in the southern segment is slower and shallower than in the north (1.8 cm/yr at 45°- 50°) (DeMets et al., 2010). North of Dominica, the 50 km wide Kallinago depression separates two distinct volcanic chains (Figure 1-7). The outer arc, to the east, is the remnant of earlier volcanism and is known as the Limestone Caribees, while the inner arc, known as the Volcanic Caribees, to the west, began activity in the Burdigalian (~20 Ma) and is still active today. South of Dominica, the older and younger igneous arcs are superimposed. The Tiburon and Barracuda, aseismic ridges, both of which trend ESE-WNW, are currently being subducted beneath the Lesser Antilles Arc.

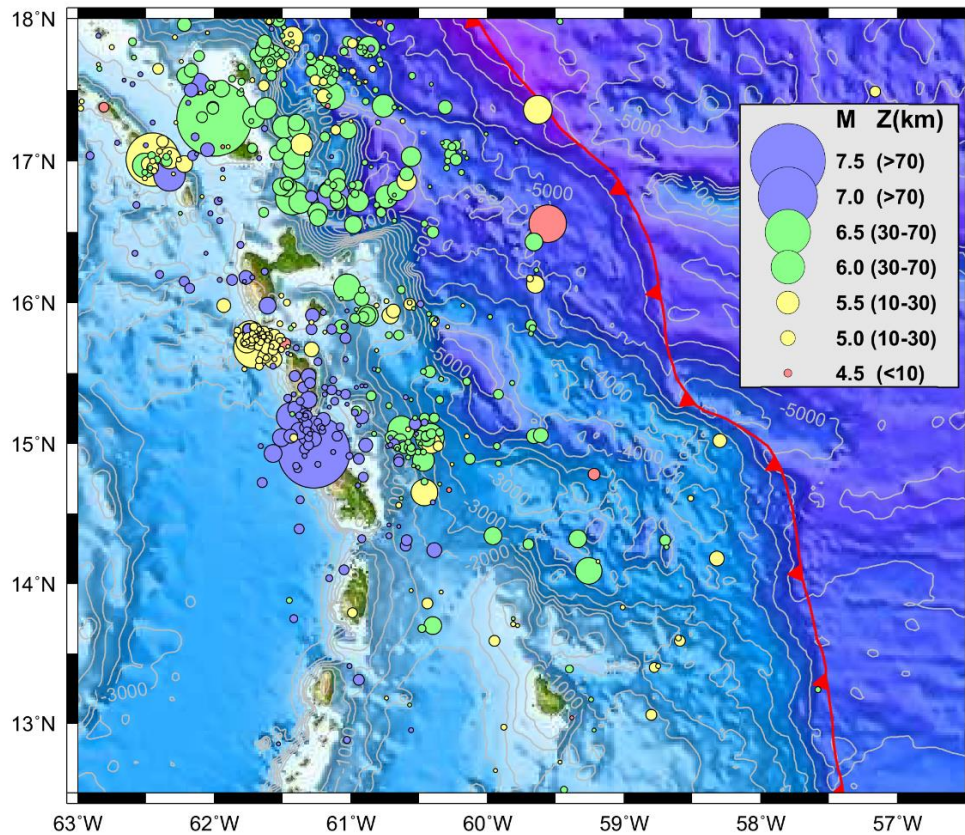


Figure 1-6 Lesser Antilles Arc regional seismicity

(Smith et al., 2013, DeMets et al., 2010, Mann et al., 2002)

Figure reproduced from Smith et al., 2013: Regional seismicity from the IRIS and NEIC catalogs for all earthquakes of magnitude greater than M4 from 1906 to 2010.

Magnitudes are shown as scaled circles and the hypo central depths and coded using the colors shown in the legend in the upper right. Topography and bathymetry from ETOPO1, which were reformatted and released by NOAA

(<http://www.ngdc.noaa.gov/mgg/global/global.html>). Contours are in meters. The trace of the intersection of the crystalline lithospheres of the North American or South American plates and the overriding Caribbean plate is modified from Mann et al., 2002. Note the increased seismicity north of 15°N and the high concentration of shallow crustal seismicity along the arc.

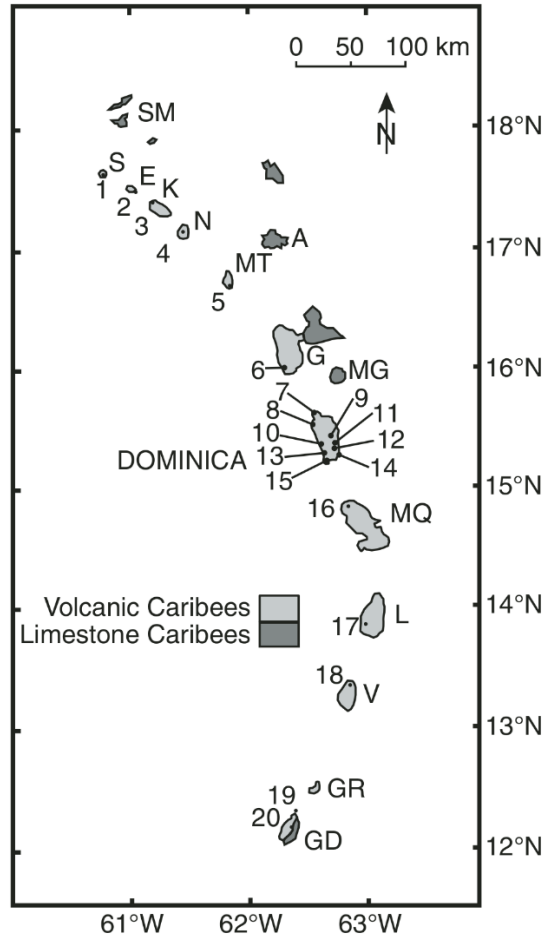


Figure 1-7 Map of Lesser Antilles

Reproduced from Smith et al. (2013): Map showing location of potentially active volcanoes: 1-Mount Scenery; 2-The Quill; 3-Mount Liamuiga; 4-Nevis Peak; 5-Soufrière Hills; 6-La Soufrière; 7-Morne aux Diabes; 8-Morne Diablotins; 9-Morne Trois Pitons; 10-Wotten Waven caldera; 11-Valley of Desolation; 12-Watt Mountain; 13-Morne Anglais; 14-Grand Soufrière Hills; 15-Morne Plate Pays; 16-Mount Pelée; 17- Soufrière volcanic center; 18- Soufrière; 19-Kick ‘em Jenny (submarine); Mount St. Catherine. Also shown is the subdivision of the Lesser Antilles into Limestone Caribee and Volcanic Caribee island arcs (after Roobol and Smith, 2004). Islands are S-Saba; E-St. Eustatius; SM-St. Martin; K-St. Kitts; N-Nevis; MT-Montserrat; A-Antigua; G-Guadeloupe; L-St. Lucia; V-St. Vincent; GR-Grenadines; GD-Grenada.

Of particular interest here is the island of Dominica (Figure 1-8). The predominantly andesitic volcanic island sits in the Central Lesser Antilles, either side of which, differences exist in the tectonics and the resulting morphology of the arc system. At this location in the arc, the subducted slab has a dip angle of  $\sim 50^\circ$ -  $60^\circ$  and subduction is nearly normal (James, 2008). The Wadati-Benioff zone is at its deepest here, with earthquakes reaching a maximum depth of  $\sim 210$  km (Smith et al., 2013). Dominica should be free from significant arc-parallel extension that is present both to the north, due to sinistral oblique subduction, and to the south, due to dextral oblique subduction (DeMets et al., 2000).



Figure 1-8 Location of Dominica within the Lesser Antilles

## Chapter 2

### GPS Data

#### 2.1 Campaign GPS Data Acquisition

GPS data from the Island of Dominica have been collected during GPS campaigns that began in 2001. The University of Arkansas Geodesy Lab began geodetic measurements of the Island by installing and occupying nine sites (James, 2008). Expansions of the network have been completed over the years; three sites were added in 2003, six were added in 2004, five were added in 2006, and the final four were added in 2007 to complete the 27 site network (James, 2008). Each of the sites consists of a stainless steel Bevis pin drilled and then epoxied into bedrock, a building, or other edifice deemed stationary with reference to the surrounding landscape. Details regarding each individual site are available in the site descriptions located in the Appendix of this manuscript.

A variety of equipment was used to collect GPS data. During the 2011 and 2012 field campaigns, 4 types of mounts were used: 0.2 m and 0.5 m spike mounts, a 1.5 m tetrapod, and a standard surveyor's tripod with a tribrach. The type of mount used for any given site was dictated by the environment of the individual sites. The receiver/antenna combination was either an Ashtech  $\mu$ -Z receiver with a Dorn-Margolin choke ring antenna or a Trimble R7 receiver with a Zephyr geodetic antenna. Both receivers are dual frequency and record L1 and L2 code and phase data. A typical 12 volt lead-acid car battery with a solar panel was used to power each station. Data was collected at each site for three consecutive UTC days with a 30 second sampling interval and an elevation mask of  $10^\circ$ . At the end of a site occupation, the data from the receiver was downloaded using receiver specific software onto a laptop and transferred to the server at UTA using WinSCP.

## 2.2 Continuous GPS Data Acquisition

Continuous GPS data were obtained from the open data archive at UNAVCO ([www.unavco.org](http://www.unavco.org)). Since the focus of this work is the Caribbean, the data collected are from sites within the Continuously Operating Caribbean Observational Network (COCONet - <http://coconet.unavco.org>). COCONet is an NSF-funded, internationally collaborative effort aimed at developing a large-scale geodetic and atmospheric infrastructure in the Caribbean that forms the backbone for a broad range of geoscience and atmospheric investigations (Braun et al., 2012)

## 2.3 GPS Data Processing

All GPS data for this study have been processed using an absolute point positioning strategy using GIPSY-OASIS II (versions 6.1.2 and 6.2). GIPSY (GNSS-Inferred Positioning SYstem) and OASIS (Orbit Analysis and Simulation Software), together, comprise a software package that has been developed by the Jet Propulsion Laboratory (JPL) and is maintained by the Near Earth Tracking Applications and Systems groups. For our purposes, this software will be used for terrestrial positioning (Webb and Zumberge, 1995; Gregorius, 1997; Turner, 2010). The initial calculated positions are non-fiducial and in the free frame, or satellite reference frame. These positions are then translated, rotated, and scaled into the International GNSS Service 2008 (IGS08), using X-files from JPL (Zumberge et al., 1997), and then into a more useable, plate-based reference frame with the DeMets et al. (2000, 2007) version of the GPS-derived Euler pole for the Caribbean to examine site velocities relative to the fixed Caribbean plate.

GIPSY – OASIS II (GOAll) was developed to solve for precise positions from GPS data collected in the field and consists of numerous individual programs and modules that can be tailored to suit the needs of any user. For GOAll to be used, the raw

data, or GPS observables, must be converted from the receiver specific formatting to the Receiver Independent Exchange Format (RINEX) using TEQC (Estey and Meertens, 1999) and named according to GIPSY format, which then allows the data to be run in an automated manner using a UNIX script originally authored by Charles DeMets and significantly modified over the years by Glen S. Mattioli. Turner (2003) provides a detailed description of the steps involved in the processing of GPS data using GIPSY-OASIS II software to calculate precise point positions, these steps are presented here with minor modifications.

1. The program Ninja translates the rinex files into a FORTRAN binary file, removes outliers, and detects cycle slips. The data are decimated into 300 second intervals and data for each satellite are merged into a qm file.
2. Individual qm files are merged into a single file, the QMfile, by the program merge\_qm. A namelist is created from the QMfile called qregress.nml.
3. The qregress.nml namelist is used to derive qregress, which does the physical modeling of the receiver measurements. In our analysis scheme, qregress uses final precise satellite orbits, clocks, and earth orientation parameters provided by JPL. Qregress applies the physical models (receiver location time dependence, tidal effects, polar motion and earth rotation, nutation, procession, perturbation, rotation, geocenter offset, and coordinate scaling) to the orbits and observations and outputs a regress file, rgfile, which contains the parameter partials and nominal values.
4. The rgfile is used by the program wash\_nml to create a wash.nml file. The rgfile and the wash.nml files are the input for the preprefilter, prefilter, and filter modules. The filter module runs the Square Root Information Filter, which processes small batches of data sequentially and produces the accume.nio, smooth.nio, and uinv.nio files.
5. Smapper follows the filtering process and smoothes and maps the covariance, sensitivity, and solution of the parameter estimation.
6. Postfit computes the post-fit data residuals.
7. Postbreak searches for cycle slips missed by Ninja and modifies the QMfile if cycle slips are detected and reruns GIPSY.
8. Edtpnt2 adds or deletes data points to or from the filtered solution to remove outliers. After Edtpnt2 is run, smapper and postfit are rerun.
9. The stacov module produces the final solution files in text format.



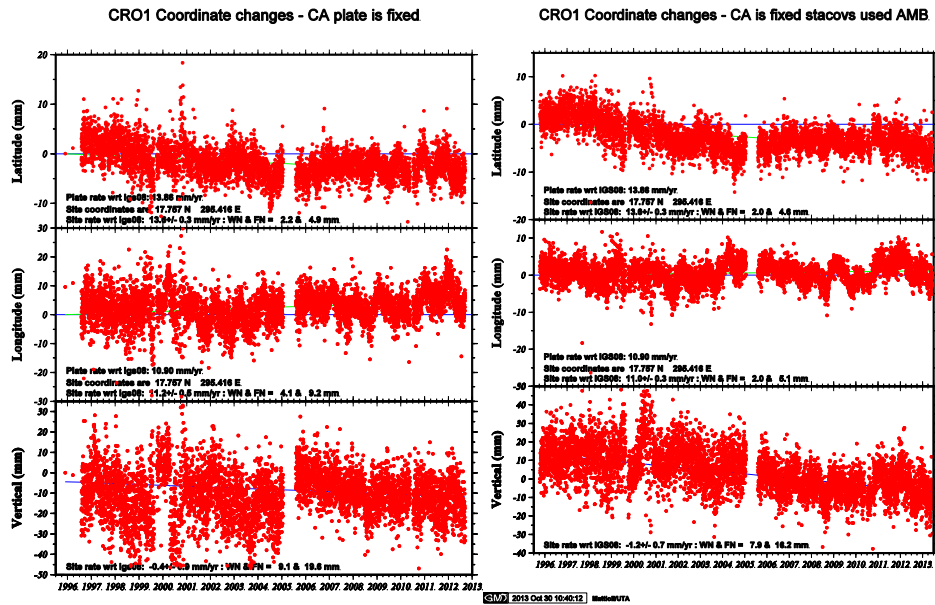
## 2.4 GOAll - 6.1.2 vs. 6.2

The data were initially processed using GOAll version 6.1.2, but discrepancies prompted an evaluation of the processing system, whereby, it was determined that version 6.2 generated more precise results. The 6.2 version provides for the resolution of the ambiguity that exists within the first cycle of data collected by the GPS receivers. The most notable improvement is seen in the vertical velocity component, which is a result of the software and processing scheme incorporating the antenna's absolute phase center information into the analysis, in addition to using VMF1 grid files for tropospheric estimates. Figure 2-1 compares time series for site CRO1, using various versions of the GOAll software: a) version 6.1.2, b) version 6.2 with ambiguity resolution and c) version 6.2 without ambiguity resolution. Note that for sites with large amounts of data (CRO1 has almost 18 years of continuous data), the north and east components of the velocity show very little variation. The vertical velocity in this example is  $-0.4 \pm 0.9$  mm/yr when processed with version 6.1.2 versus  $-1.2 \pm 0.7$  mm/yr when processed with version 6.2, which incorporates the phase center specifications for the antenna used at this site. For sites with fewer data (CN07 has been collecting data for approximately 1 year), larger variations are seen in all three velocity components. Figure 2-2 compares time series for the site CN07 using various versions of GOAll: a) version 6.1.2, b) version 6.2 with ambiguity resolution, c) version 6.2 without ambiguity resolution, and d) version 6.2 with ambiguity resolution and an antenna offset correction. It is interesting to note that even when using version 6.2, which incorporates the antenna phase center information, there still exists, in some cases, an offset in the time series due to a change in the antenna type. On January 30, 2013 at site CN07, the antenna was changed from a Trimble model 57971 to a Trimble model 59800. An offset in the vertical component is apparent in Fig. 2-2 (b) and the correction for the offset can be seen in Fig. 2-2 (d). Table 2-1 outlines the

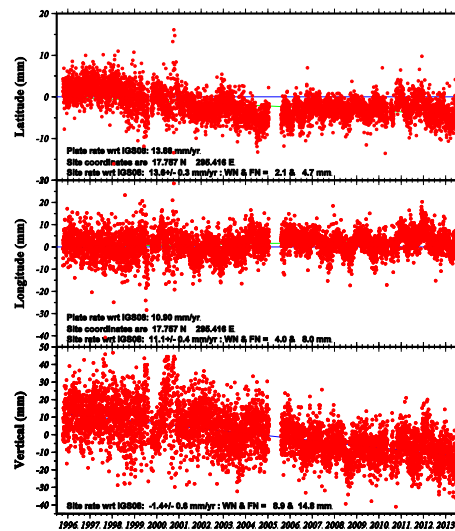
velocity values generated by the various versions of the software for both of these sites. It is clear to see that for sites with shorter observation time spans, the variations in the processing have a much larger impact on the result. The most obvious discrepancy for site CN07 is in the vertical component where there is an approximately 22 mm difference between the result that was calculated using the absolute phase center information for the two different antennas and the result that also made a correction for the offset that still existed after the absolute phase centers were considered. Inconsistencies are expected to be more commonly observed in the vertical component; however, for CN07, we also see a significant variation in the east component, which is nearly within error of the previous estimates, but still is noteworthy. For this study, if an offset was observed and corrected, the final velocity values used for the kinematic analysis were those generated by the version 6.2 with ambiguity resolution and offset corrections. Offset corrections can be seen in the times series in Appendix B.

Table 2-1 Velocity summary for sites CRO1 and CN07  
 Values generated with various versions of GOAll relative to ITRF08.

SITE CRO1 (observation span 17.67 yr)		rate in mm/yr		
GOAll version		north	east	vertical
6.1.2		13.6 ± 0.3	11.2 ± 0.5	-0.4 ± 0.9
6.2 without ambiguity resolution		13.6 ± 0.3	11.1 ± 0.4	-1.4 ± 0.7
6.2 with ambiguity resolution		13.6 ± 0.3	11.0 ± 0.3	-1.2 ± 0.7
SITE CN07 (observation span 1.09 yr)		rate in mm/yr		
GOAll version		north	east	vertical
6.1.2		7.3 ± 1.4	-3.4 ± 2.1	-28.5 ± 8.0
6.2 without ambiguity resolution		8.3 ± 1.3	-8.3 ± 1.8	25.1 ± 5.4
6.2 with ambiguity resolution		8.5 ± 1.3	-6.5 ± 1.5	24.5 ± 5.2
6.2 w/amb and offset correction		9.4 ± 1.3	-4.3 ± 1.4	2.3 ± 3.0



(a) (b)  
CRO1 Coordinate changes - CA is fixed stacovs used no\_AMB



(c)

Figure 2-1 Comparative time series for site CRO1.  
 a) GOAll version 6.1.2 b) GOAll version 6.2 with ambiguity resolution  
 c) GOAll version 6.2 without ambiguity resolution. CRO1 is located on St. Croix.

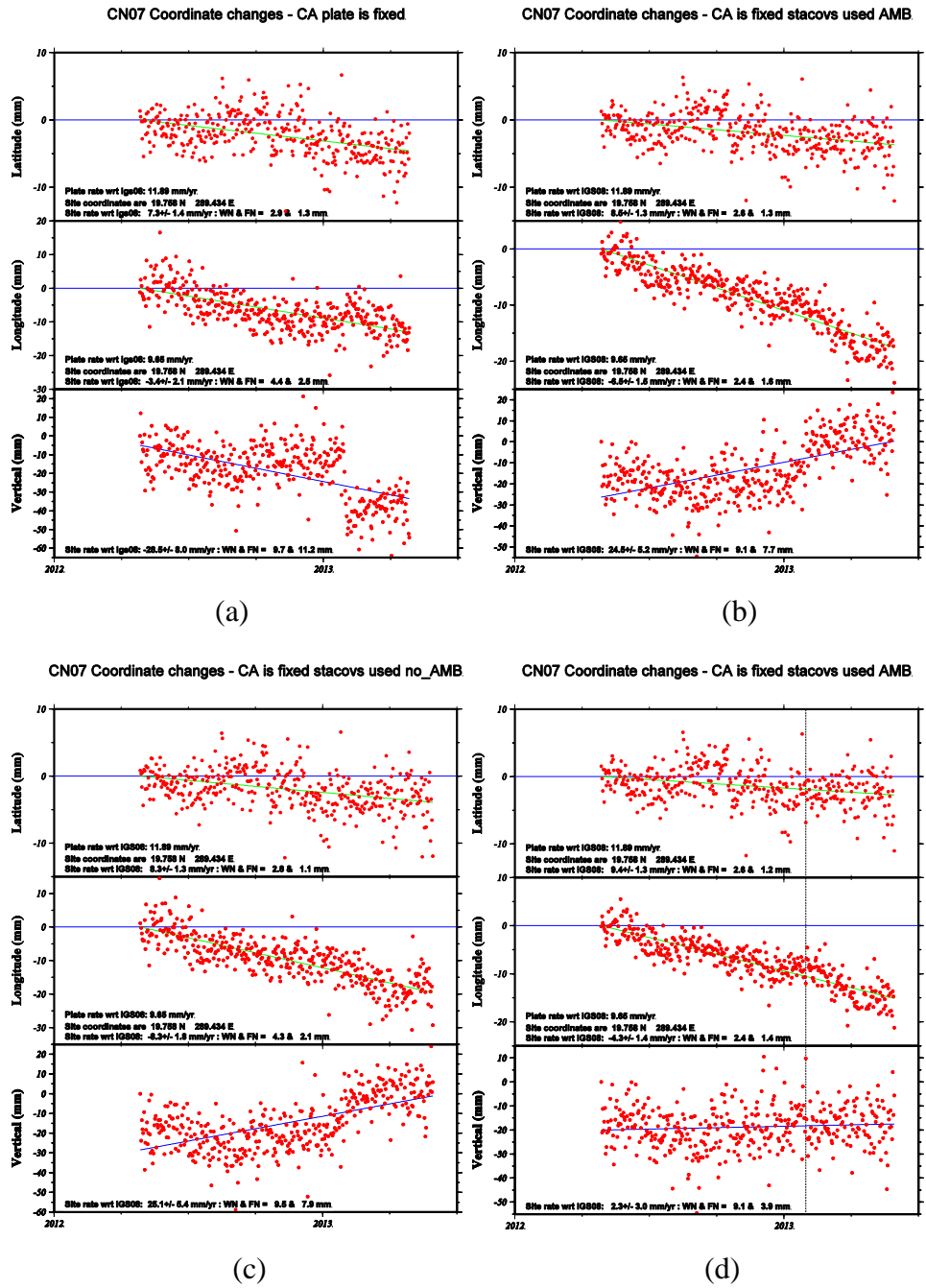


Figure 2-2 Comparative time series for site CN07. CN07 is located in Puerto Plata, Dominican Republic. a) GOAll v. 6.1.2 b) GOAll v. 6.2 with ambiguity resolution c) GOAll v. 6.2 without ambiguity resolution d) v. 6.2 with ambiguity resolution and offset correction. Vertical dashed line marks the antenna change from TRM57971 to TRM59800, no radome is used at this site.

## Chapter 3

### Geodetic Observations of Dominica, Lesser Antilles

#### 3.1 Introduction

Although people living in close proximity to volcanoes have always been able to observe changes in the Earth's surface prior to an eruption, it has only been within the last century that measurements of ground deformation have been used to infer subsurface activity. It is the desire of volcanologists, who work in the field of monitoring volcano behavior, that precise surface deformation measurements may one day be used as a predictive tool to forecast eruptions. Today, surface displacements can be measured using space-based observing platforms and these measurements are routinely used in numerical models that evaluate the rheologic and geometric conditions (Poland et al., 2006).

The Commonwealth of Dominica is a volcanic island located in the central portion of the Lesser Antilles Arc on the eastern edge of the Caribbean Sea (Figure 3-1). The Island is approximately 750 km<sup>2</sup> and has one of the highest concentrations of potentially active volcanoes in the world (Smith et al., 2013).



Figure 3-1 Location of Dominica

As a result of earthquake swarms in the southern portion of the Island in 2001, the University of Arkansas Geodesy Lab completed the installation and occupation of nine sites in the summer of 2001. Expansions of the Dominica GPS network have included three additional sites in 2003, six additional sites following a seismic swarm in 2004, and the final four sites were added in 2007 to complete the 27 station network (James, 2008) (Figure 3-4). Analysis of the data collected between 2001 and 2007, appeared to indicate that a geodetic signature was emerging as a result of some type of intrusive igneous activity (James, 2008), perhaps the pressurization of a shallow magma chamber. The residual velocities for Dominica were still relatively small with respect to their errors in 2008. Field campaigns were conducted during the summers of 2011 and 2012, during which 22 of the previously established 27 sites were re-occupied. Specifics regarding each individual site are located in Appendix A of this manuscript. The additional data has reduced the site velocity errors to reasonable values in order to make a conclusion regarding the relationship between geodetic signatures observed and any tectonic, seismic, or volcanic activity on Dominica.

### 3.2 Volcanic History of Dominica

The volcanics on the Island are predominantly andesitic and display a range of morphologies, which indicates a variation in eruption style through time. The geology of the Island (Figure 3-2) can be divided into 4 stratigraphic divisions based on age: Division 1 (upper Miocene) is dominated by mafic volcanism; Division 2 (upper Pliocene to lower Pleistocene) is characterized by the development of two large stratovolcanoes over a 2 million year period; Division 3 (lower to upper Pleistocene) represents a general hiatus in major activity, and Division 4 (upper to Pleistocene to Holocene) is characterized by the formation of numerous Pelean centers throughout the island (Smith et al., 2013). The

igneous activity that began as minimally contaminated basaltic magmas ponding at the crust-mantle boundary was followed by fractionation and rise of the magma, which generated distinct basic and intermediate suites. The mid-crustal magma chambers that sat below the stratovolcanoes then served as barriers to the continued rise of magma, which resulted in the Division 3 quiescence. The magma eventually found its way around the chambers as numerous sills were emplaced into the lower crust. The sills served to reactivate the volcanism, which was then dominated by andesitic and dacitic composition. A mid-crustal batholith was postulated to exist below Dominica as a result of the amalgamation of the various chambers and an illustration of evolution is presented in Figure 3-3 (Smith et al., 2013). Dominica's volcanics are in contrast to a typical system, where each individual volcano is underlain by an independent volcanic system, with a unique composition, that, over a period of 0.5-1 million years will evolve and eventually become extinct (Christiansen, 1979). It has been proposed that when a magma reaches a crystallization state of >50%, that magma can no longer be erupted (Carmichael, 2002). This means that what was once a feeder system for a volcano can become the barrier to more magma rising, and even if the magma finds its way to the surface, it remains geochemically distinct from other volcanic centers (Gunn et al., 1974, Smith and Roobol, 1990). Such is not the case with Dominica, where the products of the numerous volcanic centers are remarkably homogeneous, which suggests that magma mixing within the batholith was very efficient (Smith et al., 2013). This same type of system, on a smaller scale, can be seen under the Soufriere Volcanic Complex on St Lucia (Schmitt et al., 2010). The development of an extensive zone of melting due to a sustained mantle basalt flux is attributed to the fact that the leading edge of the Caribbean plate is undergoing near normal convergence with the subducting North and South American plates (Smith et al., 2013). Convergence becomes more oblique as one moves away

from Dominica, both to the north and the south along the Lesser Antilles (DeMets et al., 2000; 2007). Another factor that will support a sustained flux of material from the mantle is the steeply descending slab that is seen at Dominica. The Waditi-Benioff Zone beneath central and western portions of the island are deeper than that for any other island, with the exception of a small portion beneath northern Martinique (Smith et al., 2013). Also unique to Dominica are calderas, which are not common in oceanic island-arc settings (Hughes and Mahood, 2008). The calderas at Morne Trois Pitons and Wotten Waven are evidence that the system has had the capability of generating large-scale eruptions. These two calderas along with Morne Diablotins have generated a total volume of ignimbrite in excess of 60 km<sup>3</sup> (Carey and Sigurdsson, 1980). Geothermal features coincident with the “seismo-thermal” zones indicate that the system is still active, and currently, the country, with the assistance of Iceland, is drilling test wells to ascertain the viability of harnessing the Island’s geothermal potential.

The last magmatic eruption on Dominica was ~450 years ago and current active volcanism is concentrated in “seismo-thermal” zones, which are a reflection of the “live” portions of the amalgamated batholith. It stands to reason that monitoring this system will not only provide data about surface deformation related to igneous activity, but would also provide valuable information for Dominica’s emergency management response teams, in the event that the current status of the system changes in the near future.



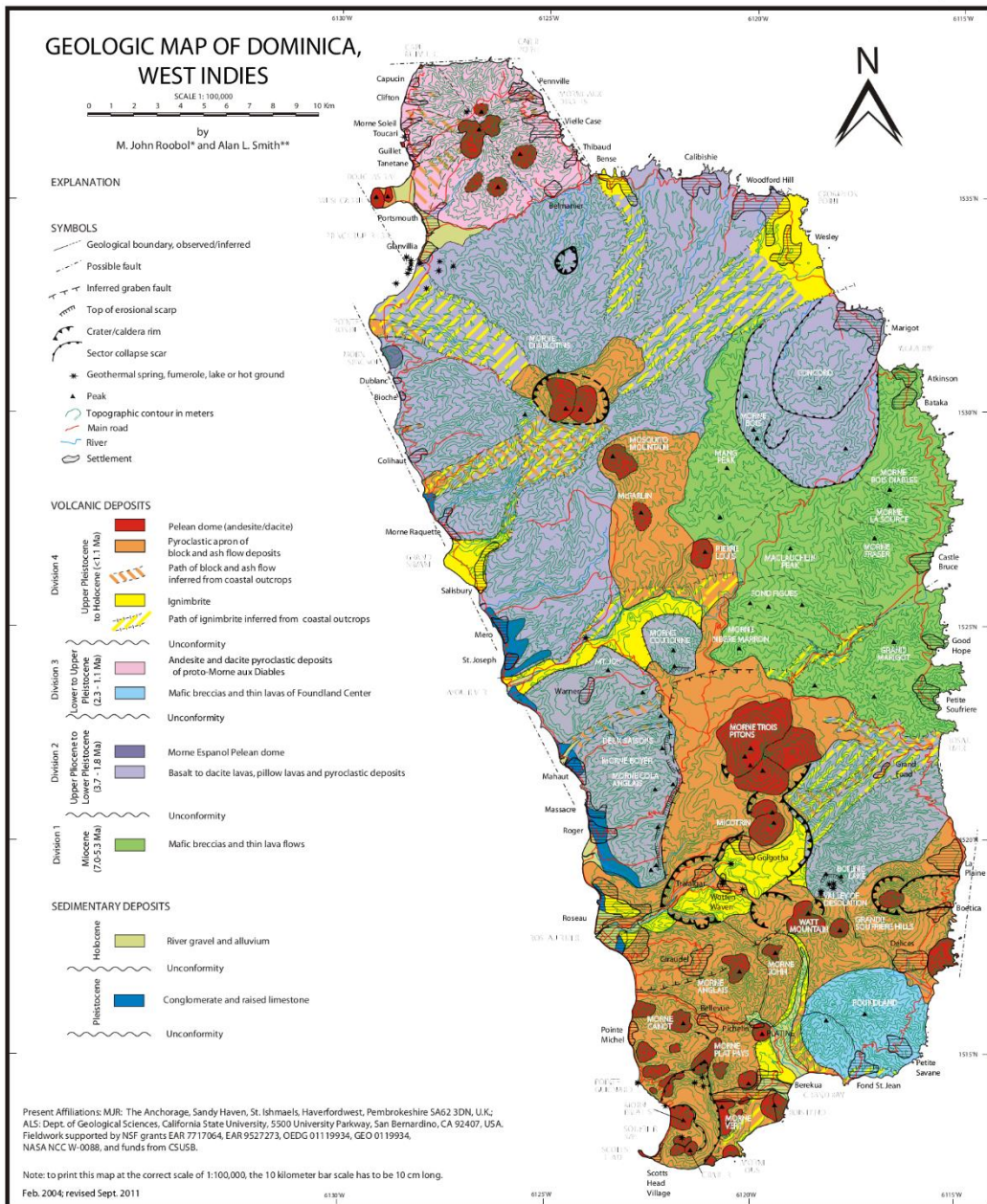


Figure 3-2 Geologic map of Dominica from Smith et al. (2013)

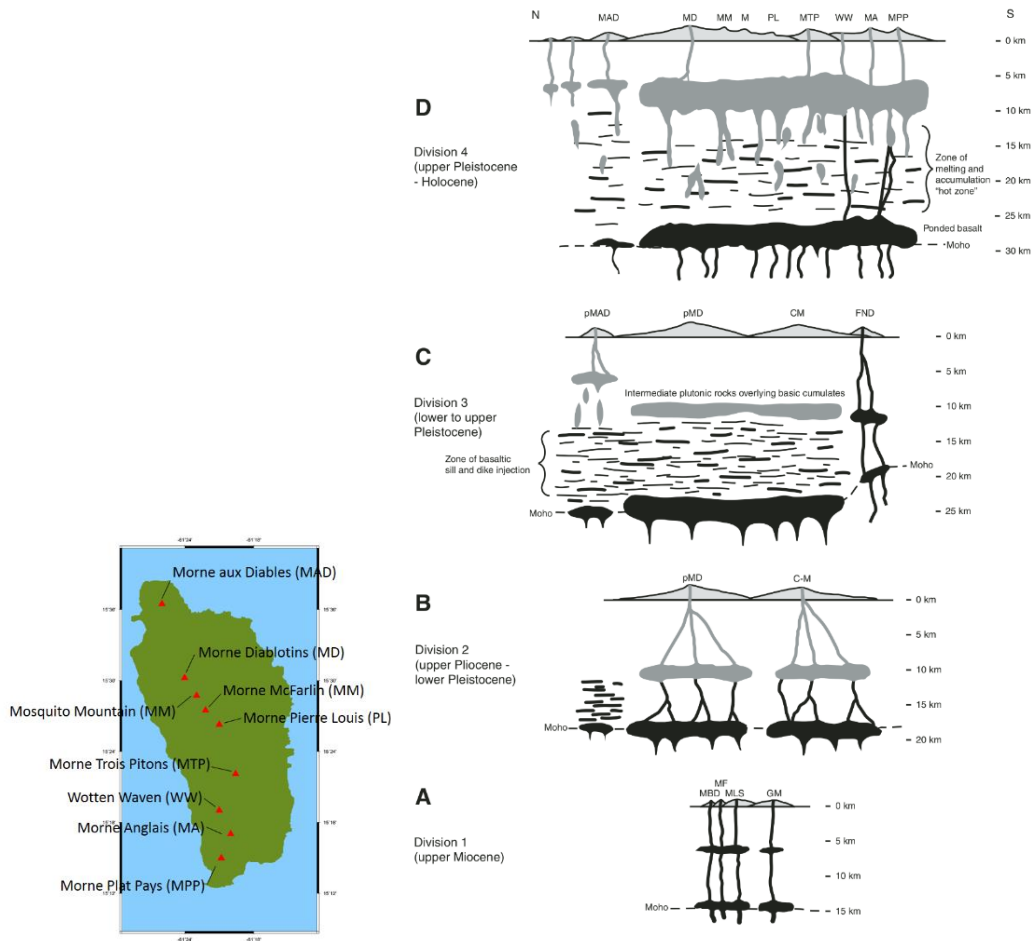


Figure 3-3 A petrogenetic model for the geologic evolution of Dominica (Smith et al., 2013). Site map at left. Diagrammatic sketches to show the development of magmatic systems on Dominica over time. Horizontal and vertical scales are the same, height of volcanic centers not to scale. **(A) Stratigraphic Division 1** – upper Miocene: independent volcanic systems involving ponding of mantle-derived basalt at the crust mantle boundary (~15 km) and mid-crustal magma chambers that become more developed over time; MBD-Morne Bois Diabes, MF-Morne Fraser, MLS-Morne La Source, GM-Grand Marigot. **(B) Stratigraphic Division 2** – upper Pliocene to lower Pleistocene: two separate volcanic systems - proto-Morne Diablotins (pMD) in the north and Cochrane-Mahaut (CM) in the south. More extensive development of basaltic accumulation zone at crust-mantle boundary (~18 km) and well-developed mid-crustal magma chambers under each center. Mantle derived basaltic magmas continue to reach surface from lower accumulation zone. Initiation of basaltic sill and/or dike injection under future proto-Morne aux Diabes. **(C) Stratigraphic Division 3** – lower to upper Pleistocene: development of large crust-mantle zone of accumulation (26 km) beneath most of Dominica and formation of a mid-crustal “proto-pluton” under proto-Morne Diablotins (pMD) and Cochrane-Mahaut (CM) centers that effectively blocks the rise of

Figure 3-3 continued:

new magma, causing termination of activity at these centers. Continued influx of basaltic magma accommodated by the injection of lower crustal sills and/or dikes that has the effect of progressively heating up the lower crust. Development of a zone of melting and magma accumulation under proto-Morne aux Diabes stratovolcano (PMAD) in the north. Rise of basaltic magma through unaltered oceanic crust (Moho = ~20 km) in the south produced a mid-crustal magma chamber that was the source for the Foundland stratovolcano (FND). **(D) Stratigraphic Division 4** – upper Pleistocene to Holocene: Increase in mantle flux continues injection of sills and/or dikes beneath most of southern and central Dominica, producing a “hot zone” under the island and generation of intermediate and hybrid magmas. The “proto-pluton” is no longer a barrier to the rise of intermediate magmas. Greatest flux is under southern Dominica, as suggested by the presence of most of the potentially active centers and the caldera-forming eruptions of Morne Trois Pitons (MTP) stratovolcano and Wotten Waven caldera (WW). Mid-crustal magma chambers expand and eventually merge to form mid-crustal batholith under most of the island. Expansion of magmatic system beneath Morne aux Diabes (MAD) to form new volcanic zone under northern Dominica and the surrounding seafloor. MD-Morne Diablotins, MM-Mosquito Mountain, M-Morne Anglais, MPP-Morne Plat Pays. Format for sketches modified from de Silva (2008). Figure reproduced from Smith et al. (2013).

### 3.3 Results

A time series plot has been generated for each campaign GPS observation station (Figure 3-4) in Dominica and these are presented in Figure 3-5 through Figure 3-24. The results were analyzed with an absolute point positioning strategy using GOAll version 6.2, and final precise orbits, clocks and earth orientation parameters obtained from Jet Propulsion Laboratory (JPL). The reference frame used was IGS08. The plots include all available data for the particular site, the red dots are the daily position estimates, the blue lines are the predicted plate rates in IGS08 held fixed (horizontal) and the green lines are the least squares best fit site rates in IGS08 with respect to the Caribbean plate rate (CA). White noise (WN) and flicker noise (FN) amplitudes are lowest in the north direction and highest in the vertical, and it has been established that white noise in the vertical component is higher for stations located in tropical regions ( $\pm 23^\circ$ ) (Mao et al., 1999). Table 3-1 is the velocity summary for the Dominica campaign

GPS sites; note that FN values are at the default level and that the default estimate for Random Walk Noise (RWN) is fixed at 1 mm/sqrt (yr) of monument noise.

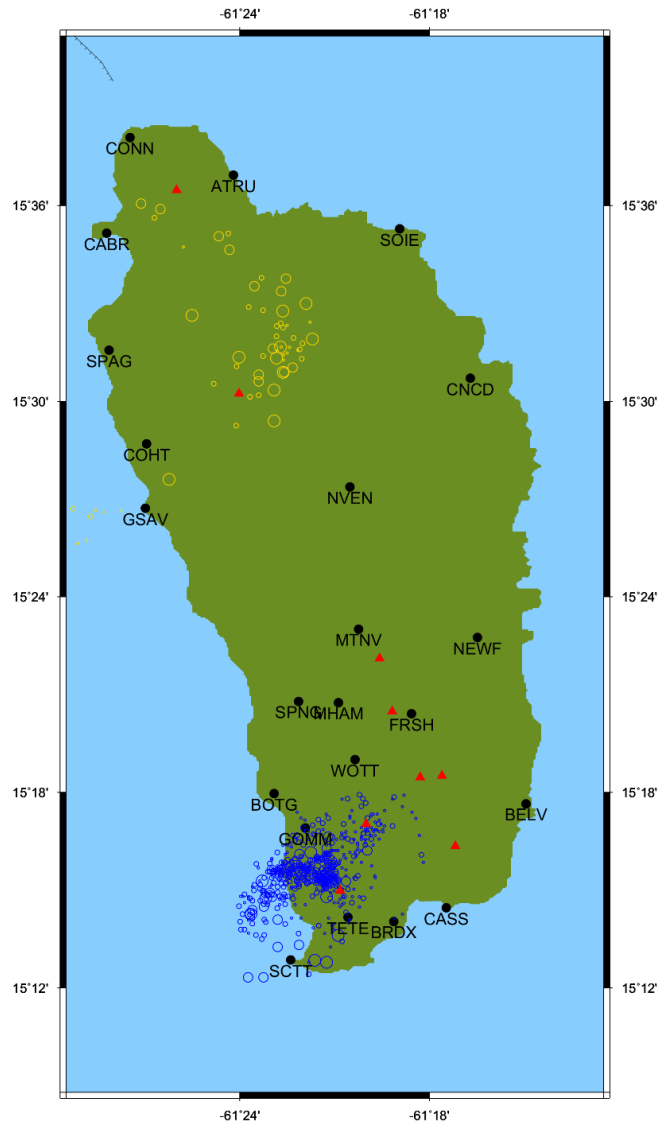
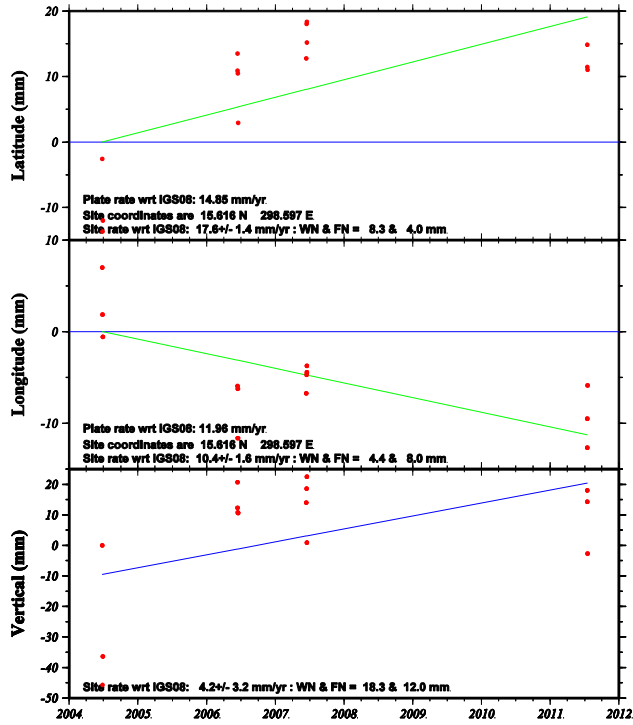


Figure 3-4 Dominica campaign GPS site location map  
Black dots indicate the location of GPS sites with associated marker name, red triangles are volcanic centers, gold circles mark the 2001 seismic swarm and blue circles mark the 2004 seismic swarm. Epicenter data courtesy of the Seismic Research Unit at the University of the West Indies.

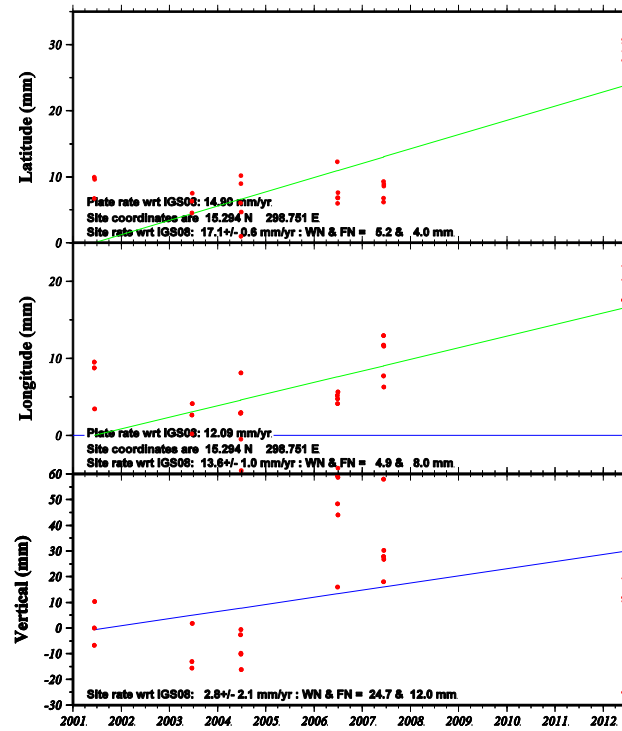
ATRU Coordinate changes - CA is fixed stacovs used AMB



2013 Oct 21 19:15:11 MetNet/UTA

Figure 3-5 Time series for site ATRU

BELV Coordinate changes - CA is fixed stacovs used AMB

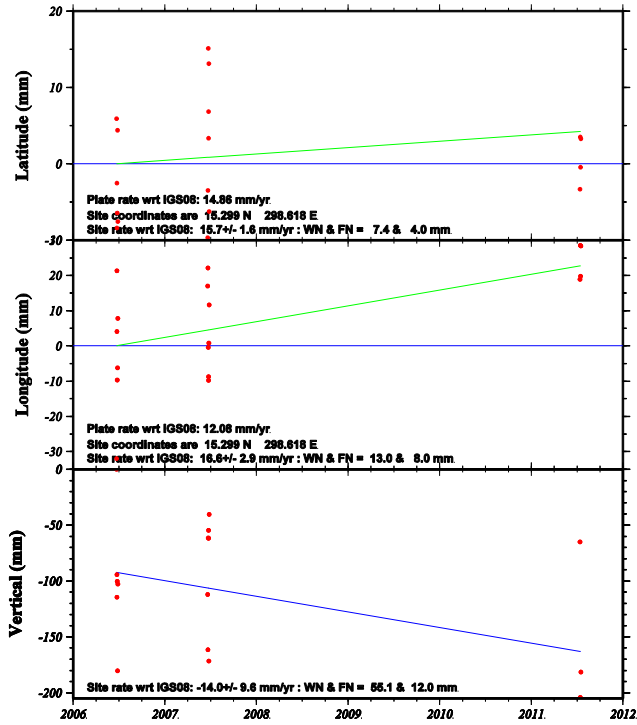


2013 Oct 21 19:21:39 MetNet/UTA

Figure 3-6 Time series for site BELV

Red dots are the daily position estimates (16 – 24 hr occupations). The blue lines are the predicted plate rates in IGS08 held fixed (horizontal). The green lines are the least squares best-fit site rates in IGS08 with respect to the Caribbean plate rate (CA). WN = white noise and FN = flicker noise estimates.

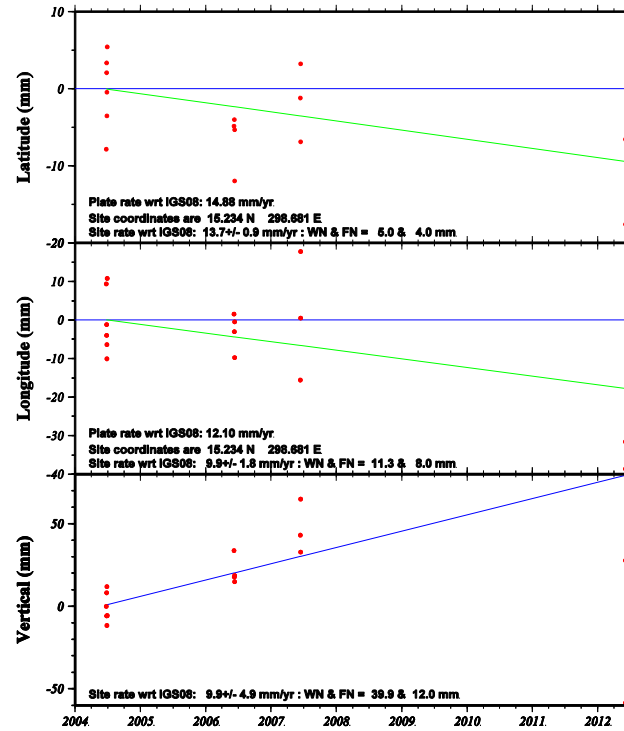
**BOTG Coordinate changes - CA is fixed stacovs used no\_AMB**



SM 2013 Jun 11 11:22:49 MetNet/UTA

Figure 3-7 Time series for site BOTG

**BRDX Coordinate changes - CA is fixed stacovs used AMB**

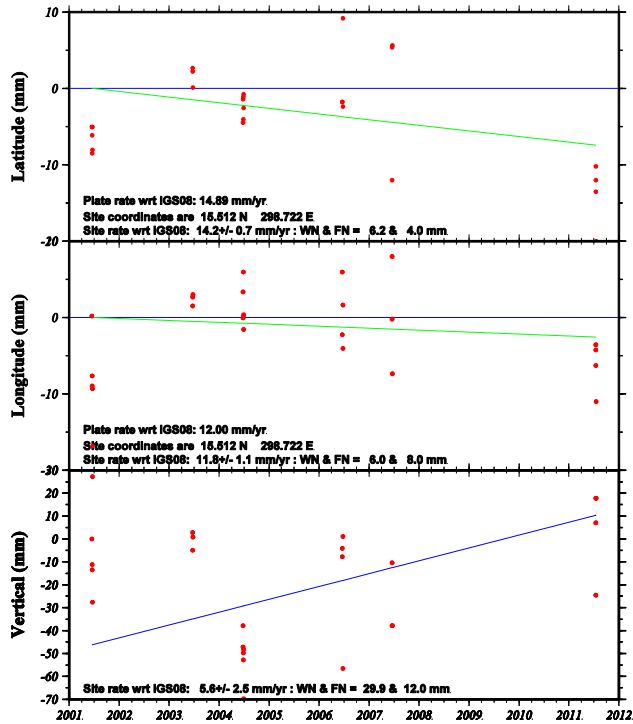


SM 2013 Jun 11 11:28:26 MetNet/UTA

Figure 3-8 Time series for site BRDX

Red dots are the daily position estimates (16 – 24 hr occupations). The blue lines are the predicted plate rates in IGS08 held fixed (horizontal). The green lines are the least squares best-fit site rates in IGS08 with respect to the Caribbean plate rate (CA). WN = white noise and FN = flicker noise estimates.

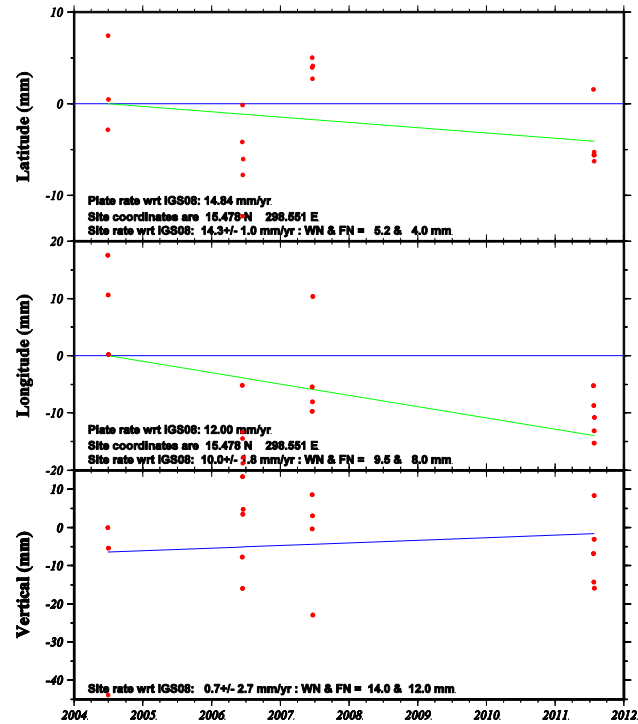
CNCD Coordinate changes - CA is fixed stacovs used AMB



SM 2013 Jun 11 13:03:34 MetUWATA

Figure 3-9 Time series for site CNCD

COHT Coordinate changes - CA is fixed stacovs used AMB

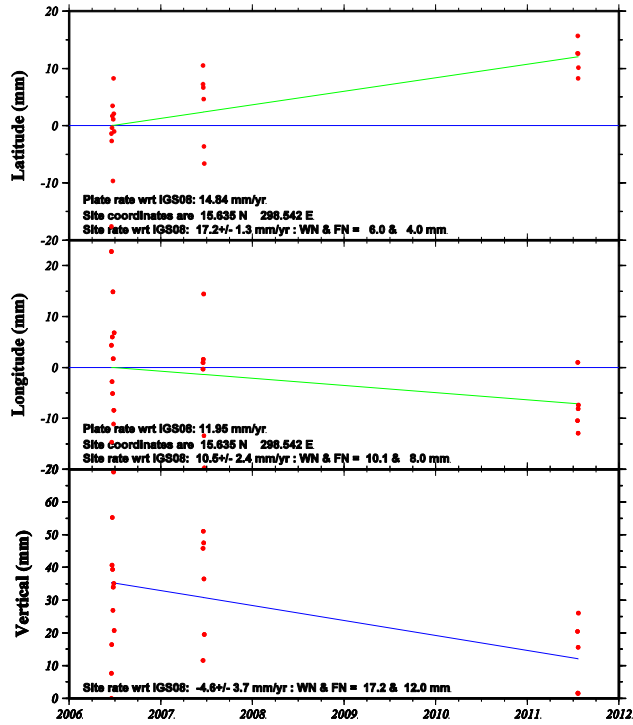


SM 2013 Jun 11 13:06:28 MetUWATA

Figure 3-10 Time series for site COHT

Red dots are the daily position estimates (16 – 24 hr occupations). The blue lines are the predicted plate rates in IGS08 held fixed (horizontal). The green lines are the least squares best-fit site rates in IGS08 with respect to the Caribbean plate rate (CA). WN = white noise and FN = flicker noise estimates.

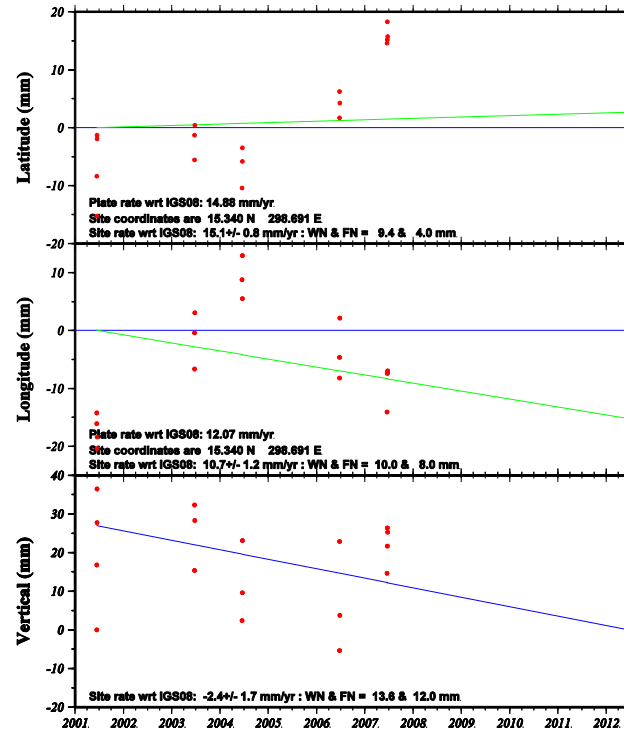
CONN Coordinate changes - CA is fixed stacovs used AMB



2013 Jun 11 13:12:00 MetNet/UTA

Figure 3-11 Time series for site CONN

FRSH Coordinate changes - CA is fixed stacovs used AMB



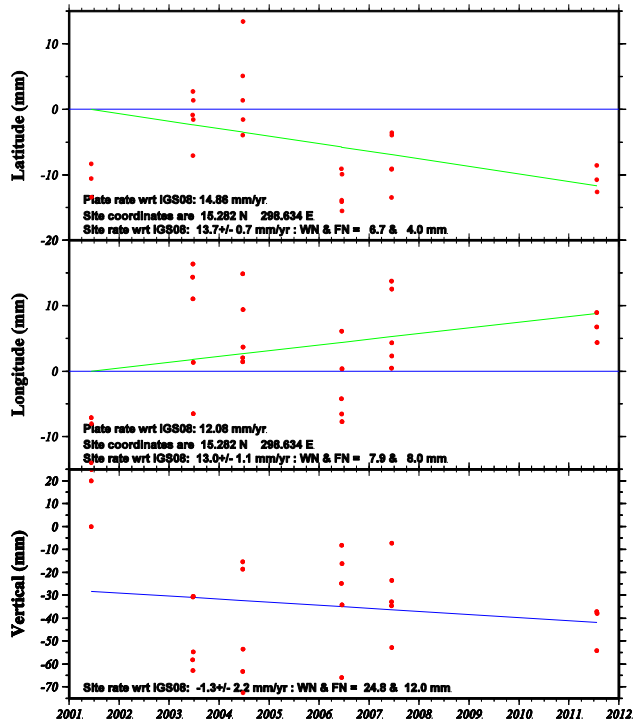
2013 Jun 11 14:38:57 MetNet/UTA

Figure 3-12 Time series for site FRSH

Red dots are the daily position estimates (16 – 24 hr occupations). The blue lines are the predicted plate rates in IGS08 held fixed (horizontal). The green lines are the least squares best-fit site rates in IGS08 with respect to the Caribbean plate rate (CA). WN = white noise and FN = flicker noise estimates.



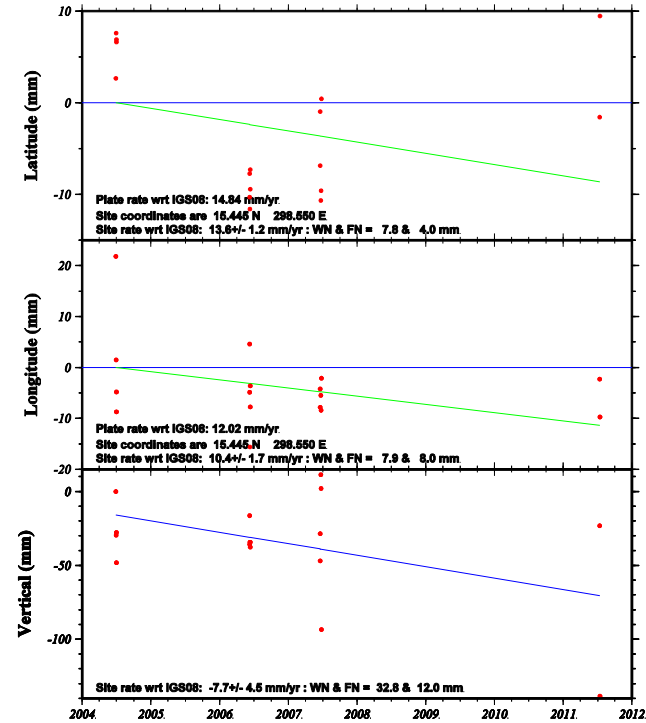
GOMM Coordinate changes - CA is fixed stacovs used AMB



2013 Jun 11 14:43:28 MetNet/WUTA

Figure 3-13 Time series for site GOMM

GSAV Coordinate changes - CA is fixed stacovs used AMB

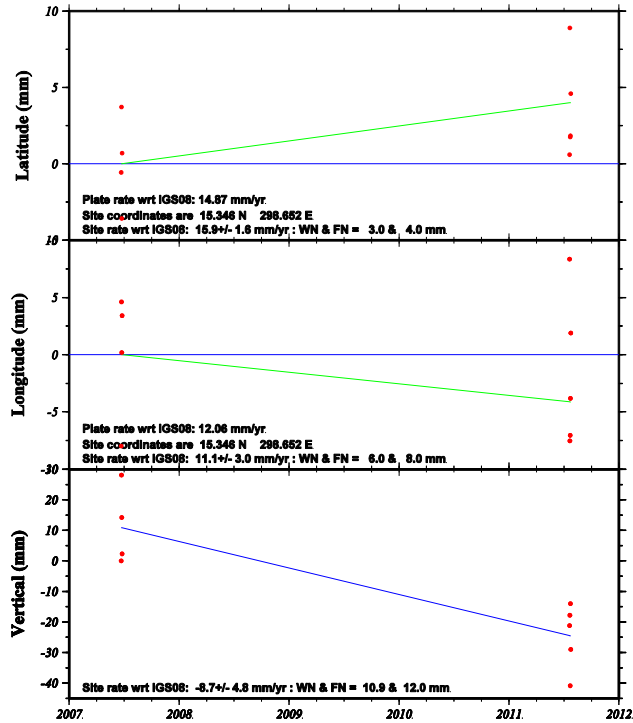


2013 Jun 11 14:48:31 MetNet/WUTA

Figure 3-14 Time series for site GSAV

Red dots are the daily position estimates (16 – 24 hr occupations). The blue lines are the predicted plate rates in IGS08 held fixed (horizontal). The green lines are the least squares best-fit site rates in IGS08 with respect to the Caribbean plate rate (CA). WN = white noise and FN = flicker noise estimates.

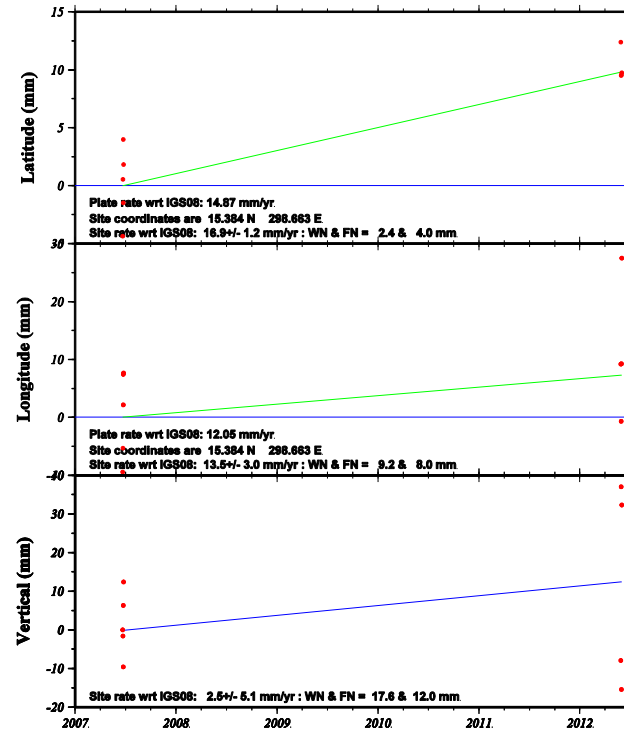
MHAM Coordinate changes - CA is fixed stacovs used AMB



2013 Jun 11 15:10:03 MetUWATA

Figure 3-15 Time series for site MHAM

MTNV Coordinate changes - CA is fixed stacovs used AMB

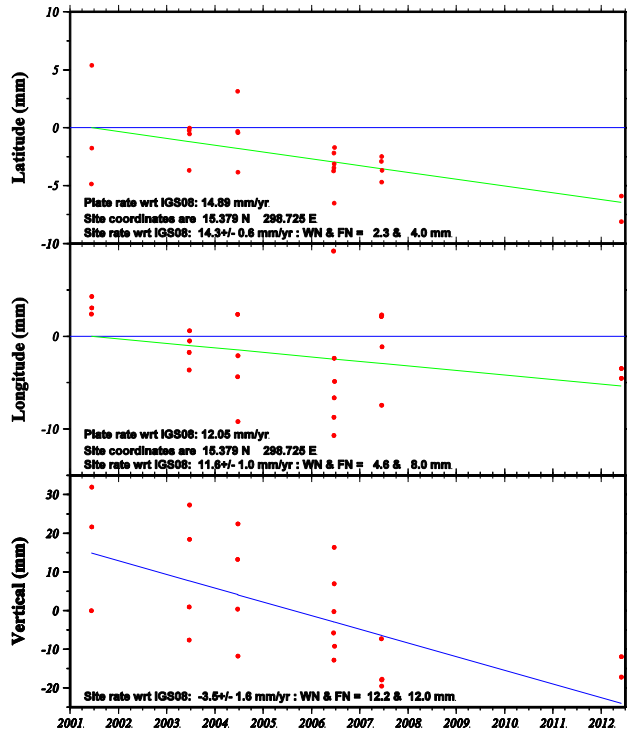


2013 Jun 11 15:02:52 MetUWATA

Figure 3-16 Time series for site MTNV

Red dots are the daily position estimates (16 – 24 hr occupations). The blue lines are the predicted plate rates in IGS08 held fixed (horizontal). The green lines are the least squares best-fit site rates in IGS08 with respect to the Caribbean plate rate (CA). WN = white noise and FN = flicker noise estimates.

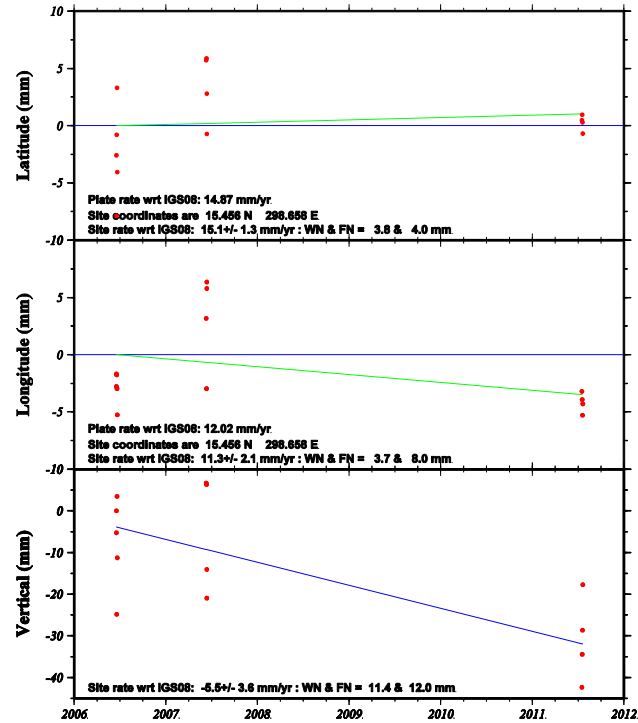
NEWF Coordinate changes - CA is fixed stacovs used AMB



SM 2013 Jun 11 15:06:21 MetUWTA

Figure 3-17 Time series for site NEWF

NVEN Coordinate changes - CA is fixed stacovs used AMB

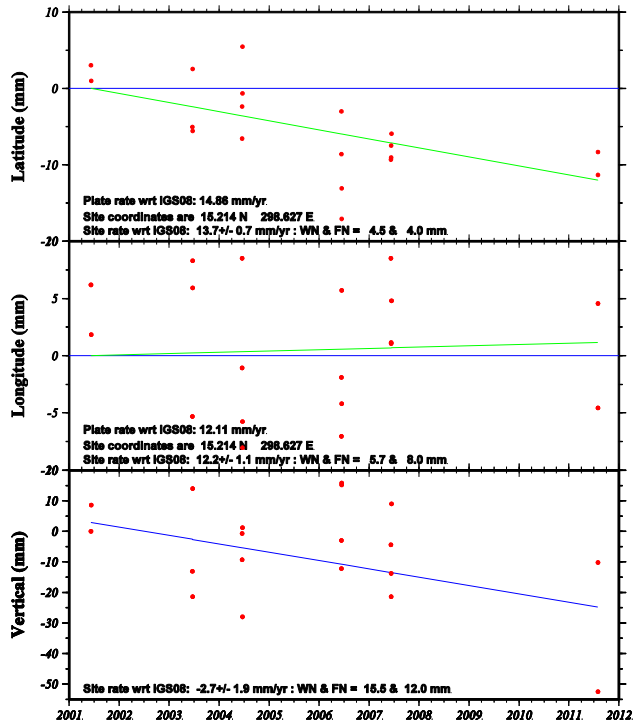


SM 2013 Jun 11 15:22:02 MetUWTA

Figure 3-18 Time series for site NVEN

Red dots are the daily position estimates (16 – 24 hr occupations). The blue lines are the predicted plate rates in IGS08 held fixed (horizontal). The green lines are the least squares best-fit site rates in IGS08 with respect to the Caribbean plate rate (CA). WN = white noise and FN = flicker noise estimates.

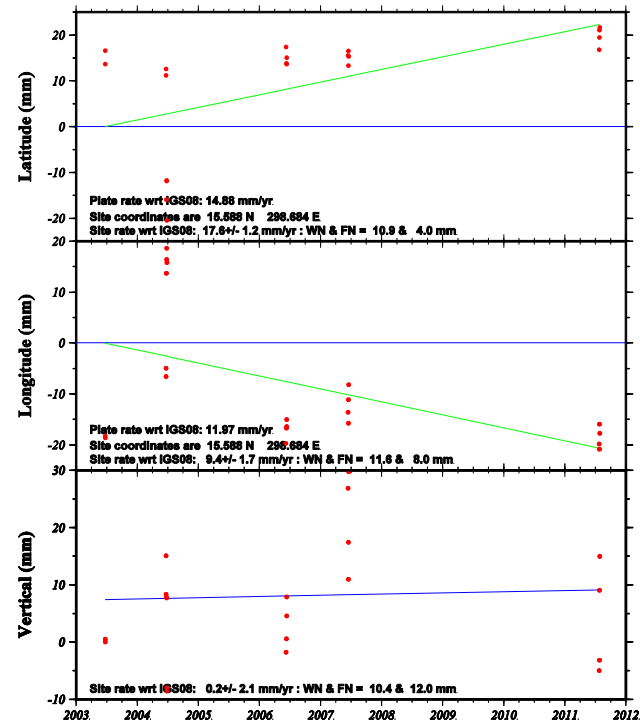
SCTT Coordinate changes - CA is fixed stacovs used AMB



2013 Jun 11 16:53:11 MetUW/UTA

Figure 3-19 Time series for site SCTT

SOIE Coordinate changes - CA is fixed stacovs used AMB

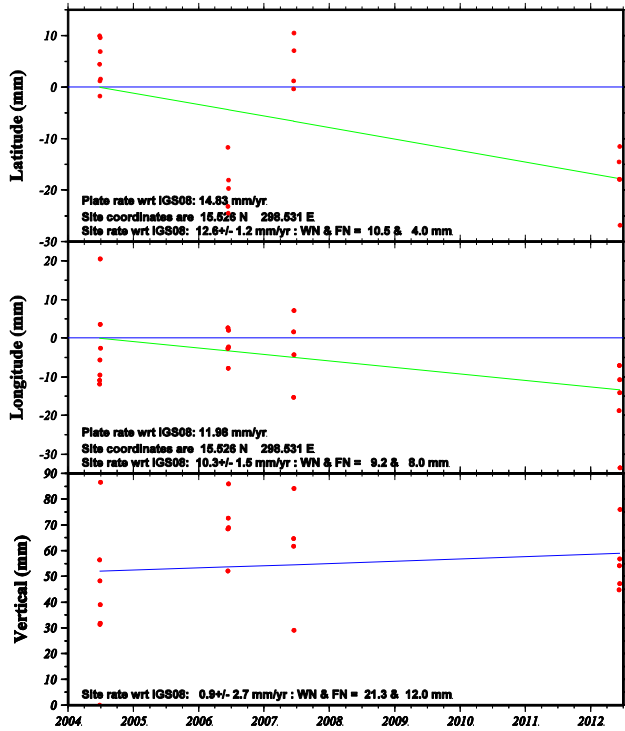


2013 Jun 11 16:59:39 MetUW/UTA

Figure 3-20 Time series for site SOIE

Red dots are the daily position estimates (16 – 24 hr occupations). The blue lines are the predicted plate rates in IGS08 held fixed (horizontal). The green lines are the least squares best-fit site rates in IGS08 with respect to the Caribbean plate rate (CA). WN = white noise and FN = flicker noise estimates.

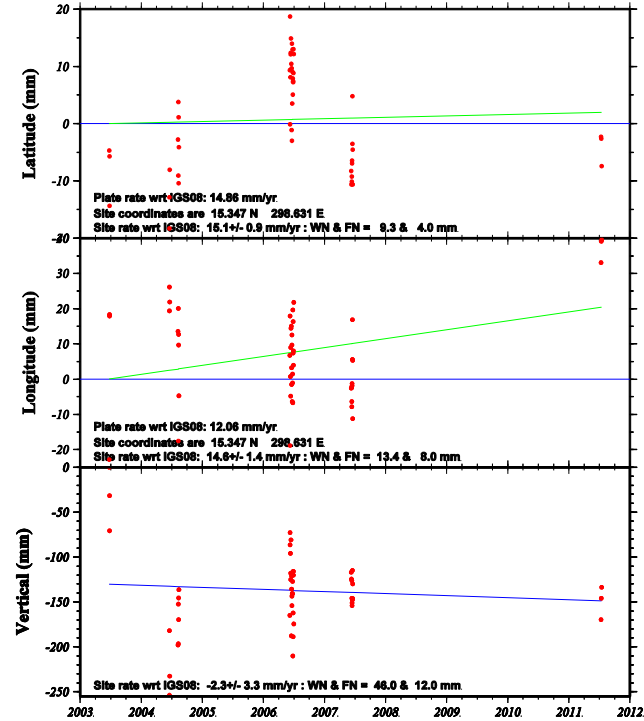
SPAG Coordinate changes - CA is fixed stacovs used AMB



2013 Jun 11 16:33:20 MetUWATA

Figure 3-21 Time series for site SPAG

SPNG Coordinate changes - CA is fixed stacovs used AMB

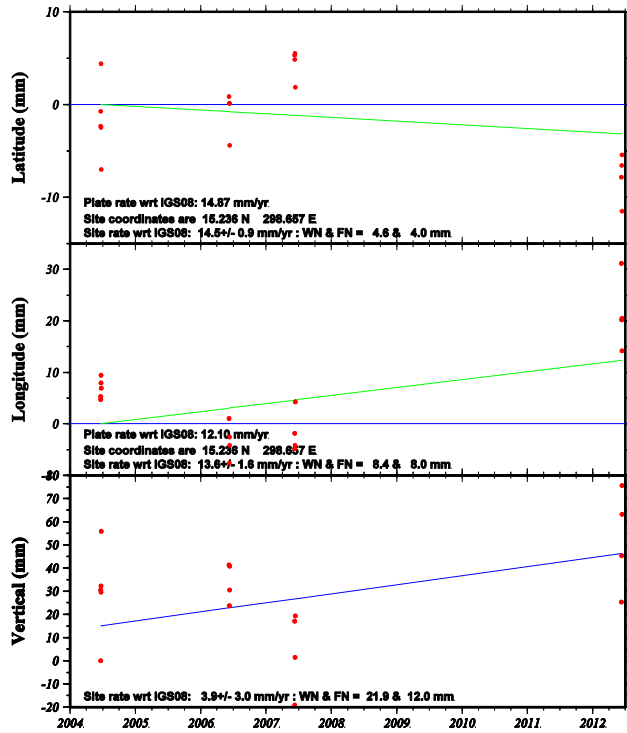


2013 Jun 11 17:20:22 MetUWATA

Figure 3-22 Time series for site SPNG

Red dots are the daily position estimates (16 – 24 hr occupations). The blue lines are the predicted plate rates in IGS08 held fixed (horizontal). The green lines are the least squares best-fit site rates in IGS08 with respect to the Caribbean plate rate (CA). WN = white noise and FN = flicker noise estimates.

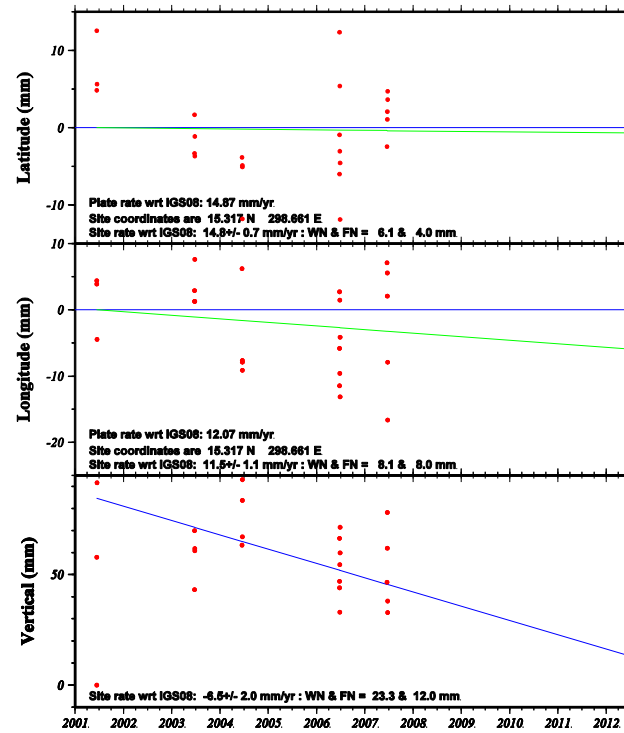
TETE Coordinate changes - CA is fixed stacovs used AMB



2013 Jun 11 16:32:29 MetrolIUTA

Figure 3-23 Time series for site TETE

WOTT Coordinate changes - CA is fixed stacovs used AMB



2013 Jun 11 16:36:05 MetrolIUTA

Figure 3-24 Time series for site WOTT

Red dots are the daily position estimates (16 – 24 hr occupations). The blue lines are the predicted plate rates in IGS08 held fixed (horizontal). The green lines are the least squares best-fit site rates in IGS08 with respect to the Caribbean plate rate (CA). WN = white noise and FN = flicker noise estimates.

Table 3-1 Dominica site velocity summary

Sites are sorted by time span of data available. Location is given in degrees of latitude (Lat), longitude (Long) and height above ellipsoid (HAE) in meters. North (Vn), East (Ve), and vertical (Vv) velocities are presented in a fixed-Earth reference frame as well as a fixed-Caribbean reference frame (revised from DeMets et al., 2007, personal communication to Glen S. Mattioli). WN= white noise, FN=flicker noise and rwn=random walk. Note that all flicker noise values are the default since the number of observations falls below the threshold.

Site ID	Lat (N)	Long (E)	HAE (m)	IGS2008 (mm/yr) - No Common Mode Correction												CAR rate		CAR Fixed Velocity (mm/yr)								Span	Obs
				Vn	Err	WN	FN	Ve	Err	WN	FN	Vv	Err	WN	FN	rwn	Vn	Ve	Vn	Err	Ve	Err	Vv	Err	Epoch		
FRSH	15.340	298.691	724.100	15.1	0.8	9.4	4.0	10.7	1.2	10.0	8.0	-2.4	1.7	13.6	12.0	1.0	14.88	12.07	0.22	0.80	-1.37	1.20	-2.40	1.70	2001.4452-2012.4358	10.9906	21
BELV	15.294	298.751	161.098	17.1	0.6	5.2	4.0	13.6	1.0	4.9	8.0	2.8	2.1	24.7	12.0	1.0	14.90	12.09	2.20	0.60	1.51	1.00	2.80	2.10	2001.4397-2012.4303	10.9906	25
WOTT	15.317	298.661	229.847	14.8	0.7	6.1	4.0	11.5	1.1	8.1	8.0	-6.5	2.0	23.3	12.0	1.0	14.87	12.07	-0.07	0.70	-0.57	1.10	-6.50	2.00	2001.4452-2012.4331	10.9879	25
CASS	15.241	298.709	-33.596	14.0	0.6	4.4	4.0	11.8	1.1	7.8	8.0	0.2	1.8	14.9	12.0	1.0	14.89	12.10	-0.89	0.60	-0.30	1.10	0.20	1.80	2001.4288-2012.4167	10.9879	20
NEWF	15.379	298.725	143.599	14.3	0.6	2.3	4.0	11.6	1.0	4.6	8.0	-3.5	1.6	12.2	12.0	1.0	14.89	12.05	-0.59	0.60	-0.45	1.00	-3.50	1.60	2001.4425-2012.4194	10.9769	23
SCTT	15.214	298.627	21.765	13.7	0.7	4.5	4.0	12.2	1.1	5.7	8.0	-2.7	1.9	15.5	12.0	1.0	14.86	12.11	-1.16	0.70	0.09	1.10	-2.70	1.90	2001.4342-2011.5795	10.1452	19
CABR	15.586	298.530	97.718	11.1	0.9	10.2	4.0	12.1	1.3	13.1	8.0	5.1	3.1	40.4	12.0	1.0	14.83	11.96	-3.73	0.90	0.14	1.30	5.10	3.10	2001.4342-2011.5767	10.1425	26
GOMM	15.282	298.634	209.167	13.7	0.7	6.7	4.0	13.0	1.1	7.9	8.0	-1.3	2.2	24.8	12.0	1.0	14.86	12.08	-1.16	0.70	0.92	1.10	-1.30	2.20	2001.4397-2011.5575	10.1178	26
CNCD	15.512	298.722	-24.548	14.2	0.7	6.2	4.0	11.8	1.1	6.0	8.0	5.6	2.5	29.9	12.0	1.0	14.89	12.00	-0.69	0.70	-0.20	1.10	5.60	2.50	2001.4534-2011.5411	10.0877	25
SOIE	15.588	298.684	-34.642	17.6	1.2	10.9	4.0	9.4	1.7	11.6	8.0	0.2	2.1	10.4	12.0	1.0	14.88	11.97	2.72	1.20	-2.57	1.70	0.20	2.10	2003.4726-2011.5685	8.0959	20
SPNG	15.347	298.631	306.878	14.7	0.9	9.7	4.0	16.1	1.9	23.2	8.0	-6.4	3.5	48.5	12.0	1.0	14.86	12.06	-0.16	0.90	4.04	1.90	-6.40	3.50	2003.4753-2011.5329	8.0575	47
TETE	15.236	298.657	414.407	14.5	0.9	4.6	4.0	13.6	1.6	8.4	8.0	3.9	3.0	21.9	12.0	1.0	14.87	12.10	-0.37	0.90	1.50	1.60	3.90	3.00	2004.4658-2012.4495	7.9836	17
SPAG	15.526	298.531	324.523	12.6	1.2	10.5	4.0	10.3	1.5	9.2	8.0	0.9	2.7	21.3	12.0	1.0	14.83	11.98	-2.23	1.20	-1.68	1.50	0.90	2.70	2004.4795-2012.4467	7.9672	21
BRDX	15.234	298.681	244.109	13.7	0.9	5.0	4.0	9.9	1.8	11.3	8.0	9.9	4.9	39.9	12.0	1.0	14.88	12.10	-1.18	0.90	-2.20	1.80	9.90	4.90	2004.4768-2012.4249	7.9481	15
COHT	15.478	298.551	239.061	14.3	1.0	5.2	4.0	10.0	1.8	9.5	8.0	0.7	2.7	14.0	12.0	1.0	14.84	12.00	-0.54	1.00	-2.00	1.80	0.70	2.70	2004.4904-2011.5685	7.0781	17
ATRU	15.616	298.597	-35.766	17.6	1.4	8.3	4.0	10.4	1.6	4.4	8.0	4.2	3.2	18.3	12.0	1.0	14.85	11.96	2.75	1.40	-1.56	1.60	4.20	3.20	2004.4822-2011.5411	7.0589	14
GSAV	15.445	298.550	8.936	13.6	1.2	7.8	4.0	10.4	1.7	7.9	8.0	-7.7	4.5	32.8	12.0	1.0	14.84	12.02	-1.24	1.20	-1.62	1.70	-7.70	4.50	2004.4904-2011.5329	7.0424	16
CONN	15.635	298.542	57.543	17.2	1.3	6.0	4.0	10.5	2.4	10.1	8.0	-4.6	3.7	17.2	12.0	1.0	14.84	11.95	2.36	1.30	-1.45	2.40	-4.60	3.70	2006.4589-2011.5575	5.0986	22
NVEN	15.456	298.658	293.570	15.1	1.3	3.8	4.0	11.3	2.1	3.7	8.0	-5.5	3.6	11.4	12.0	1.0	14.87	12.02	0.23	1.30	-0.72	2.10	-5.50	3.60	2006.4589-2011.5493	5.0904	13
BOTG	15.299	298.618	-21.352	15.1	1.7	7.9	4.0	14.9	2.8	12.1	8.0	-0.9	9.1	52.1	12.0	1.0	14.86	12.08	0.24	1.70	2.82	2.80	-0.90	9.10	2006.4726-2011.5384	5.0658	17
MTNV	15.384	298.663	526.173	16.9	1.2	2.4	4.0	13.5	3.0	9.2	8.0	2.5	5.1	17.6	12.0	1.0	14.87	12.05	2.03	1.20	1.45	3.00	2.50	5.10	2007.4699-2012.4139	4.9441	9
MHAM	15.346	298.652	616.336	15.9	1.6	3.0	4.0	11.1	3.0	6.0	8.0	-8.7	4.8	10.9	12.0	1.0	14.87	12.06	1.03	1.60	-0.96	3.00	-8.70	4.80	2007.4726-2011.5603	4.0877	9

### 3.4 Data Analysis and Discussion

In order to evaluate the current data and compare it to data collected by previous researchers, all position estimates must be in the same reference frame. Figure 3-25 shows the site velocities published by James (2008), generated using data from 2001 through 2007, processed as absolute point positions with GIPSY-OASIS II (GOAll) v. 5, in the IGS2005 reference frame using final precise Earth orientation parameters, clocks and orbits from JPL. These initial results suggested that there may be observable surface deformation on Dominica. For example, in the northern part of Dominica, sites CONN, ATRU, SOIE, and CABR appear as if they may be pointed away from a crustal magmatic source, which may be an indicate the inflation of that source. The errors for these velocities, as indicated by the red ovals in the figure are too large, however, to make any robust conclusion. In fact, in most cases, the errors are as large, or larger, than the values themselves. The IGS2005 data products were deprecated by JPL in August 2011. A major reprocessing effort was undertaken by the JPL orbit analysis group (Desai et al., 2012) to generate new orbits, clocks and ephemerides using updated Earth models including solid Earth tides and loading, tropospheric models, and absolute phase center corrections for both the GPS SV emitters and ground based tracking stations.

Accordingly, since I collected data post 2011 and wanted to take advantage of the new JPL data products in IGS08, I reprocessed all the data from Dominica as well as across the Caribbean using the same methods, models and GOAll version as used by JPL. The data presented here is in the IGS08 reference frame. Figure 3-26 presents James' data reprocessed using GOAll (v. 6.2) in the IGS08 reference frame. The reprocessing with the updated software and new reference frame are broadly similar. The minimal effect of the upgraded software may partially be due to the fact that the



Dominican GPS sites do not use radomes. A radome will effect the GPS signal, which must be corrected properly, and it has been shown that with the new processing software, the misreporting of the type of radome in the metadata produces erroneous results. A notable difference in azimuth is seen at sites SPAG and BOTG, but the variations fall within error. Figure 3-27 is the James (2008) data plus data collected during the 2011 and 2012 field seasons. These are processed with GOAll version 6.2 in the IGS08 reference frame. It is clear to see that the additional data has drastically reduced the velocity errors for all the sites. Nine of the sites have a decade's worth of data, which now allows confident conclusions about the surface velocity field to be made.

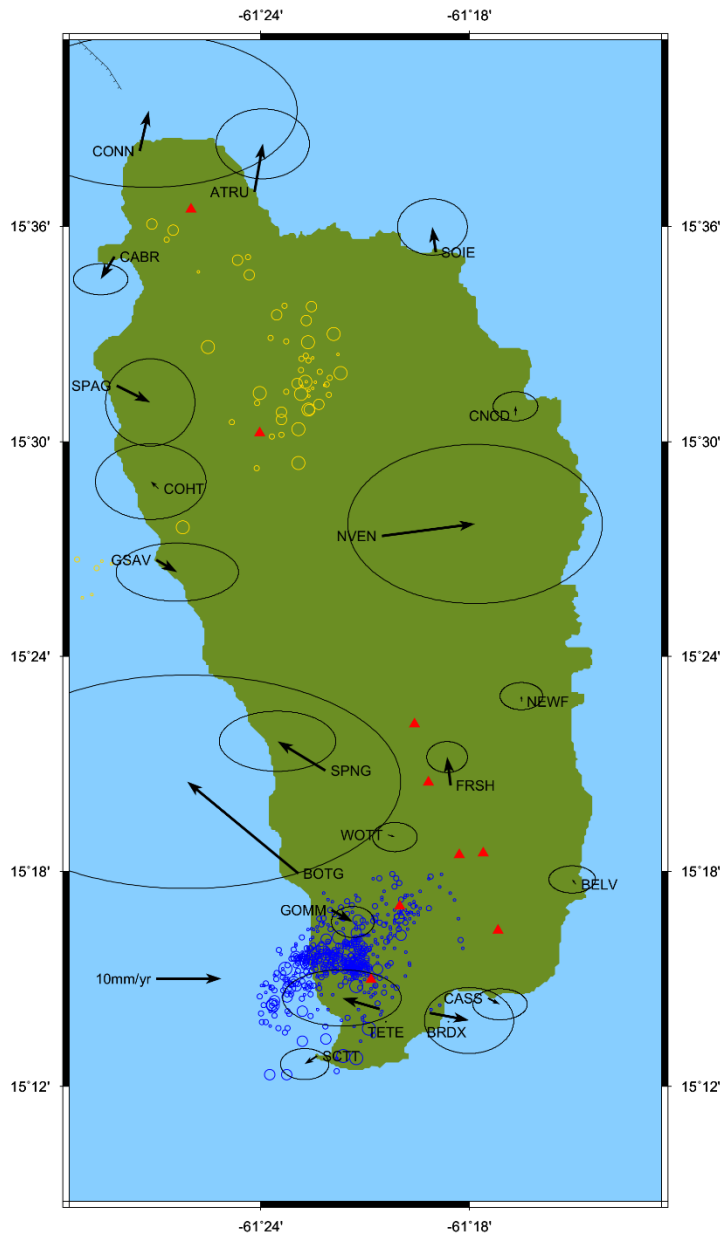


Figure 3-25 Dominica horizontal velocities reported by James (2008) Values are 2001-2007 data processed with GIPSY-OASIS II (v. 5) in the IGS05 reference frame. Red triangles are volcanic centers, blue circles are epicenters of 2001 seismic swarm, yellow circles are epicenters of 2004 seismic swarm (data courtesy of the Seismic Research Center at the University of the West Indies). Error ellipses are  $1 \sigma$ .

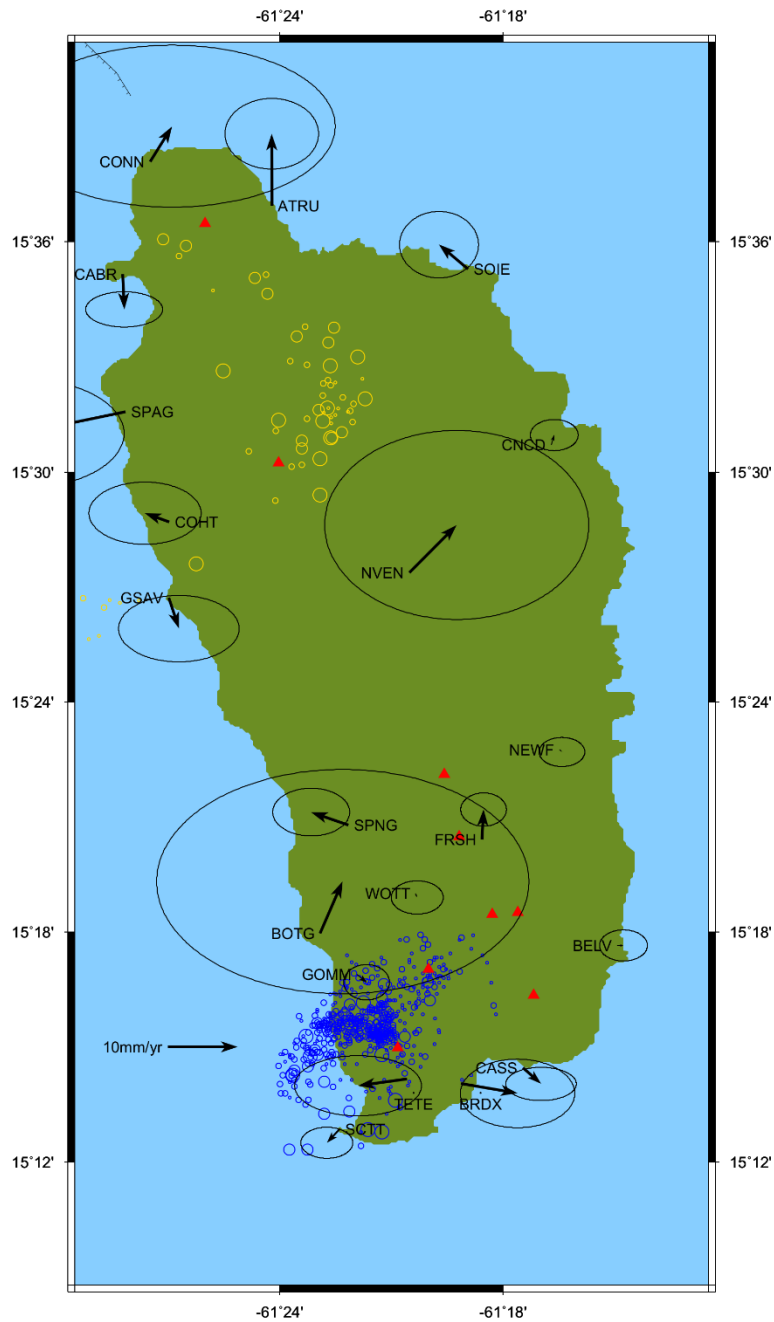


Figure 3-26 Dominica horizontal velocities (2001-2007). Values are 2001-2007 data reprocessed with GIPSY-OASIS II (v 6.2) in the IGS08 reference frame. Red triangles are volcanic centers, blue circles are epicenters of 2001 seismic swarm, yellow circles are epicenters of 2004 seismic swarm (data courtesy of the Seismic Research Center at the University of the West Indies). Error ellipses are  $1 \sigma$ .

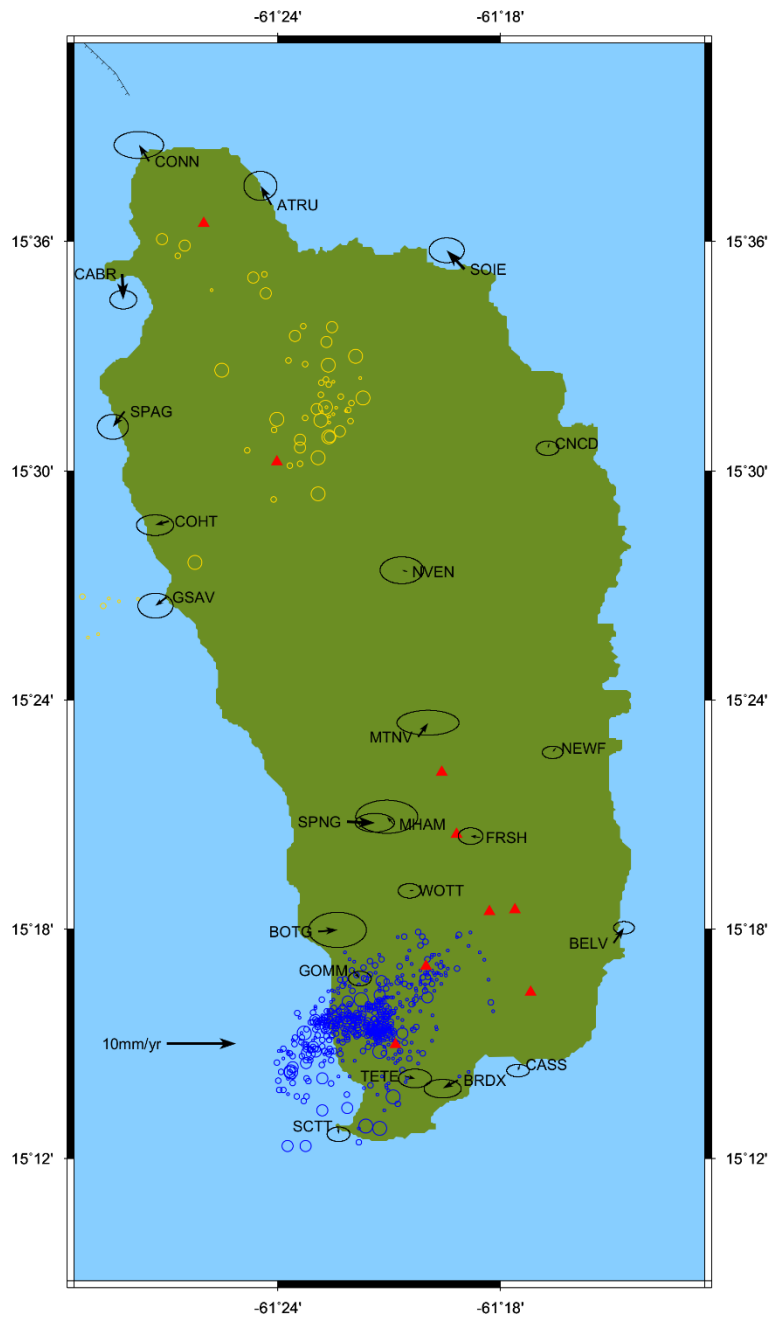


Figure 3-27 Dominica residual horizontal site velocities (2001-2012). Values are 2001-2012 data, processed using GIPSY-OASIS II (v. 6.2) in the IGS08 reference frame. Red triangles are volcanic centers, blue circles are epicenters of 2001 seismic swarm, yellow circles are epicenters of 2004 seismic swarm (data courtesy of the Seismic Research Center at the University of the West Indies). Error ellipses are  $1 \sigma$ .

Although most of the Dominica site velocities do not exhibit significant residual velocity, some minor motion can be identified. In Figure 3-28 A, the northern sites of SOIE, ATRU, and CONN seem to have a sinistral motion with respect to sites CABR, SPAG, COHT and GSAV along the trace delineated by the 2004 seismic swarm, which is designated by yellow circles. This motion is consistent with data presented by Smith et al., 2013 and the models of van Benthem, 2013. In Figure 3-28, image C shows focal mechanisms for earthquakes in the central Lesser Antilles. Note the shallow earthquake focal mechanisms in the area of Dominica, Figure 3-28 C (colored yellow in a red oval), the majority of which indicate sinistral strike slip motion (Smith et al., 2013). Although the convergence at Dominica is considered nearly normal, there is a slight obliquity to both the CA-NA and CA-SA relative motion vectors defined by MORVEL (DeMets et al., 2010) and presented by Smith et al. (2013) (Figure 3-28 B). For a rate of 20 mm/yr, a simple calculation of the obliquity of convergence yields an arc-parallel rate of ~3.5 mm/yr to the northwest. Northwest motion on the forearc side would generate sinistral motion along faults in the area of the 2004 seismic swarm. Van Benthem (2013) presents a map of principle stress directions for the Caribbean. Note the location of Dominica (Figure 3-28 B), with the principle stress arrows in the vicinity, indicating a tensional environment. The conditions here are consistent with those necessary for the emplacement of a NW-trending dike, as is seen on Monserrat to the north (Wadge et al. 1984; Mattioli et al.; 1998; Linde et al., 2010).

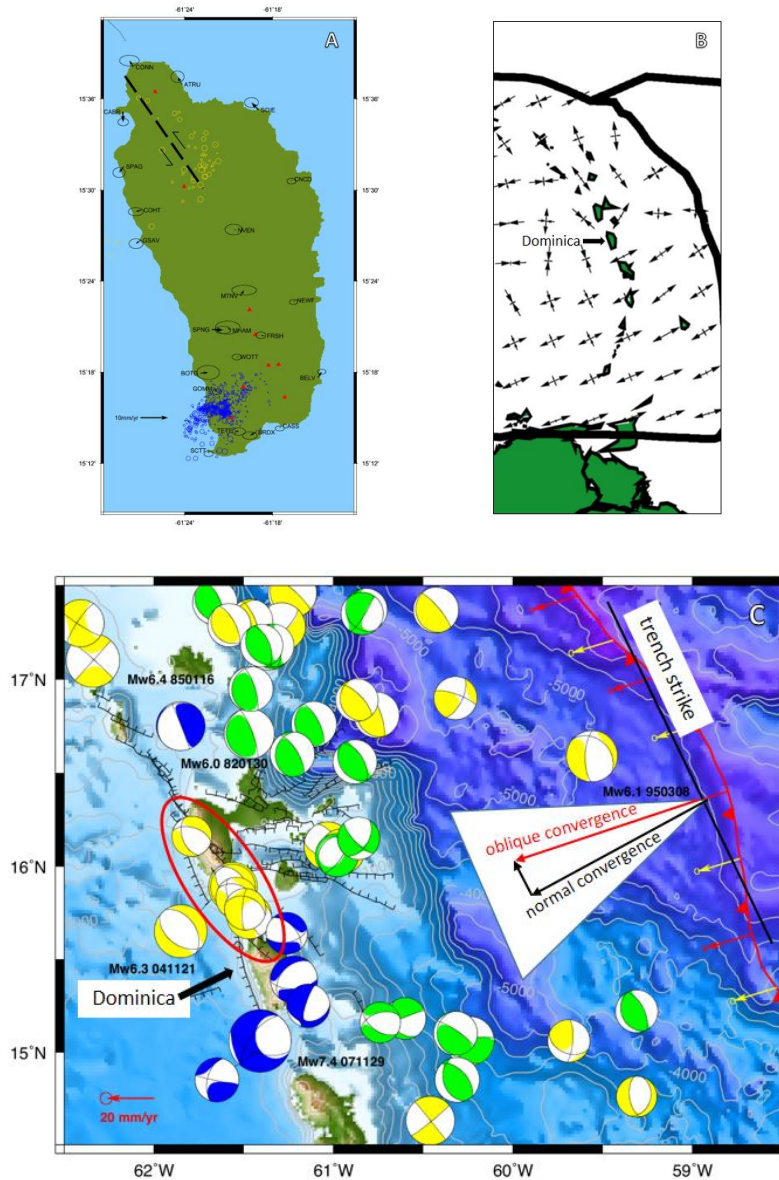


Figure 3-28 Dominica surface deformation  
 (A) Dominica velocity map as described in Figure 3-27 with possible sinistral strike-slip motion marked by dashed black line. (B) Principal stress directions (van Benthem, 2013). (C) Focal mechanisms are from the Global CMT project (Ekstrom et al., 2012, <http://www.globalcmt.org>). Mapped faults are from various sources including Feuillet et al., 2002 and Roobol and Smith, 2004. Moment tensor solutions are color coded as follows: yellow (shallow, 10-30 km), green (intermediate, 30-70 km), and blue (deep, >70 km). Yellow vectors indicate South America-Caribbean motion and red vectors indicate North America-Caribbean motion (DeMets et al., 2010). Figure modified based on Smith et al. (2013).

If you ignore the direction of the residual velocity, in general, the horizontal velocities (Figure 3-27) in the northern part of Dominica are greater than in the south, while the vertical component velocities show the opposite, such that, velocities in the south are greater than in the north (Figure 3-29). The central, eastern portion of the island, consisting of sites CNCD, NVEN, NEWF, MHAM, FRSH and WOTT appear to be very stable, with almost zero motion with respect to the Caribbean plate. The lack of movement at WOTT is surprising however, since it is close to currently active geothermal features and the location of geothermal test wells. SPNG and BOTG show small easterly directed motion, but there does not seem to be any distinguishable pattern among the horizontal velocities of the southern sites with respect to the 2001 seismic swarm (designated by blue circles). The vertical velocity field, however, may show a pattern such that the sites north (SPNG, WOTT, MHAM, FRSH, BOTG, and NEWF) of the 2001 seismic swarm show subsidence, while the sites (BELV, BRDX, and TETE) south of the swarm show uplift (Figure 3-29). The subsidence demonstrated by sites WOTT and MHAM may be attributed to the fact that they are located within, or on the borders of, caldera structures identified in Figure 3-2. The elongate pattern seen in the distribution of motion associated with the seismic swarms could also be consistent with the emplacement of dikes.

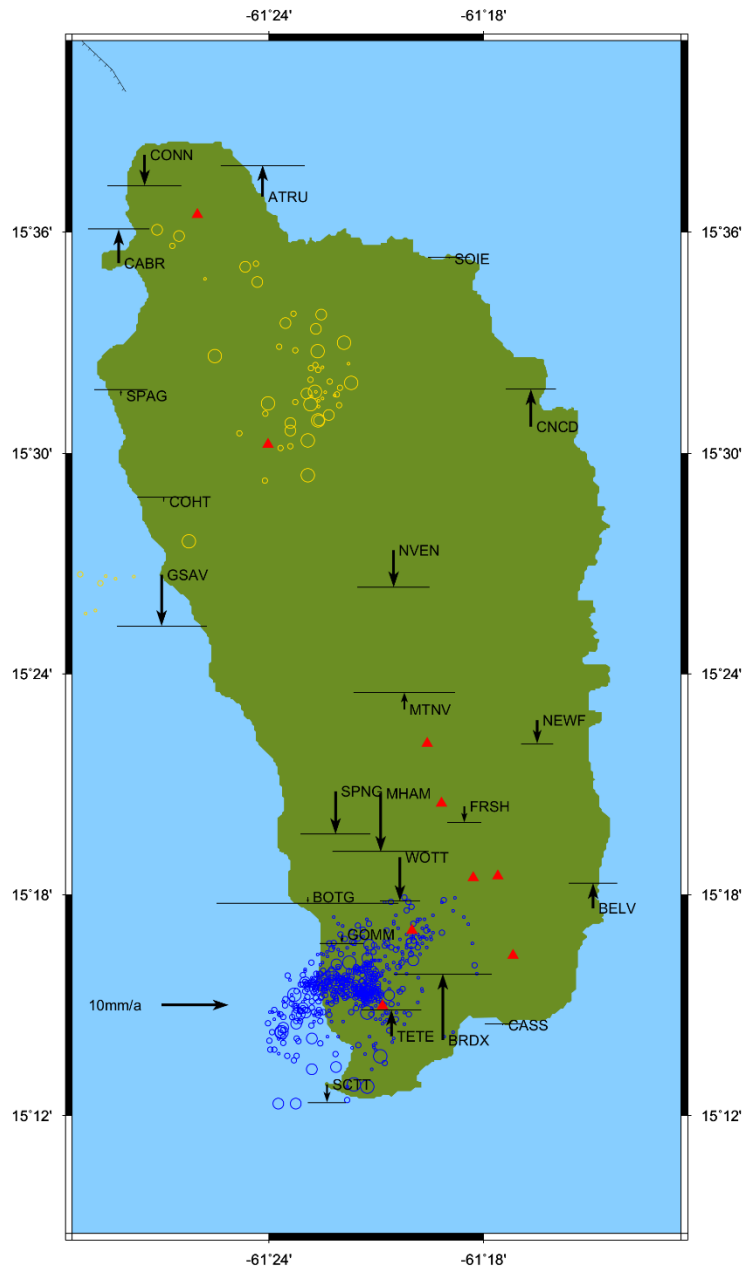


Figure 3-29 Dominica vertical site velocities (2001-2012)  
 Values are 2001-2012 data, processed using GIPSY-OASIS II (v. 6.2) in the IGS08 reference frame. Black arrows indicate up or down vertical motion, thin black line at the end of each arrow is the  $1 \sigma$  error associated with that vector. Red triangles are volcanic centers, blue circles are hypocenters of 2001 seismic swarm, while yellow circles are hypocenters of 2004 seismic swarm.



### 3.5 Conclusion

GPS data collection on the Island of Dominica has proven to be challenging in a variety of ways. The climate is conducive to high weathering rates, the infrastructure is generally substandard, and the topography and vegetation make observations nearly impossible in many areas. Yet, despite the challenges, over a span of a decade, teams have been successful collecting high precision GPS data. Evaluation of the data by James (2008) after the 2007 field season suggested that a recognizable surface deformation signature, associated with recent shallow seismicity, was going to emerge. Figure 3-26 and Figure 3-27 are horizontal velocity maps of the Dominica campaign GPS data. Figure 3-26 is the data used by James, 2008, reprocessed in IGS08, and Figure 3-27 is the same data plus additional epochs of data collected in 2011 and 2012. It is clear that the addition of the 2011 and 2012 data has served to reduce the error on the horizontal velocities significantly. It is also evident that there is no significant and easily discernable signature related to volcanic processes present in the velocities. The velocity field for Dominica indicates that the points measured are generally tracking the motion of the Caribbean plate. If, in fact, there is subtle subsurface igneous activity, it has been demonstrated that intermittent (bi-annual) campaign GPS is not an effective monitoring tool to observe subtle surface deformation changes in a tropical environment. The last eruptions on Dominica occurred approximately 450 years ago, and since then, the island has only experienced shallow seismic swarms, geothermal activity and phreatic activity (Smith et al., 2013). The low deformation rate observed here suggests that a majority of the batholith is partially solidified, and that any volcanic activity is a result of basaltic injection at the base of the batholith (Smith et al., 2013). Perhaps Dominica is entering a new phase in its volcanic history, one that will be dominated by the behavior of its mid-level island-arc batholith. The fact that there seems to be no significant residual surface

deformation in Dominica relative to the Caribbean plate, suggests that inclusion of the velocities from Dominica may help define the motion of the eastern part of the Caribbean plate.

## Chapter 4

### The Caribbean Plate

#### 4.1 Introduction

One of the issues distinctive to the Caribbean plate, which renders the determination of its motion problematical, is the lack of any subaerial landmass in its interior. In an attempt to study and mitigate the natural hazards that occur in the Caribbean, the Continuously Operating Caribbean GPS Observational Network (COCONet) was initiated in 2011 (Braun et al., 2012). The purpose of this NSF-funded international consortium is to develop a large-scale geodetic and atmospheric infrastructure in the Caribbean to serve as the backbone for a wide range of geoscience investigations. The network currently collects data from a combination of 60+, previously established and newly installed stations. COCONet data, in conjunction with campaign GPS data will be analyzed to evaluate the motion and rigidity of the Caribbean plate. Since the campaign GPS data from Dominica has shown that the island is closely tracking the Caribbean plate at a majority of the 27 sites, data from some of those sites will be useful in constraining the motion of the easternmost edge of the plate. All data from the Caribbean sites were processed as described in Chapter 2. Figure 4-1 is a map showing the locations of the sites used for this study; Table 4-1 and Table 4-2 are velocity summaries of those sites.

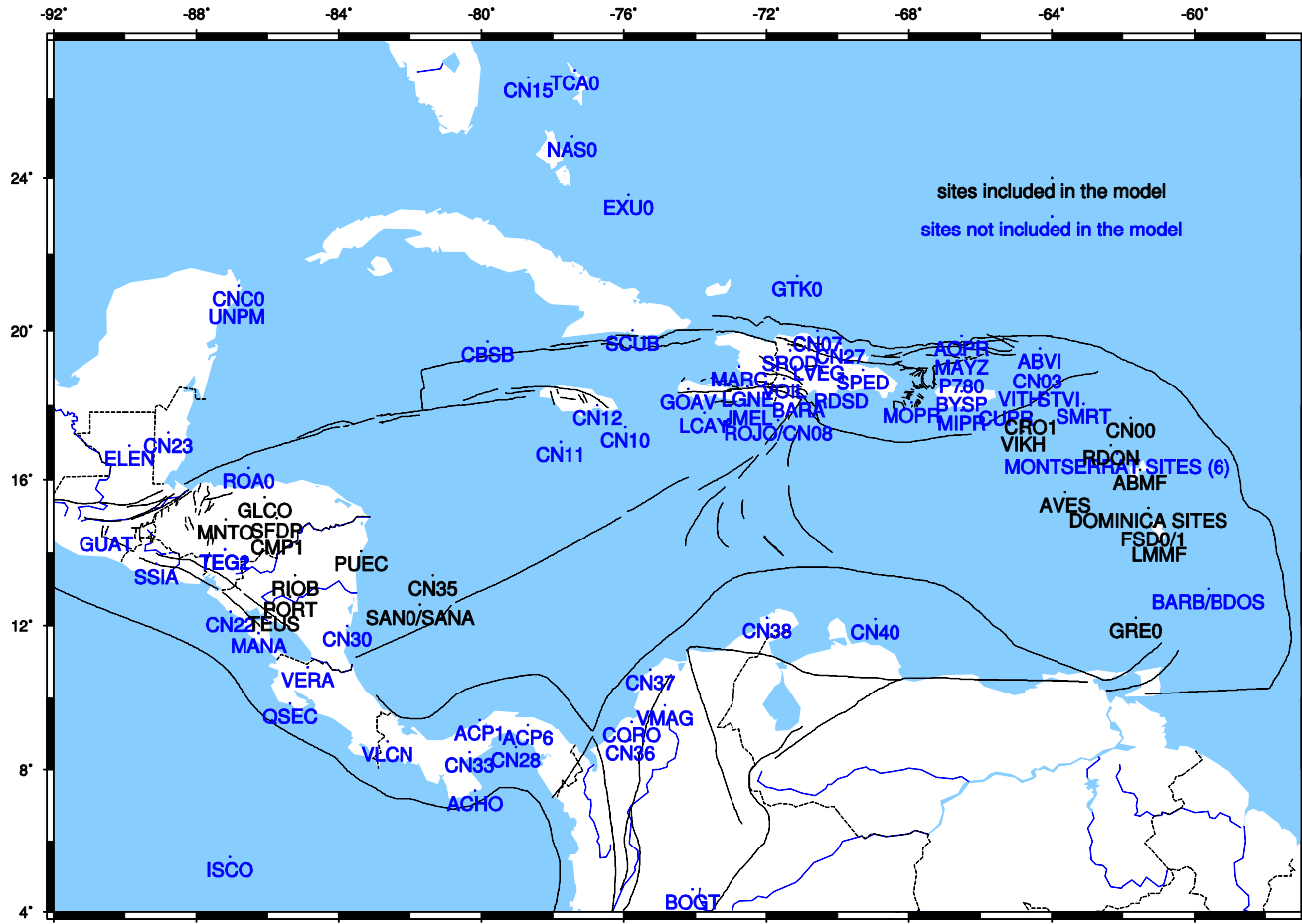


Figure 4-1 Caribbean GPS station site map  
Site locations available from UNAVCO at <http://www.unavco.org>. Black lines delineate putative faults, site names in black were used for inversion.

Table 4-1 Caribbean wind velocity summary, sorted by site ID.

Site name	Site ID	Lat (N)	Long (E)	HAE (m)	IGS2008 (mmyr)/No Common Mode Correction												CAR rate			CAR Fixed Velocity (mmyr)			Span	No. Obs				
					Vn				Vv				Vw				Vn	Vv	Vw	Vn	Vv	Vw						
					Error	WN	FN	FN	Error	WN	FN	FN	Error	WN	FN	FN	Error	WN	FN	FN	Error	WN			FN	FN		
Les Abymes, Guadeloupe	ABMF	16.262	298.472	-27.688	14.4	0.8	2.3	2.2	12.0	0.9	2.4	2.7	2.3	8.2	8.9	10	14.81	11.70	-0.41	0.80	0.30	0.90	2.50	2.30	2010.6671-2013.511	2.8438	977	
Anequá, Virgin Islands	ABVI	18.730	295.668	-37.653	15.2	0.8	2.3	1.4	8.5	1.1	3.4	2.7	0.3	2.3	6.5	6.9	10	13.94	10.54	1.26	0.80	-2.04	1.10	0.30	2.30	2011.0973-2013.3822	2.9849	632
Acochotes, Panama	ACHD	7.415	279.827	33.074	10.7	1.2	2.4	1.6	20.8	1.6	2.4	2.7	-1.0	3.2	6.7	5.9	10	8.46	14.39	2.24	1.20	1.61	1.60	-1.00	3.00	2011.3849-2013.7582	1.3763	490
Sherman, Panama	ACP1	9.231	280.050	10.390	11.3	0.6	2.2	2.4	17.0	0.6	2.1	2.3	-0.7	1.1	7.0	6.3	10	8.54	13.59	2.76	0.60	3.41	0.60	-0.70	1.10	2008.8156-2013.4260	4.6105	1245
Panama	ACPB	9.239	280.592	941.097	12.2	0.9	2.8	2.1	17.1	0.6	2.2	2.6	-0.5	1.1	6.7	6.8	10	8.74	13.60	3.46	0.90	3.50	0.60	-0.50	1.10	2008.7883-2013.4260	4.6378	1269
Montserrat	ARS	16.741	297.766	62.208	13.5	1.0	3.3	12.5	12.3	1.0	6.1	11.9	-4.3	2.8	12.8	12.7	10	14.60	11.17	-1.15	1.00	0.83	1.00	-4.30	2.80	2004.2309-2013.4288	9.1979	2440
Aneco Observatory, PR	ACPR	18.347	293.246	317.458	13.3	1.3	1.6	8.7	12.4	1.4	1.4	0.1	2.3	8.0	3.1	10	13.16	10.51	0.44	1.30	-1.81	1.20	1.10	0.30	2012.1926-2013.4096	1.2170	443	
Aves Island Venezuela	AVES	15.667	296.382	-38.928	14.2	1.3	2.0	1.0	11.3	2.3	2.4	8.0	-1.4	3.9	11.9	12.0	10	14.17	11.79	0.03	1.30	-0.49	2.30	-1.40	3.90	1994.3740-1998.2479	3.8740	28
Barahona, DR CANAPE site	BARA	18.209	288.902	3.909	13.3	0.6	14.9	22.3	33.7	26.9	42.6	92.7	0.9	11.3	56.2	72.9	10	11.71	10.27	-1.49	6.50	23.43	26.90	0.90	21.30	2011.0014-2013.4288	2.4274	624
Barbados	BARB	13.008	300.391	-40.859	17.1	1.9	2.6	3.6	8.1	1.0	2.3	1.4	-4.5	3.8	9.0	7.7	10	15.39	13.00	1.71	1.90	-4.90	1.00	-4.30	3.80	1999.5000-2001.1164	1.8164	333
Barbados	BDOB	13.008	300.391	-40.859	15.2	0.5	2.0	1.0	14.2	0.8	2.1	9.3	-0.8	1.2	7.4	14.1	10	15.39	13.00	-1.49	0.50	1.20	0.80	-1.20	2.00	2004.4440-2013.3832	8.9492	2258
Boggy, Antigua	BGGY	17.045	298.139	353.631	15.4	0.4	2.3	5.2	9.9	0.3	2.3	4.0	-1.5	0.5	7.1	8.9	10	14.71	11.38	0.69	0.40	-1.48	0.30	-1.50	0.50	1998.6123-2012.9986	14.3863	3851
Bojota, Colombia	BOGT	4.640	285.919	2574.510	15.8	0.6	2.1	13.4	0.6	2.4	13.7	-42.9	1.7	8.2	41.3	10.1	10	10.67	15.59	5.13	0.60	-15.19	0.60	-42.90	1.70	1994.8781-2013.4288	18.5507	4096
Bayamon Science Park, PR	BYSF	18.406	293.638	47.156	13.2	0.9	2.6	1.4	9.1	0.9	2.3	1.6	1.5	2.1	7.8	5.3	10	13.36	10.53	-0.16	0.80	-1.43	0.90	1.50	2.10	2011.3832-2013.4096	2.0164	621
Cayman Brac, Cayman Islands	CBSB	19.712	280.167	-9.158	2.9	0.5	2.4	3.3	-8.3	0.7	2.7	6.1	-1.2	1.1	6.8	11.2	10	8.59	9.11	-6.69	0.50	-17.41	0.70	-1.20	1.10	2006.8836-2013.4288	7.5452	2052
UW-Madison site in Honduras	CMP1	14.509	274.285	389.225	5.4	1.7	4.6	4.0	11.7	2.4	4.2	8.0	-8.8	6.2	15.3	12.0	10	6.37	11.22	-0.97	1.70	0.48	2.40	-6.80	5.20	2000.1926-2006.4068	5.2142	62
Barbuda	CN00	17.669	298.214	-24.029	11.6	3.9	2.0	4.0	11.2	7.4	1.6	2.3	0.8	11.1	7.3	10	14.74	11.15	-2.14	3.80	0.05	7.40	18.60	11.10	2012.6207-2013.4096	0.7689	282	
North Sound British Virgin Islands	CN03	18.491	295.598	286.355	25.3	12.5	2.1	4.0	23.8	24.1	2.6	8.0	21.3	37.4	7.2	10.0	10	13.92	10.63	11.38	12.50	13.17	24.10	21.30	37.40	2013.1466-2013.3822	0.2356	86
Puerto Rico, Dominican Republic	CN04	19.758	298.434	-34.216	9.4	1.3	2.6	1.2	-4.3	1.4	2.4	1.4	2.3	3.0	9.1	3.9	10	11.89	9.65	-2.49	1.30	-13.95	1.40	2.30	2012.3122-2013.4096	1.0886	394	
Caro Rigo, Dominican Republic	CN08	17.903	288.326	-19.168	10.1	1.3	2.4	1.1	11.8	1.6	3.0	1.5	7.7	5.0	8.5	6.7	10	11.51	10.36	-1.41	1.30	1.44	1.60	7.70	5.00	2012.3320-2013.3411	1.0091	353
Montst Cay, Jamaica	CN10	17.222	282.216	-12.814	6.5	0.9	2.1	1.2	9.2	1.1	2.1	2.0	-2.2	3.1	6.5	7.3	10	9.34	10.41	-2.84	0.90	-1.21	1.10	-2.20	3.10	2011.7164-2013.2342	1.5178	552
Pedro Cay, Jamaica	CN11	17.202	282.216	-12.814	6.5	0.9	2.1	1.2	9.2	1.1	2.1	2.0	-2.2	3.1	6.5	7.3	10	9.34	10.41	-2.84	0.90	-1.21	1.10	-2.20	3.10	2011.7164-2013.2342	1.0688	620
UW-Madison site in Honduras	CN12	18.005	283.251	167.861	3.5	1.3	3.0	1.6	3.4	1.9	2.8	24.8	-24.8	2.6	10.9	3.7	10	9.72	10.03	-6.22	1.30	-6.63	1.40	-24.80	2.60	2012.1598-2013.4288	1.2689	460
Grand Bahama, Bahamas	CN15	26.557	281.307	-29.072	4.4	1.3	2.7	1.6	-11.3	1.2	2.4	1.2	-5.7	3.9	8.4	9.0	10	9.01	6.05	-4.61	1.30	-17.35	1.20	-5.90	2.10	2011.4753-2013.2128	13.375	414
Ponelnia, Nicaragua	CN22	12.384	272.955	26.478	7.6	1.2	3.0	1.5	1.5	1.5	2.3	2.3	6.6	4.8	11.2	8.8	10	5.86	12.13	-1.74	1.20	-13.63	1.10	-6.70	4.80	2012.4007-2013.4288	3.918	419
Belmopan, Belize	CN23	17.621	271.221	53.228	-6.2	1.5	2.4	1.1	-6.9	1.8	2.5	1.6	1.8	3.6	3.6	5.6	10	5.18	9.89	-11.56	1.50	-15.79	1.80	19.60	3.60	2012.5669-2013.4288	0.9618	303
Cabo Francos Viej, Dom. Rep.	CN27	19.667	290.060	-23.107	8.7	1.6	3.1	1.0	-3.9	1.9	2.9	1.1	38.4	4.2	9.5	3.7	10	12.10	9.74	-3.40	1.60	-13.64	1.60	38.40	4.20	2012.6298-2013.4260	0.7822	289
Costadora, Panama	CN29	8.625	280.965	23.426	4.8	28.7	2.3	4.0	-2.2	53.0	1.9	8.0	-12.1	-8.5	6.4	12.0	10	8.88	13.92	-4.08	28.70	-14.12	53.00	-12.10	-84.50	2013.1586-2013.3055	0.1068	40
Bluefield, Nicaragua	CN30	11.994	276.228	27.749	-0.3	1.2	2.7	1.5	8.3	1.4	2.8	1.9	-1.0	3.8	8.8	6.5	10	7.11	12.38	-7.41	1.20	-4.08	1.40	-1.00	3.80	2015.1189-2013.4288	1.3099	644
Perenone, Panama	CN33	8.487	279.673	74.384	10.8	2.1	3.4	4.3	20.0	19.9	2.7	3.7	-2.3	3.2	9.3	6.6	10	8.40	13.95	2.40	2.10	6.05	1.90	-2.30	3.20	2011.8616-2013.4288	1.5671	569
Old Town, Colombia	CN35	10.736	276.637	45.597	3.0	4.0	2.2	4.0	9.2	7.7	2.3	8.0	16.2	11.6	7.3	12.0	10	8.02	11.85	-5.02	4.00	-2.65	7.00	16.20	11.60	2012.6899-2013.4288	0.7389	268
Restrepo, Colombia	CN37	12.820	284.173	12.933	7.1	4.3	4.0	2.2	1.4	2.2	1.5	1.5	1.5	1.5	1.5	1.5	10	13.03	10.53	-0.16	0.80	-1.43	0.90	1.50	2.10	2012.4007-2013.4288	3.918	419
Galerazamba, Colombia	CN37	10.379	284.737	-0.923	22.7	4.0	2.0	4.0	8.8	7.6	2.4	8.0	15.5	11.5	7.2	10.0	10	10.25	13.14	12.45	4.00	-4.34	7.60	15.50	11.50	2012.6462-2013.4205	0.7744	205
Cerceno, Colombia	CN38	12.222	288.012	8.191	9.5	1.0	4.0	12.8	7.4	2.2	8.0	12.2	11.2	7.6	12.0	11.0	10	11.40	12.69	-1.90	3.00	0.11	7.40	12.20	11.00	2012.6626-2013.4288	0.7662	277
Curicao, Colombia	CN40	12.280	291.042	31.014	12.0	1.0	3.1	19.9	12.9	0.9	2.2	1.6	1.9	2.3	6.6	5.7	10	12.43	12.84	-0.43	1.00	0.06	1.90	2.30	2011.5521-2013.4260	1.8740	677	
Cancun, Mexico	CN42	21.175	273.179	-2.186	0.7	1.3	2.1	-0.0	0.6	1.6	3.1	-1.0	-1.2	2.2	8.8	10.1	10	13.03	10.53	-0.16	0.80	-1.43	0.90	1.50	2.10	2012.4007-2013.4288	5.3486	1752
Corozal, Colombia	CN43	9.328	284.712	153.367	11.2	1.2	1.5	10.0	12.3	1.7	4.0	3.8	7.7	7.2	10.4	13.73	10.96	1.20	-3.73	1.20	4.00	3.80	2011.2013-2013.4041	1.4137	510			
St. Croix, Virgin Islands	CRO1	17.757	295.416	-34.070	13.6	0.3	2.0	4.6	11.0	0.3	2.1	5.2	-1.2	1.0	8.4	24.2	10	13.86	10.90	-0.26	0.30	0.10	0.30	-1.20	1.00	1996.7922-2013.4260	17.6438	10270
Culebra Island, PR	CUL1	18.307	294.717	-32.502	13.6	0.6	2.4	1.2	8.9	0.6	2.3	1.9	-1.2	1.3	8.1	8.6	10	13.64	10.63	-0.14	0.50	-1.73	0.60	-1.20	1.30	2006.8320-2013.4096	4.5776	616
Santa Elena, Guatemala	ELEN	16.916	270.132	115.966	1.2	0.4	1.9	5.0	-7.8	0.4	1.8	0.4	0.4	2.4	6.7	37.9	10	4.76	10.02	-3.56	0.40	-17.82	0.40	2.40	2007.9356-2013.4288	11.4653	2870	
Exuma Int Airport, Bahamas	EXU1	23.564	284.127	-21.823	5.1	0.5	2.0	2.1	-8.4	0.5	1.9	2.2	-1.0	0.9	6.3	6.8	10	10.03	7.62	-4.93	0.50	-17.02	0.50	-1.00	0.90	2007.4918-2013.4288	5.9370	1826
Martinique Volcano Observatory	FS00	14.735	298.853	481.809	15.8	1.2	4.3	10.3	13.1	32.1	15.4	8.0	17.0	13.9	8.0	12.0	10	14.93	12.30	0.97	1.30	-0.30	3.70	-6.90	13.70	1994.3986-1999.8671	5.4685	14
Martinique Volcano Observatory	FS01	14.735	298.853	481.809	16.3	1.7	6.2	4.0	13.3	2.1	4.7	8.0	-8.4	14.7	12.0	10	14.93	12.30	1.17	1.20	-2.50	2.70	0.30	2.00	2012.4007-2013.4288			



## 4.2 The 1-plate model

The currently accepted definition for the motion of the Caribbean with respect to the ITRF, which serves as the foundation for this study, is presented by DeMets et al. (2007), and Figure 4-2 is a velocity map of the 15 sites from that study. The GPS processing software, methods and global reference frame have been updated since 2007, so it is necessary to reprocess all the data using the current software version and reference frame, so direct comparisons can be made. Figure 4-2 presents three sets of velocity vectors. The black arrows are the velocity vectors from Demets et al. (2007) with respect to ITRF2005. The first step was to update the original data to the current reference frame. The current global reference frame is ITRF2008, which outperforms ITRF2005 in terms of determining station positions and velocities (Altamimi et al., 2011). The improvement in the IGS solutions are a result of, among other things, new absolute phase center offsets and more advanced tropospheric modelling. The precise orbit and clock files, used by GIPSY-OASIS II for terrestrial positioning, have also been recalculated by JPL and the combination of the newest software and products will yield better results than those processed analyzed by DeMets et al. (2007). The red arrows represent the same data, for the same epochs, reprocessed with GOAll v. 6.2 in the ITRF2008 reference frame. Finally, any additional data collected between 2007 and 2013 were added and also processed in GOAll v. 6.2 in the IGS08 reference frame. The last revision to the site velocities is represented by the yellow vectors in Figure 4-2.

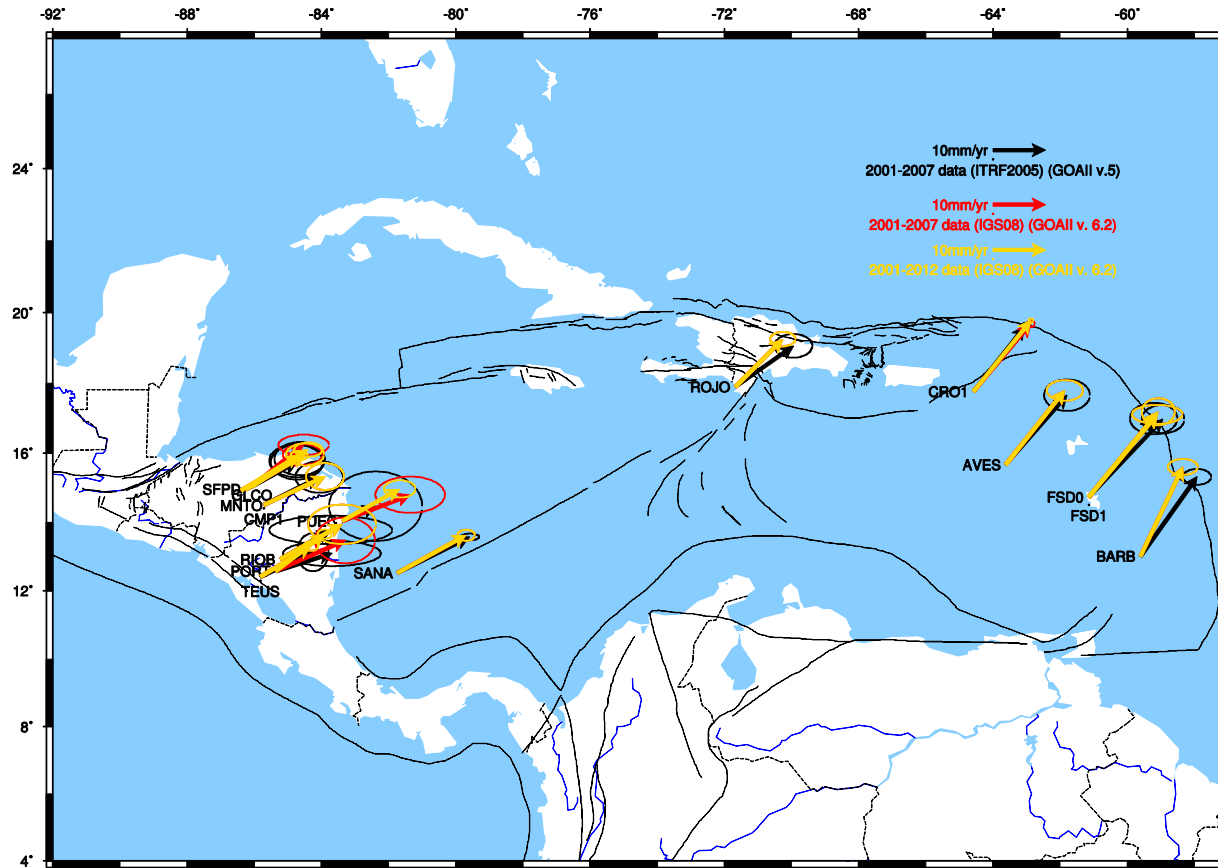


Figure 4-2 Demets et al. (2007) velocity vectors and updated values. Black arrows are Demets, 2007 original values with respect to ITRF2005. Red arrows are the 2007 sites and epochs, but processed with updated software and reference frame. Yellow arrows are the red arrows plus any additional data available from 2007 to the present.



The process of updating the reference frame (black arrows to red arrows), resulted in minor directional changes, but in a few cases, a notable change in the resulting rate. In general, the ITRF2008 results are rotated towards the north relative to the ITRF2005 results. For example, the ITRF2005 north and east velocities for PUEC (eastern Nicaragua) were  $2.8 \pm 4.4$  and  $6.4 \pm 5.9$  (DeMets et al., 2007), respectively, and when reprocessed with respect to ITRF2008, the north and east velocities are now  $6.1 \pm 1.1$  and  $11.0 \pm 2.0$ . All of the sites, when reprocessed in ITRF2008 versus ITRF2005 yield an improvement in the velocity uncertainty. Between 2006 and 2013 additional data were collected at sites GLCO, MNTO, PORT, PUEC, TEUS, and CRO1. These data have been included in the yellow velocity vectors shown in Figure 4-2. Any site with updated data produces an additional reduction in error and some minor variations in direction are also apparent.

In order to define a best-fitting angular velocity vector for Caribbean plate motion relative to IGS08, the velocities of the 15 original sites will be inverted using an inversion algorithm written by DeMets (the code, called GCCM was provided to G. Mattioli). The north and east components for each site are weighted in the inversion by the reciprocal of their squared 1 sigma uncertainties, ensuring that velocities from sites with long continuous time series contribute more to the final solution than those occupied infrequently (DeMets et al., 2007). The inversion of the velocities generates an estimate of an Euler pole for the motion defined by the specified set of sites. An Euler pole is the fixed point around which a rigid body will rotate on a sphere (Fowler, 1990).

In order to test the validity of the current 1-plate model for the Caribbean, the inversion for: 1) the original sites with the original epochs, updated to the current reference frame and 2) the original sites with all data available through 2013. The results

are listed in Table 4-3, and inversion input files and inversion results are available in Appendix E.

Table 4-3 Best-fitting Caribbean plate velocity vector information

Best-fitting Caribbean plate angular velocity vector information					
plate pair	no. of sites	angular velocity vector			reduced $\chi^2$
		$\lambda$	$\phi$	$\omega$	
		(°N)	(°E)	°m.y. <sup>-1</sup>	
CA-ITRF2000 published value by Demets et al., 2007	15	36.30	-98.50	0.2550	0.54
CA-IGS08 (original epochs - GOAll v. 6.2)	15	37.49	-102.62	0.2423	1.33
CA-IGS08 (all data available through 2013 - GOAll v. 6.2)	15	37.02	-103.18	0.2438	1.71

Small variations are seen in the latitude ( $\lambda$ ), longitude ( $\phi$ ), and rotation ( $\omega$ ) of the estimated Euler pole, but the increase in the reduced  $\chi^2$  value is of concern here.  $\chi^2$  is the sum of the squared weighted residual values from the inversion output. The reduced  $\chi^2$  is the  $\chi^2$  divided by the degrees of freedom, and is a statistical measure of the goodness of fit (Bevington, 1969). The reduced  $\chi^2$  value should decrease as a model improves its fit to the data. The reduced  $\chi^2$  value of the inversion including only the original dataset was 1.33, while the reduced  $\chi^2$  for the inversion with the enhanced dataset was 1.71. In this case, adding additional GPS data (*i.e.* extending the time-series) to the existing model, changed the velocity estimates, and thus resulted in a worse fit. The degraded fit suggests that the 15 site, 1-plate model defined by Demets et al. (2007) may no longer be valid, and a new more complex model needs to be developed.

Perhaps the addition of more sites will improve the fit of the model. Figure 4-3 presents the 117 COCONet and campaign sites that were analyzed for consideration as part of the Caribbean plate. All sites were processed as described in Chapter 2 and the time series are located in Appendix B. Once the sites were processed, they were sorted

by their deviation from the currently accepted plate motion. Any site outside of  $2\sigma$  variation were not included and sites within  $2\sigma$  variation underwent further scrutiny. Any site whose velocity is affected by a zone of plate boundary deformation, or has been established in the literature to be part of another plate also was excluded. Data from some sites in the highly concentrated GPS campaign region of Dominica were eliminated to reduce spatial redundancy. This process narrowed the list of 117 sites down to 24 that are considered “on plate” and these are designated by red arrows in Figure 4-3.

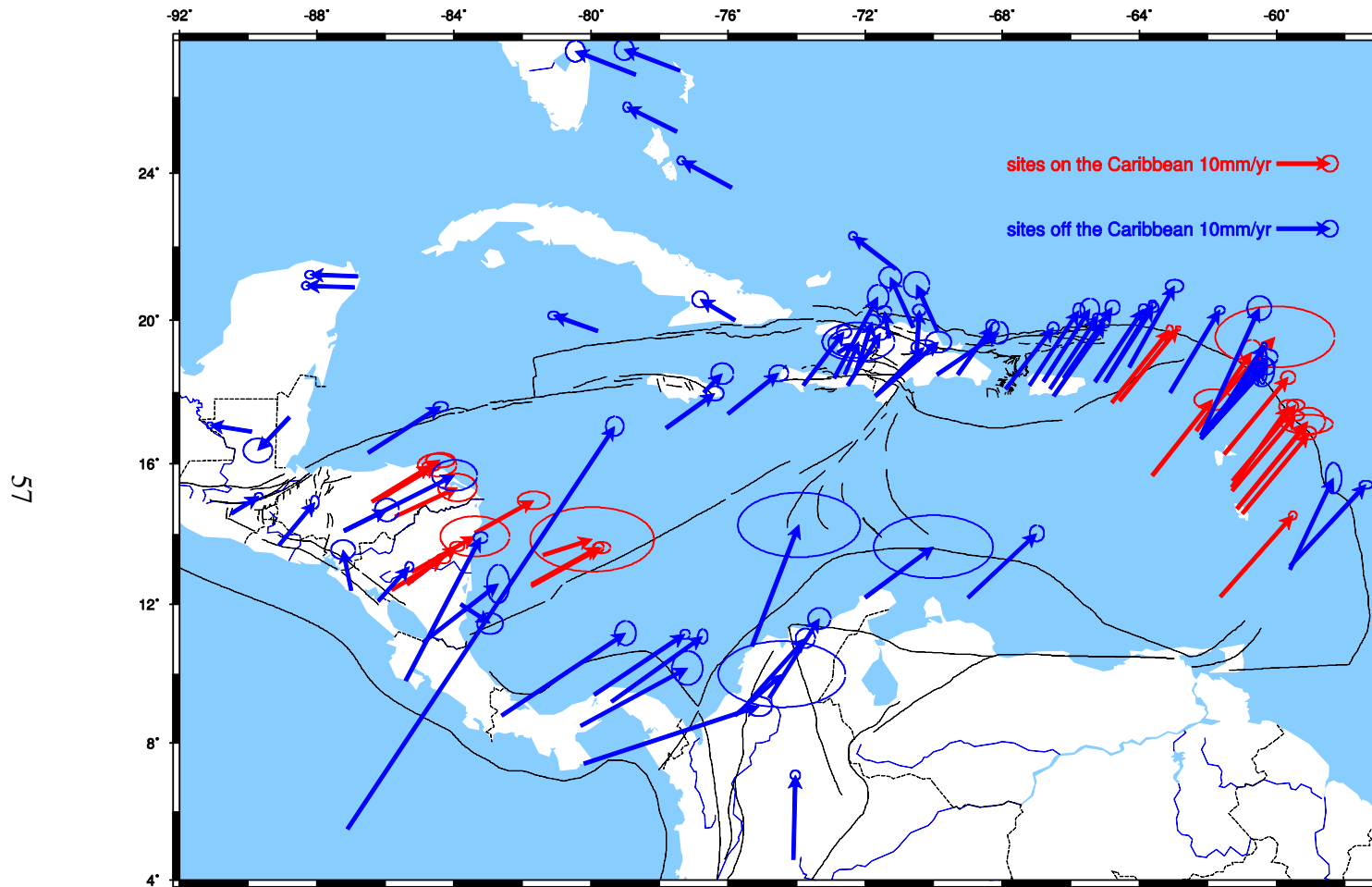


Figure 4-3 Caribbean horizontal site velocities  
Red arrows are on-plate and blue arrows are off-plate.

Table 4-4 Occupation history and velocities

	country	site	lat (°N)	long (°W)	station days occupied per calendar year													site velocity mm yr <sup>-1</sup> with respect to IGS08															
					2000	2001	2002	2003	2004	2005	2006	2007	2008	2009	2010	2011	2012	2013	North	East													
1	Honduras	CMP1	14.5090	85.7146	3					2									5.8 ±2.0	13.0 ±2.7													
2	Honduras	GLCO	15.0300	86.0699	2				3	2					4				7.0 ±1.2	11.2 ±2.0													
3	Honduras	MNTO	14.9170	86.3805	3				3						3				6.7 ±1.0	10.7 ±1.4													
4	Honduras	SFDP	14.9660	86.2449	3				3										6.7 ±2.1	12.0 ±3.1													
5	Nicaragua	PORT	12.5731	85.3671	3		4	4			4		4				4		7.4 ±0.8	9.8 ±1.2													
6	Nicaragua	PUEC	14.0421	83.3820		4		4			4								6.5 ±1.7	10.6 ±2.5													
7	Nicaragua	RIOB	12.9209	85.2206	4		4	4											6.2 ±3.3	11.2 ±6.8													
8	Nicaragua	TEUS	12.4098	85.8136	5		5	5			4						4		5.9 ±0.6	9.7 ±0.9													
9	Columbia	SANA	12.5238	81.7294	1994 (9), 1996 (3), 1998 (6), 2000 (6), 2003 (5)														44	7.2 ±0.7	13.1 ±1.1												
10	Virgin Isl.	CRO1	17.7569	64.5843	1995-2002 (2285)													362	360	168	363	361	360	354	287	364	362	157	13.6 ±0.3	11.0 ±0.3			
11	Venezuela	AVES	15.6670	63.6183	1994 (18), 1998 (10)																								14.3 ±2.0	10.3 ±2.8			
12	Matinique	FSD0	14.7348	61.1467	1994 (4), 1998 (6), 1999 (4)																								15.9 ±1.7	12.0 ±3.9			
13	Matinique	FSD1	14.7349	61.1465	1994 (5), 1998 (11), 1999 (4)																								16.3 ±1.7	13.3 ±2.1			
14	Ant./Barb.	RDON	16.9340	62.3460														217	85	15.2 ±1.9	11.2 ±2.2												
15	Grenada	GRE0	12.2220	61.6400														188	360	354	326	365	363	103	15.2 ±0.5	13.5 ±0.7							
sites added																																	
16	Guadeloupe	ABMF	16.2623	61.5275																122	353	317	185		14.4 ±0.8	12.0 ±0.9							
17	Martinique	LMMF	14.5948	60.9962																122	355	362	184		15.0 ±0.8	12.5 ±0.9							
18	Columbia	SANO	12.5800	81.7160																24	360	354	363	365	257	103	6.9 ±0.6	12.1 ±0.8					
19	Virgin Isl.	VIKH	17.7160	64.7980							118	263	236	306	360	362	363	103								13.6 ±0.6	10.8 ±0.6						
20	Barbuda	CN00	17.6685	61.7856																		132	150			12.6 ±3.8	11.2 ±7.4						
21	Columbia	CN35	13.3755	81.3629																		114	154			3.0 ±4.0	9.2 ±7.7						
22	Dominica	CASS	15.2409	61.2911		4		3	5		3	4											3			13.7 ±0.9	11.8 ±1.8						
23	Dominica	CNCD	15.5118	61.2783		5		3	6		4	3											4			14.7 ±1.0	11.5 ±1.4						
24	Dominica	FRSH	15.3402	61.3094		4		3	4		3	4											4			14.5 ±1.2	10.7 ±1.5						
sites removed																																	
	Barbados	BARB	13.0879	59.6091	192	26	1999 (115)																							17.1 ±1.9	8.1 ±1.0		
	Dom. Rep.	ROJO	17.9040	71.6745		2	1994 (9), 1995 (2), 1998 (3)																									9.1 ±0.9	9.1 ±1.6

### 4.3 The 2-plate model

The data from the 24 sites (Figure 4-3) that appear to move with the Caribbean plate are inverted to see how the result compares to the DeMets et al. (2007) 15 site, 1-plate model. BARB and ROJO have been removed from the original 15 sites, and 11 new sites have been added). I have chosen to remove BARB and ROJO because their velocities are inconsistent with the sites considered “on-plate”. BARB, in Barbados is likely affected by active shortening of the accretionary wedge (Speed et al., 1982), and ROJO, in the Dominican Republic is very near the Enriquillo-Plaintain Garden fault which experiences slip on the order of ~20 mm/yr (Manaker et al., 2008). Visual inspection of the velocity map for these sites (Figure 4-3, red vectors) suggests that there are two distinct populations of horizontal velocity vectors. To better visualize the differences in azimuth between the two populations, the velocities are plotted on a compass diagram (Figure 4-4, inset), and it appears to verify that there are two distinct vector populations

for the 24 sites considered “on plate”: The eastern site velocities are represented by the blue arrows and the western site velocities by the red arrows in Figure 4-4. The western site velocities have a greater easterly component, while the eastern sites display stronger northerly motion.

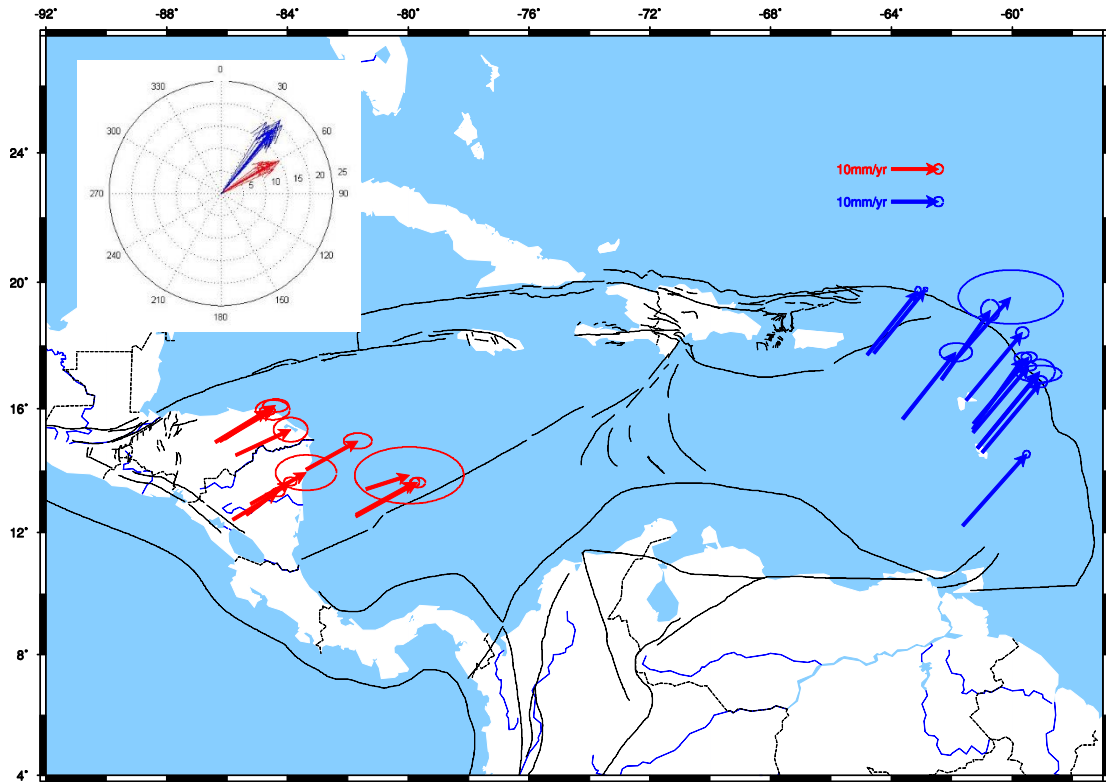


Figure 4-4 Horizontal velocities for sites on the Caribbean plate. Arrows represent horizontal velocity vectors with respect to IGS08, blue arrows represent the eastern Caribbean sites and the red arrows represent the western Caribbean sites. Inset is a compass plot of Caribbean velocity vectors, azimuth and magnitude in mm/yr is shown.

Since it appears that the eastern and western sites have unique and independent motion, I will test whether a 2-plate model fits all the reprocessed data better by examining both options. First, the 24 sites are inverted, assuming all sites are on 1 plate, with respect to a fixed IGS08 reference frame and the reduced  $\chi^2$  is 0.75. When the inversion is run using 2 plates, with the sites split into an eastern group and a western group, the 2-plate model yields a reduced  $\chi^2$  of 0.60. Although the resulting reduced  $\chi^2$  value is improved, the F-ratio test must be employed to confirm that the improvement is not merely an artifact of adding three additional adjustable parameters (Stein and Gordon, 1984). There are 3 adjustable parameters for a 1-plate model, which are, latitude, longitude, and rotation rate of the pole. A 2-plate model doubles the adjustable parameters to 6, since a latitude, longitude and rotation rate must be defined for 2 poles. The equation for the F test for the validity of adding  $n^{\text{th}}$  term is shown below (Stein and Gordon, 1984):

$$F = \frac{\frac{\chi^2(r) - \chi^2(p)}{p - r}}{\frac{\chi^2(p)}{N - p}}$$

$N$  = number of data

$p$  = degrees of freedom for a 2-plate model

$r$  = degrees of freedom for a 1-plate model

The F value calculated,  $F = 4.94$ , for  $v_1 = 3$  and  $v_2 = 42$ , generates a 99.5% confidence that a 2-plate model is a statistically significant improvement over the 1-plate model.

Figure 4-5 (A, B) shows and Table 4-5 Site data importance values by site, which is the percentage that each site contributes to the final solution. A continuous site with a long occupation history is weighted more in the inversion than the data from campaign

sites that are intermittently occupied. These data importance values are determined from the relative uncertainties of the individual site velocities and the site location with respect to other sites and the pole of rotation (Minster et al., 1974). The DeMets et al. (2007) values are also shown in Figure 4-5 (A) and Table 4-5. It is important to note that their solution relies heavily on site CRO1 (~41%), which was a concern stated by the authors at the time of publication. The heavy reliance of the model on CRO1 (St. Croix) forced DeMets et al. (2007) to consider the possibility that the assumption that CRO1 accurately records the motion of the undefining Caribbean lithosphere may be incorrect. Enough data has been collected from the eastern Caribbean (Table 4-5 and Figure 4-5 B), since the DeMets et al. (2007) study, such that the plate motion model's dependence on CRO1 has been reduced to 17.7% (Table 4-5). The site data importances, in general, are more evenly distributed both numerically and spatially. The east versus west site data importance for DeMets et al. (2007) was 62% versus 38%, whereas the value for the 24-site 2-plate model is 49% versus 51%. The data are now nearly equally weighted, so neither region of the Caribbean plate has a dominating effect on the resulting kinematic model.

The spatial distribution of the site data importance is now adequate to support improved confidence in the inversion results. Figure 4-6 is a map showing the derived Euler poles for the Caribbean as determined by various authors. Although there are small variations seen in the pole of rotation based on the reference frame and the software version used, all of the poles for models that hold the Caribbean as a single rigid plate, plot in the similar vicinity. Note that if the Caribbean is considered as two plates, the pole for the east-Caribbean is farther east than all other results and the pole for west-Caribbean shows significant disparity, with its location north of 58°N. Another important feature is that the pole estimation determined by Altamimi et al. (2007) for the Caribbean

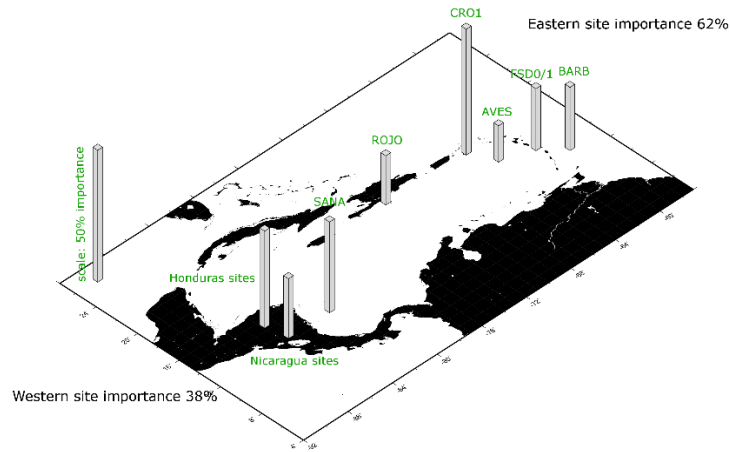


is based on 3 sites: St. Croix, Puerto Rico, and Barbados. I have excluded data from Barbados and Puerto Rico from my inversions, because of their proximity to zones of active deformation and thus I would consider this pole location to be the least reliable.

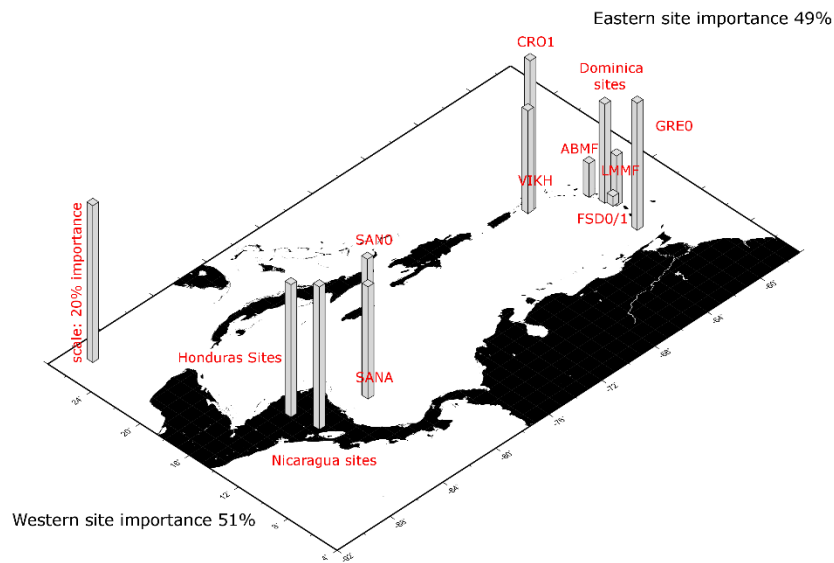
Table 4-5 Site data importance values

site importance (%)		
Miller, 2013	DeMets, 2007	site
17.7	41.7	CRO1
12.5	17.7	Honduras sites
8.5	14.8	SANA
1.2	6.3	FSD0/1
15.2	5.9	Nicaragua sites
0.5	2.9	AVES
14.2	new site	SANO
11.3	new site	GRE0
7.1	new site	VIKH
6.6	new site	Dominica sites
2.6	new site	LMMF
1.9	new site	ABMF
0.7	new site	RDON
0.3	new site	CN35
0.1	new site	CN00
removed from inversion	6.5	BARB
removed from inversion	4.3	ROJO
100%	100%	total
east versus west importance		
49.0%	62.0%	eastern sites
51.0%	38.0%	western sites

Values for velocities of Caribbean GPS sites used to derive the best-fitting CA-ITRF2008 angular velocity vector. Values for DeMets et al. (2007) 15-sites.



(A)



(B)

Figure 4-5 Data importance

Data importance values for velocities of Caribbean and Central American GPS sites used to derive the best-fitting Caribbean-ITRF2008 angular velocity vector. Values plotted are those that contributed >1% to the solution. All importance values are listed in Table 4-5. (A) Values for DeMets et al. (2007) 15-site 1-plate model. (B) Values for 24-site 2-plate model. Note the different scales for (A) and (B).

Table 4-6 Best fitting Caribbean angular velocity vectors

Best-fitting Caribbean plate angular velocity vector information				
plate pair	no. of sites	angular velocity vector		
		$\lambda$ (°N)	$\phi$ (°E)	$\omega$ °m.y. <sup>-1</sup>
CA-ITRF2005 published value by Altamimi et al.	3	39.32	-104.28	0.2410
CA-ITRF2005 published value by Demets et al., 2007	15	36.30	-98.50	0.2550
CA-IGS08 data through 2007, reprocessed	15	37.49	-102.62	0.2423
CA-IGS08 data through 2013, reprocessed	15	37.02	-103.18	0.2438
CA-IGS08, 1-plate model result	24	37.19	-101.95	0.2545
CA(east)-IGS08, 2-plate model result	14	35.79	-97.18	0.2802
CA(west)-IGS08, 2-plate model result	10	58.51	-145.36	0.1321

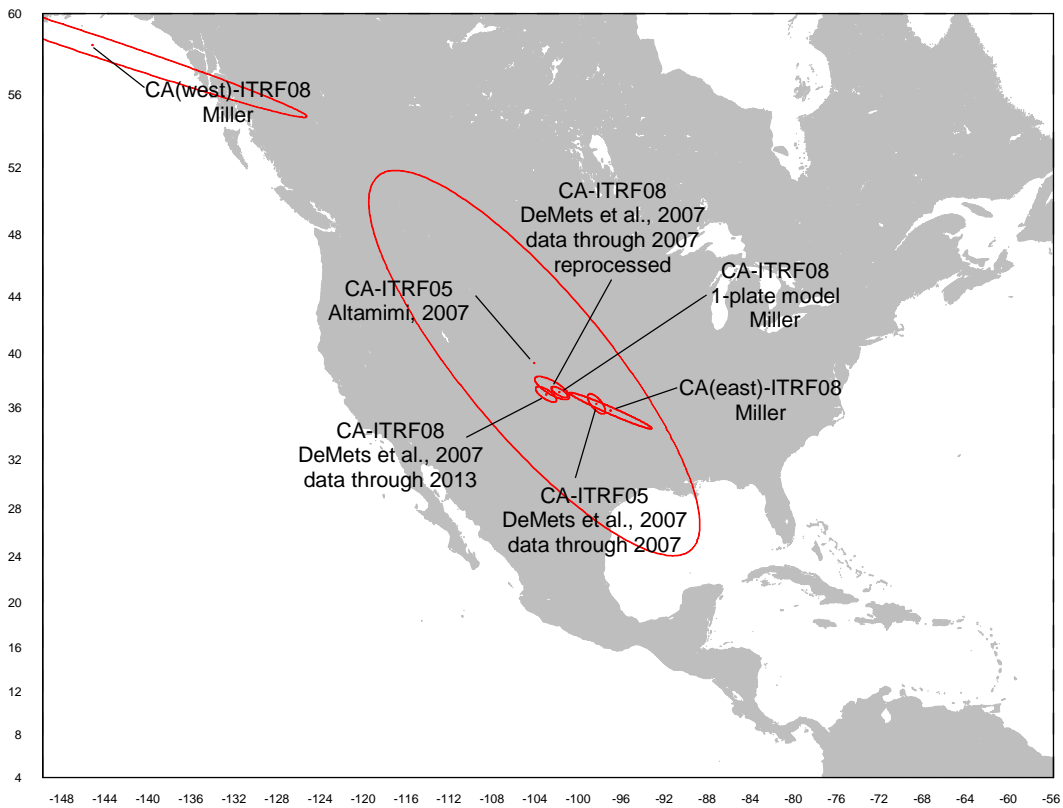


Figure 4-6 Euler pole locations.  
Error ellipses are 1  $\sigma$ .

#### 4.4 The rigidity of the Caribbean plate

Based on the F-test, I can infer that the east and west Caribbean are moving at different rates and directions, and since we can see in Figure 4-7, that despite the fact that there is very little seismicity in the interior of the Caribbean, I conclude that there is ongoing internal deformation and therefore the Caribbean plate is non-rigid. To investigate possible structures that may serve as a boundary between east and west Caribbean blocks, and a location where such deformation might occur, I consider geomorphologically prominent features, the locations of known and putative faults, and observed earthquake hypocenters (Figure 4-7).

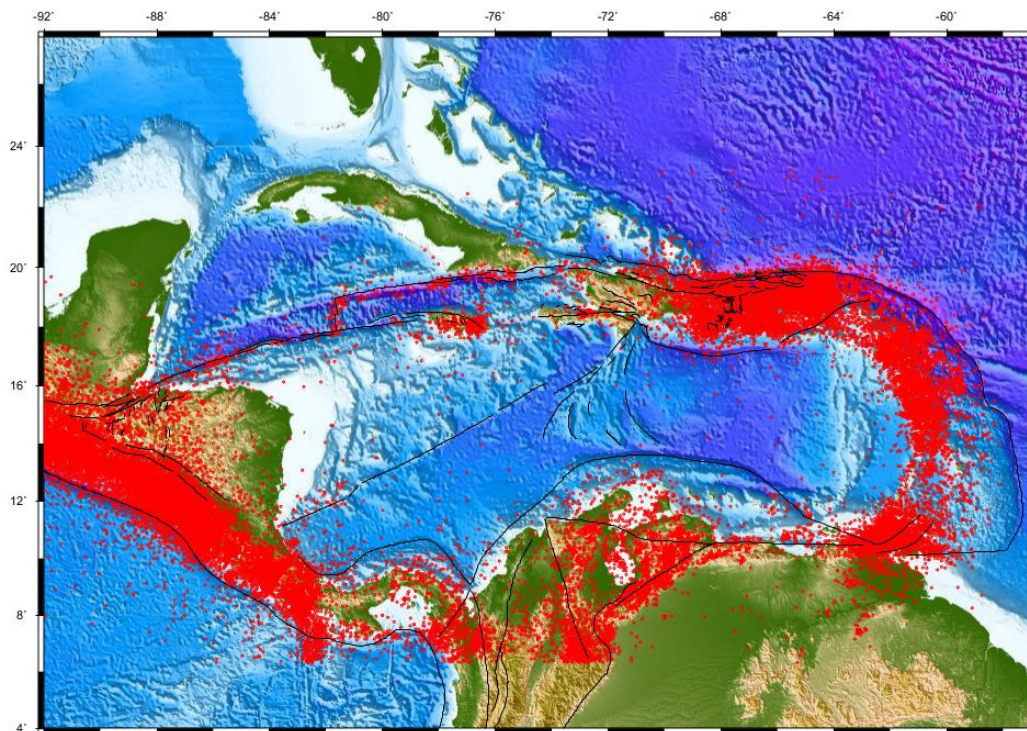


Figure 4-7 Faults and earthquakes of the Caribbean  
Red circles are earthquake hypocenters (IRIS data, <http://www.iris.edu>). Black lines delineate putative faults.

Two features that appear to separate the Caribbean into east and west sections are the Lower Nicaraguan Rise and the Beata Ridge (Figure 1-5). Mauffret and Leroy (1999) conclude on the basis of marine seismic profiles, that the Beata Ridge shows clear evidence of compression and transpression. They estimate that the ridge has accommodated  $9 \pm 1.5 \text{ mm yr}^{-1}$  of shortening since the early Miocene. To test this proposal, we use the 2-plate model, based on the inversion of the 24 sites (10 on the western block and 14 on the eastern block) and the derived poles to predict the relative motion of the east and west sections relative to each other along both the Beata Ridge and the Lower Nicaraguan Rise. The results for the predicted motion along the Lower Nicaraguan Rise are presented in Figure 4-8 and Figure 4-9. I calculate less than 1 mm of relative motion between the east and west sides of the Lower Nicaraguan Rise, which indicates that it is not a likely candidate for the location of any significant intraplate deformation. The 2-plate model, however, predicts an average velocity of 3 mm/yr along the Beata Ridge with the motion oblique to the boundary (Figure 4-10 and Figure 4-11). This prediction corroborates the transpressional environment described by Mauffret and Leroy (1999), which includes a pop-up structure, reverse faults, and an inverted basin, identified through interpretation of seismic reflection profiles.

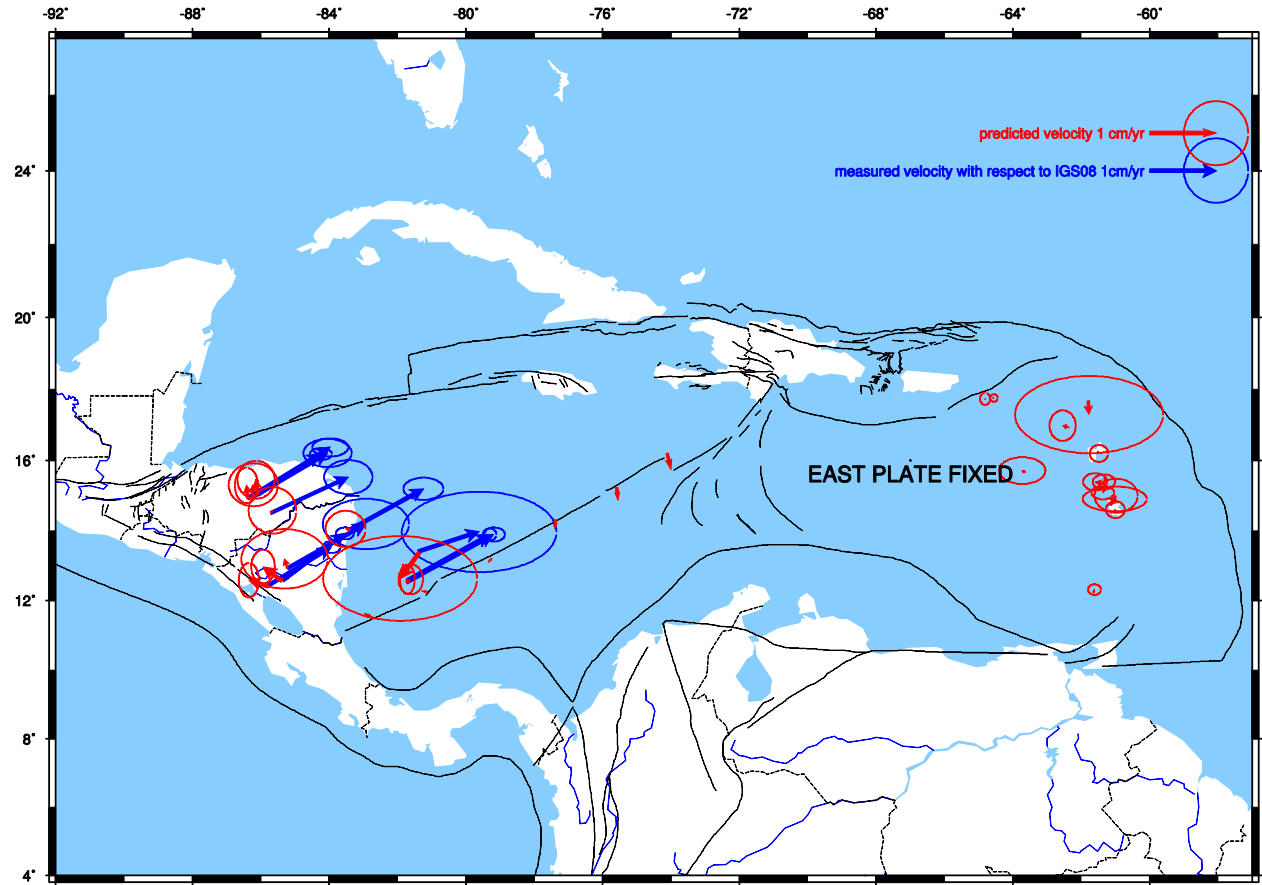


Figure 4-8 Motion along Lower Nicaraguan Rise with respect to a fixed east plate. Red arrows are motion predicted by a 2-plate model with respect to a fixed east plate. Blue arrows are velocities measured with respect to IGS08. Error ellipses are 1  $\sigma$ .

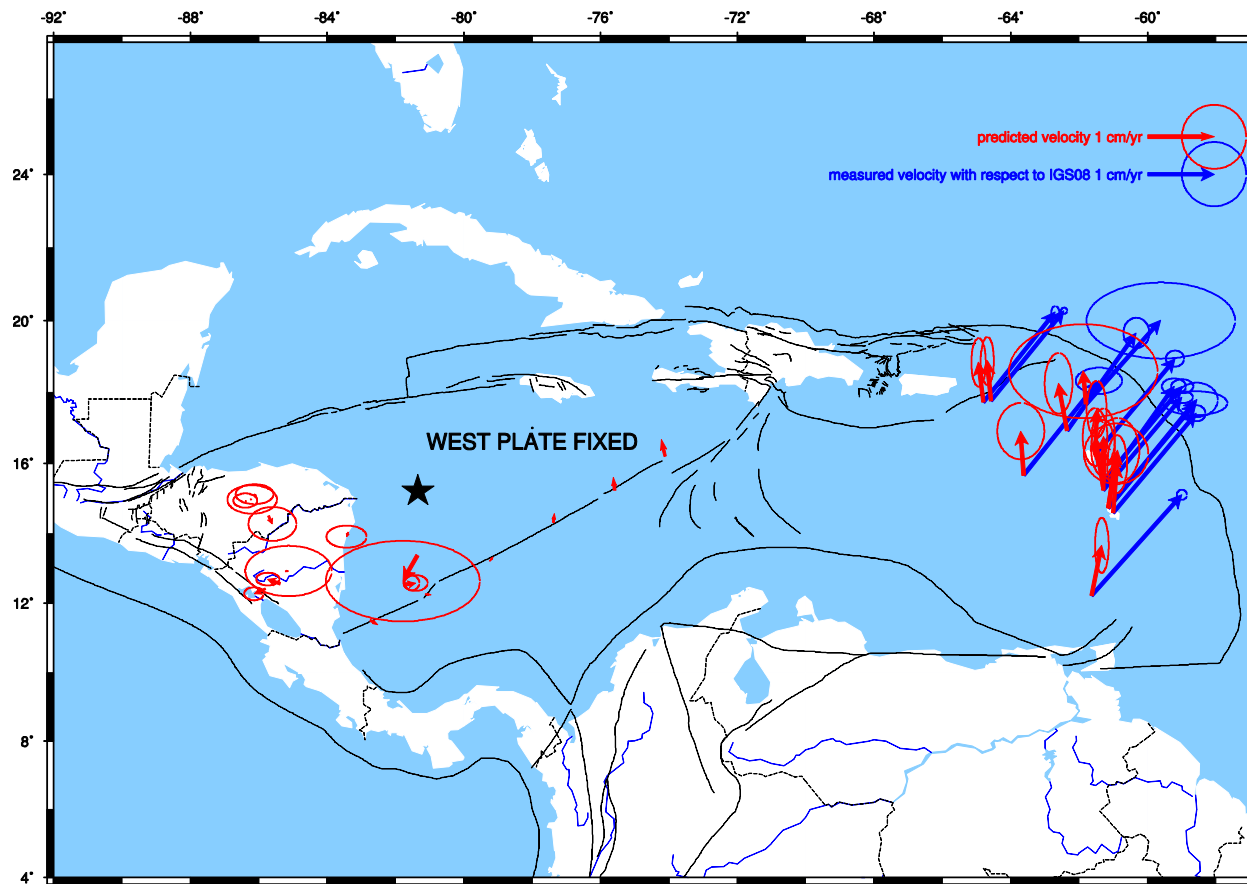


Figure 4-9 Motion along Lower Nicaraguan Rise with respect to a fixed west plate. Red arrows are motion predicted by a 2-plate model with respect to a fixed east plate. Blue arrows are velocities measured with respect to IGS08. Black star is predicted Euler pole for the rotation of Caribbean-east with respect to a fixed Caribbean-west.. Error ellipses are  $1 \sigma$ .

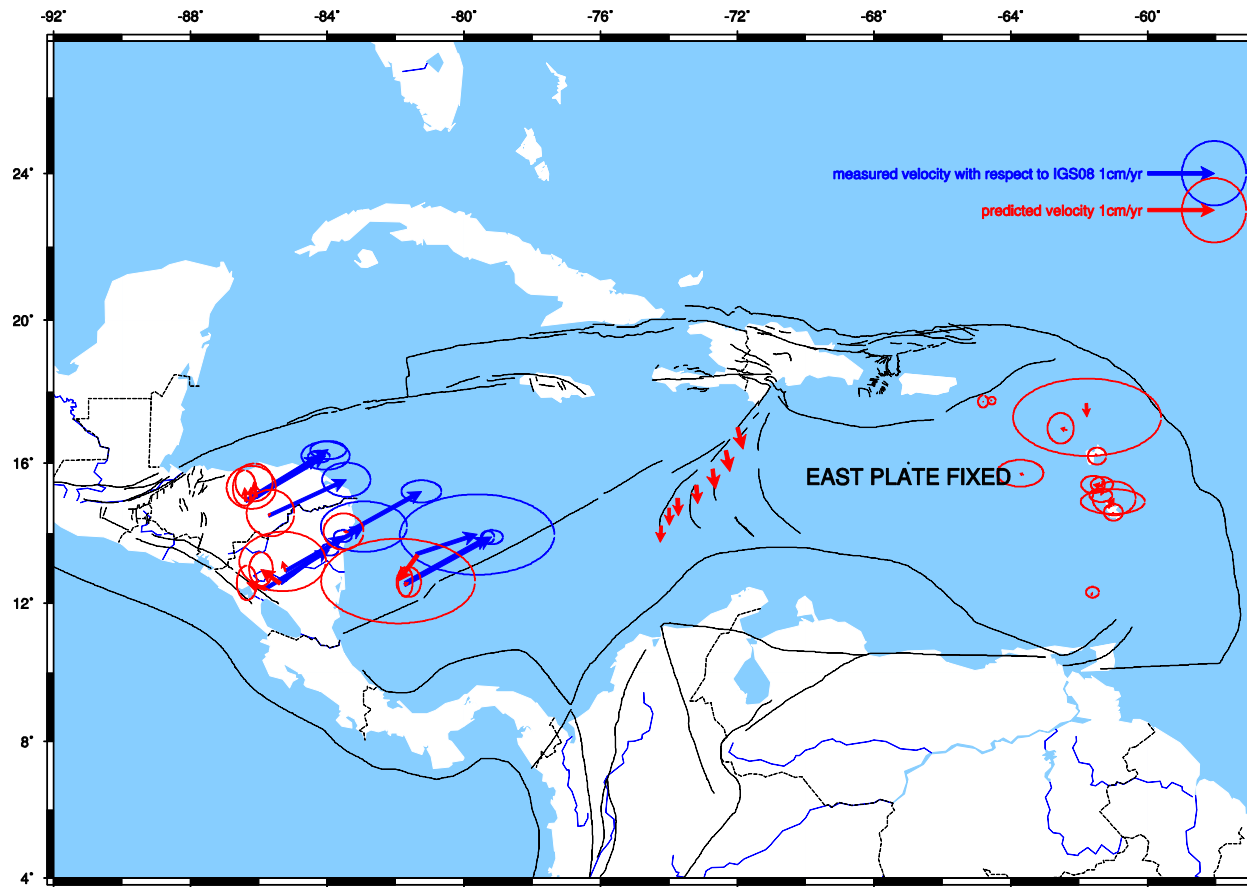
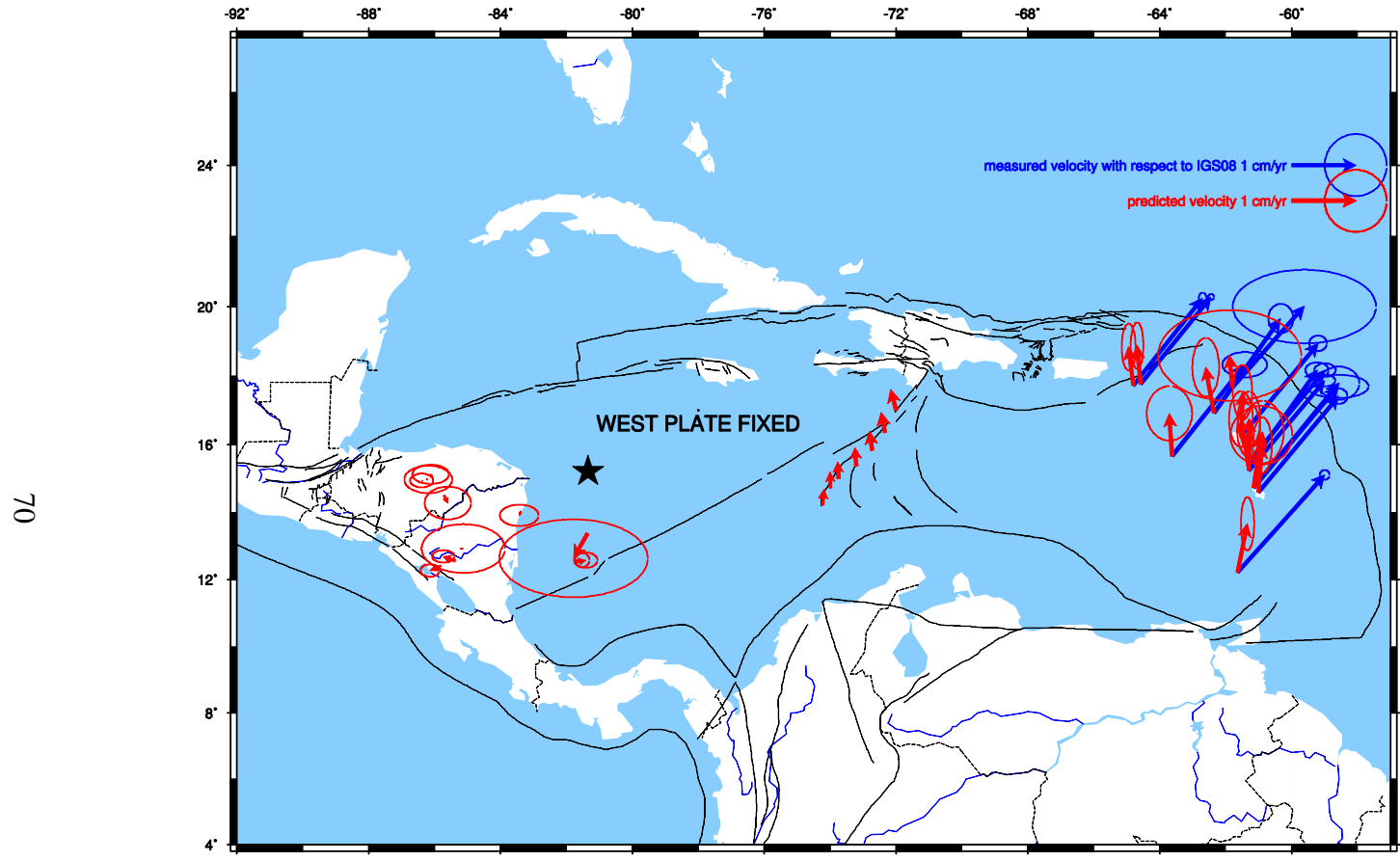


Figure 4-10 Motion along the Beata Ridge with respect to fixed east plate. Red arrows are motion predicted by a 2-plate model with respect to a fixed east plate. Blue arrows are velocities measured with respect to IGS08. Error ellipses are  $1 \sigma$ .





70

Figure 4-11 Motion along the Beata Ridge with respect to fixed west plate. Red arrows are motion predicted by a 2-plate model with respect to a fixed east plate. Blue arrows are velocities measured with respect to IGS08. Black star is predicted Euler pole for the rotation of Caribbean-east with respect to a fixed Caribbean-west. Error ellipses are  $1 \sigma$ .

Once new Caribbean poles for a 2-plate model are adopted, a re-plotting of the residual velocity maps is required, using the new Caribbean-east and Caribbean-west rates. Minimal change is expected for sites in the eastern block the previous model and the one that was used for the initial kinematic analysis (DeMets et al., 2007) was overly dependent on the eastern sites to define its pole. Figure 4-12 shows the Dominica residual velocity rates plotted in black for the 1-plate model and red for the 2-plate model. The red is superimposed on the black since the difference is virtually insignificant. The scale has been magnified in this image to make the vectors easier to see. The western sites show more variation in the residuals (Figure 4-13), due to the large disparity in the location of the Euler pole when the western sites are isolated.

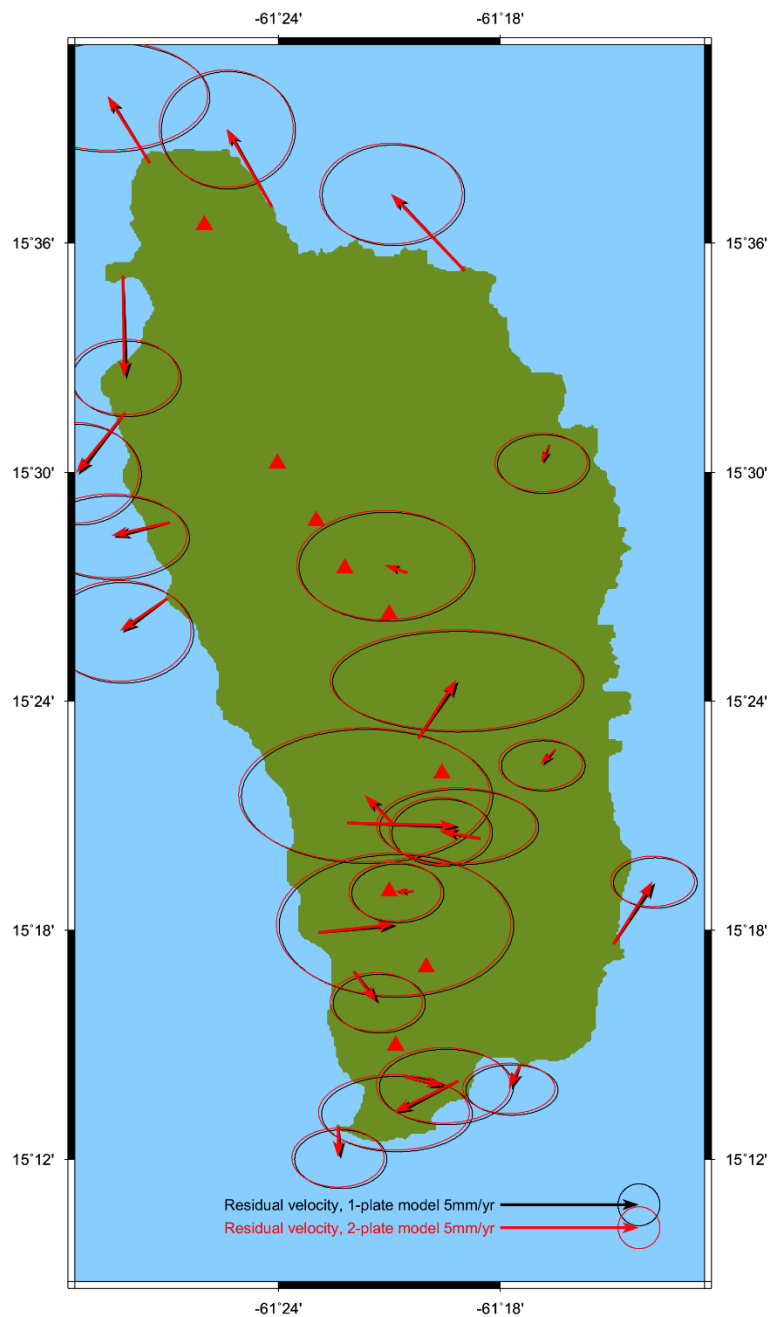


Figure 4-12 Dominica residual velocities, 1-plate model versus 2-plate model. Black arrows represent residual velocity with respect to a fixed 1-plate Caribbean. Red arrows represent residual velocity with respect to a fixed East Caribbean plate. Error ellipses are  $1 \sigma$ . Note scale difference between this figure and figures 3-26 and 3-27.

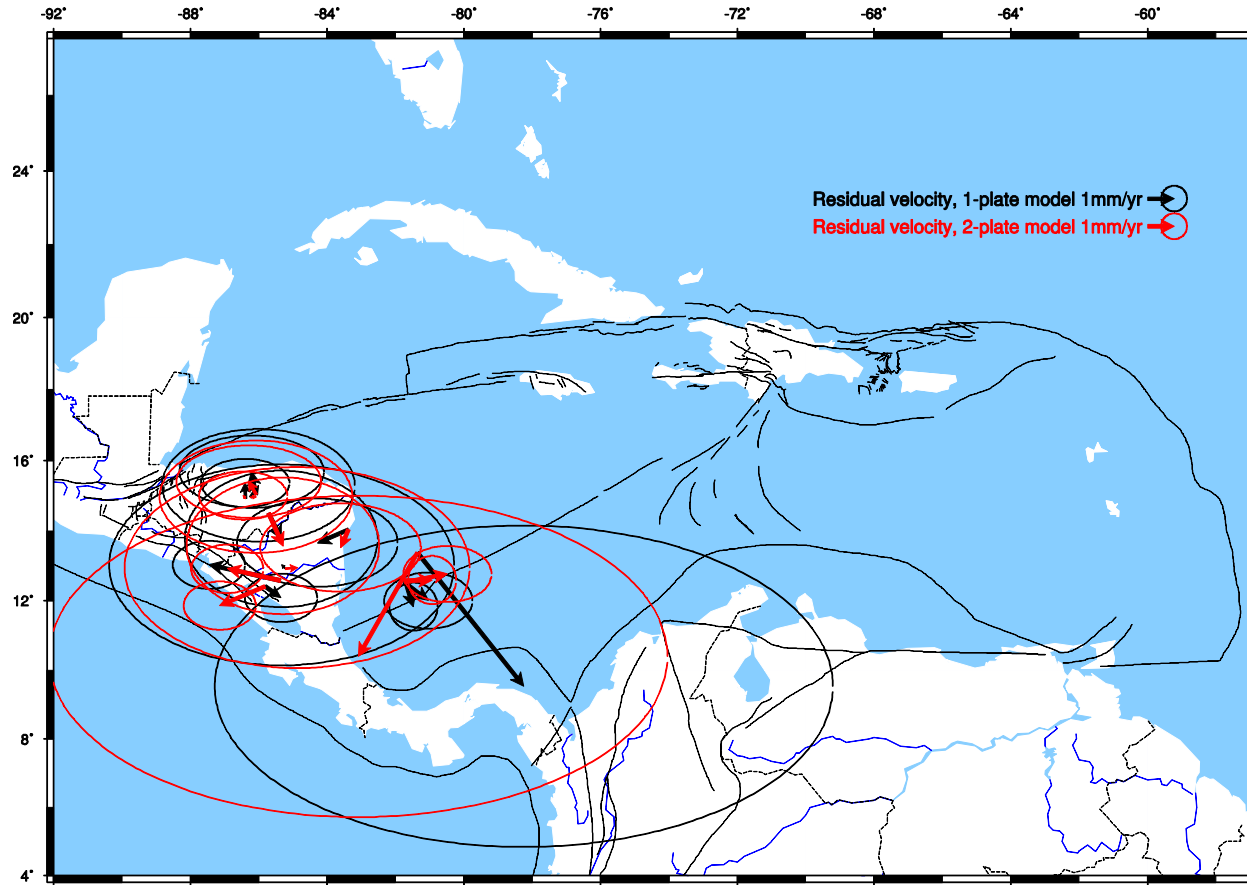


Figure 4-13 Western site residual velocities, 1-plate model versus 2-plate model. Black arrows represent residual velocity with respect to a fixed 1-plate Caribbean. Red arrows represent residual velocity with respect to a fixed West Caribbean plate. Error ellipses are  $1\sigma$ .

#### 4-5 Kinematic versus dynamic model of the Caribbean

A dynamic model of the Caribbean is presented by van Benthem (2013), which supports the kinematic 2-plate model I have proposed. He identifies the forces contributing to the dynamics of the Caribbean plate as: (1) pull by the Maracaibo slab, which is largely counteracted by slab resistive forces, (2) frictional forces with the surrounding plates, perhaps combined with (3) trench suction at the southern Lesser Antilles (van Benthem, 2013). Figure 4-14 presents van Benthem's map of principle stresses for the Caribbean. Note that in the area of Beata Ridge (marked with a red oval), where we suspect a transpressional environment, the primary stress direction is compressional and oriented approximately E-W.

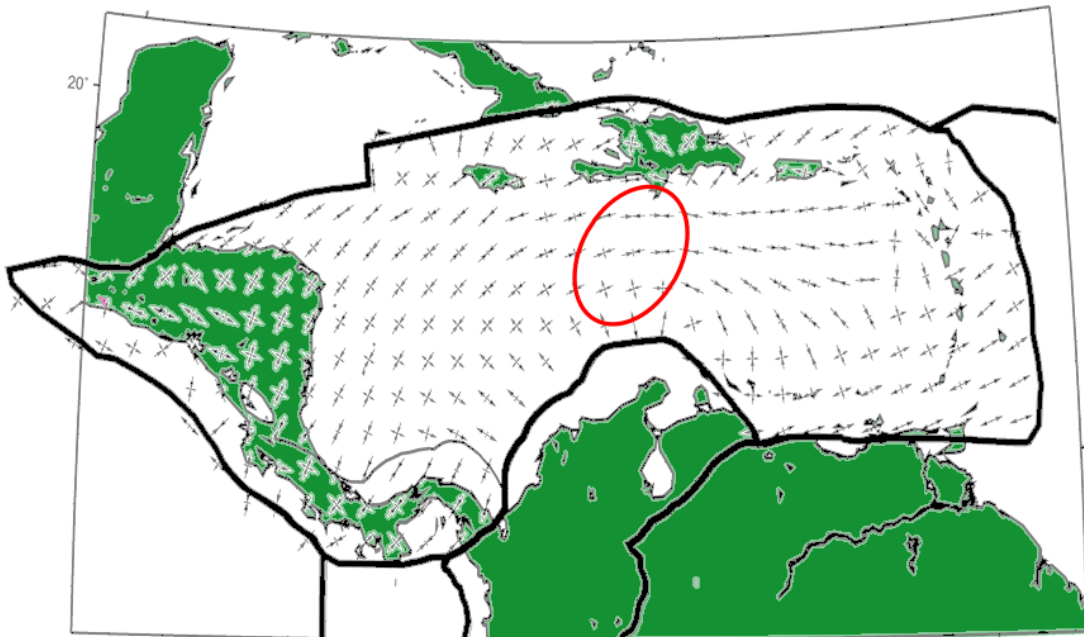


Figure 4-14 Caribbean principle stress directions (van Benthem, 2013)  
Red oval marks the area of the Beata Ridge.

Van Benthem (2013) also identifies mechanisms for plate boundary deformation in the NE Caribbean as “Bahamas collision” and “slab edge push”. His “slab edge push” model predicts uplift for the interior of the Caribbean plate, roughly at the location of the Beata Ridge (Figure 4-15) (van Benthem, 2013). In both models, predicted strain rates are higher for eastern versus western Caribbean, with a demarcation that lies along the Beata Ridge.

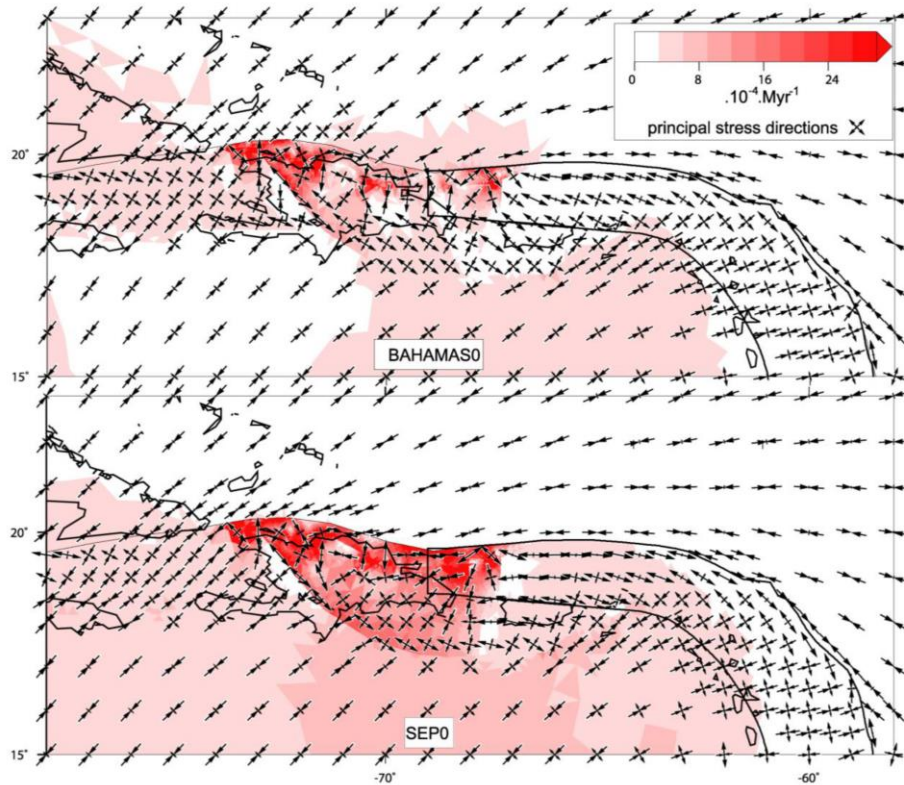


Figure 4-15 Caribbean effective strain rate (van Benthem, 2013)  
Strain rate is  $\text{Myr}^{-1}$ . Black crosses denote the principle strain rate directions. The top panel is the Bahamas collision model for present day and the bottom panel is the slab edge push (SEP) model for present day.

#### 4-6 Conclusion

It is with confidence that I conclude that the east and west sides of the Caribbean display unique motion and that the Caribbean is not a single rigid plate. E-W shortening is likely occurring in the area of the Beata Ridge, a theory supported by seismic data, kinematic and dynamic modeling. The adoption of a 2-plate model would have implications in various areas of Caribbean studies, including geodesy and neotectonics. Poles associated with a 2-plate model highlight the inconsistencies with the Euler pole for the Caribbean plate as defined by ITRF2008. Any models used to assess regional hazards associated with plate motion would need to be reevaluated, especially for the Western Caribbean.

Appendix A  
Dominica Campaign Site Descriptions



Modified from James, 2008

#### ATRU

Site is located at Atru Bay on the coast near the north end of Dominica (fig. A-1). The end of the journey to this site requires a descent down a steep switch backed driveway to a plot of land that was for sale in 2011. At the end of the driveway, there is a relatively flat open field (fig. A-1) to the Atlantic Ocean. Once parked at the end of the driveway, you will be facing east to the Atlantic. Park here and head out on foot south/southeast across the field approximately 100 yards to a grove of palms. There is a subtle opening in the trees, which may once have been a "trail". Enter the trees and follow the "trail" towards the ocean. As you emerge from the trees, it is necessary to scale down a small (3-5 m) drop to the rocks on the shore. Once at the bottom, you are very near the site. The pin is located in a boulder approximately 2 m from the base of the ~5 m cliff you just scaled down. The cliff may be a source of multipath interference and certainly limits the sky view available to the west of this site. Antenna should be elevated as much as possible to reduce the influence of this cliff. The site is not secure, however there is relatively low traffic and as such, security is not a major concern.

Installation: June 2004, stainless steel Bevis pin set with epoxy in a 0.5" hole in andesitic bedrock.

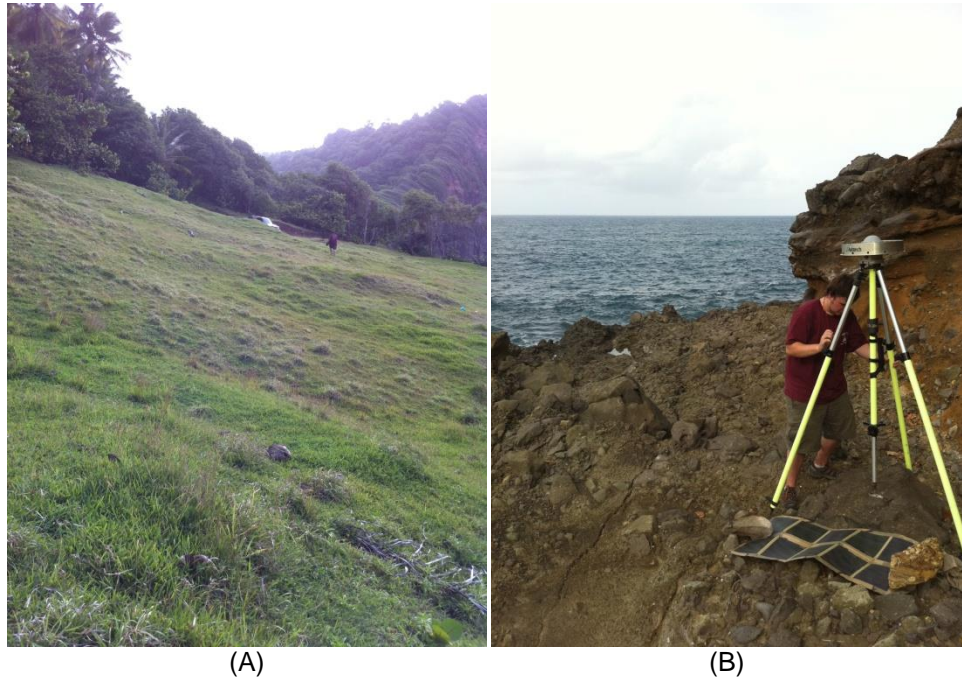


Figure A-1 Dominica campaign site (A) ATRU, 2012 looking back across the field from the palm grove towards the parking area (B) ATRU, 2012

#### BELV

Site is located in an andesite boulder on a hillside at Belvedere Estates on the east coast of Dominica. There is a road (two strips of concrete) that will take you this location. The road has some precarious spots so proceed with caution. The landowner is Edward Joseph, he is very friendly and if present, can show you where the pin is located. When you get close using GPS, look for a shed (fig. A-2). Park near the shed, cross the road and cut through the trees. The boulder is located in the field just north of the shed. The field is no longer used for grazing cows as it had been in the past so the vegetation was chest high. You will need a machete for this site. Edward cut a path for us and cleared around the boulder.

*Installation:* June 2001, stainless steel Bevis pin set with epoxy in a 0.5" hole.

Site requires either a tripod or tetrapod for setup due to a small mounting area on the surface of the boulder.



Figure A-2 Dominica campaign site (A) BELV, 2012 Edward Joseph's shed, place to park and cross through trees (B) BELV, 2012 (C) BELV, 2006 (D) BELV, 2006

#### BOIL

This site is on the shore of boiling lake and is a 16 mile round trip on foot.

Installation: 2007

## BOTG

Site is located in a mostly buried boulder at the Botanical Gardens in Roseau (fig. A-3). The boulder is located inside a fence with a locked gate that contains the parrot house. Access is very limited so coordination with the Forestry Division is required. Permissions were required from not only the Forestry Division, but from the person in charge of the Aviary. A new addition to the site in 2011 was an RV (fig. A-3) that is parked very near the pin and will not be removed. Proximity to the Parrot House as well as the height of the surrounding fence means that tripod or tetrapod antennae mount is preferred.

*Installation:* June 2006, stainless steel Bevis pin set with epoxy in a 0.5" hole.



Figure A-3 Dominica campaign site (A) BOTG, 2011 (B) BOTG, 2011

## BRDX

Site located in andesite boulder in a small orchard above a farm just east of TETE (fig. A-4). Take the roads most of the way up to the site and park near the cell tower. Take the path that leads away from the cell tower through the trees to an open field. The site has been overgrown with trees that may require trimming. The landowner was in the process of planting something in the open field so site may be obscured in future visits.

*Installation:* June 2004, stainless steel Bevis pin set with epoxy in a 0.5" hole.

Any type of antenna mount may be used.



Figure A-4 Dominica campaign site (A) BRDX, 2011 (B) BRDX, 2011

#### CABR

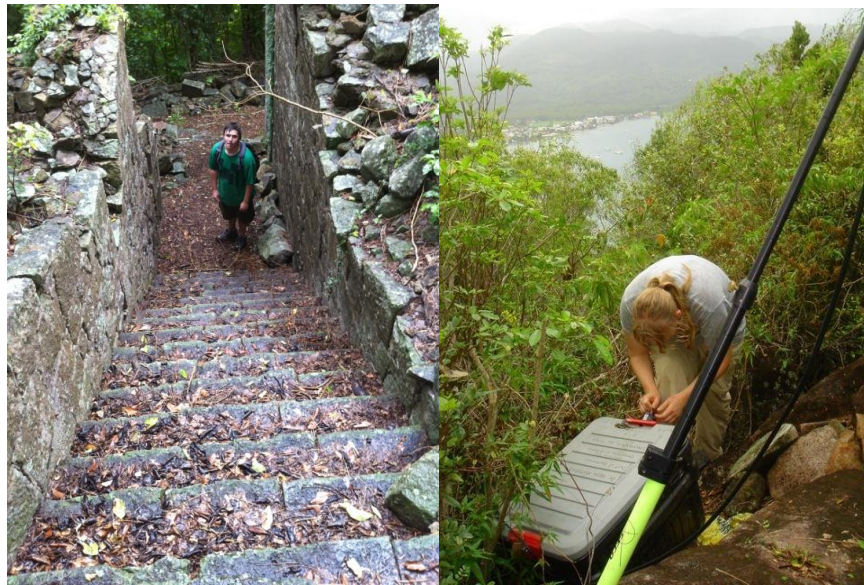
Government permission from the Forestry Division is needed in order to work at this location. In 2011 and 2012 permission was granted by Jacqueline Andre. In 2012, the department instituted a lengthy application process for working in the parks. An exception was granted for us since we were working with the Office of Disaster Management. It was necessary however, to first get permission from the Office of Disaster Management before requesting the permission from the Forestry Division.

Site is located in Cabrits National Park at the North end of the Island (fig. A-5). As you enter the park (which may require finding someone to lift the gate) you will pass a building on the left associated with the ship docks. After passing the docks, you should be able to see a four sided archway. You need to drive through the archway (even though it looks like it is for foot traffic) and head uphill. Before heading through the arch, find a park representative to show the permission letter to and confirm that it is ok to set up equipment. The road up the hill is narrow and cobblestone as you pass through the outer wall of Fort Shirley. Pass the restored portion of the fort and look for a newer

concrete road and follow it uphill a little bit further. There is an old dirt road (4 wheel drive required) that leads over to the parade grounds (fig. A-5) just north of the fort, take this road or park and walk from here. Cross the parade grounds (which may require clearing a path), enter the forest on the other side and look for the ruins of the commandants quarters (fig. A-5). Follow the trail that leads up the hill from here, cross through the ruins of the Douglas Bay Battery (fig. A-5) and keep going. Near the end of the trail, you should find some small cannons. If you are looking along the firing trajectory of the cannons, the site is behind you. Bushwhack to the highest point you can find, the pin is located in an andesite boulder (fig. A-5) most likely overgrown with trees. Depending on where you park, the hike to the site will be a 1-2 mile roundtrip so plan accordingly.

*Installation:* June 2001, stainless steel Bevis pin set with epoxy in a 0.5" hole.

Any type of antenna mount may be used, but a tetrapod is the best choice.



(A)

(B)



Figure A-5 Dominica campaign site (A) CABR, 2011 Ruins of the Douglas Bay Battery must be passed through to reach the site (B) CABR, 2006 (C) CABR, 2011, ruins of the commandant's quarters (D) CABR, 2011, parade grounds overgrown, follow the signs to Douglas Bay Battery

#### CASS

Site is located in bedrock on the southern coast, at Zandoli Inn (fig. A-6).

Permission may be gained from Jen (the owner) who may be reached by email through the Zandoli Inn website (<http://www.zandoli.com>). The groundskeeper's name is Daison, he knows the location of the site and is most helpful. The site is located on the cliffs above the ocean just off of one of the hotel's walking paths. Park in the hotel parking and head towards the hotel. Take a left at the hotel and head down the stairs to the trails.

Cross the creek and continue to choose the "high road" trails. After walking 100 yards or so, parallel to the coastline, start looking for a place to cut through the trees and emerge onto rocky cliffs. The pin is located in a rock near the tree line. A spike mount is preferred for antennae setup at this site.

*Installation:* June 2001, stainless steel Bevis pin set with epoxy in a 0.5" hole

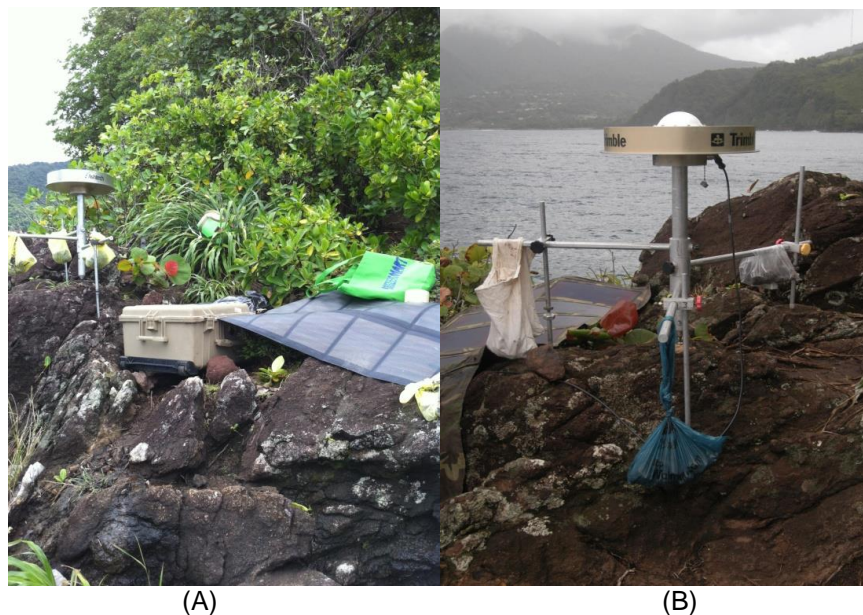


Figure A-6 Dominica campaign site (A) CASS, 2012 (B) CASS, 2006

#### CNCD

Site is located on the road that leads from the airport to Ponde Casse (fig. A-7), approximately 3.5 km after the road turns away from the ocean (this road was closed in 2011 and 2012 so 4 wheel drive was required). The site is located on a large boulder (requires scrambling up) on private property on the south side of the road. The nearest most notable landmark is the pink modern style house just to the north of the property.

The property owners were not present, but the caretakers of the property were able to grant permission for access, and showed us to and cleared the site which was quite overgrown.

*Installation:* June 2001, stainless steel Bevis pin set with epoxy in a 0.5" hole. A spike mount is preferable for this site.





Figure A-7 Dominica campaign site (A) CNCD, 2006 (B) CNCD, 2006

#### COHT

Site is located just off the main road near Colihaut (fig. A-8). The pin is located on the top of a large andesite outcrop on the south side of road which will most likely be obscured by foliage. There is a spot to pull off the road just uphill from the site. The landowner's name is Emmanuel, he lives up the mountain. The working surface around the pin is very small which makes it unsuitable for a tetrapod. A carefully placed tripod or a spike mount will work at this location.

*Installation:* June 2006, stainless steel Bevis pin set with epoxy in a 0.5" hole

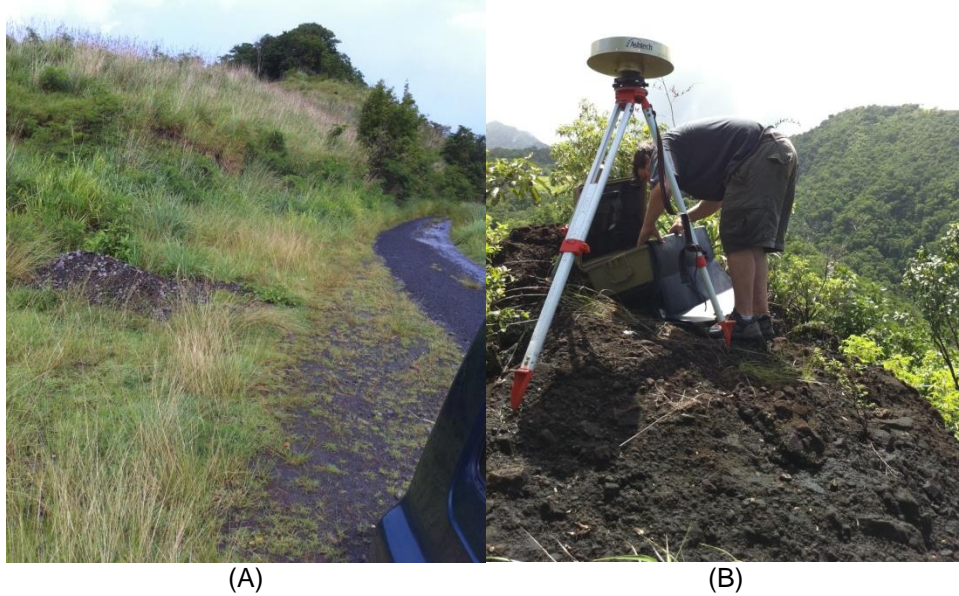


Figure A-8 Dominica campaign site (A) COHT, 2012 Place to park, site is located at the top of the peak shown (B) COHT, 2012

#### CONN

Site is located in large andesite boulder on top of a hill in a clearing at Connor Estates (fig. A-9). The owner of the property is Andre and in 2011, the property was for sale. His nephew was in the process of building the next house to the north. There is a driveway up to the property, but I do not recommend driving on it. We parked at the base and walked up towards the house. Before you get to the house, cut left through the grove of fruit trees. The boulder is located on the slope between the trees and the road. Andre is very friendly and says researchers are always welcome. A spike mount is best for this location.

*Installation:* June 2006, stainless steel Bevis pin set with epoxy in a 0.5" hole



(A)

(B)

Figure A-9 Dominica campaign site (A) CONN, 2011 (B) CONN, 2011, path up to house with new concrete

#### ELOI

Site is located in bedrock on the floor of an abandoned quarry (fig. A-10). Any type of antenna mount could be implemented at this site. This site was not occupied due to time and logistical constraints.

*Installation:* June 2003, stainless steel Bevis pin set with epoxy in a 0.5" hole.



(A)

(B)

Figure A-10 Dominica campaign site (A) ELOI, 2006 (B) ELOI, 2006

## FRSH

Site is located near the shore of Freshwater Lake in the National Park at the base of Morne Microtrin (fig. A-11). Government permissions are required in order to work on this site. The road to this location is well paved. Take the road all the way to the park, drive past the park buildings and through a green metal gate where you may park. The pin is located in a buried boulder at ground level and very difficult to find. In 2012, it was completely covered with soil and chest high foliage. A tripod or tetrapod is needed for this site.

*Installation:* June 2001, stainless steel Bevis pin set with epoxy in a 0.5" hole.

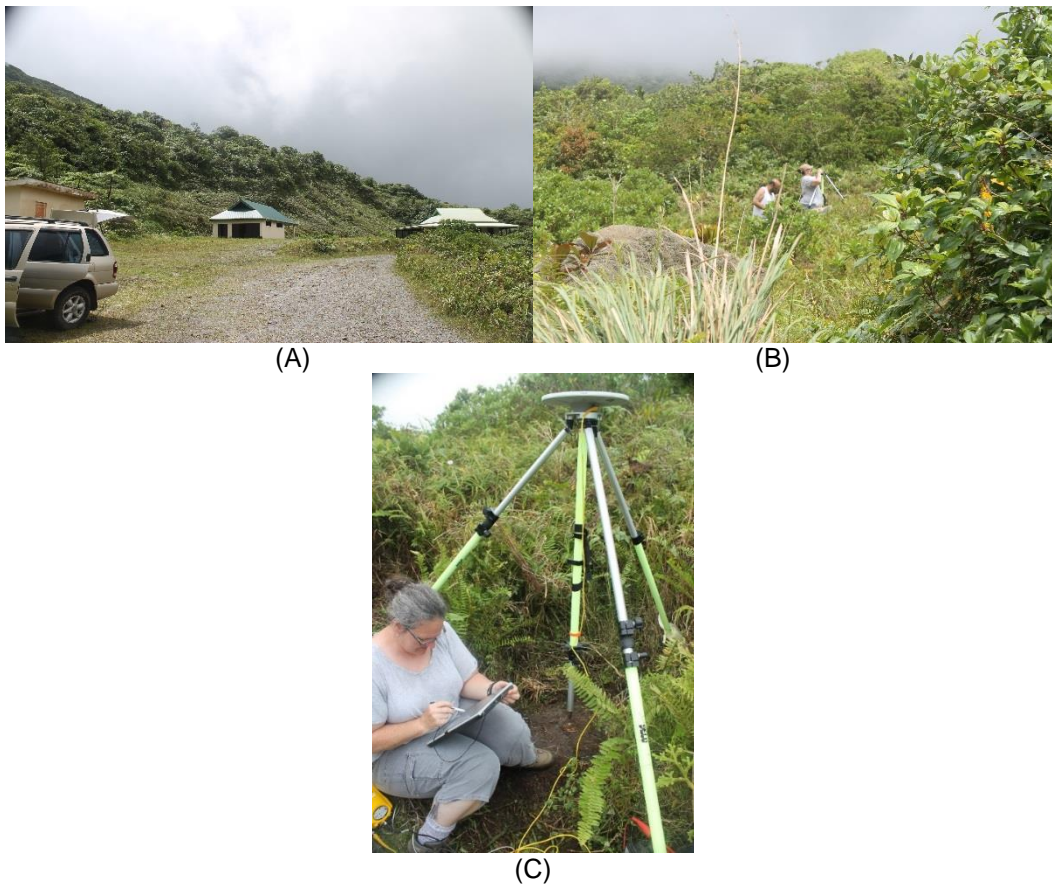


Figure A-11 Dominica campaign site (A) FRSH, 2012, looking at park entrance with lake to right and site to rear (B) FRSH, 2012, view of site from parking area (C) FRSH, 2012

## GOMM

Site is located in a small concrete roof of the pool equipment building adjacent to the pool at Gommier Estates (fig. A-12). The house belongs to the Scotia Bank, and the main office must be contacted for permission to access the site. It is easiest to make an appointment with the bank manager and visit the bank in person for permission. Once at the site, the caretakers can unlock the gate next to the pool equipment house. A spike mount is the ideal for this location.

*Installation:* June 2001, stainless steel Bevis pin set with epoxy in a 0.5" hole.

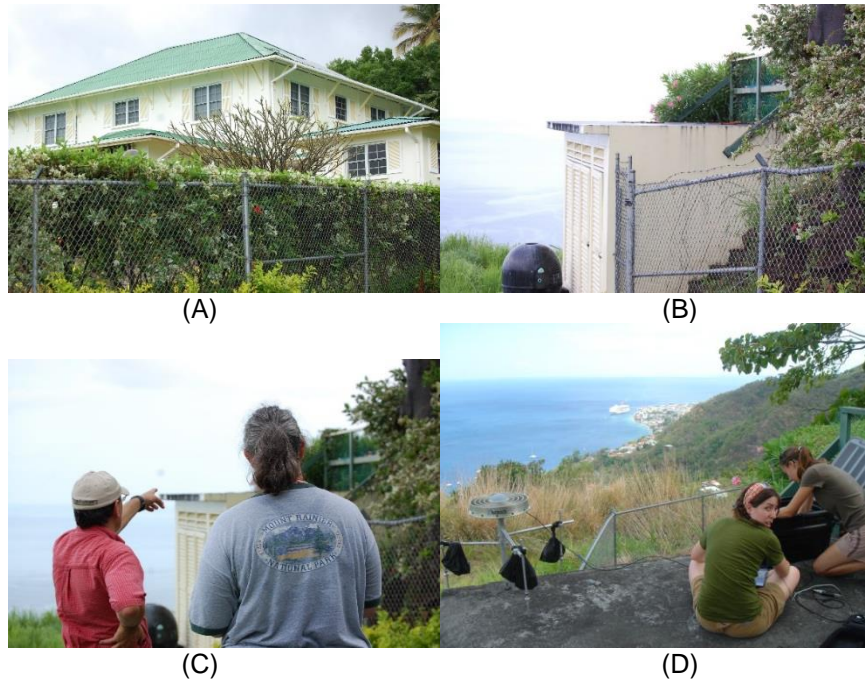


Figure A-12 Dominica campaign site (A) GOMM, 2011, the estate where the site is located (B) GOMM, 2011, view of the pool equipment building (C) GOMM, 2011, pin located very near the end of Glen Mattioli's pointed finger (D) GOMM, 2006

## GSAV

Site is on top of a large andesitic outcrop on the property of the Stonehedge Safari Hotel (fig. A-13). The road to the hotel is through a grassy field that leads to an oceanside cliff. A spike mount is required, the area around the site is very limited. A black plastic water tank has recently been installed very near the site which creates an obstruction that may cause interference. Owner is very friendly and helpful, his presence insures the security of this location.

*Installation:* June 2004, stainless steel Bevis pin set with epoxy in a 0.5" hole.



Figure A-13 Dominica campaign site (A) GSAV, 2011 Harrison Miller pointing to site  
(B) GSAV, 2011 site installed

## GUIG

Site is located in a small concrete foundation atop a hill at Point Guignard on the west coast of the island (fig. A-14). The land has changed hands twice since the site was installed. Wayne Abraham attempted unsuccessfully to find the current owner for permission. There is a fence with a locked gate and "no trespassing" signs posted so permission is required. There are stairs that lead to the site.

*Installation:* June 2006, stainless steel Bevis pin set with epoxy in a 0.5" hole.



Figure A-14 Dominica campaign site (A) GUIG, 2006 (B) GUIG, 2006

## MHAM

Site is located in a boulder in a field near Middleham Falls (fig. A-15). Follow GPS along the road to Middleham and park near the house shown in figure A-15. Cross through an orchard and head downhill from the road. The ground is very soft so a tripod/tetrapod is best. In 2011, the site was overgrown with ground cover.

*Installation:* June 2007, stainless steel Bevis pin set with epoxy in a 0.5" hole.



Figure A-15 Dominica campaign site (A) MHAM, 2011

#### MNTV

The site is located in a boulder on a slope behind a green bar/restaurant facility that is only open sporadically. The owner does not live in the country, the next door neighbor's name is Alan and he knows the location of the pin. This location is pretty close to the road and easy to get to. Park at the green guard hut shown in figure A-16, cross the courtyard and head uphill. A tripod/tetrapod is best for this location.

*Installation:* June 2007, stainless steel Bevis pin set with epoxy in a 0.5" hole.





Figure A-16 Dominica campaign site (A) MTNV, 2011 (B) MTNV, 2012 (C) MTNV, 2011, parking location (D) MTNV, 2006

## NEWF

Site is located on an andesite boulder in a field (fig. A-17). Landowner approval is required. The owner's name is Joseph (767-617-2333) and he will demand payment for land use. In 2012, he was paid \$400 (Caribbean) for 4 occupation days. Although at first meeting, he may seem confrontational, he is very helpful. If you arrange a time with him, he will clear a path to and around the site, and will assist with the transport of gear. He knows the location of the site, which will be difficult to find without him due to the overgrowth. In 2012, the boulder in figure A-17 was surrounded by head-height foliage.

Installation: June 2001, stainless steel Bevis pin set with epoxy in a 0.5" hole.

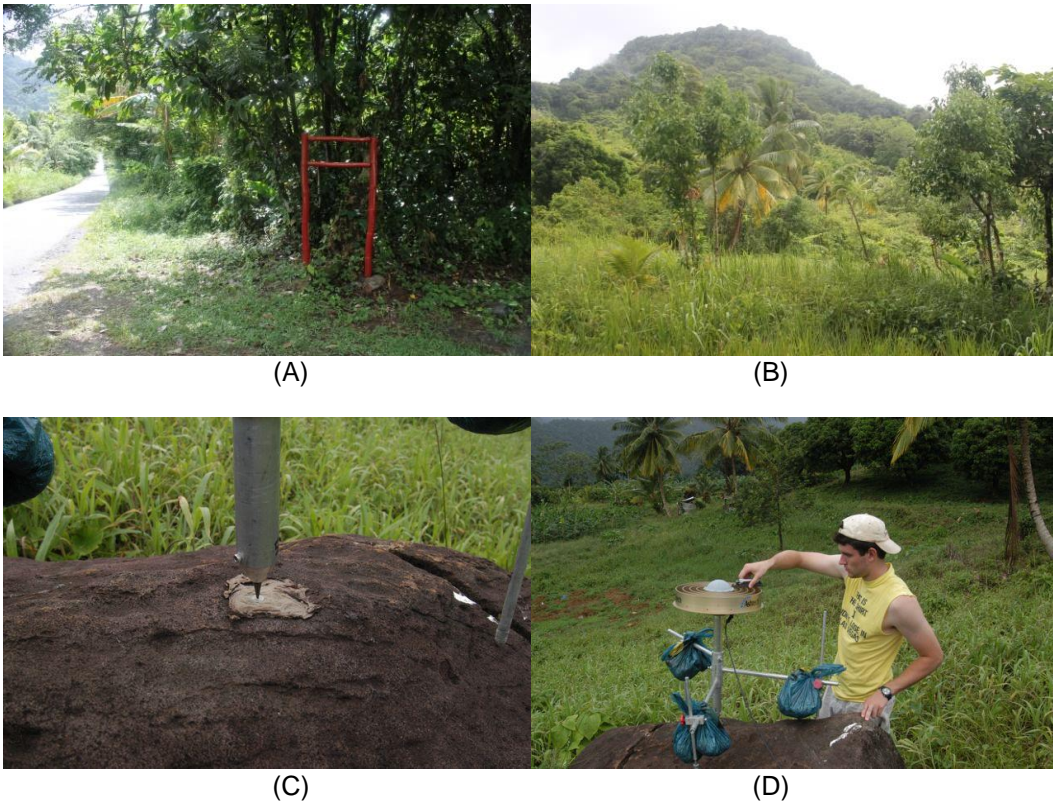


Figure A-17 Dominica campaign site (A) NEWF, 2012, location to park (B) NEWF, 2012, looking north, site is approximately 100m into the field, entirely obscured by vegetation (C) NEWF, 2006 (D) NEWF, 2006

## NVEN

Site is located in a concrete foundation at the edge of a field (fig. A-18). The road to this location is in very poor condition, four-wheel drive required. Following GPS, you will be able to drive most of the way to this site. You will walk approximately 75 yards along a dasheen field to its back edge where the slab is located. In 2011, the concrete slab was completely overgrown and not visible (fig. A-18). Any type of standard antenna mount will work for this location. The landowner is Mathew Bernard (277-6063) and he is very friendly. Notify him or a neighbor before setting up equipment.

*Installation:* June 2004, stainless steel Bevis pin set with epoxy in a 0.5" hole



(A)

(B)



Figure A-18 Dominica campaign site (A) NVEN, 2011 before cleared  
 (B) NVEN, 2011 cleared (C) NVEN, 2006 (D) NVEN, 2006

SCTT

Site is located in a boulder on top of Scott's Head at the southern tip of the Island (fig. A-19). In 2011 it had been completely covered with soil and vegetation. A narrow land bridge (rocky beach) is crossed before heading up the hill. The dirt road that leads up to the tower was drivable in 2011 and you can park and turn around at the tower. The short walk up to the peak from here begins with concrete stairs and ends with a scramble.

*Installation:* June 2001, stainless steel Bevis pin set with epoxy in a 0.5" hole



(A)



(B)

Figure A-19 Dominica campaign site (A) SCTT, 2011 view of land bridge and tower to park near (B) SCTT, 2011 installed

## SOIE

Site is located at Point La Soie on the north coast of the island (fig. A-20). Park on the shoulder and walk about 300m along a path through the orchard towards the coast. The path to take used to be a dirt road but trees have been cut down to block passage. Any mount may be used, the area surrounding the site is flat and rocky adjacent to the coast.

*Installation:* June 2003, stainless steel Bevis pin set with epoxy in a 0.5" hole



Figure A-20 Dominica campaign site (A) SOIE, 2011

## SPAG

Site is located in an andesite boulder at the base of cellular towers atop Morne Espagnole (fig. A-21). The road to the top is very steep with tight switchbacks (even by Dominica standards), it is not advisable to drive the entire way to the top. A spike mount is required for this site. The site is near the cable and wireless long-range transmission antennae.

*Installation:* June 2004, stainless steel Bevis pin set with epoxy in a 0.5" hole.



Figure A-21 Dominica campaign site (A) SPAG, 2012 (B) SPAG, 2012

## SPNG

Site sits in andesite boulder on the grounds of Springfield Estates. Take the steps that lead down to the river from the main porch and make an immediate right once at the base of the rock wall that provides support for the porch. The pin is in a boulder next to the wall that will probably be covered with foliage. A tetrapod works best at this location. AC power is available with use of extension cords from the main facility.

*Installation:* June 2004, stainless steel Bevis pin set with epoxy in a 0.5" hole

## TETE

Site located in andesite boulder near the top of Tete Morne (fig. A-22). It is in a clearing located behind a large cylindrically shaped concrete structure (fig. A-22) just before the end of the 4x4 road leading to the mountain top. Any type of antennae mount is suitable for this location. In 2012 we encountered the landowner, who was friendly, tending crops on this property.

*Installation:* June 2004, stainless steel Bevis pin set with epoxy in a 0.5" hole



Figure A-22 Dominica campaign site (A) TETE, 2012 (B) TETE, 2012, park at this location and take a path to the left of this concrete structure

## WOTT

Site located on the roof of the primary schoolhouse in Wotten Waven (fig. A-23). Either a tall ladder or a ladder placed in the bed of a truck will be required to access the site. The pin is set into the roof just behind the basketball goal. We stayed at Archbold Tropical Research Center (Springfield Guesthouse), and were able to borrow a ladder from the caretaker Desmond.

*Installation:* June 2001, stainless steel Bevis pin set with epoxy in a 0.5" hole





Figure A-23 Dominica campaign site (A) WOTT, 2012 (B) WOTT, 2012

WQ95

Site located on the roof of what used to be WQ95 radio station (fig. A-24). In 2011/2012, the building was owned by Dragon Windows ([www.dragonwindows.com](http://www.dragonwindows.com)), but no one was ever present. Numerous unsuccessful attempts in 2011/2012 were made to gain permission to install. A spike mount is required for this location.

*Installation:* June 2006, stainless steel Bevis pin set with epoxy in a 0.5" hole



Figure A-24 Dominica campaign site (A) WQ95, 2006 (B) WQ95, 2006

Appendix B  
COCONet Time Series

For all time series in this Appendix:

Red dots are the daily position estimates (16 – 24 hr occupations).

Blue lines are the predicted plate rates in IGS08 held fixed (horizontal).

Green lines are the least squares best-fit site rates in IGS08 with respect to the  
Caribbean plate rate (CA).

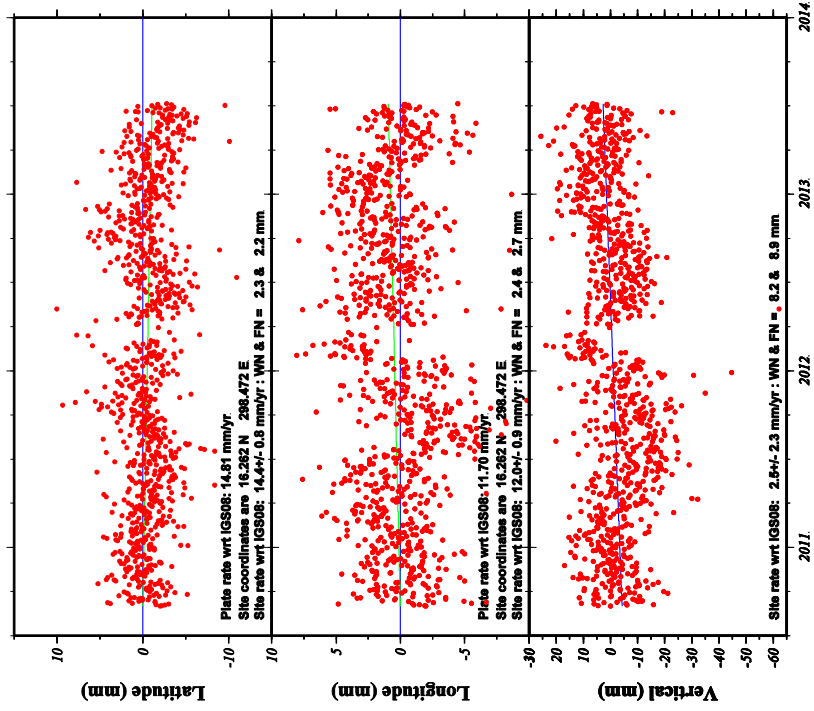
WN = white noise estimates

FN = flicker noise estimates

Black vertical dotted lines indicate when a correction has been made for an offset created  
either by a seismic event or an antenna change.

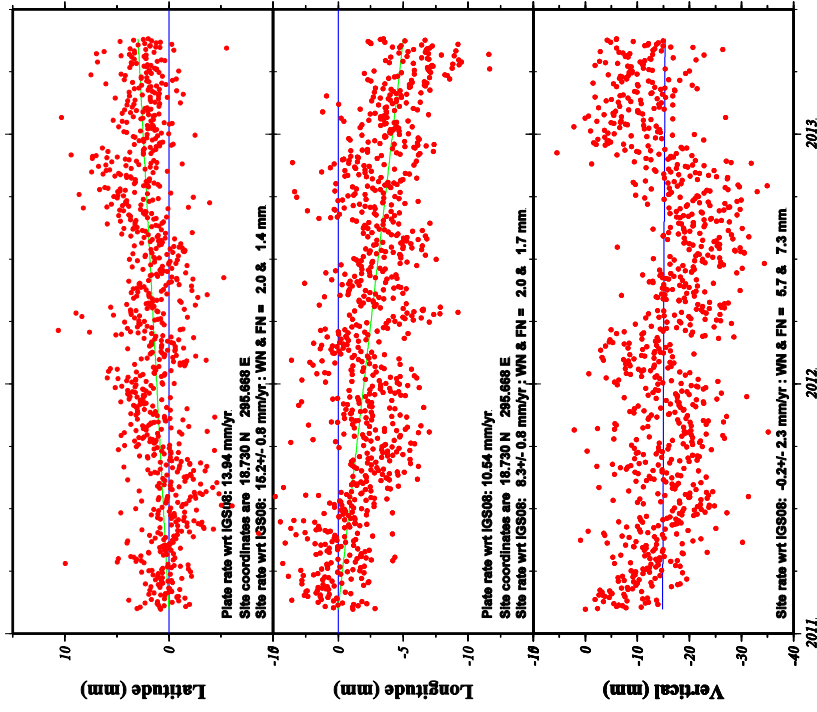
These data have been processed using GIPSY-OASIS II version 6.2, with ambiguity  
resolution on, using VMF1GRID for tropospheric corrections, and using absolute  
antenna phase center information.

ABMF Coordinate changes - CA is fixed stacovs used AMB



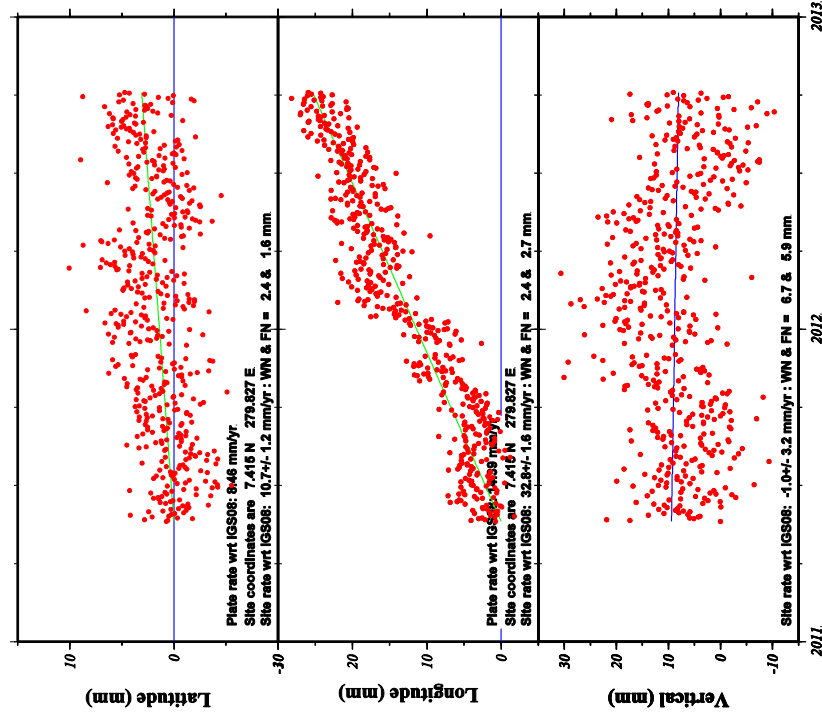
GMV 2013 Jul 17 14:24:24 | MedialUNTA

ABVI Coordinate changes - CA is fixed stacovs used AMB



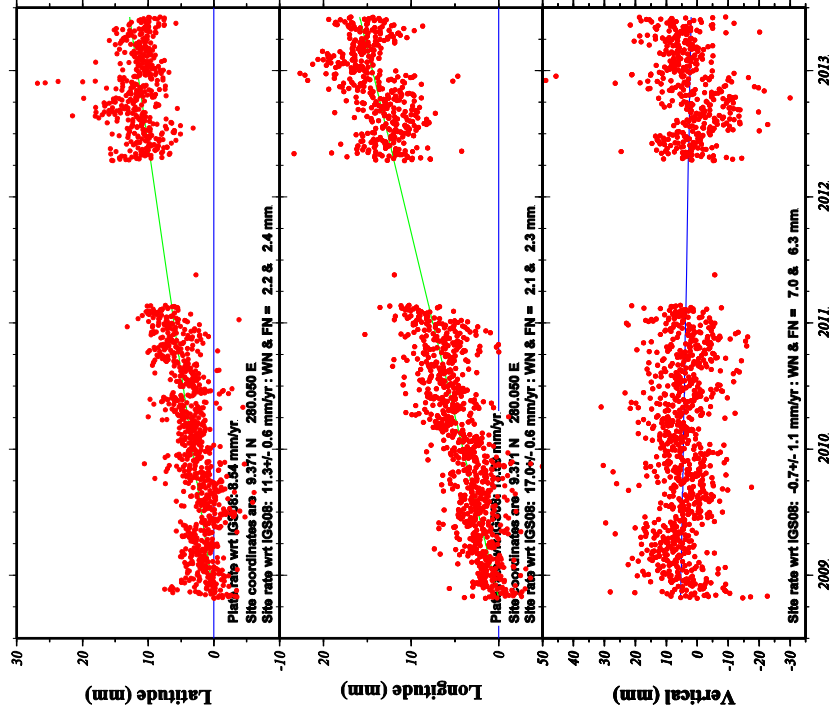
GMV 2013 Jun 13 08:38:07 | MedialUNTA

ACHO Coordinate changes - CA is fixed stacovs used AMB



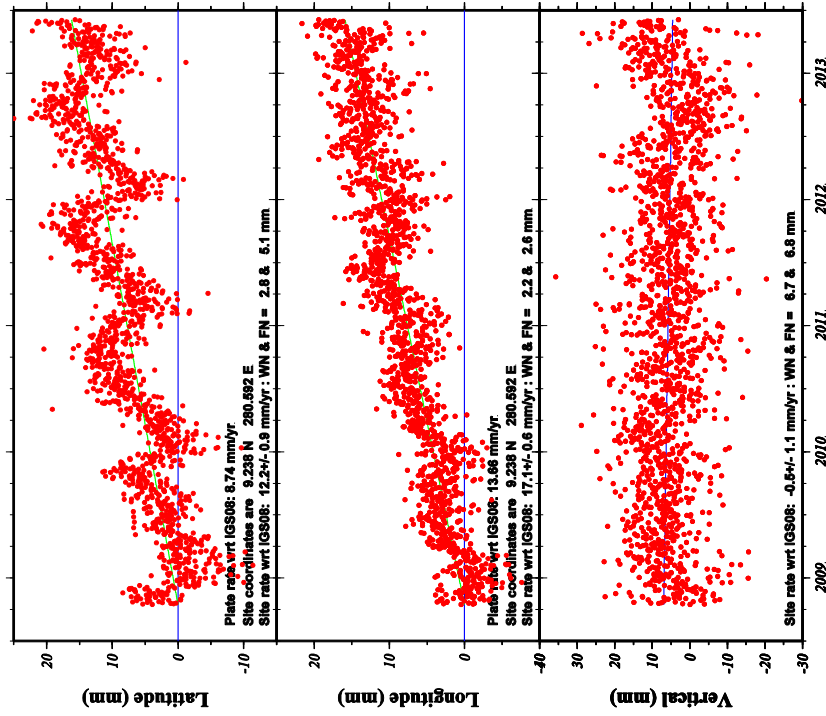
GM7 2013 Jun 18 20:16:54 Metrolab/UTA

ACP1 Coordinate changes - CA is fixed stacovs used AMB



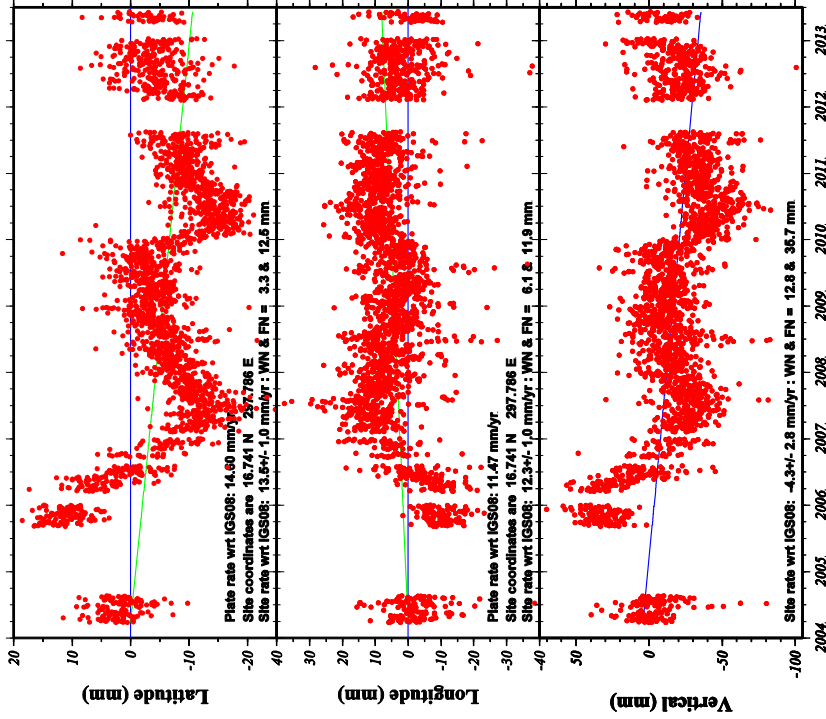
GM7 2013 Jun 19 08:20:10 Metrolab/UTA

ACP6 Coordinate changes - CA is fixed stacovs used AMB



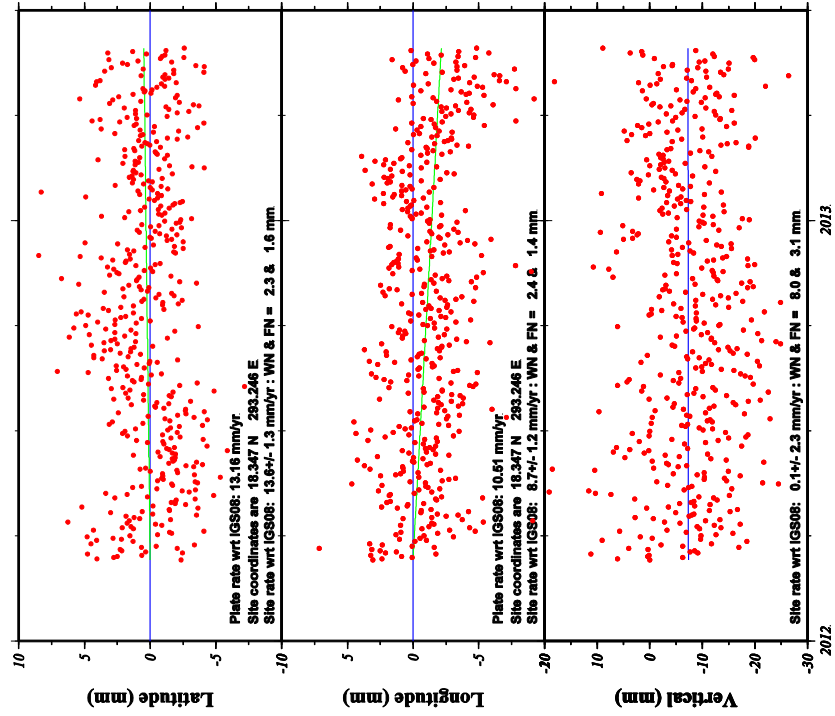
GM7 2013 Jun 25 13:44:38 | MafholoUTA

AIRS Coordinate changes - CA is fixed stacovs used AMB



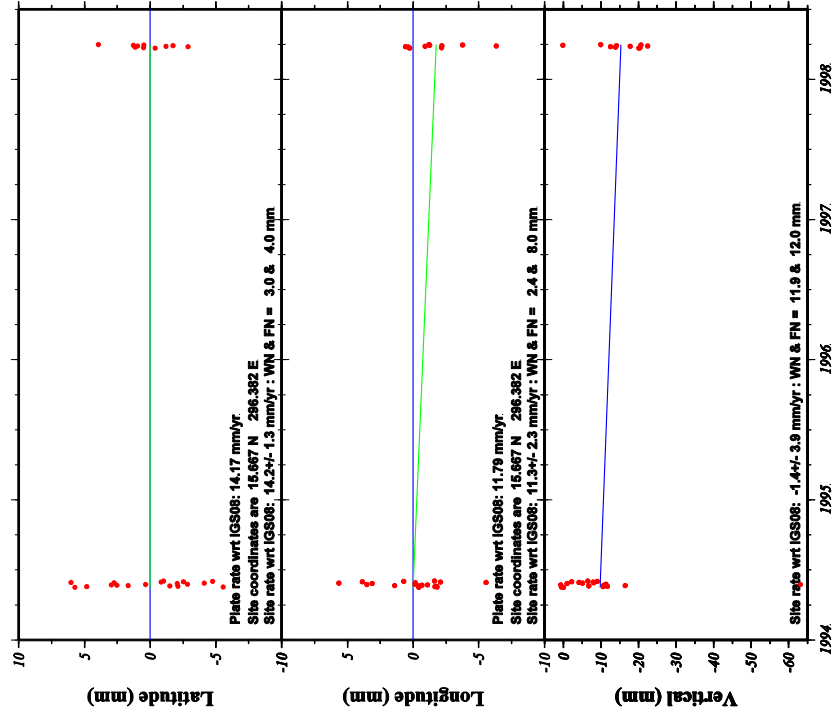
GM7 2013 Jul 03 08:20:12 | MafholoUTA

AOPR Coordinate changes - CA is fixed stacovs used AMB



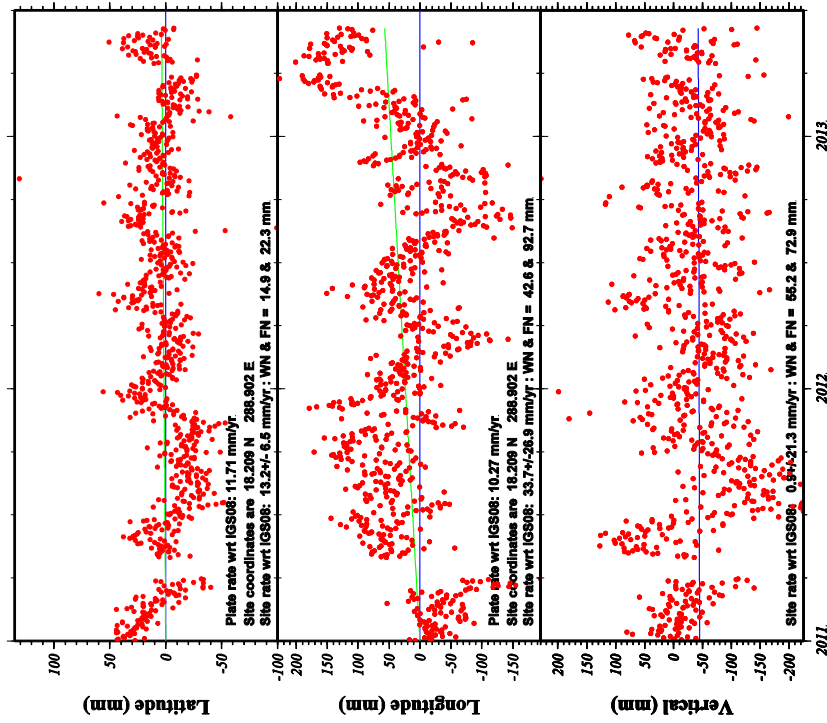
GM 2013 Jul 30 08:27:29 MATHSOUTA

AVES Coordinate changes - CA is fixed stacovs used AMB



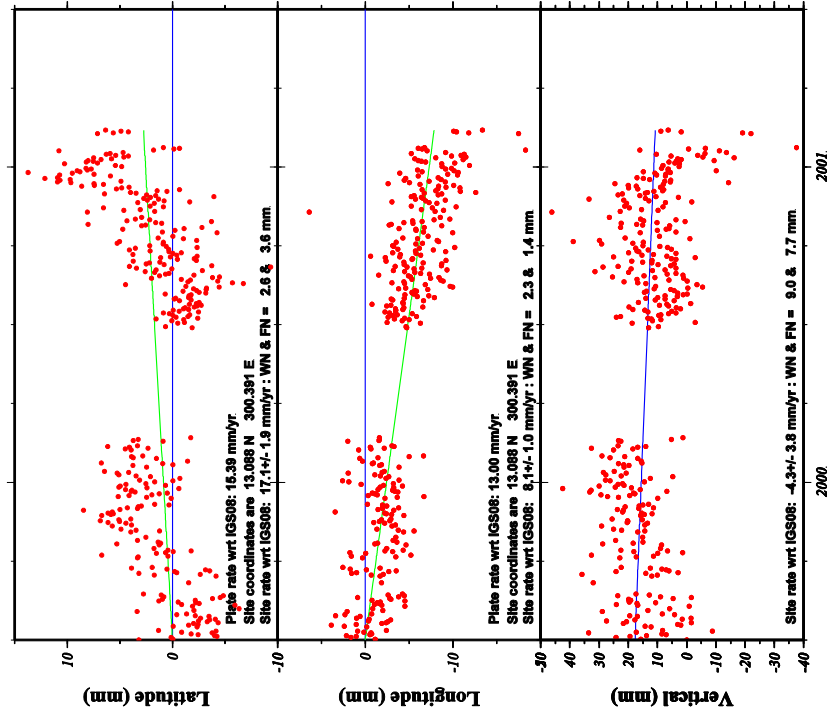
GM 2013 Jun 12 16:42:01 MATHSOUTA

**BARA Coordinate changes - CA is fixed stacovs used AMB**



GM7 2013 Jun 25 13:37:16 Msdh01UTA

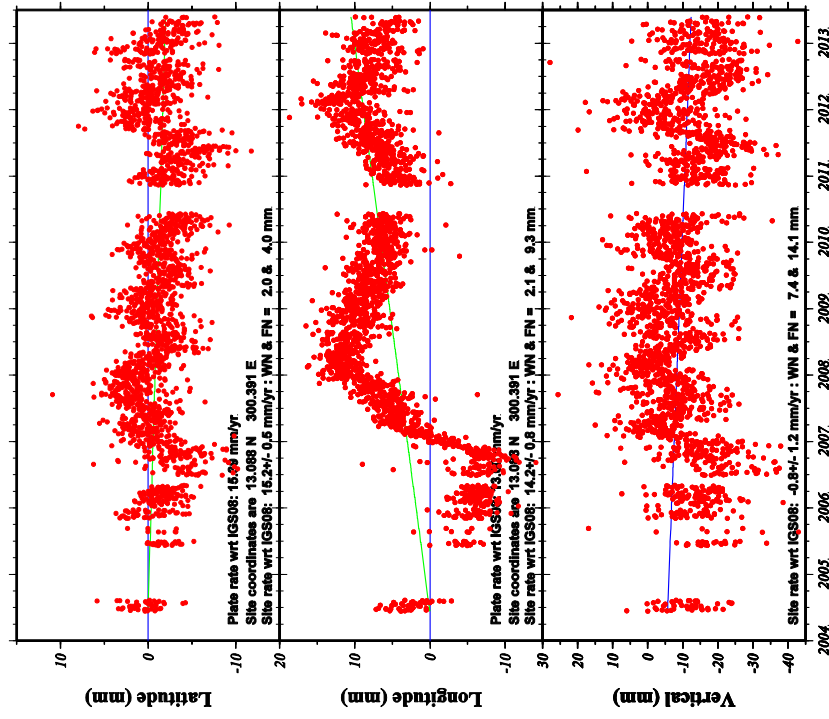
**BARB Coordinate changes - CA is fixed stacovs used AMB**



GM7 2013 Jul 22 15:12:13 Msdh01UTA

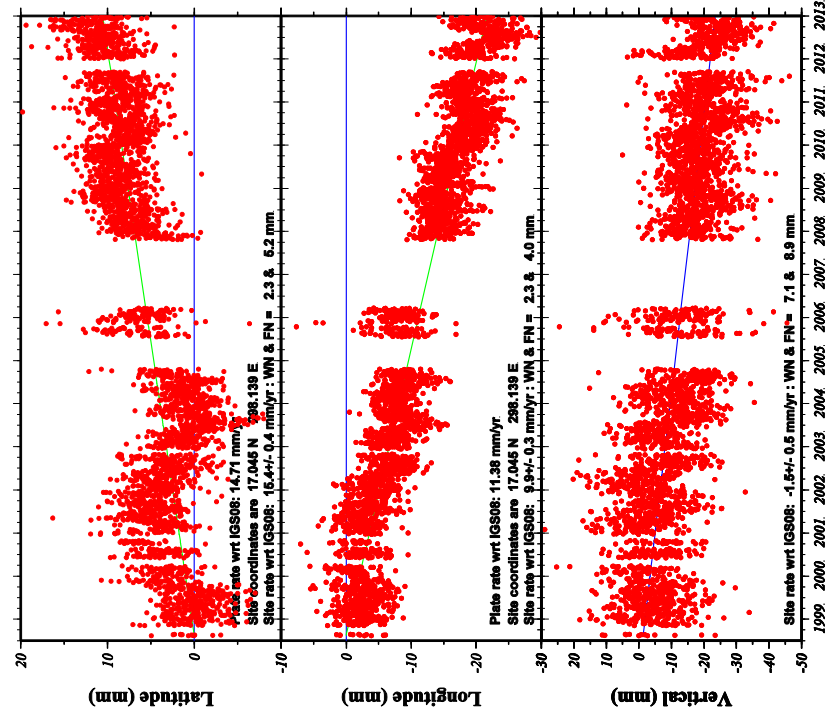


BDOS Coordinate changes - CA is fixed stacovs used AMB



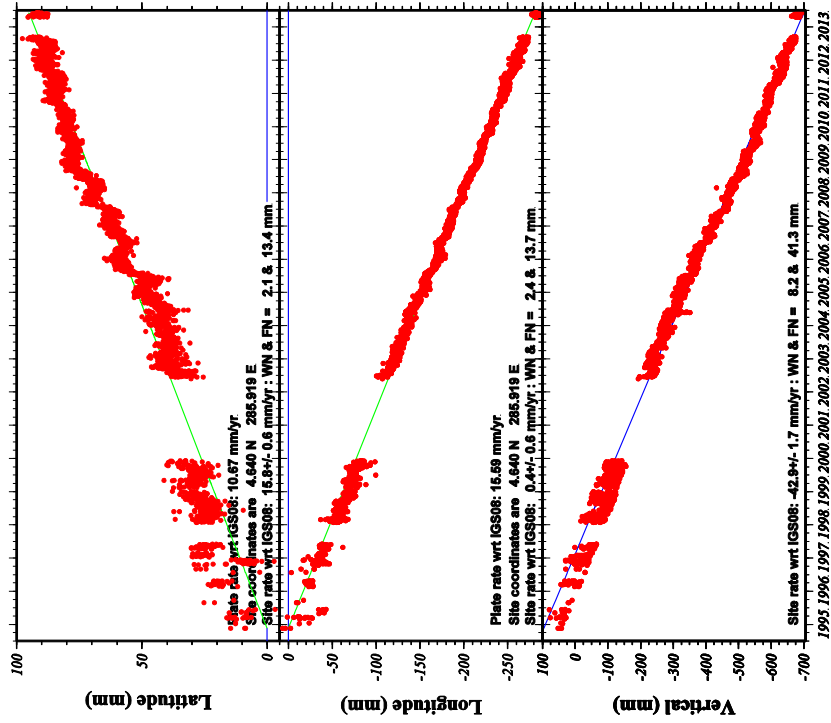
GM7 2013 Jun 28 13:27:59 Mafic/OUTA

BGGY Coordinate changes - CA is fixed stacovs used AMB



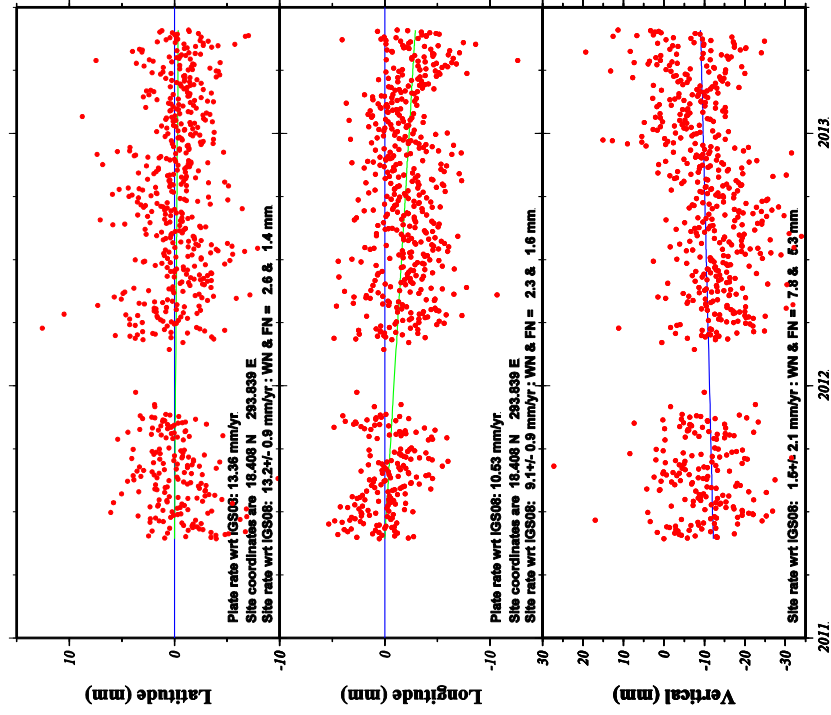
GM7 2013 Jul 03 14:15:14 Mafic/OUTA

BOGT Coordinate changes - CA is fixed stacovs used AMB



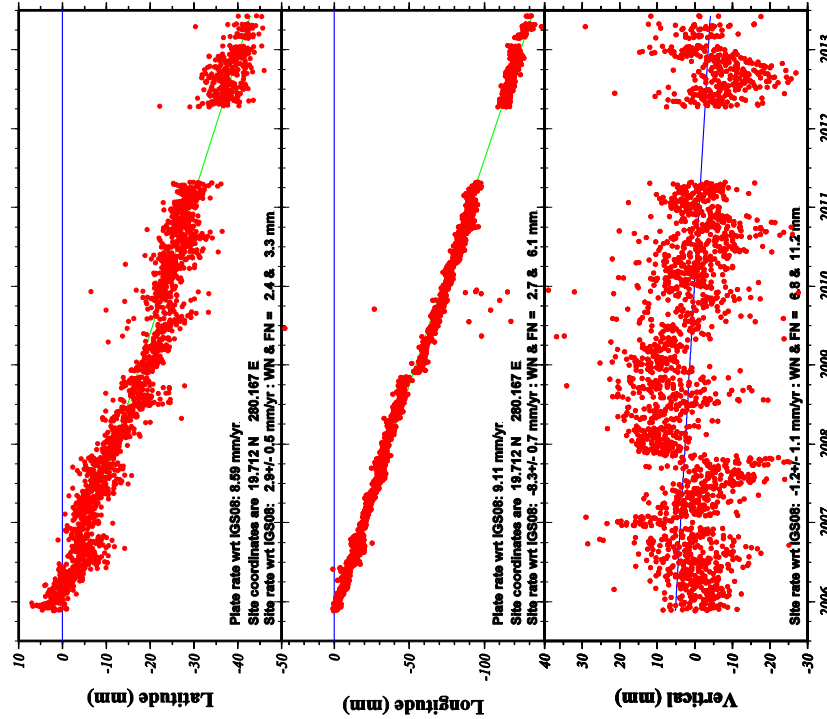
GM7 2013 Jul 30 08:47:47 | Metrolab/UTA

BYSP Coordinate changes - CA is fixed stacovs used AMB



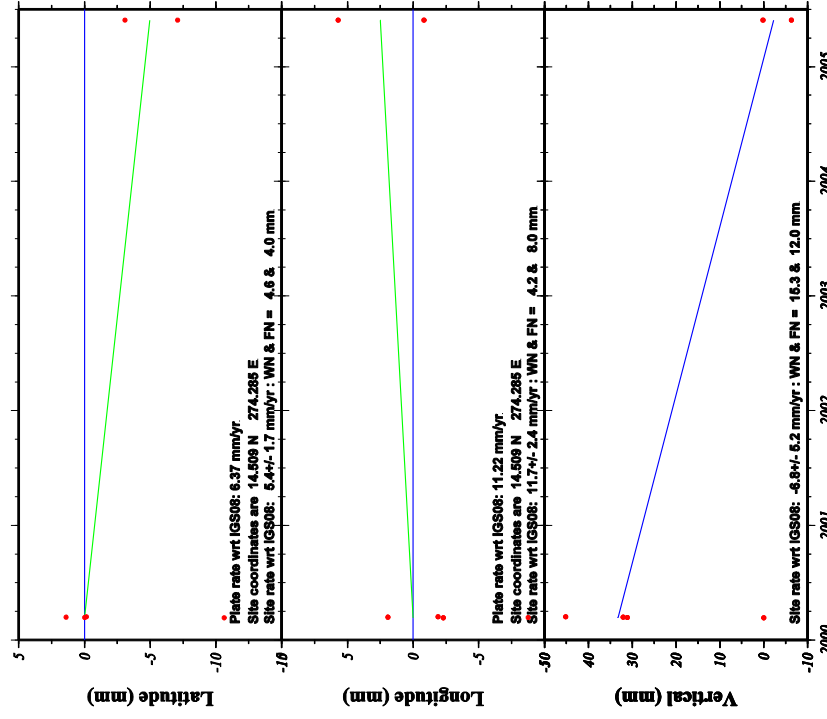
GM7 2013 Jun 13 21:00:51 | Metrolab/UTA

CBSB Coordinate changes - CA is fixed stacovs used AMB



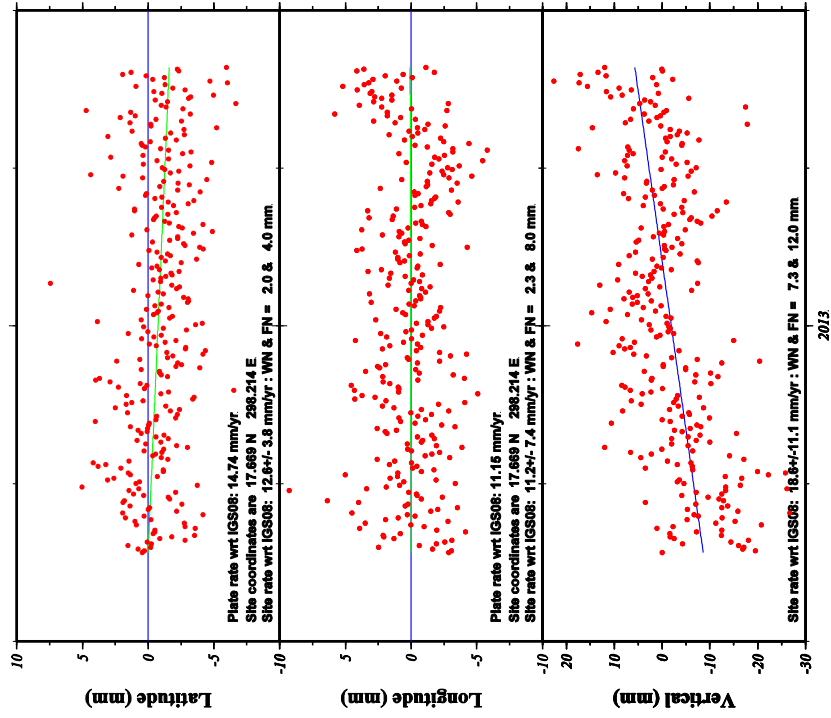
GM7 2013 Jul 01 12:57:56 | MATH607A

CMP1 Coordinate changes - CA is fixed stacovs used AMB



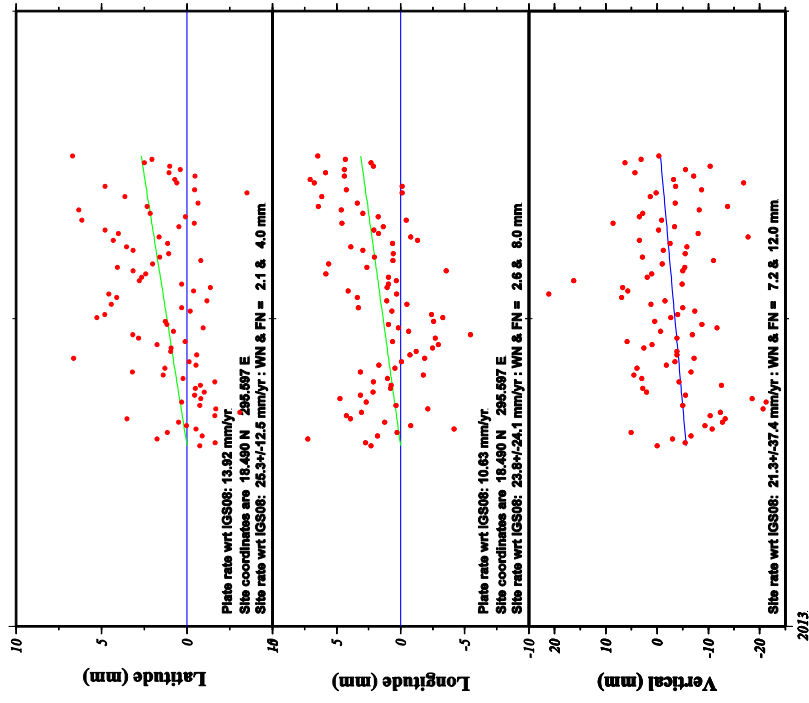
GM7 2013 Jul 22 18:25:18 | MATH607A

CN00 Coordinate changes - CA is fixed stacovs used AMB



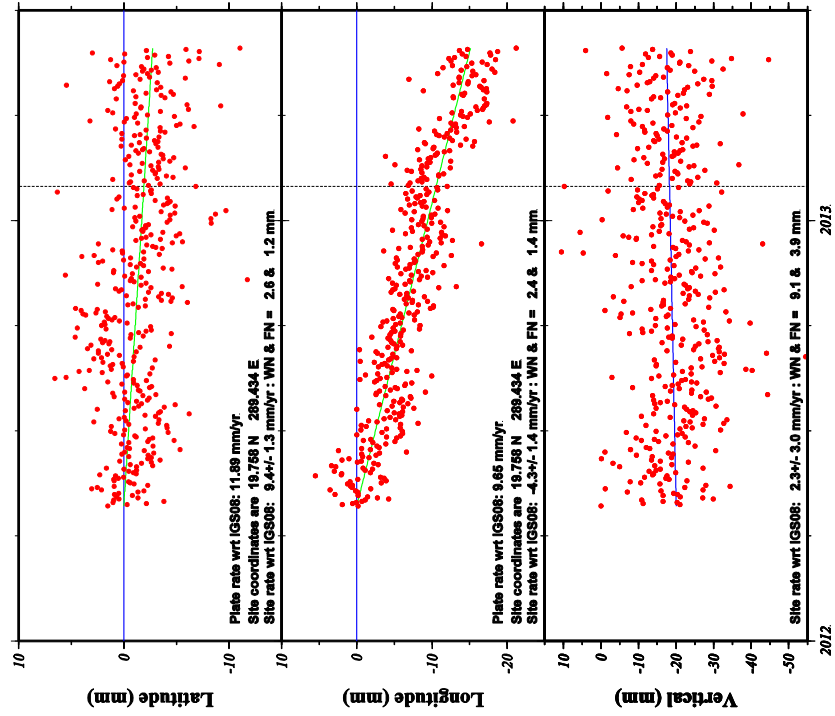
2013 Jun 12 13:35:48 MetcalUKITA

CN03 Coordinate changes - CA is fixed stacovs used AMB



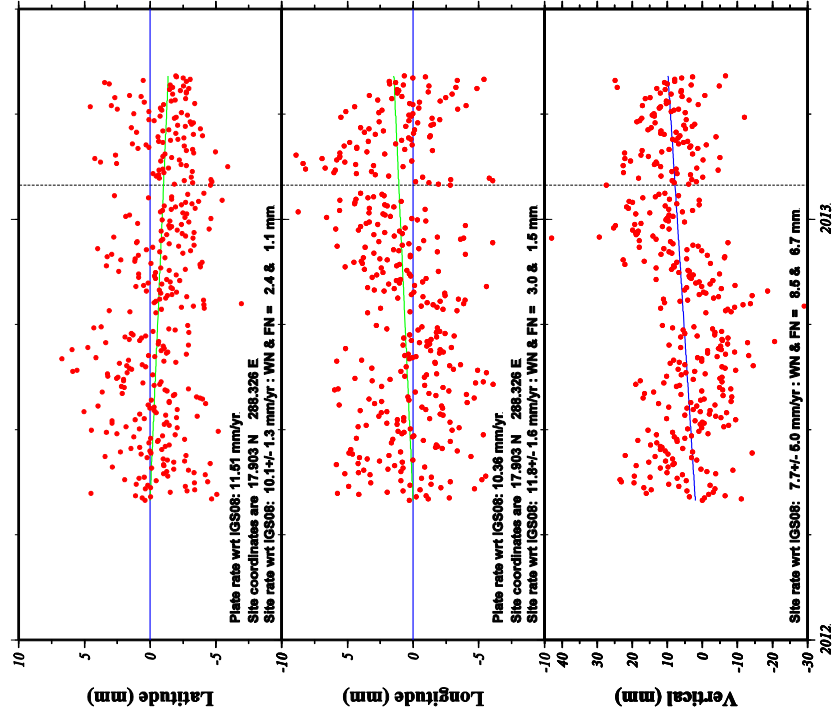
2013 Jun 21 21:45:11 MetcalUKITA

CN07 Coordinate changes - CA is fixed stacovs used AMB



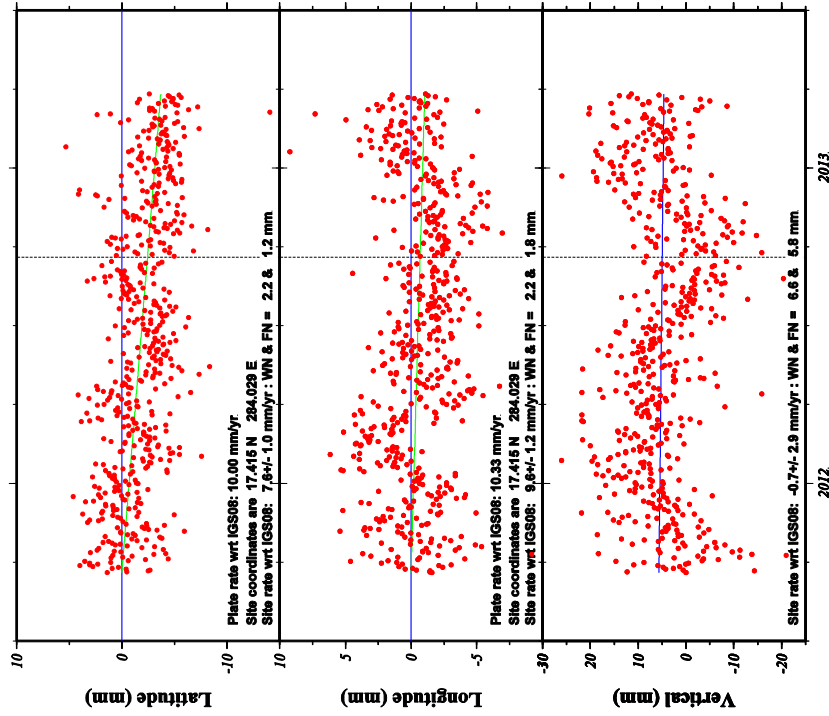
GM7 2013 Jun 21 10:42:07 MadsHolmUTA

CN08 Coordinate changes - CA is fixed stacovs used AMB



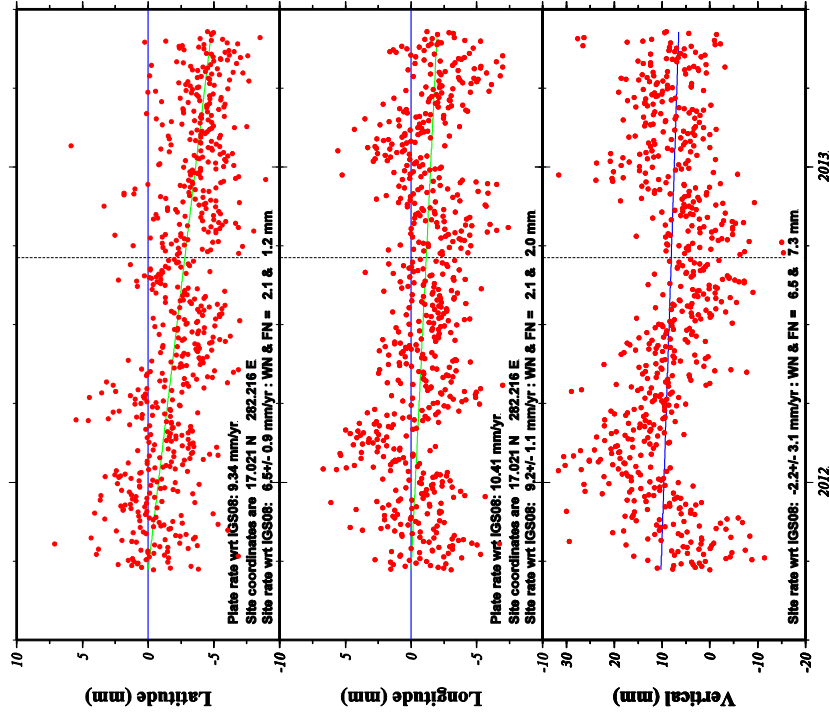
GM7 2013 Jun 21 11:27:08 MadsHolmUTA

CN10 Coordinate changes - CA is fixed stacovs used AMB



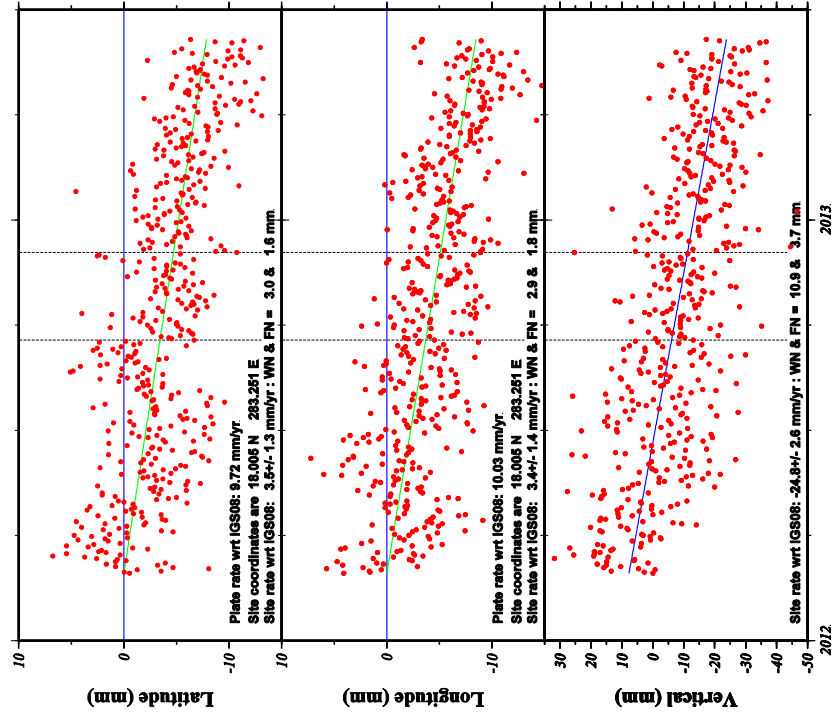
GM 2013 Oct 30 10:02:48 MetrolabUTA

CN11 Coordinate changes - CA is fixed stacovs used AMB



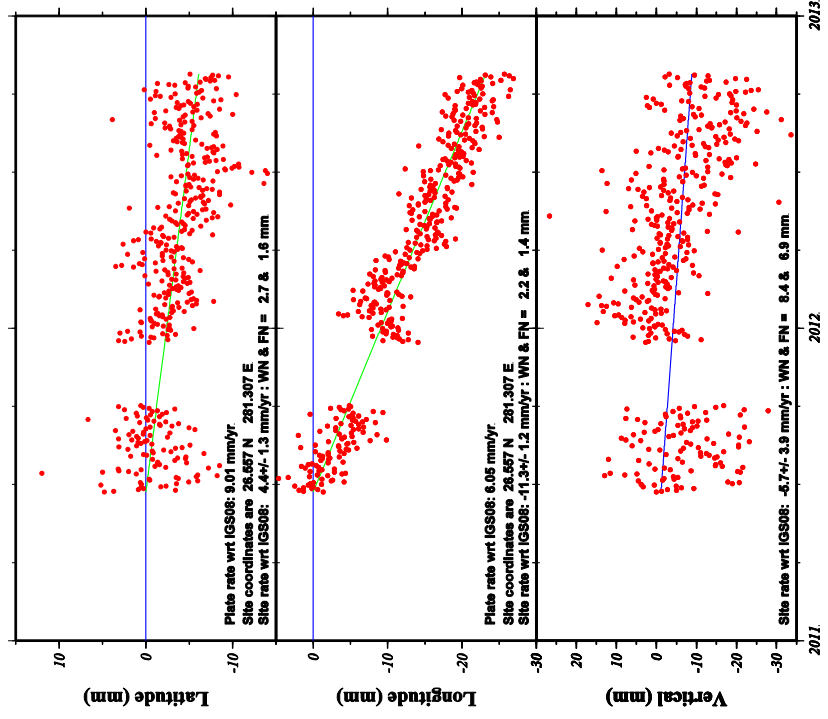
GM 2013 Oct 30 10:10:48 MetrolabUTA

CN12 Coordinate changes - CA is fixed stacovs used AMB



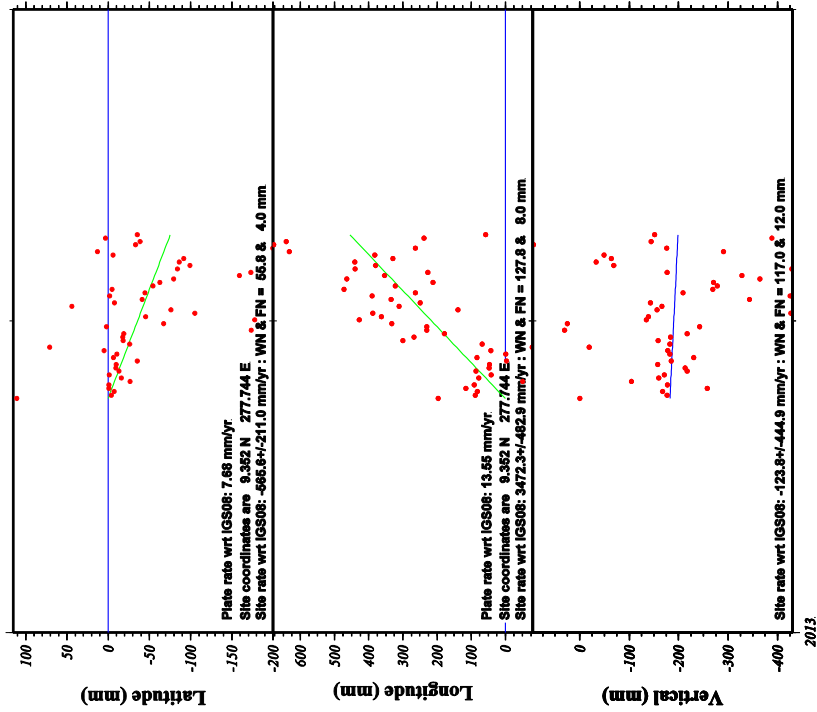
GM2 2013 Jun 22 02:46:44 MestohiUTA

CN15 Coordinate changes - CA is fixed stacovs used AMB



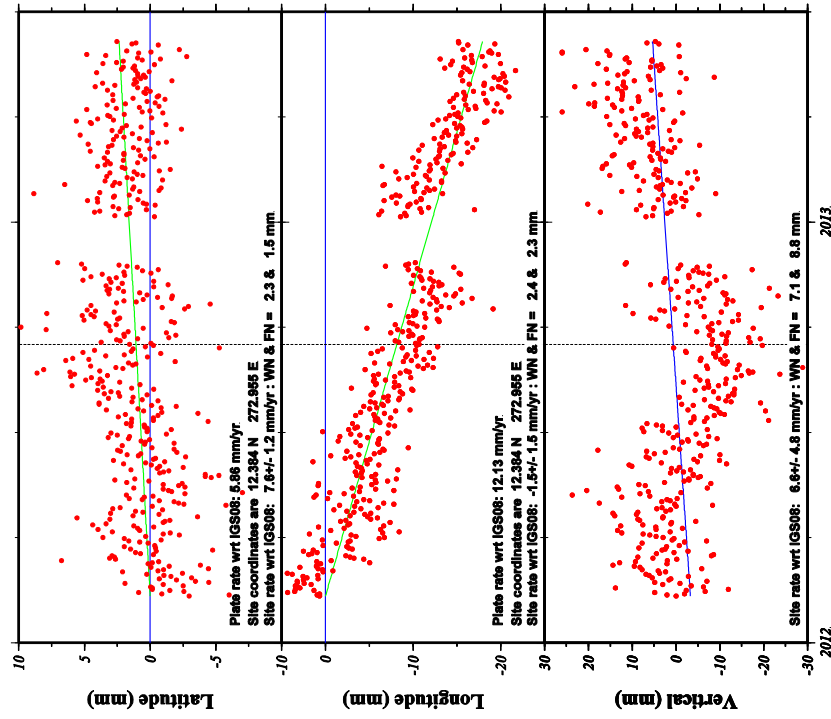
GM2 2013 Jun 22 02:59:10 MestohiUTA

CN20 Coordinate changes - CA is fixed stacovs used AMB



GMV 2013 Sep 15 11:29:47 MetcalfUTA

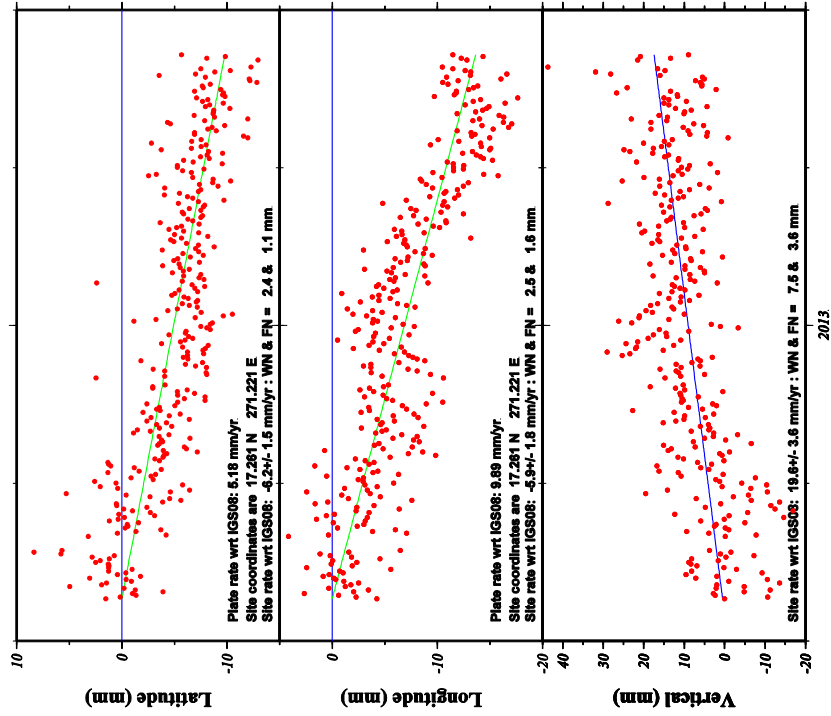
CN22 Coordinate changes - CA is fixed stacovs used AMB



GMV 2013 Jun 22 03:17:47 MetcalfUTA

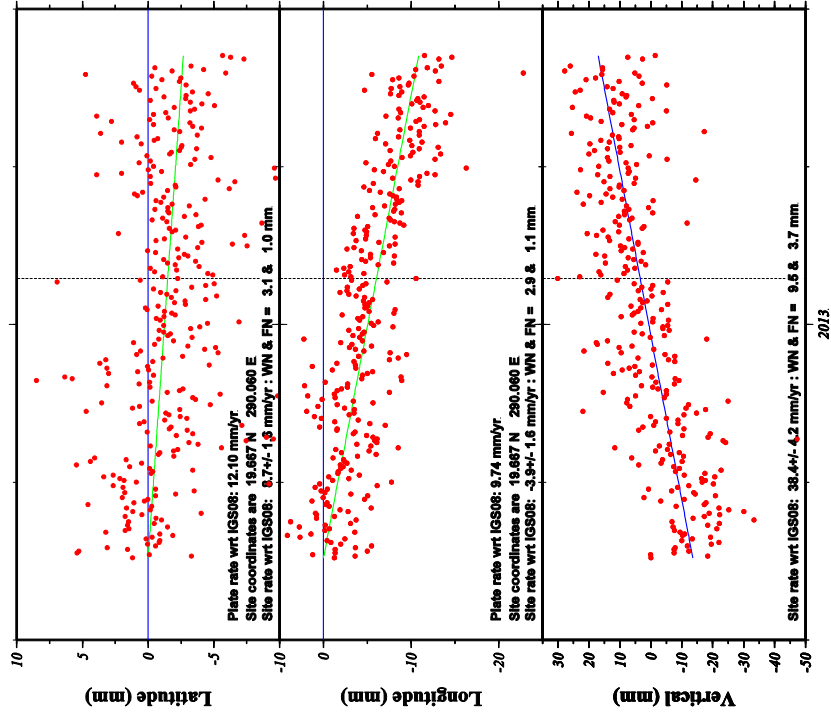


CN23 Coordinate changes - CA is fixed stacovs used AMB



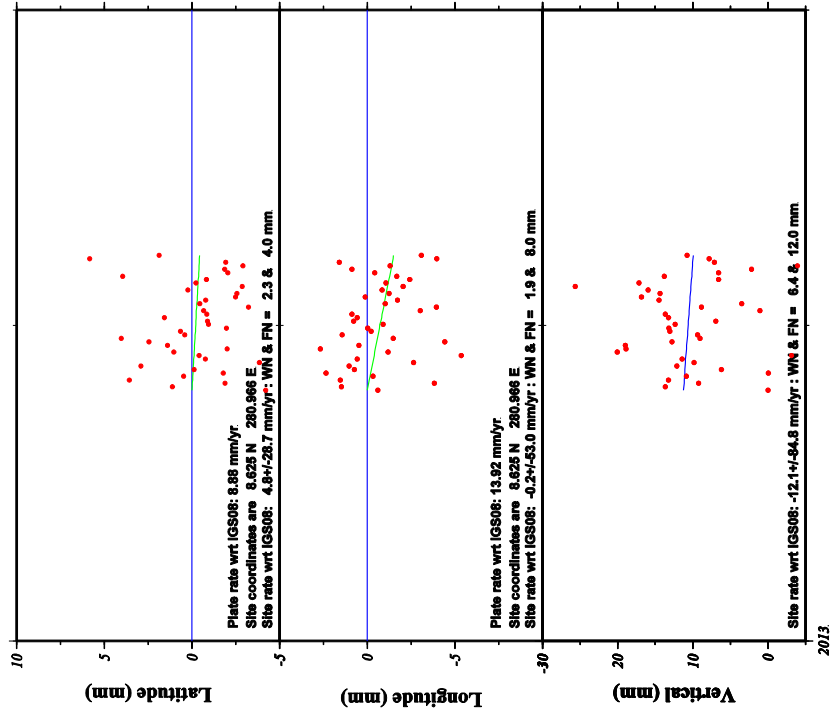
GM7 2013 Jun 22 10:34:16 MaficHUTa

CN27 Coordinate changes - CA is fixed stacovs used AMB



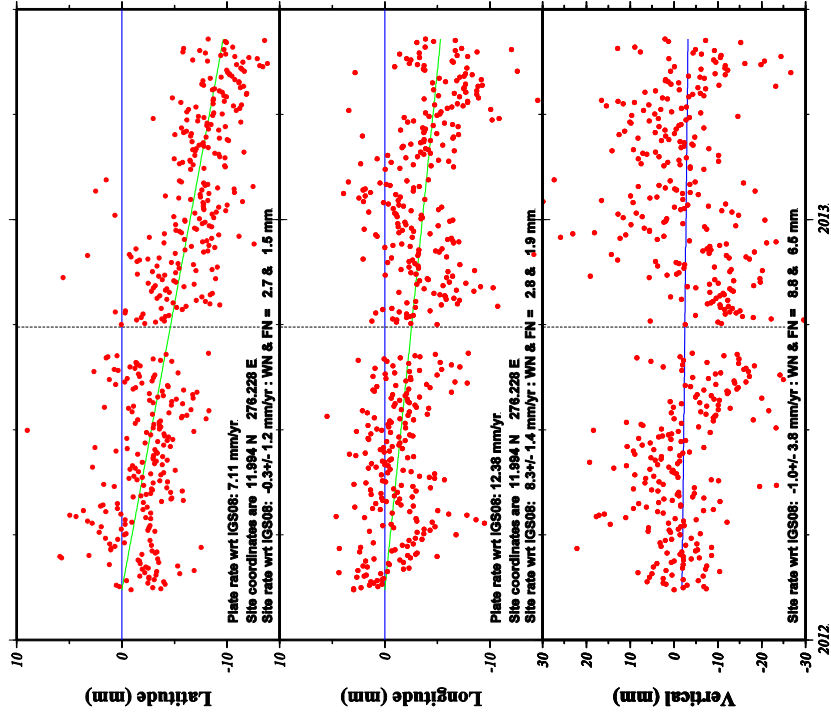
GM7 2013 Jun 23 12:34:01 MaficHUTa

CN28 Coordinate changes - CA is fixed stacovs used AMB



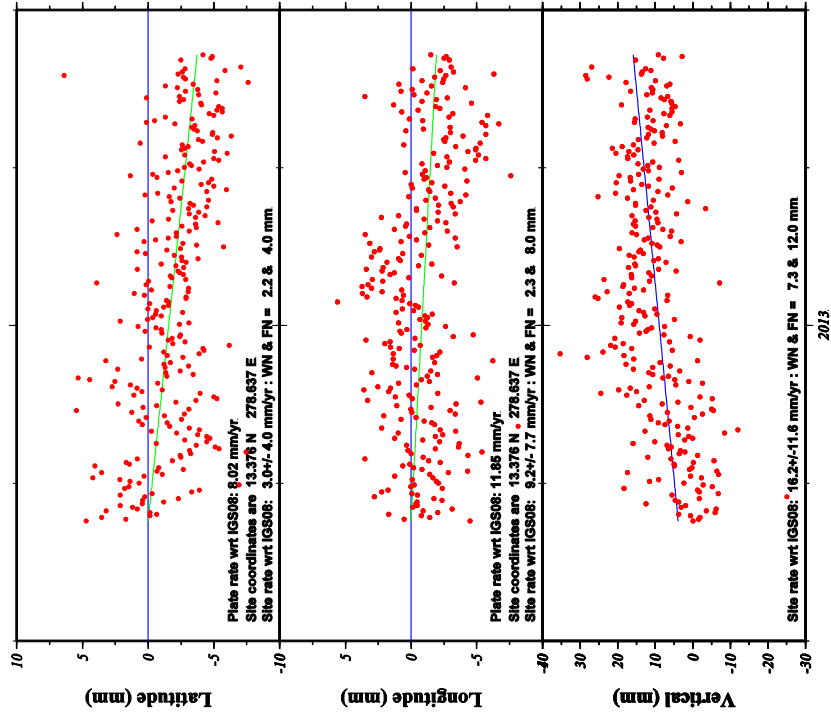
GM7 2013 Jun 22 10:42:59 MafholiUTA

CN30 Coordinate changes - CA is fixed stacovs used AMB



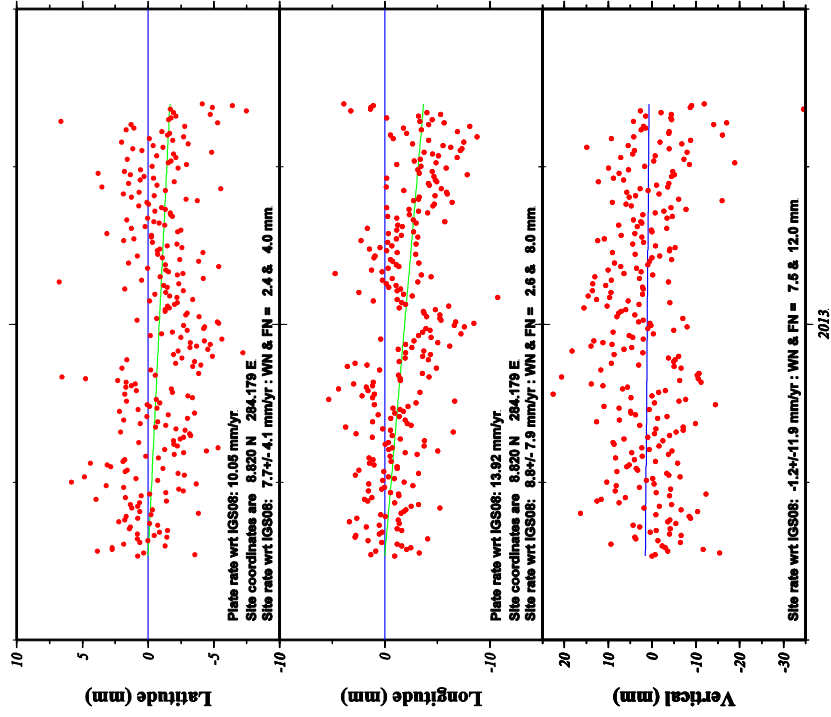
GM7 2013 Oct 30 10:21:04 MafholiUTA

CN35 Coordinate changes - CA is fixed stacovs used AMB



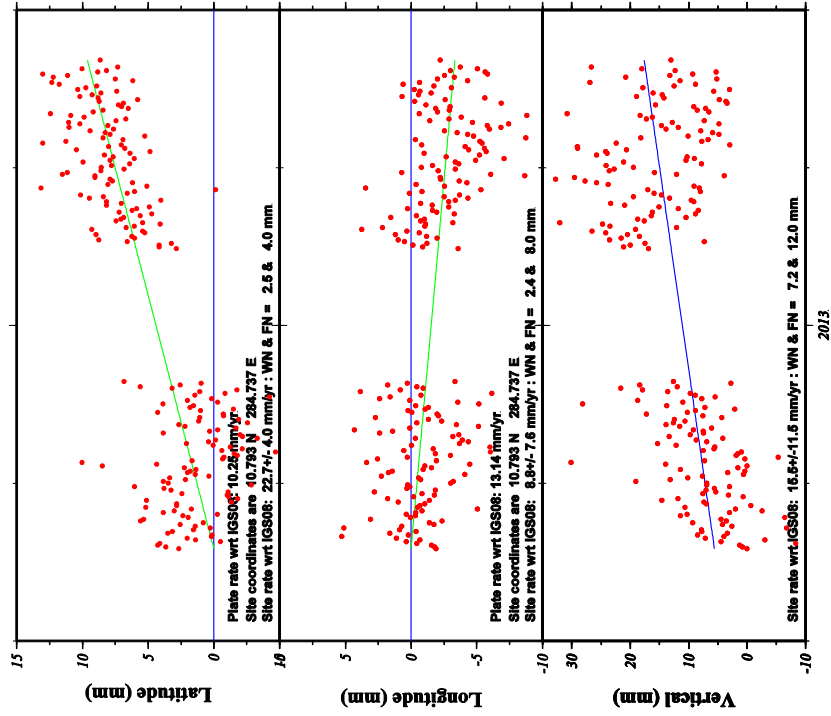
GM 2013 Jun 23 12:44:00 MaficHUTa

CN36 Coordinate changes - CA is fixed stacovs used AMB



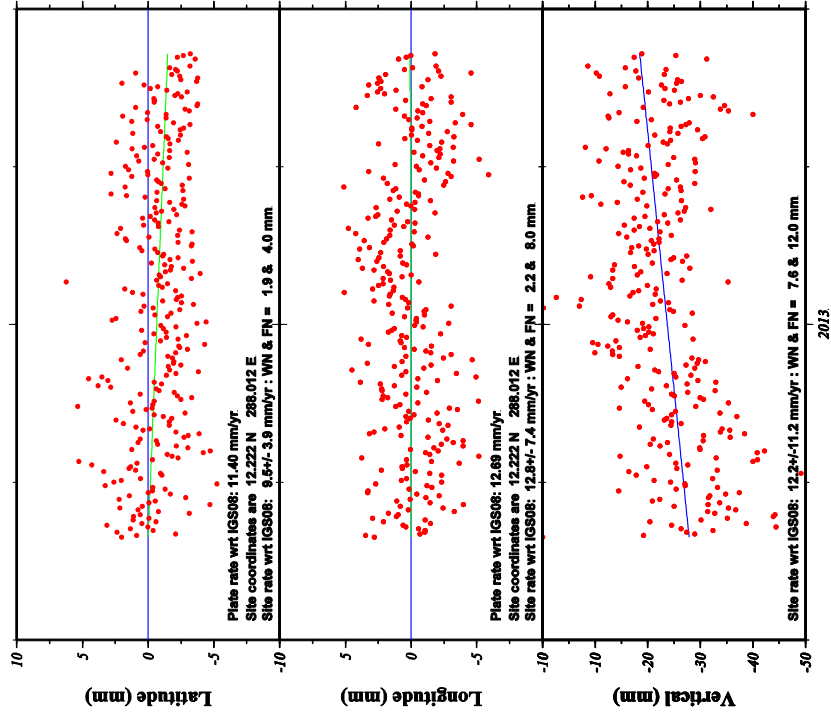
GM 2013 Jun 23 12:51:47 MaficHUTa

CN37 Coordinate changes - CA is fixed stacovs used AMB



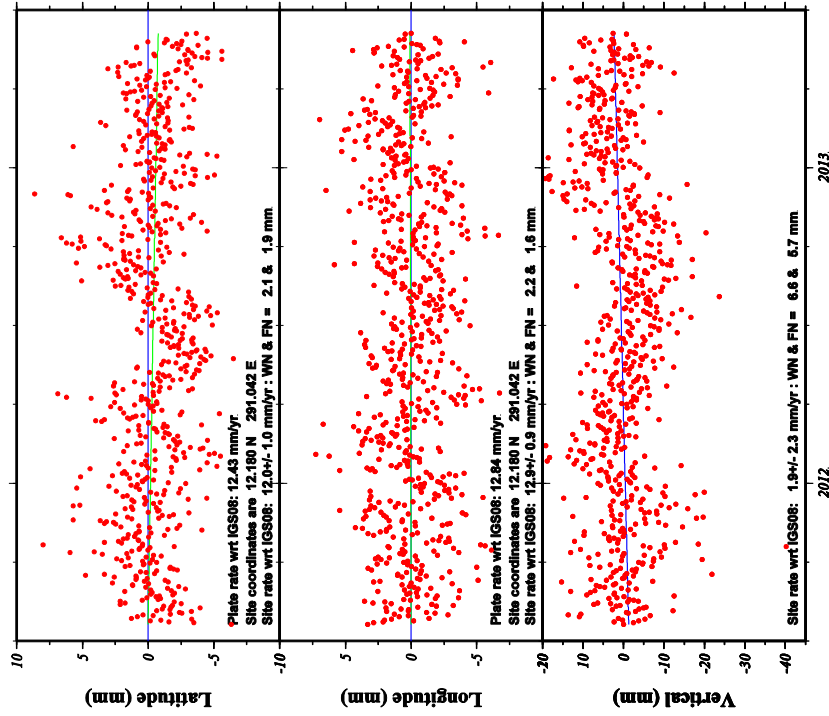
GM7 2013 Jun 24 09:48:25 MadioliUTA

CN38 Coordinate changes - CA is fixed stacovs used AMB



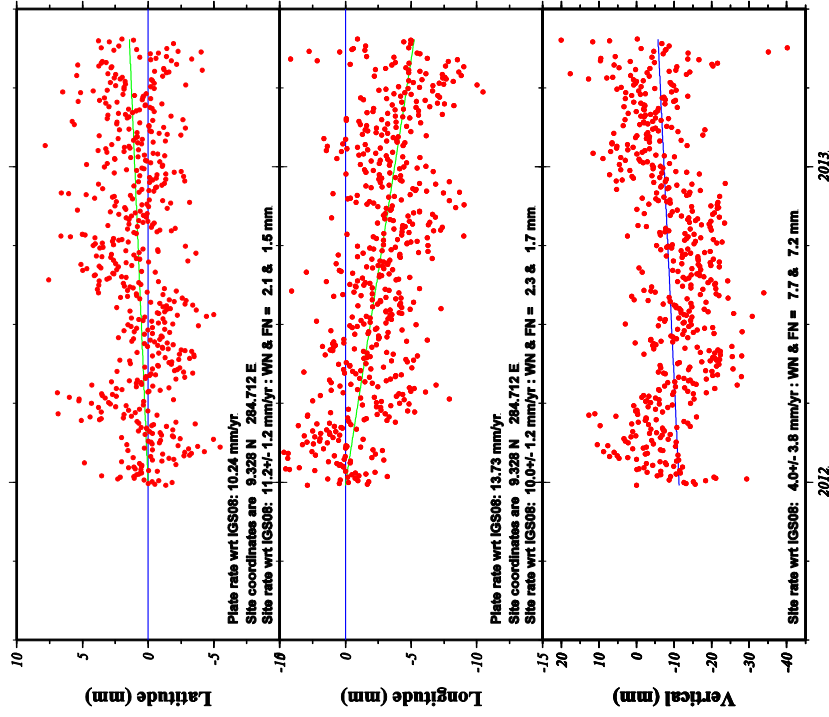
GM7 2013 Jun 24 09:40:54 MadioliUTA

CN40 Coordinate changes - CA is fixed stacovs used AMB



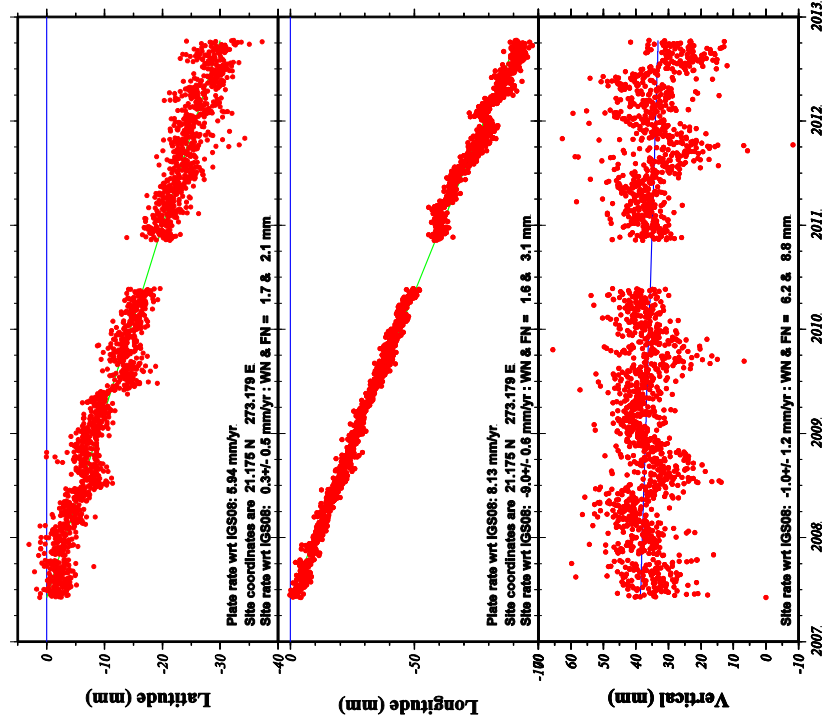
GM 2013 Jun 13 21:16:17 MadiHOUTA

CORO Coordinate changes - CA is fixed stacovs used AMB



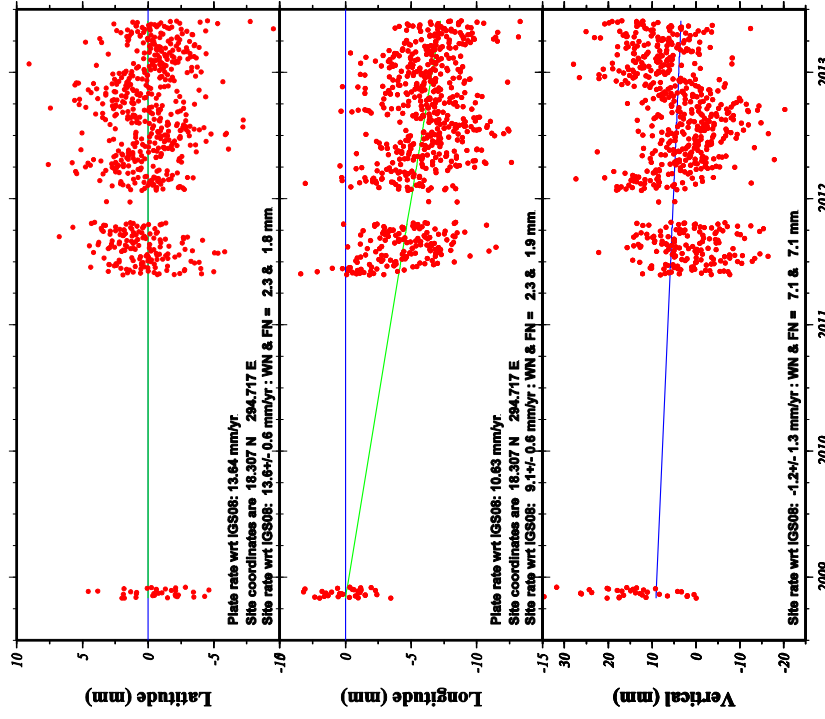
GM 2013 Jun 25 17:38:39 MadiHOUTA

CNC0 Coordinate changes - CA is fixed stacovs used AMB



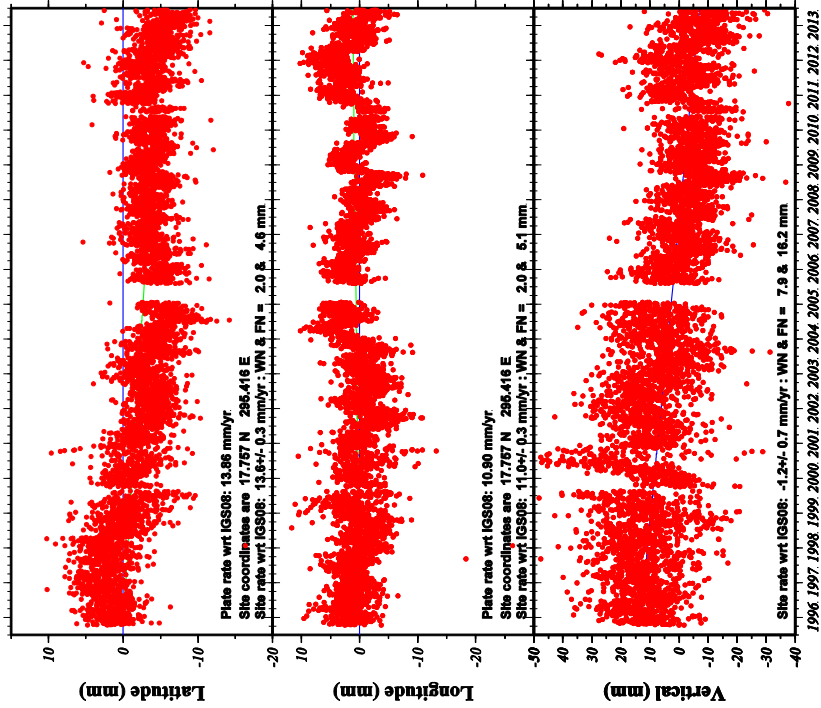
GM7 2013 Sep 15 10:16:40 MARS0107A

CUPR Coordinate changes - CA is fixed stacovs used AMB



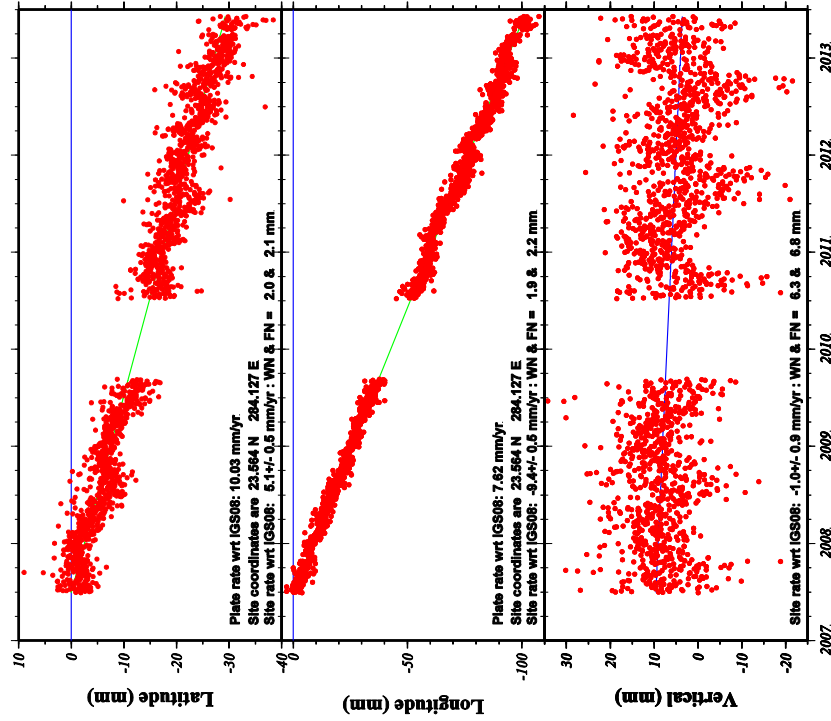
GM7 2013 Jun 28 08:30:05 MARS0107A

CRO1 Coordinate changes - CA is fixed stacovs used AMB



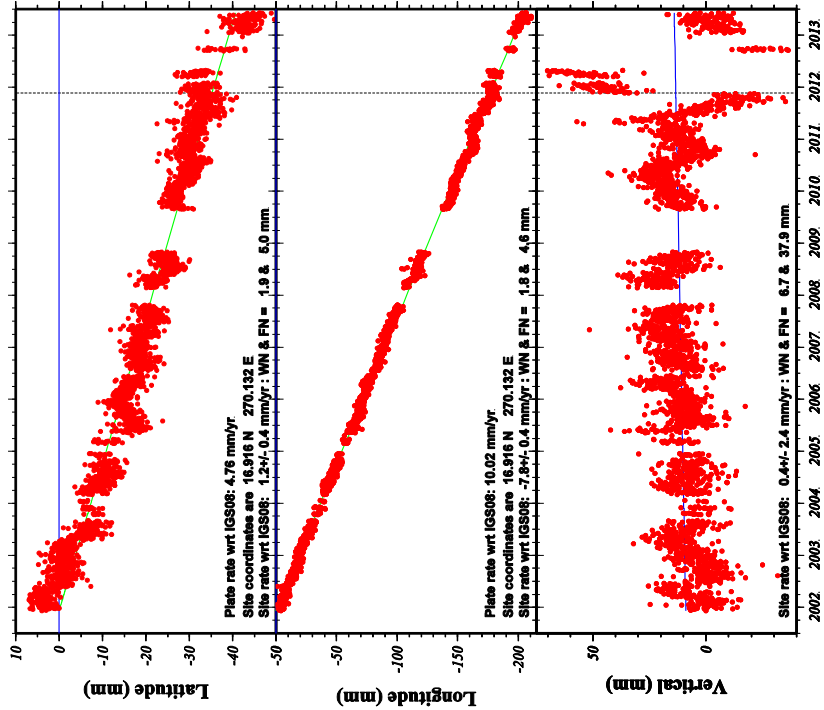
GM 2013 Oct 30 10:40:12 MATHIOLUTA

EXU0 Coordinate changes - CA is fixed stacovs used AMB



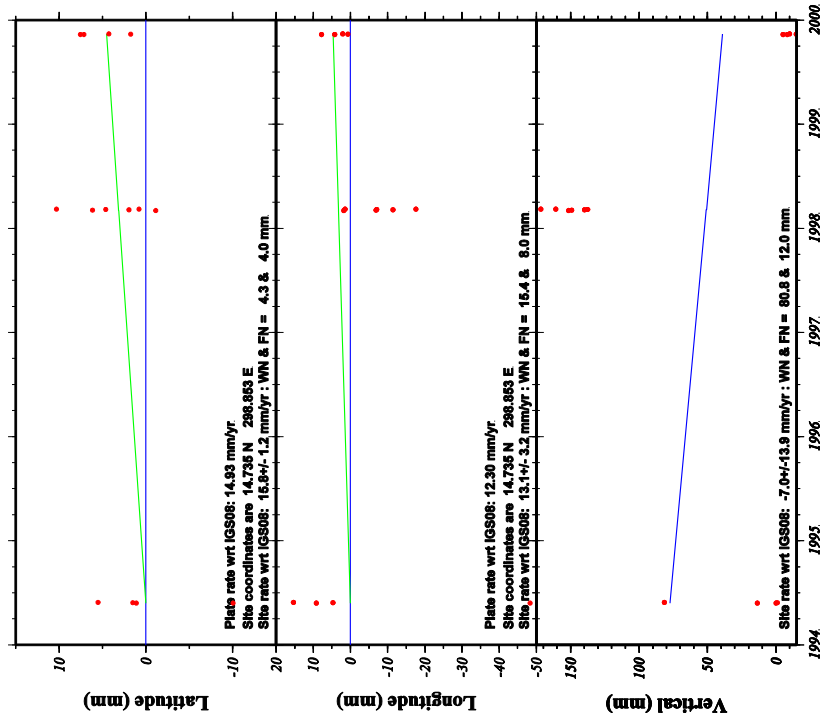
GM 2013 Jul 01 17:02:58 MATHIOLUTA

ELEN Coordinate changes - CA is fixed stacovs used AMB



GM7 2013 Sep 03 06:36:56 MetrolIUTA

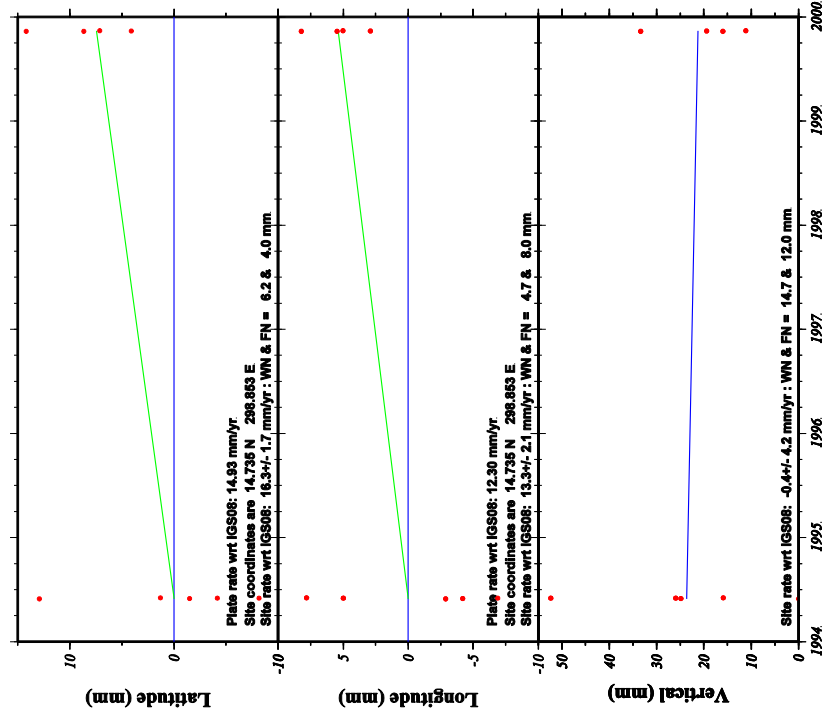
FSD0 Coordinate changes - CA is fixed stacovs used AMB



GM7 2013 Jun 20 20:58:43 MetrolIUTA

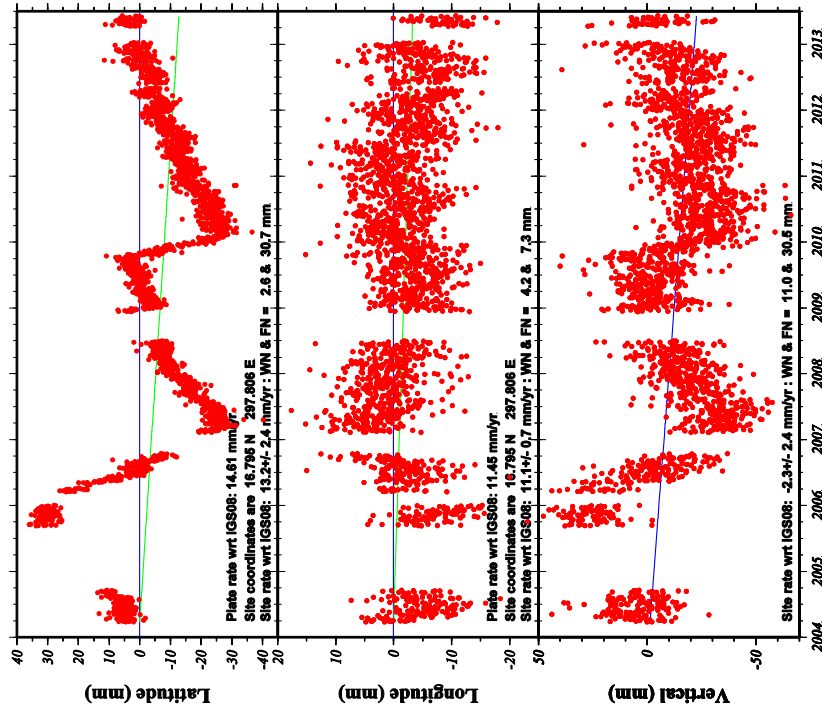


FSD1 Coordinate changes - CA is fixed stacovs used AMB



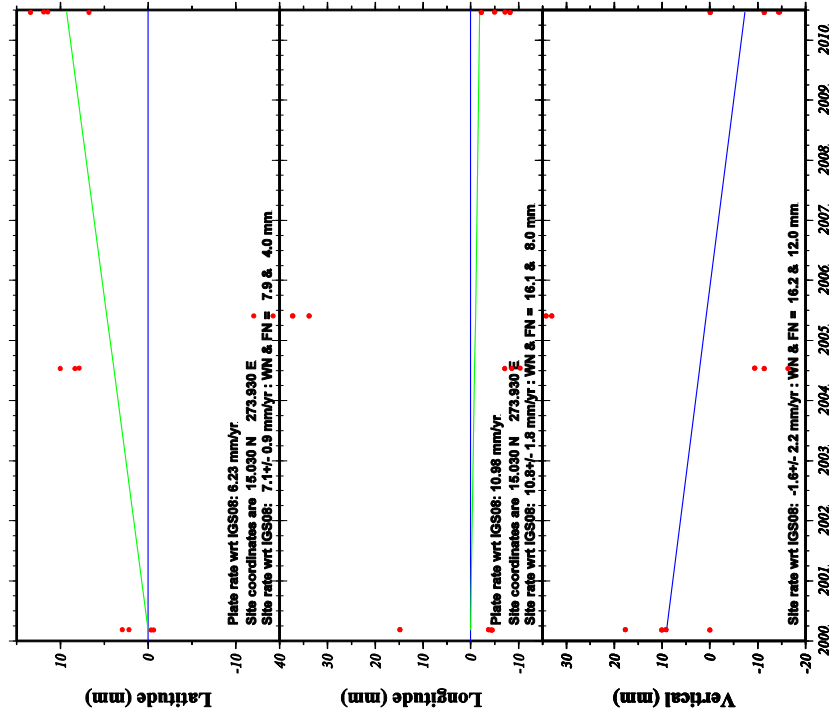
GM7 2013 Jun 20 21:11:33 MetcalfUTA

GERD Coordinate changes - CA is fixed stacovs used no\_AMB



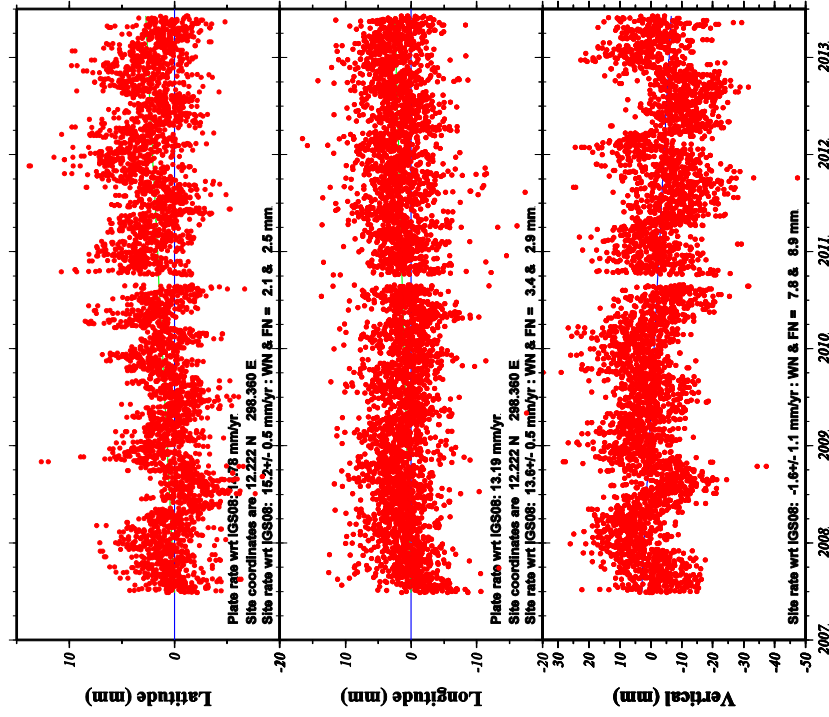
GM7 2013 Jul 30 06:16:38 MetcalfUTA

GLCO Coordinate changes - CA is fixed stacovs used AMB



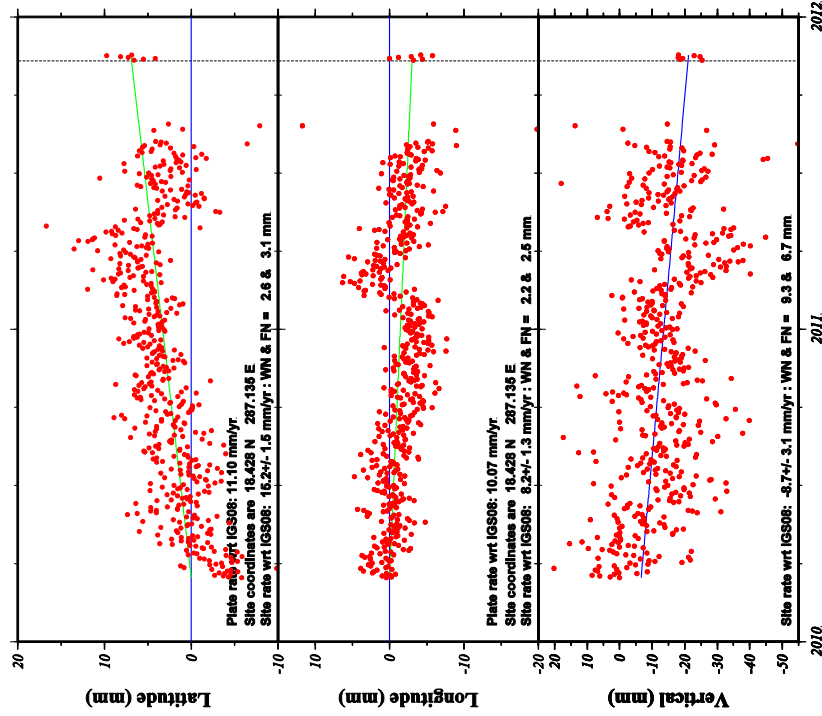
GM7 2013 Jul 30 12:42:54 | MetrolidUTA

GREO Coordinate changes - CA is fixed stacovs used AMB



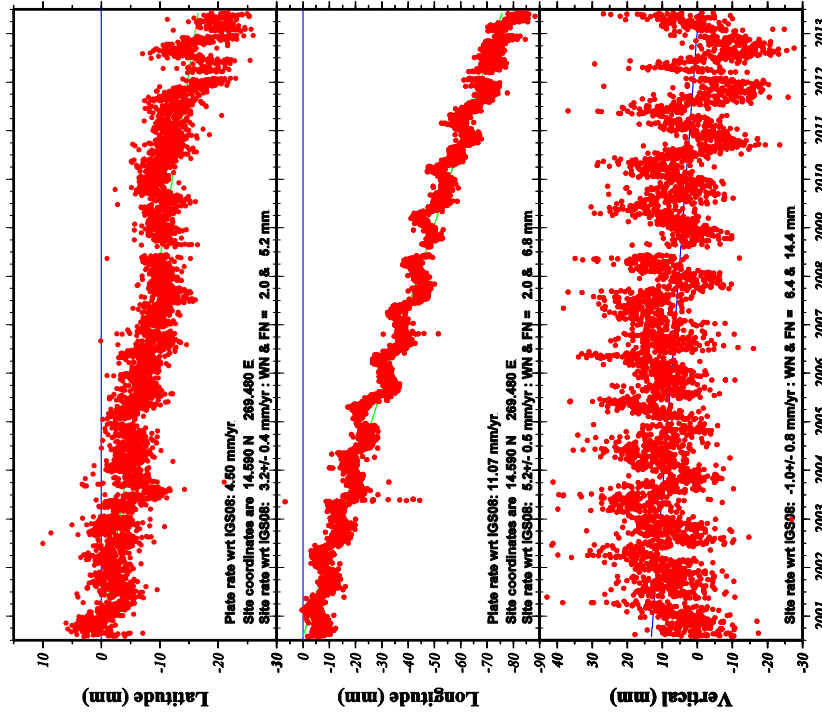
GM7 2013 Jun 15 14:18:12 | MetrolidUTA

GOAV Coordinate changes - CA is fixed stacovs used AMB



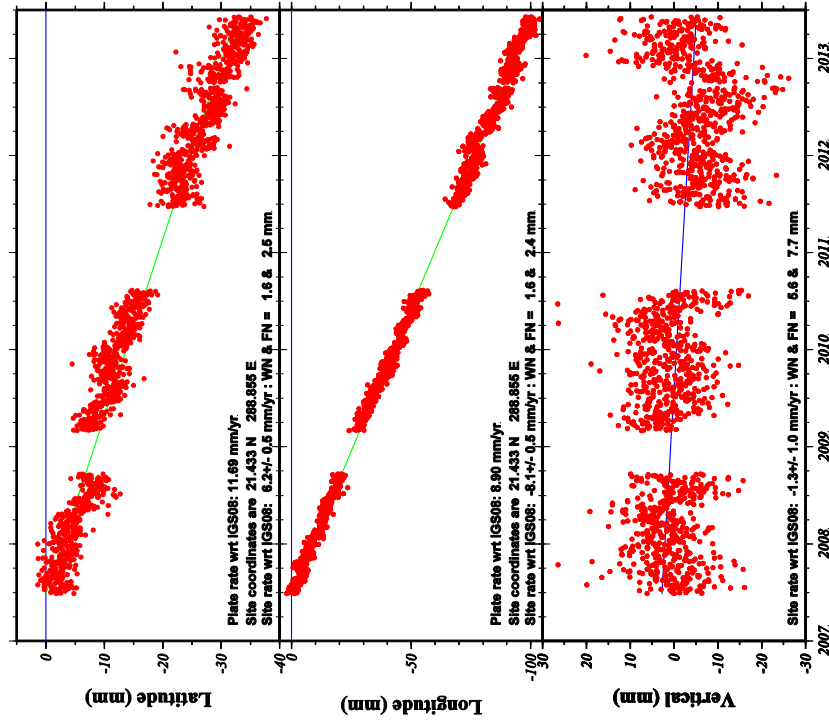
GM7 2013 Jul 02 08:48:10 MestizalUTA

GUAT Coordinate changes - CA is fixed stacovs used AMB



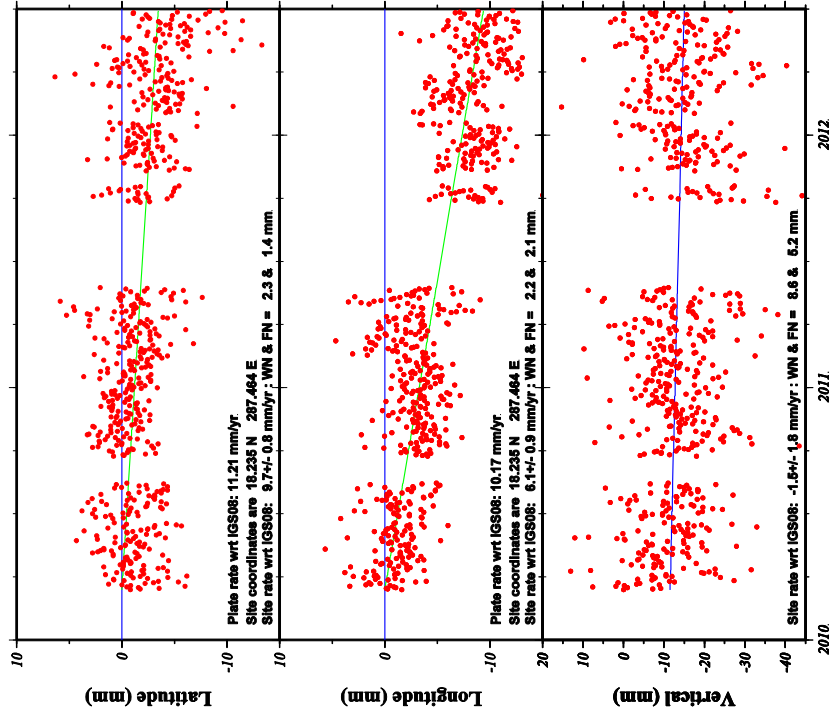
GM7 2013 Jul 01 12:14:30 MestizalUTA

GTK0 Coordinate changes - CA is fixed stacovs used AMB



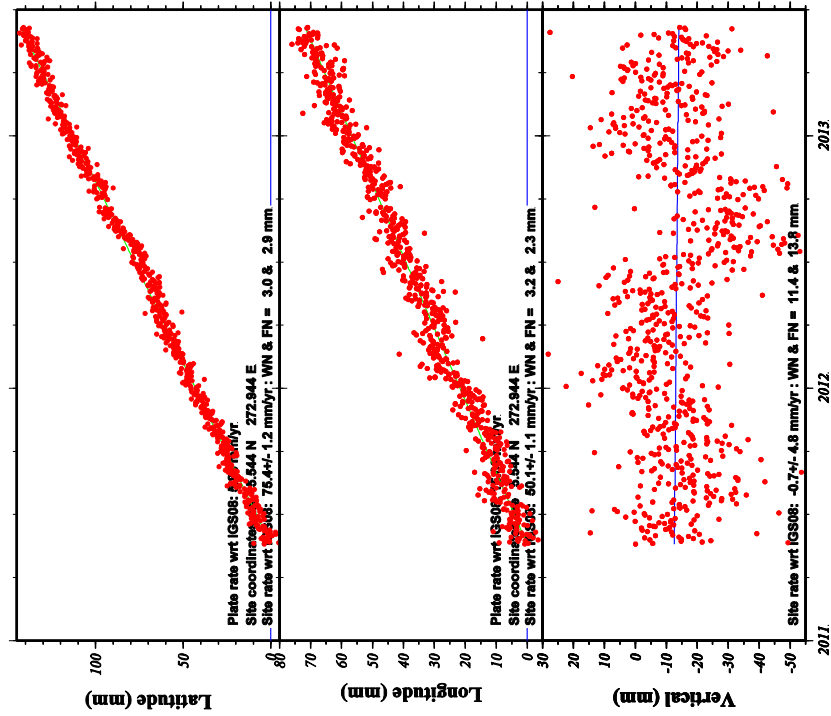
GM7 2013 Jul 01 11:23:05 | MetrolOrta

JMEL Coordinate changes - CA is fixed stacovs used AMB



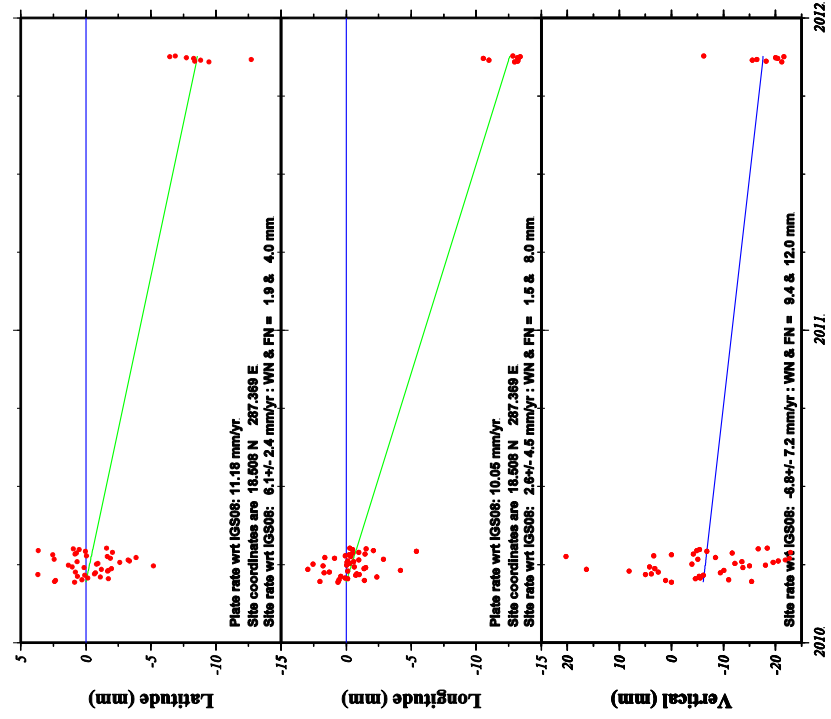
GM7 2013 Jul 08 13:03:35 | MetrolOrta

ISCO Coordinate changes - CA is fixed stacovs used AMB



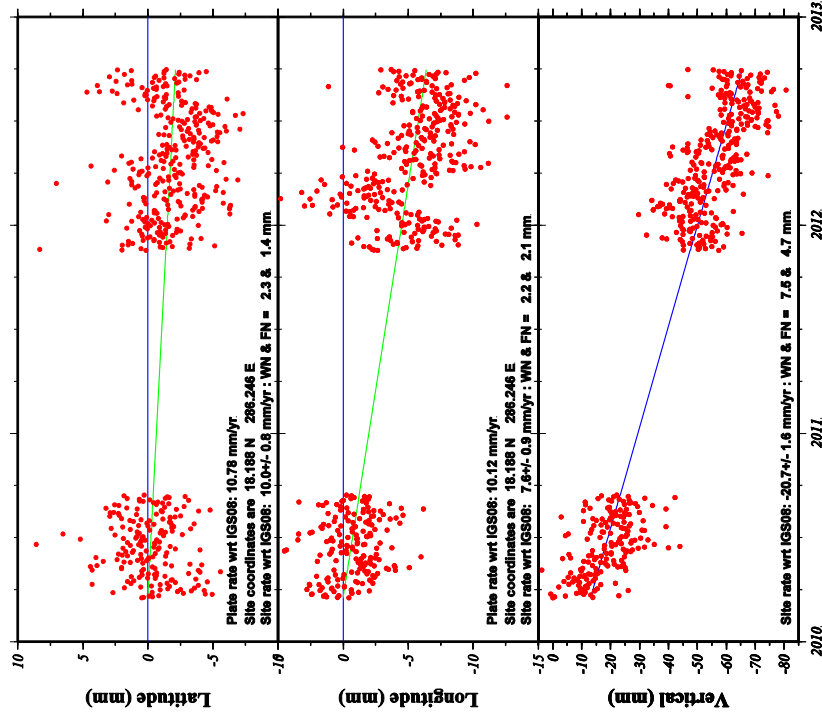
GM7 2013 Jul 01 12:28:03 MetNet/UTA

LGNE Coordinate changes - CA is fixed stacovs used AMB



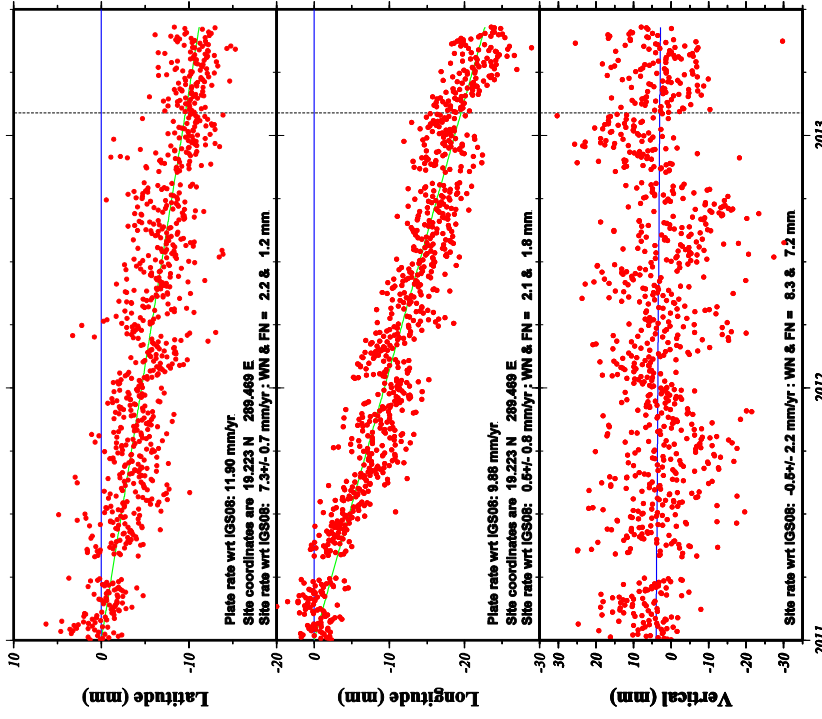
GM7 2013 Jul 03 14:35:22 MetNet/UTA

LWAY Coordinate changes - CA is fixed stacovs used AMB



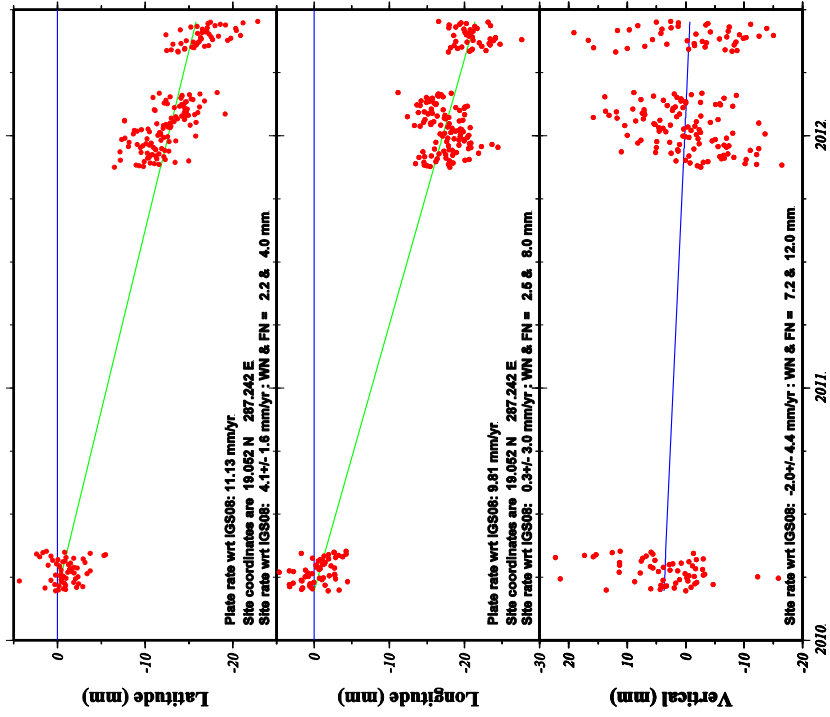
GM7 2013 Jul 01 11:16:22 MATHS@UTA

LVEG Coordinate changes - CA is fixed stacovs used AMB



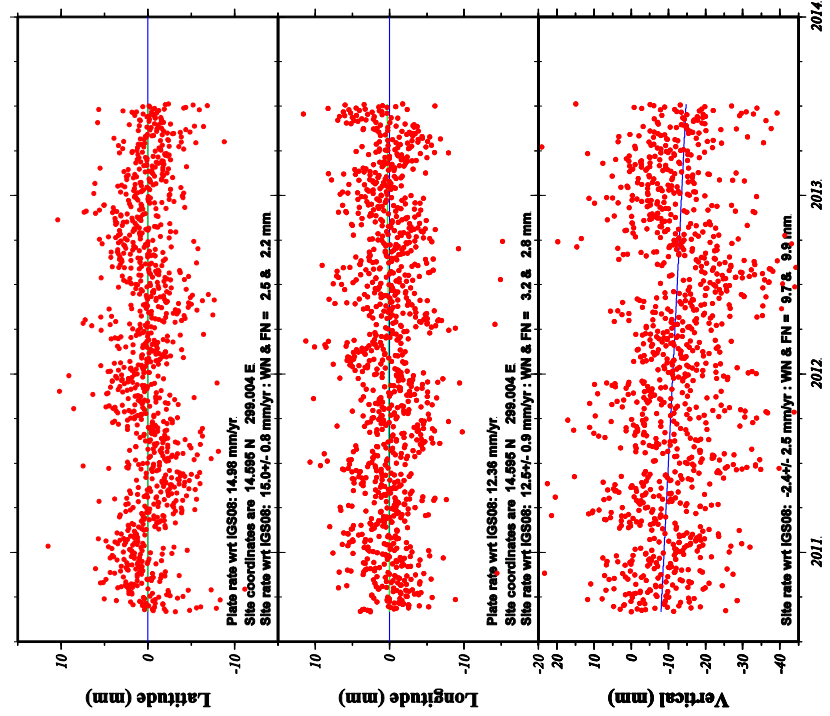
GM7 2013 Jul 09 11:16:33 MATHS@UTA

MARC Coordinate changes - CA is fixed stacovs used AMB



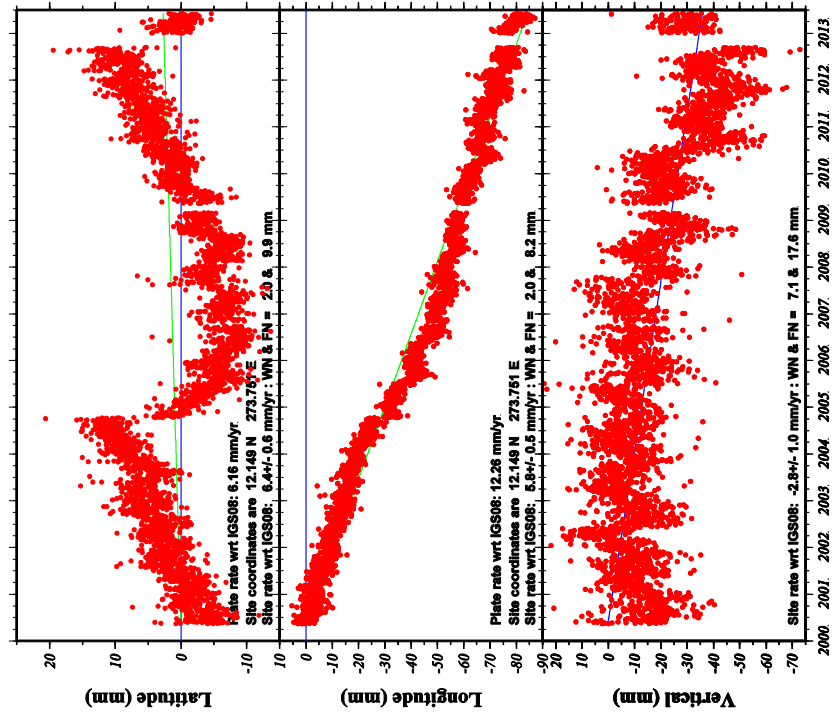
GM7 2013 Oct 30 10:56:16 MARS01UT4

LMMF Coordinate changes - CA is fixed stacovs used AMB



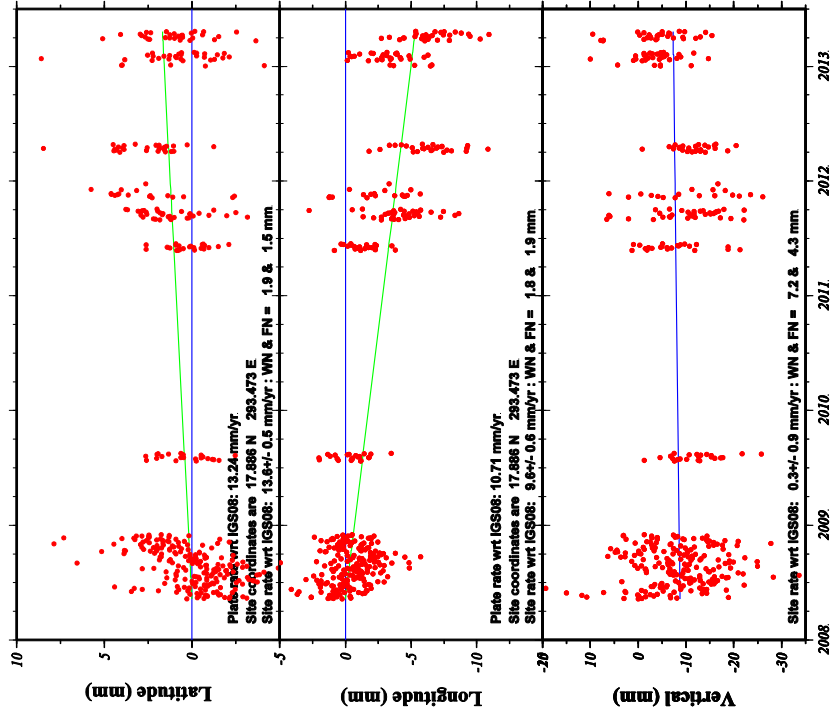
GM7 2013 Jul 18 08:47:22 MARS01UT4

MANA Coordinate changes - CA is fixed stacovs used AMB



GM7 2013 Jul 08 16:10:24 | MestrelGUTA

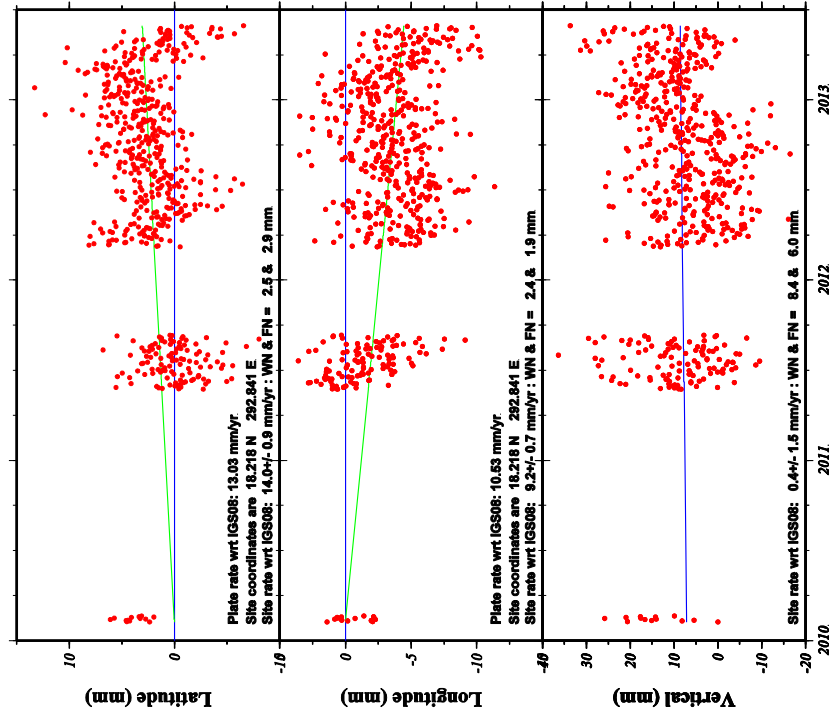
MIPR Coordinate changes - CA is fixed stacovs used AMB



GM7 2013 Jul 08 13:28:15 | MestrelGUTA

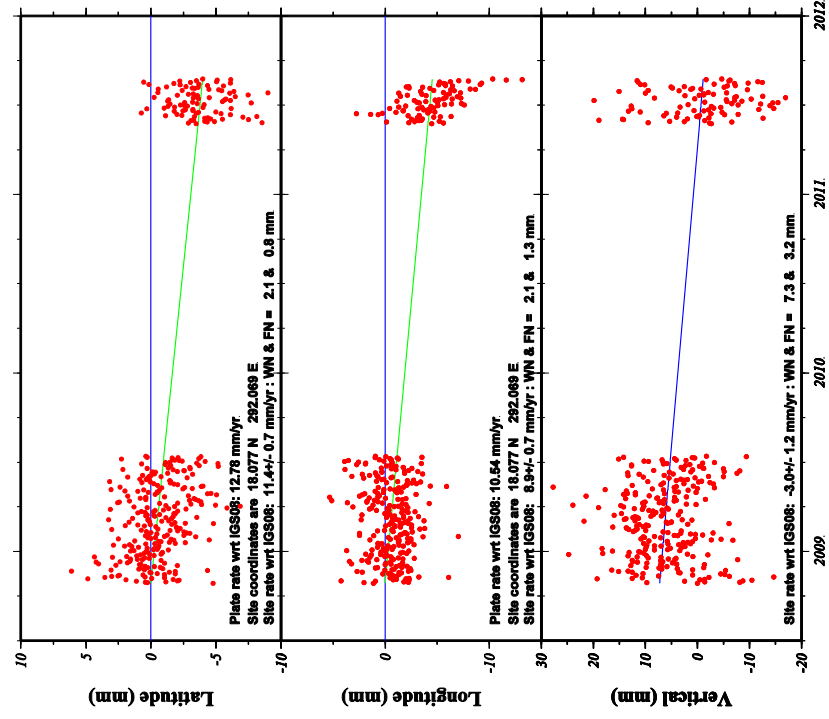


MAYZ Coordinate changes - CA is fixed stacovs used AMB



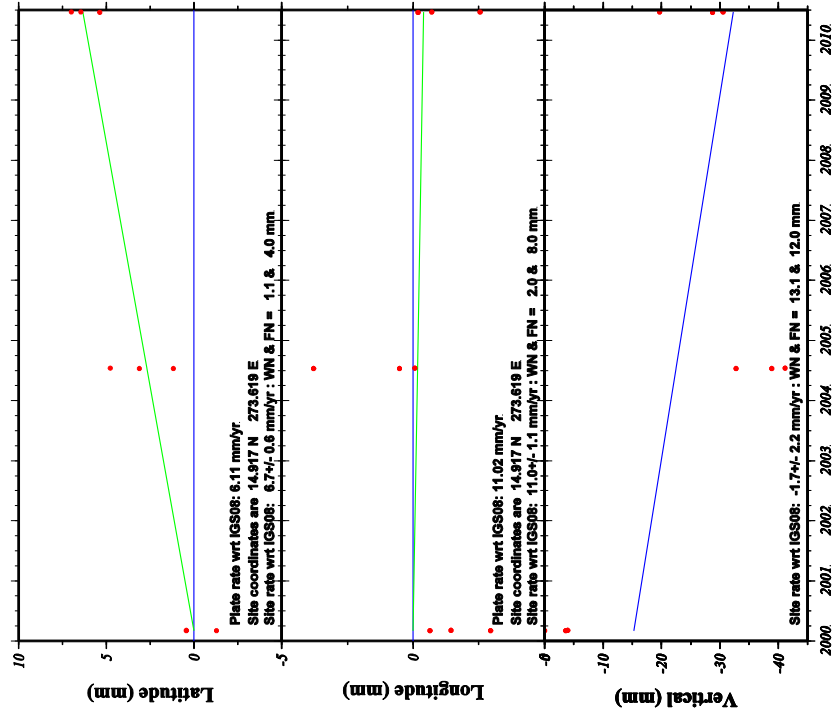
GMZ 2013 Jul 09 12:48:08 | Mutsaers/UTA

MOPR Coordinate changes - CA is fixed stacovs used AMB



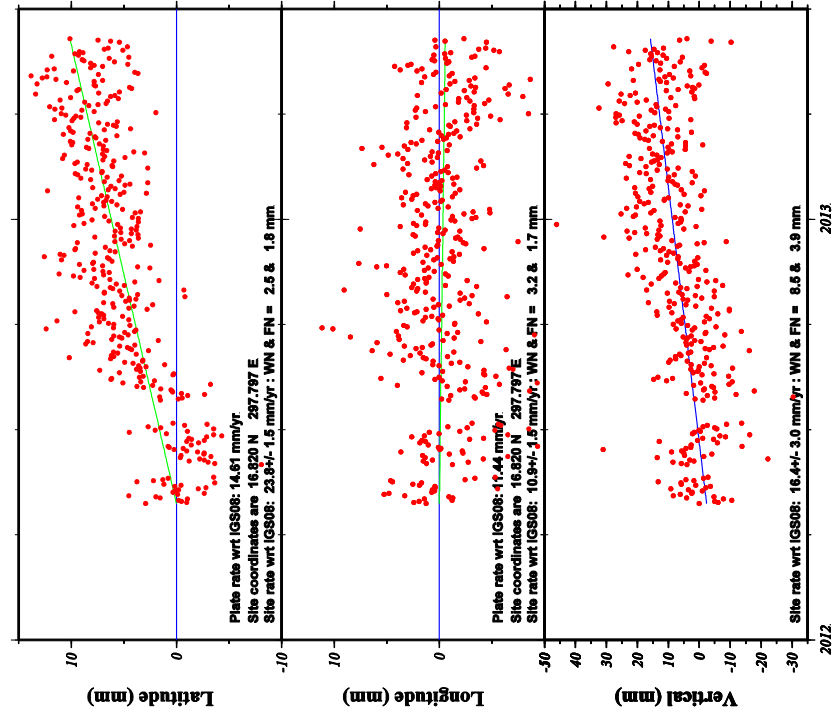
GMZ 2013 Jul 08 13:36:58 | Mutsaers/UTA

MNTO Coordinate changes - CA is fixed stacovs used AMB



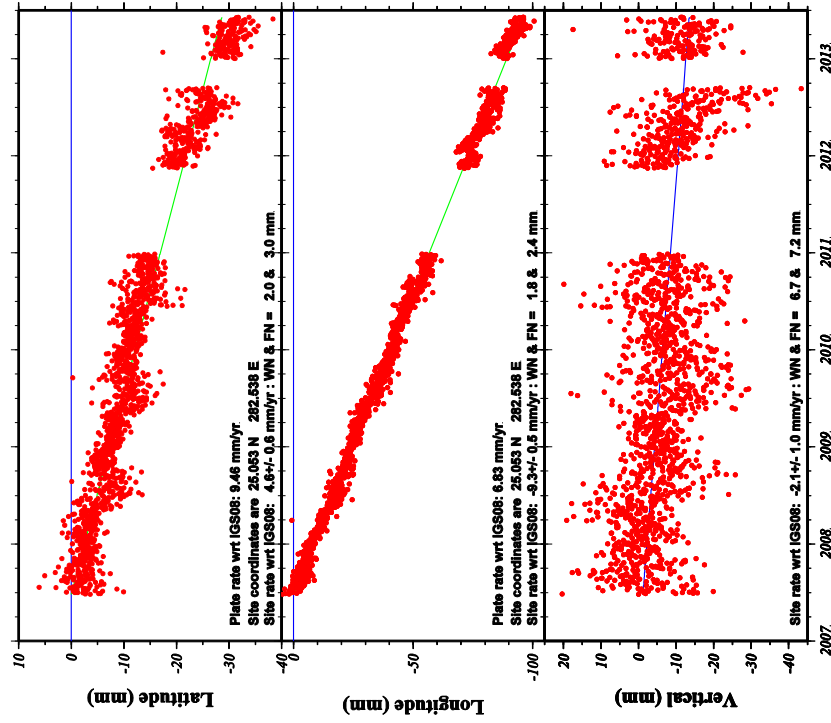
GM7 2013 Jun 15 14:38:34 Msdh01UTA

NWBL Coordinate changes - CA is fixed stacovs used AMB



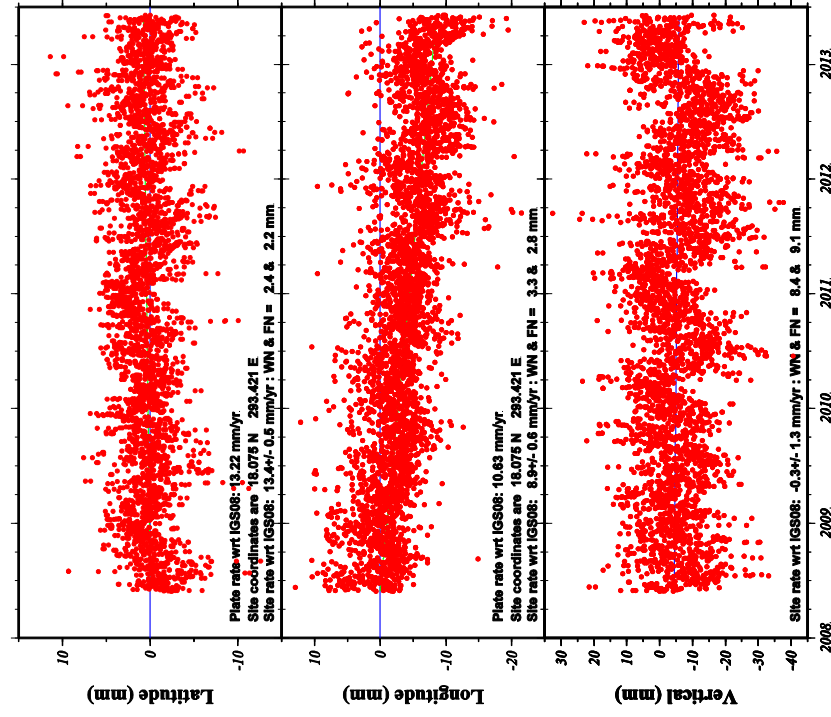
GM7 2013 Jul 09 11:30:59 Msdh01UTA

NASO Coordinate changes - CA is fixed stacovs used AMB



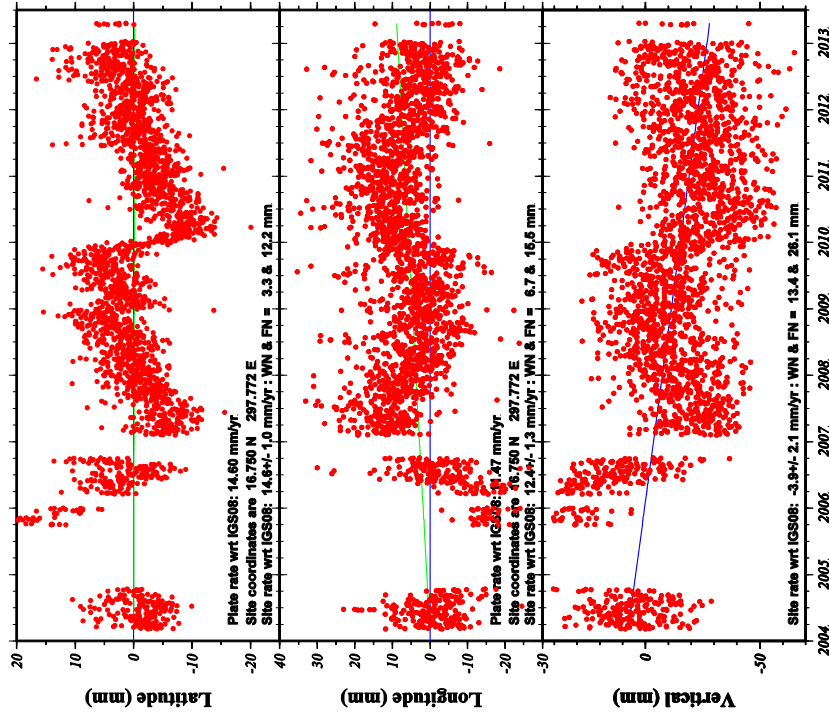
GM7 2013 Sep 14 10:06:10 Hawaii/UTTA

P780 Coordinate changes - CA is fixed stacovs used AMB



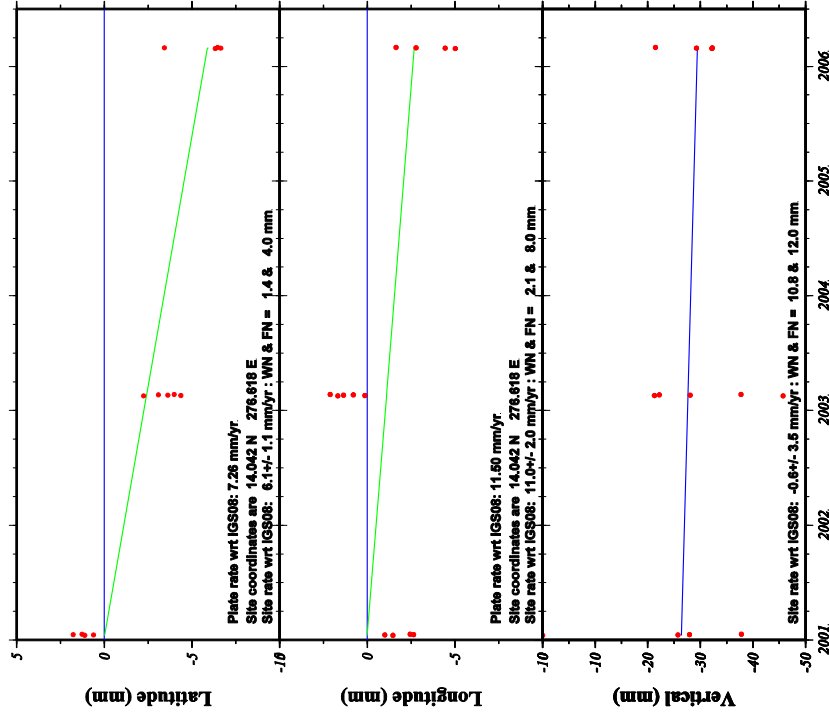
GM7 2013 Jun 17 13:25:09 Hawaii/UTTA

OLVN Coordinate changes - CA is fixed stacovs used AMB



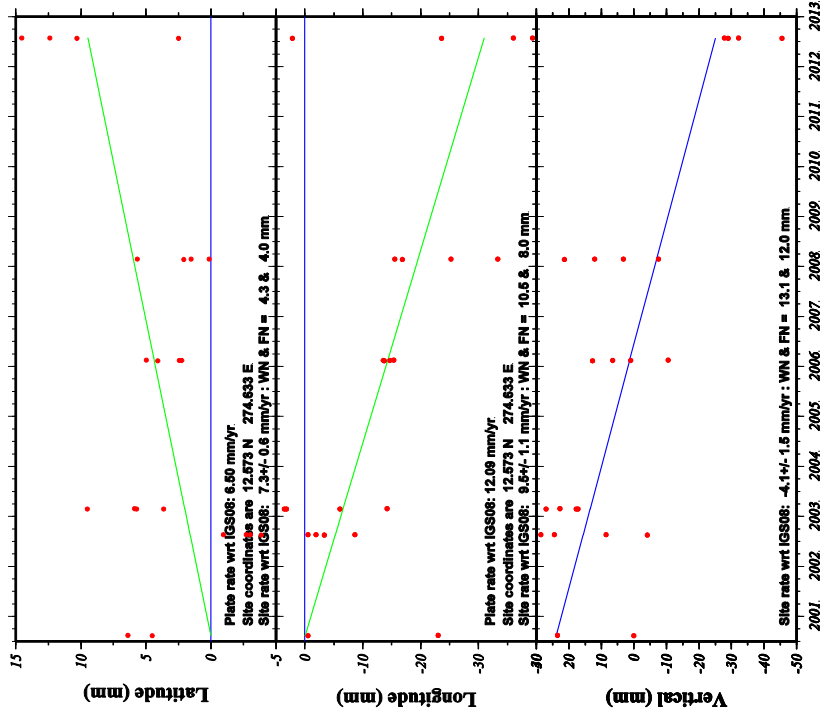
GM7 2013 Jul 08 15:40:54 | Metis@UTA

PUEC Coordinate changes - CA is fixed stacovs used AMB



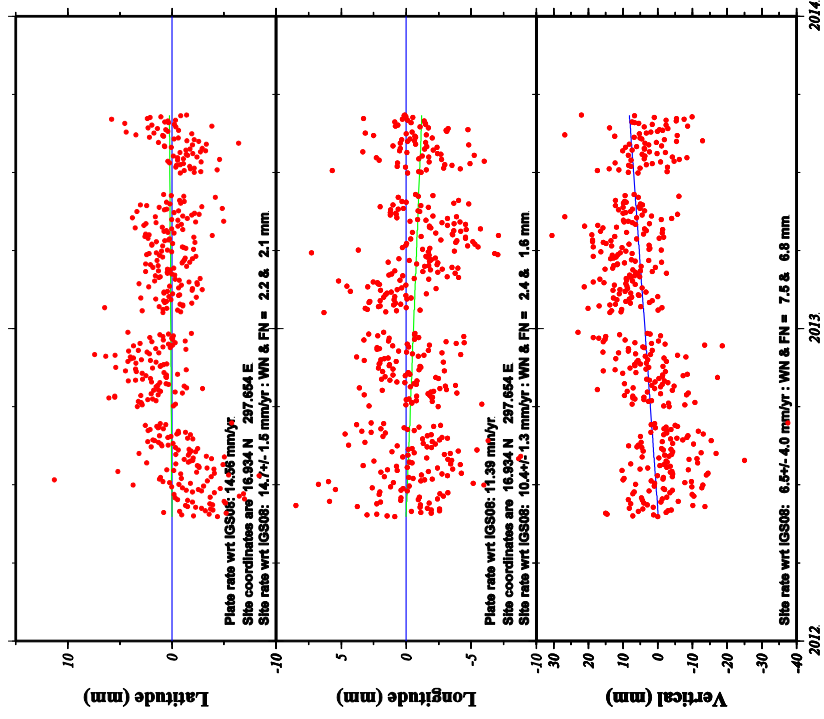
GM7 2013 Jul 30 13:10:54 | Metis@UTA

PORT Coordinate changes - CA is fixed stacovs used no\_AMB



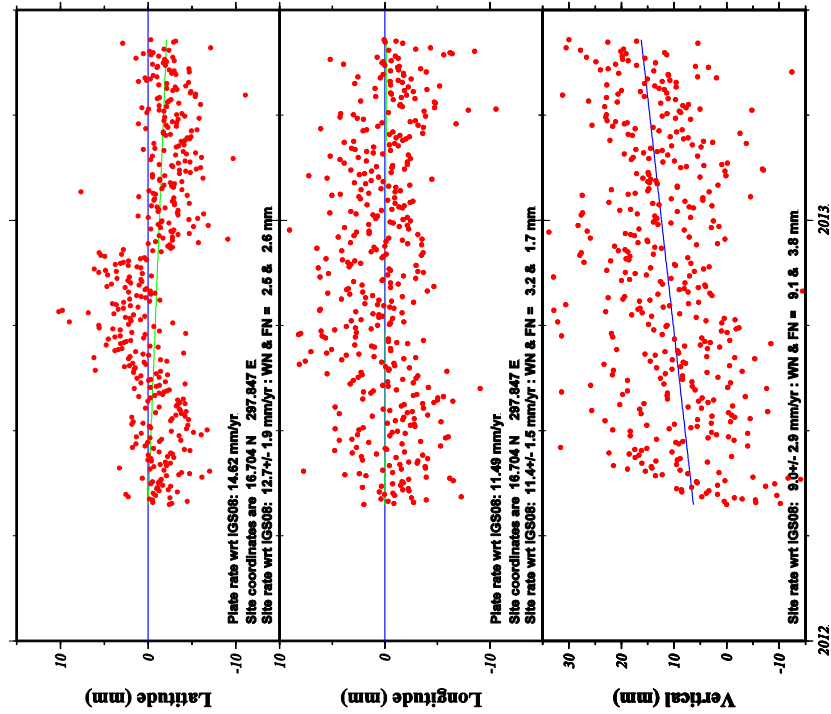
GMVP 2013 Jul 30 12:57:36 | MATHS@UTA

RDON Coordinate changes - CA is fixed stacovs used AMB



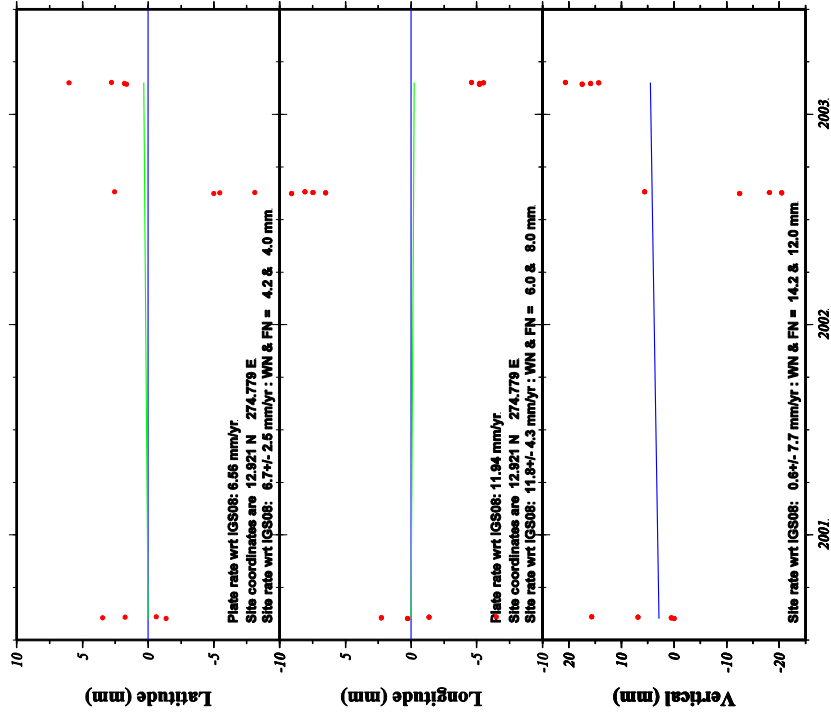
GMVP 2013 Sep 16 20:44:33 | MATHS@UTA

RCHY Coordinate changes - CA is fixed stacovs used AMB



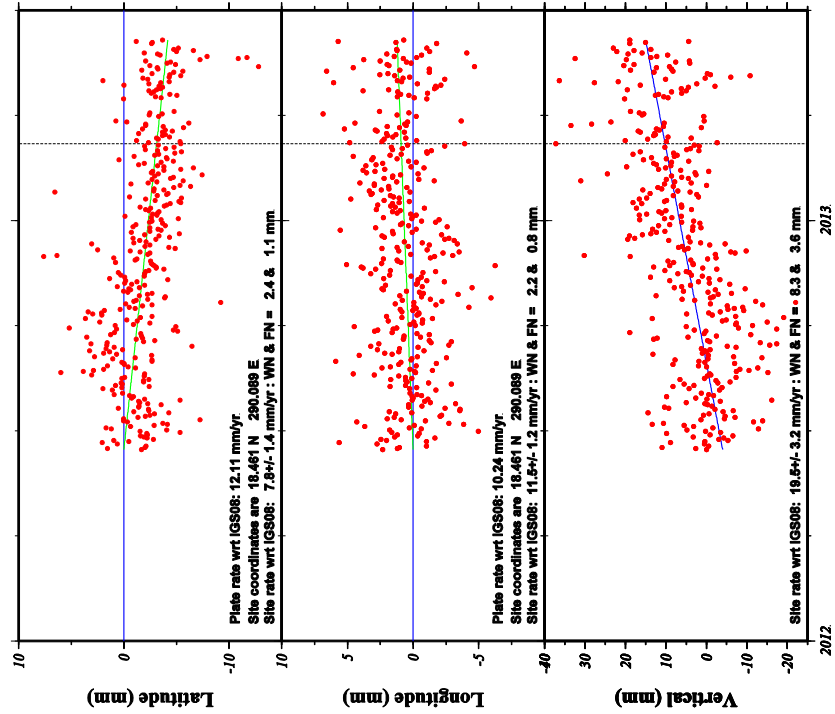
GM2 2013 Jul 09 11:40:48 | MestizolUTA

RIOB Coordinate changes - CA is fixed stacovs used AMB



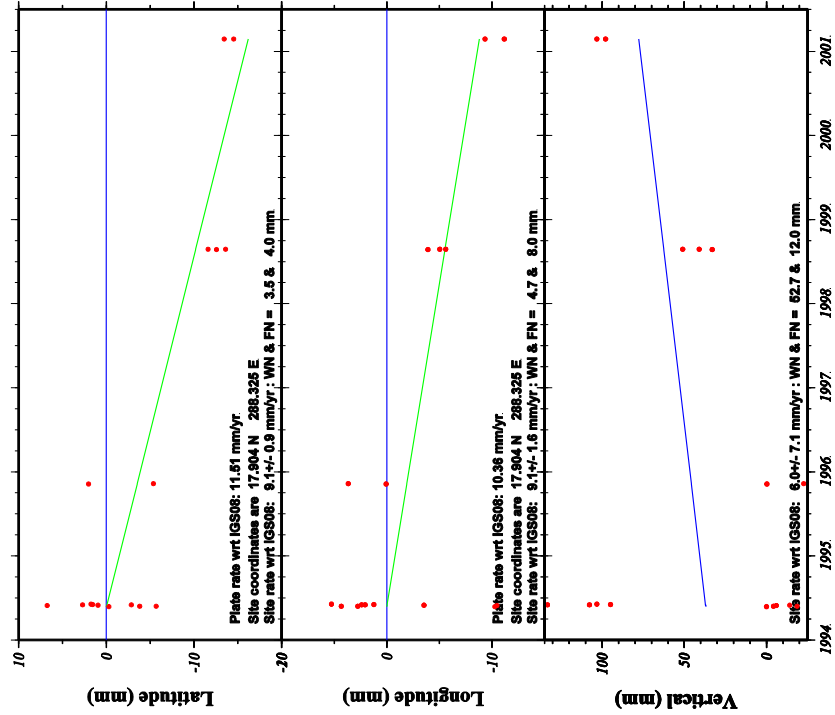
GM2 2013 Aug 08 16:17:22 | MestizolUTA

**RDSO Coordinate changes - CA is fixed stacovs used AMB**



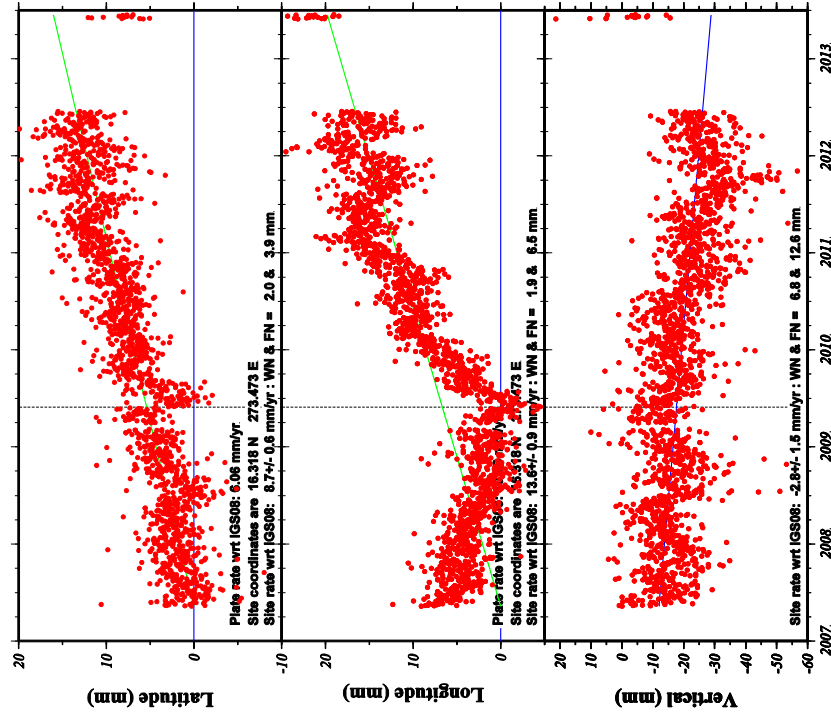
GM 2013 Jul 09 11:55:20 MATHJAZZ

**ROJO Coordinate changes - CA is fixed stacovs used AMB**



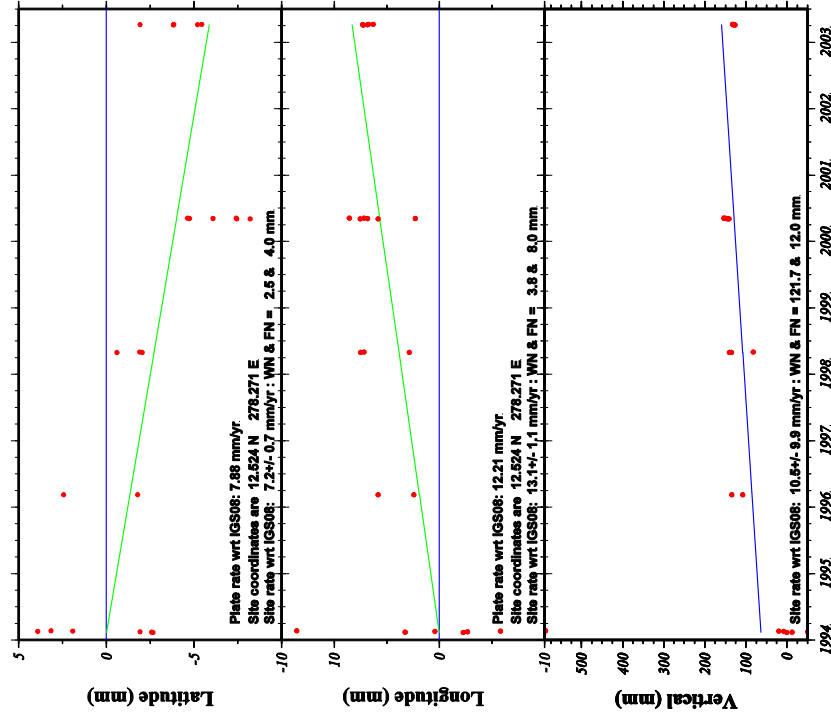
GM 2013 Aug 14 12:27:11 MATHJAZZ

ROA0 Coordinate changes - CA is fixed stacovs used AMB



GM7 2013 Sep 29 13:24:47 Hawaii/UTTA

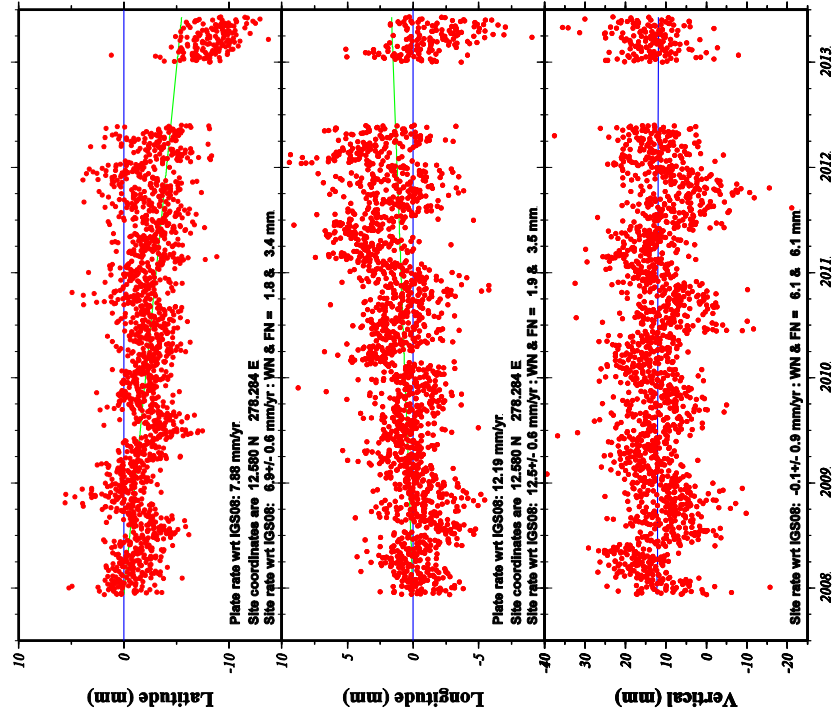
SANA Coordinate changes - CA is fixed stacovs used AMB



GM7 2013 Jul 03 08:10:48 Hawaii/UTTA

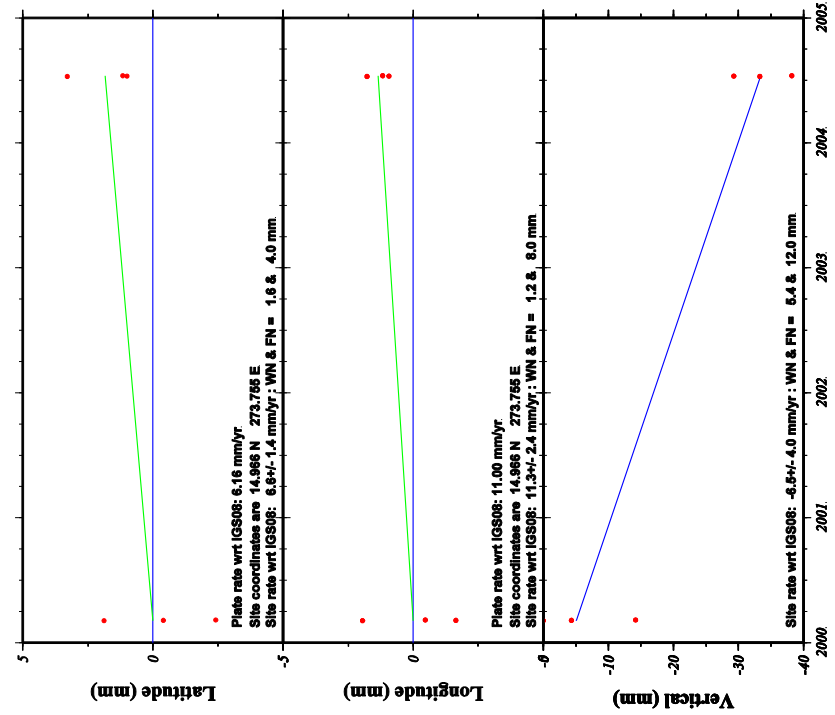


SAN0 Coordinate changes - CA is fixed stacovs used AMB



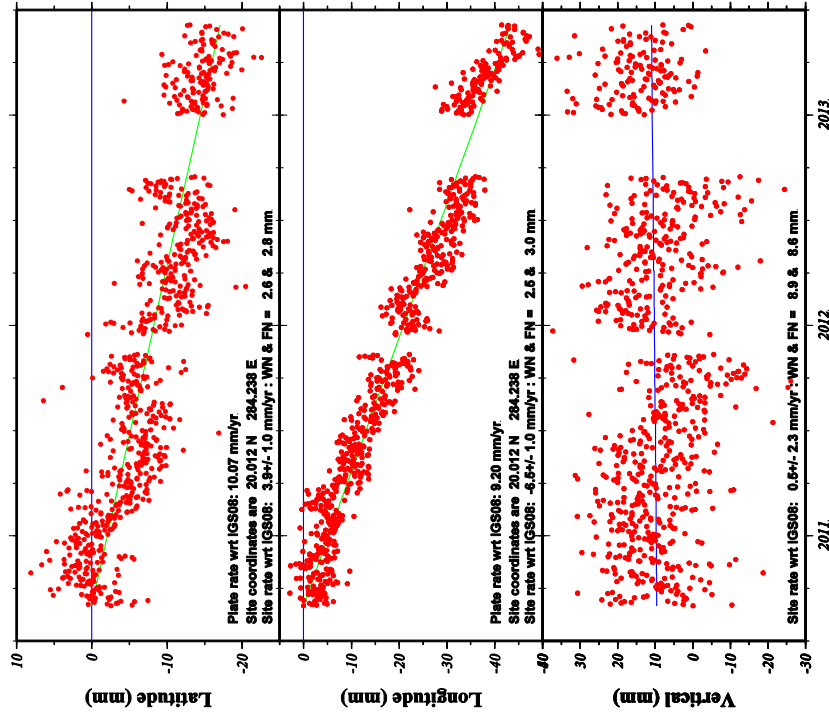
GM7 2013 Jun 20 08:38:10 Mafic04UT4

SFDP Coordinate changes - CA is fixed stacovs used AMB



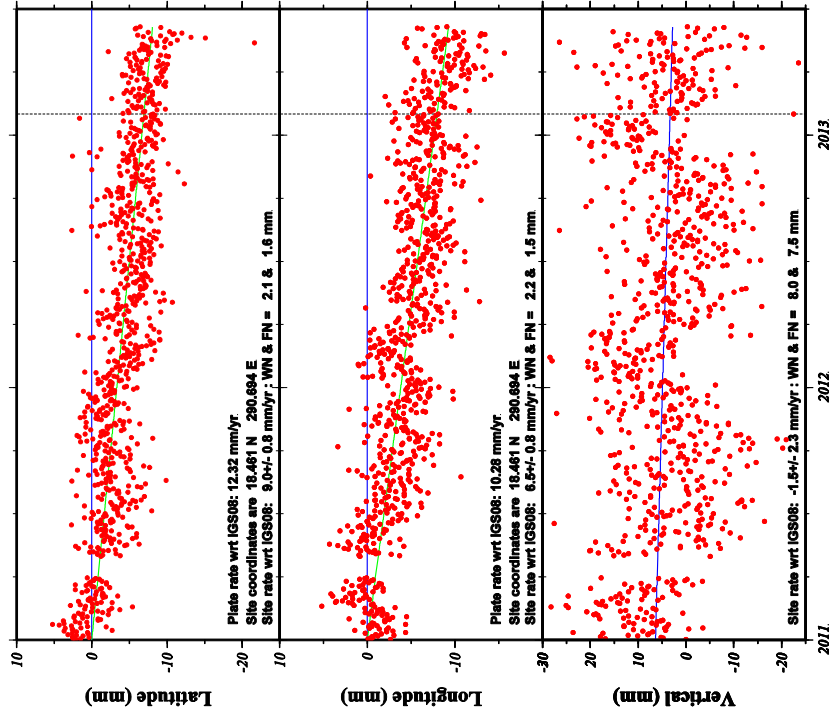
GM7 2013 Jun 16 06:50:39 Mafic04UT4

SCUB Coordinate changes - CA is fixed stacovs used AMB



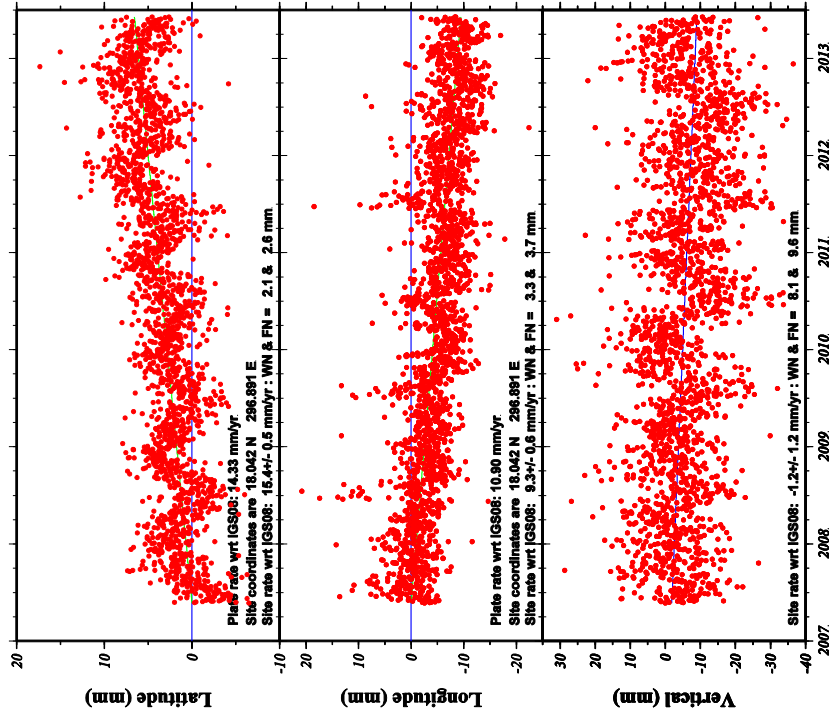
GM7 2013 Jul 31 14:18:44 | MetStacOVA

SPED Coordinate changes - CA is fixed stacovs used AMB



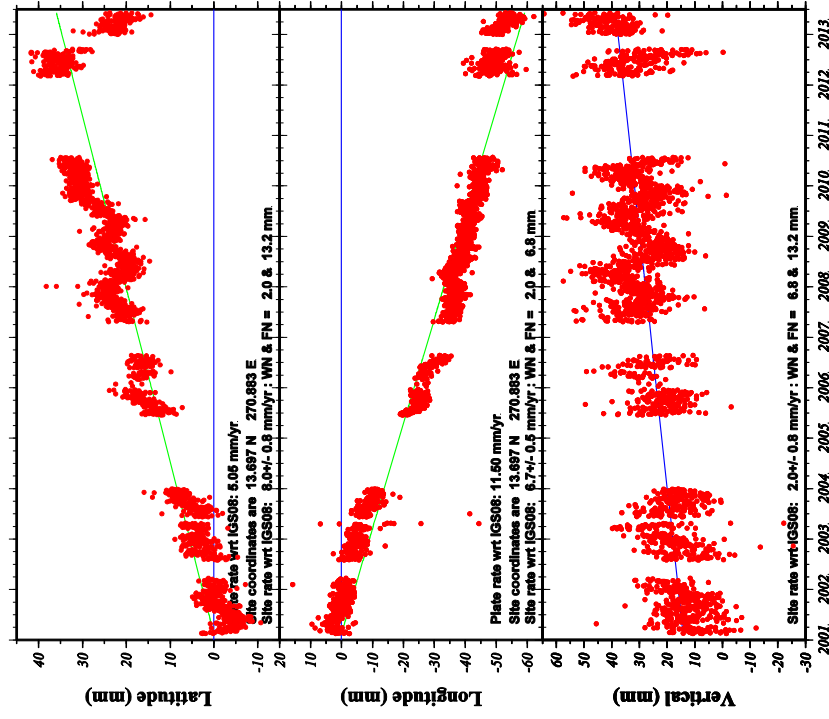
GM7 2013 Jul 10 16:50:49 | MetStacOVA

SMRT Coordinate changes - CA is fixed stacovs used AMB



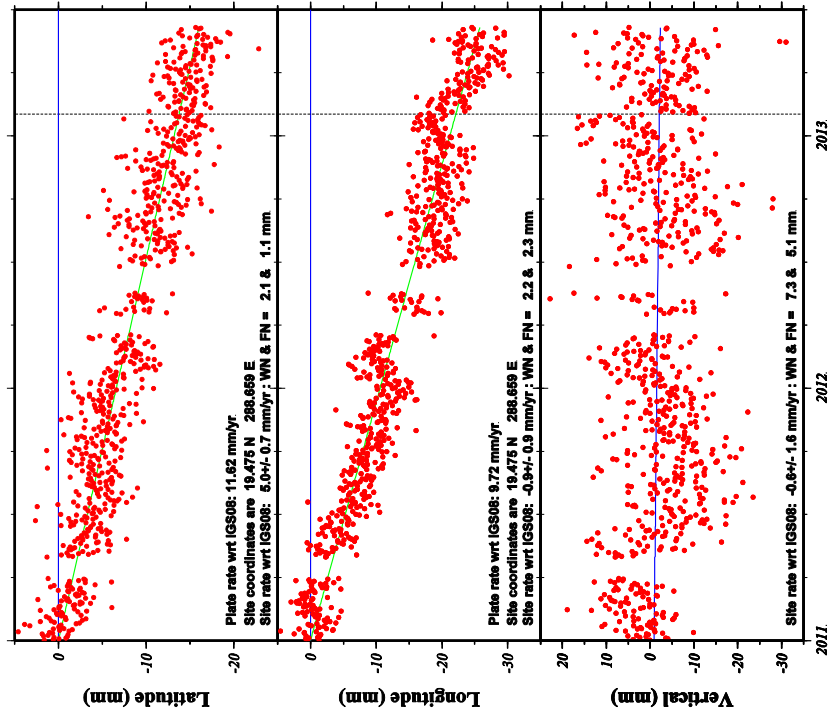
GM7 2013 Jul 10 16:44:48 | Natioli/UTA

SSIA Coordinate changes - CA is fixed stacovs used AMB



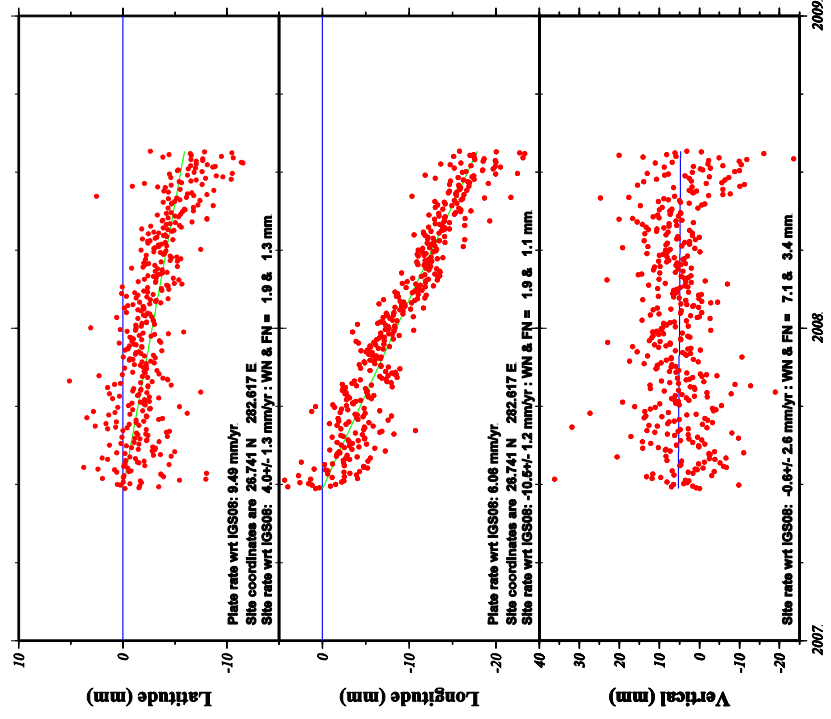
GM7 2013 Sep 07 09:15:52 | Natioli/UTA

**SROD Coordinate changes - CA is fixed stacovs used AMB**



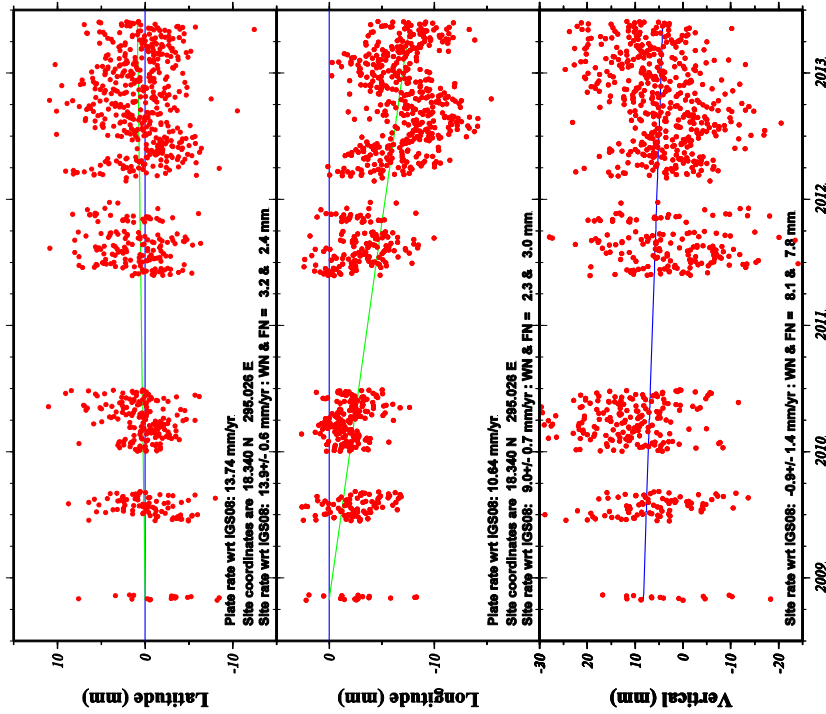
GM 2013 Jul 10 17:02:38 MARS0107A

**TCAO Coordinate changes - CA is fixed stacovs used AMB**



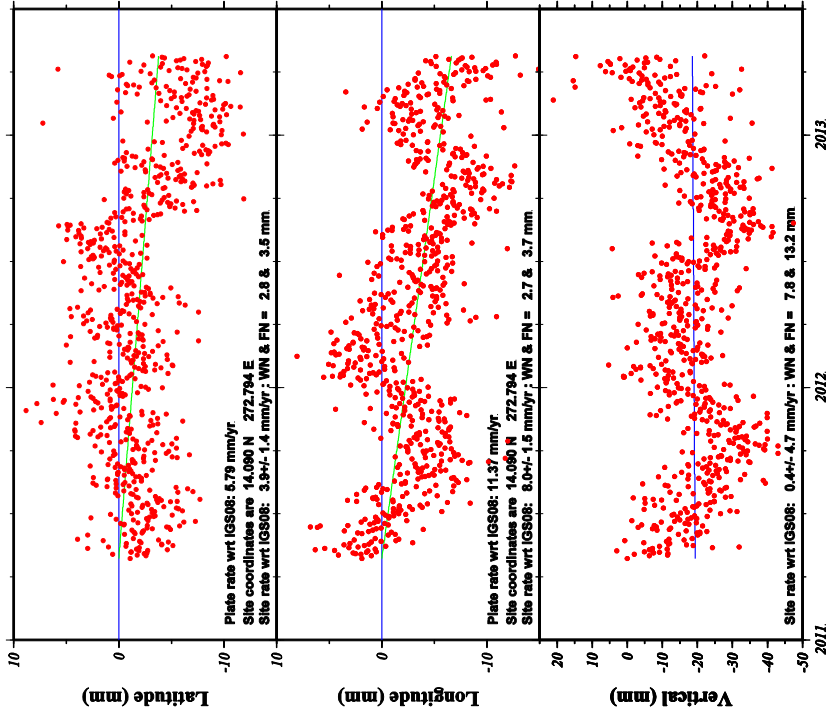
GM 2013 Aug 27 20:55:19 MARS0107A

STVI Coordinate changes - CA is fixed stacovs used AMB



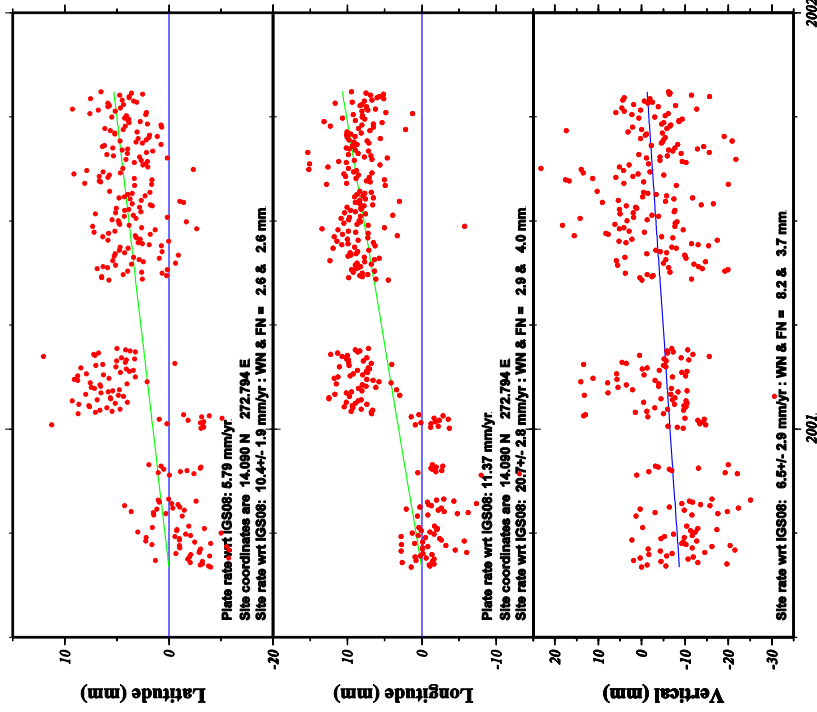
GM7 2013 Jul 11 09:32:08 | MetStacOVA

TEG2 Coordinate changes - CA is fixed stacovs used AMB



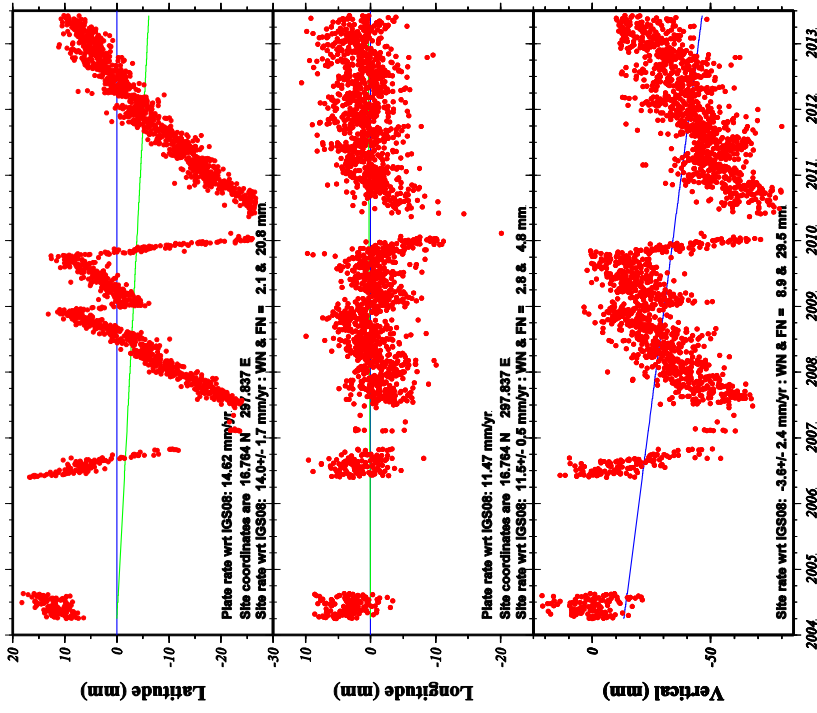
GM7 2013 Jul 10 17:28:58 | MetStacOVA

TEG1 Coordinate changes - CA is fixed stacovs used AMB



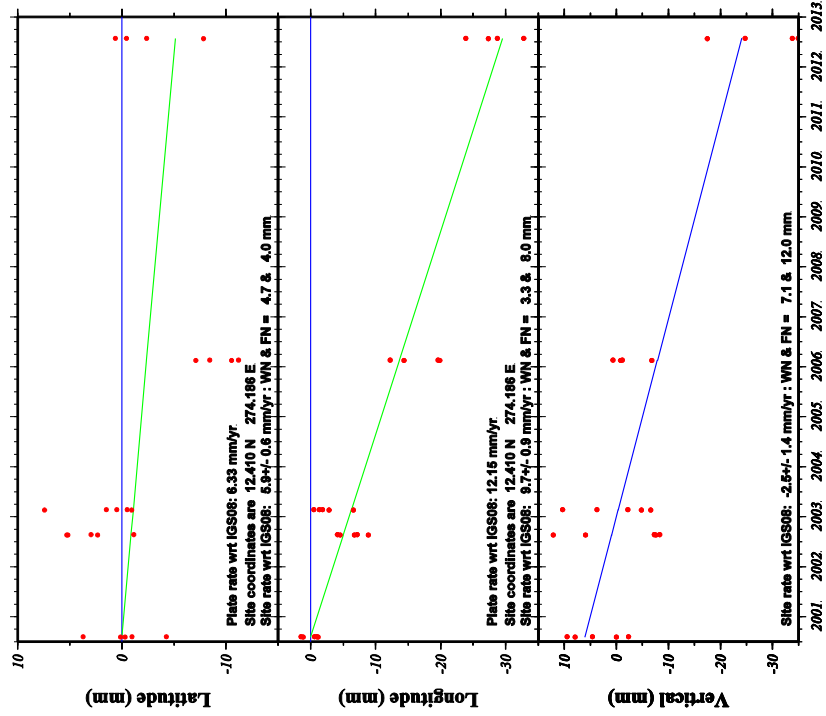
GMV 2013 Jul 10 16:29:53 Method:UTA

TRNT Coordinate changes - CA is fixed stacovs used AMB



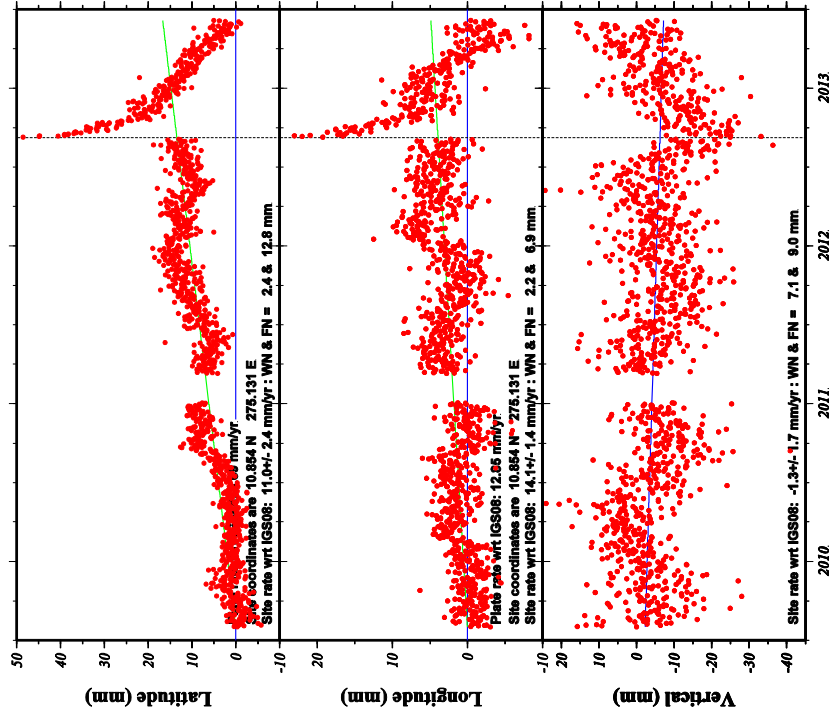
GMV 2013 Sep 07 06:25:30 Method:UTA

TEUS Coordinate changes - CA is fixed stacovs used AMB



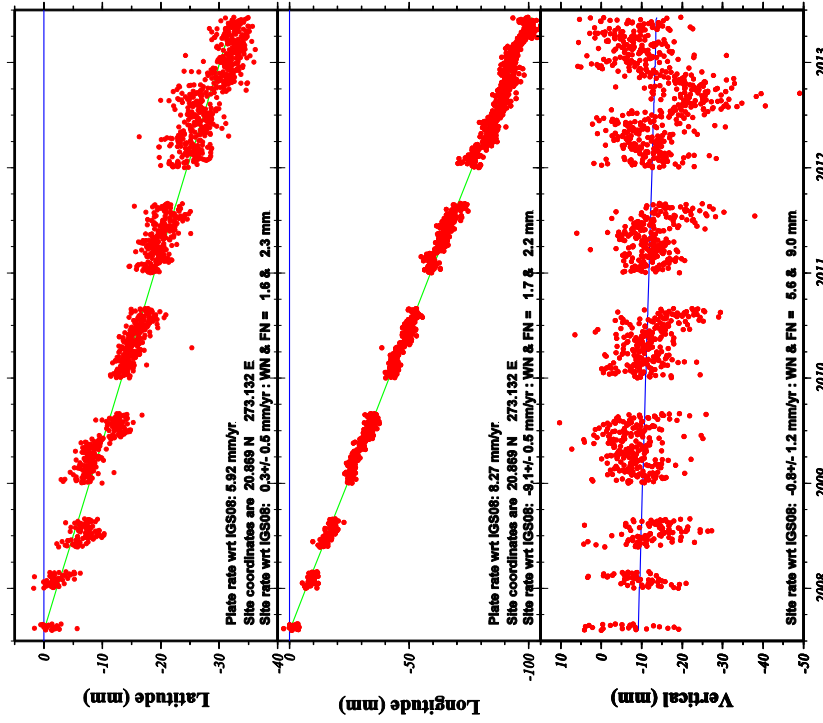
GM7 2013 Jun 13 16:18:38 MestohiUTA

VERA Coordinate changes - CA is fixed stacovs used AMB



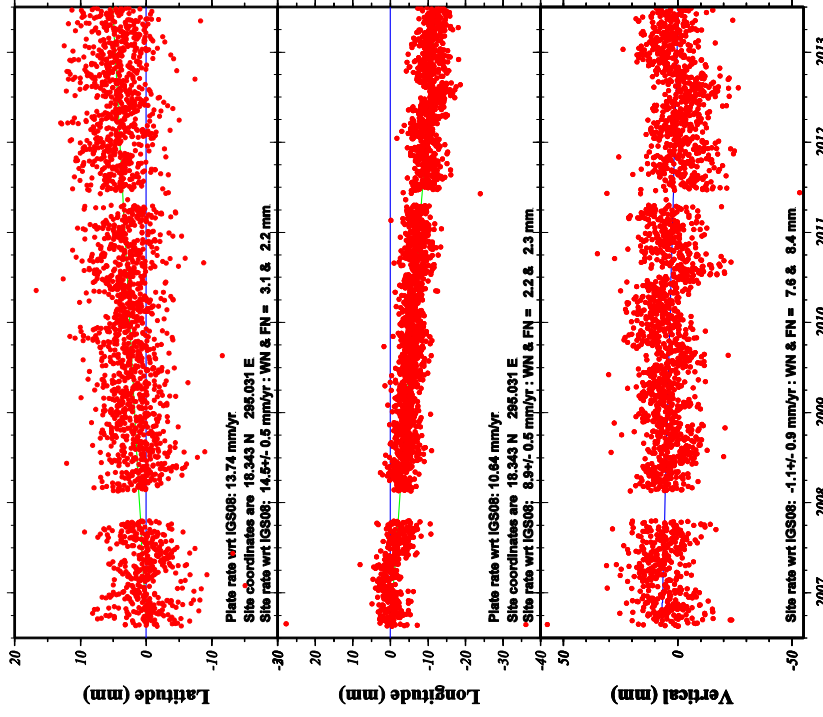
GM7 2013 Jul 11 06:52:30 MestohiUTA

UNPM Coordinate changes - CA is fixed stacovs used AMB



GM7 2013 Jul 11 08:28:09 | Metis@UTA

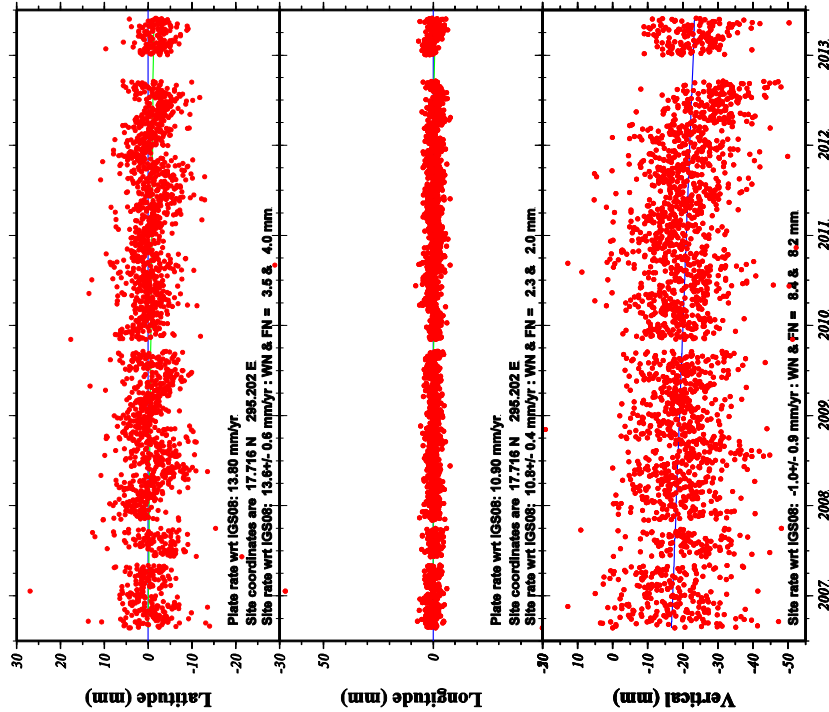
VITH Coordinate changes - CA is fixed stacovs used AMB



GM7 2013 Jul 12 08:17:03 | Metis@UTA

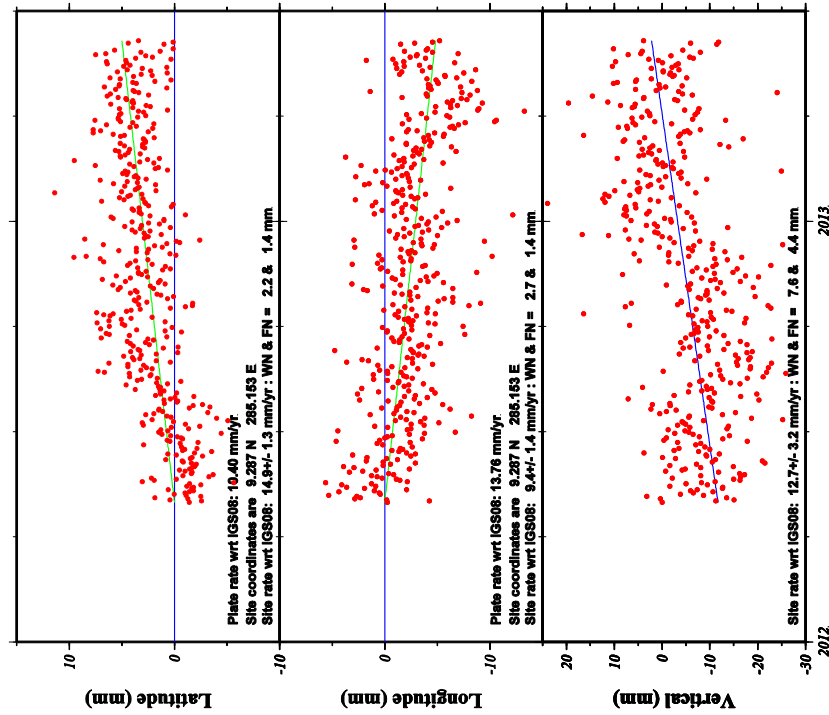


VIKH Coordinate changes - CA is fixed stacovs used AMB



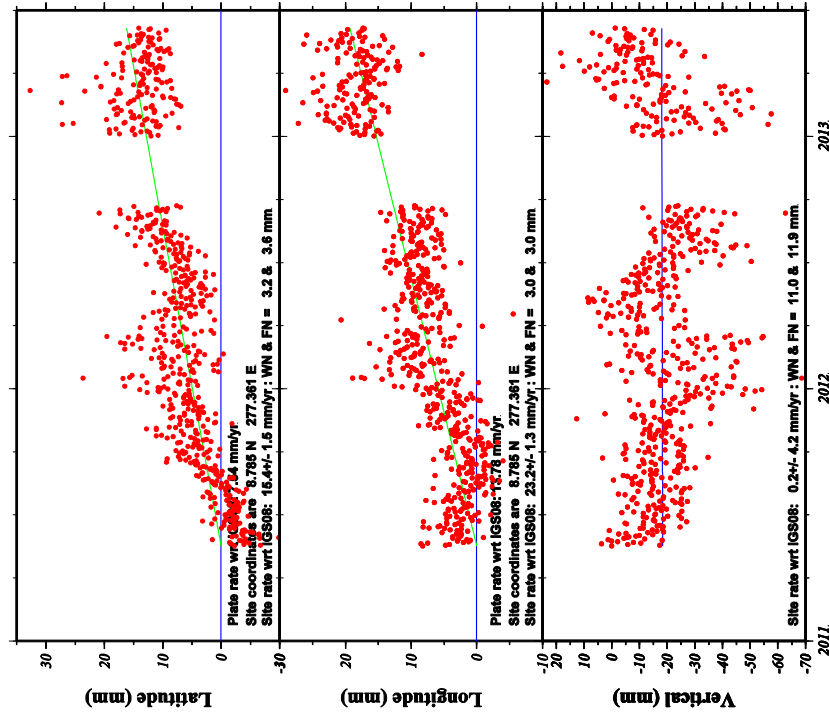
GM 2013 Jun 20 15:35:38 MedSOLUTA

VMAG Coordinate changes - CA is fixed stacovs used AMB



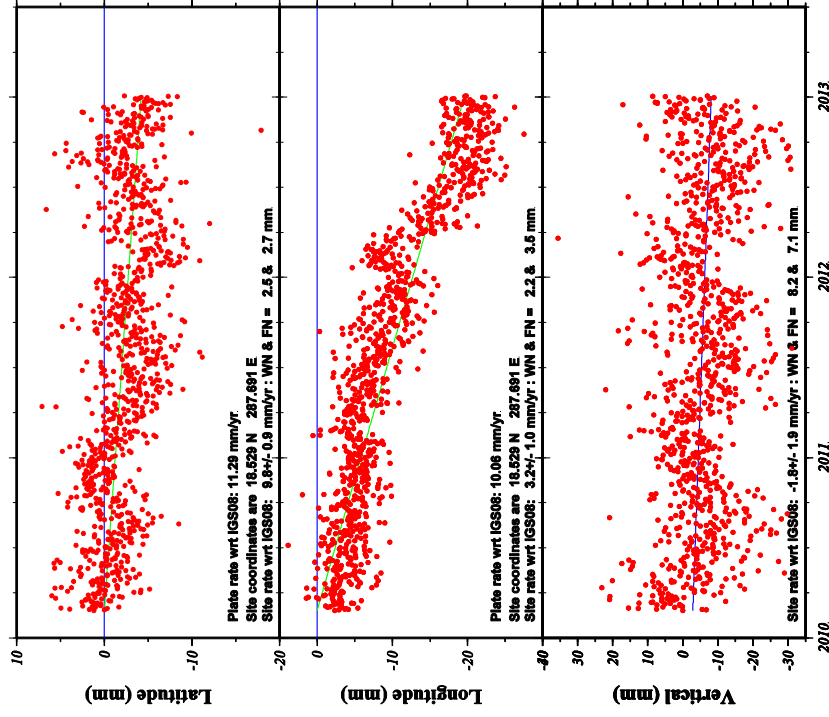
GM 2013 Jul 10 17:33:57 MedSOLUTA

VLCN Coordinate changes - CA is fixed stacovs used AMB



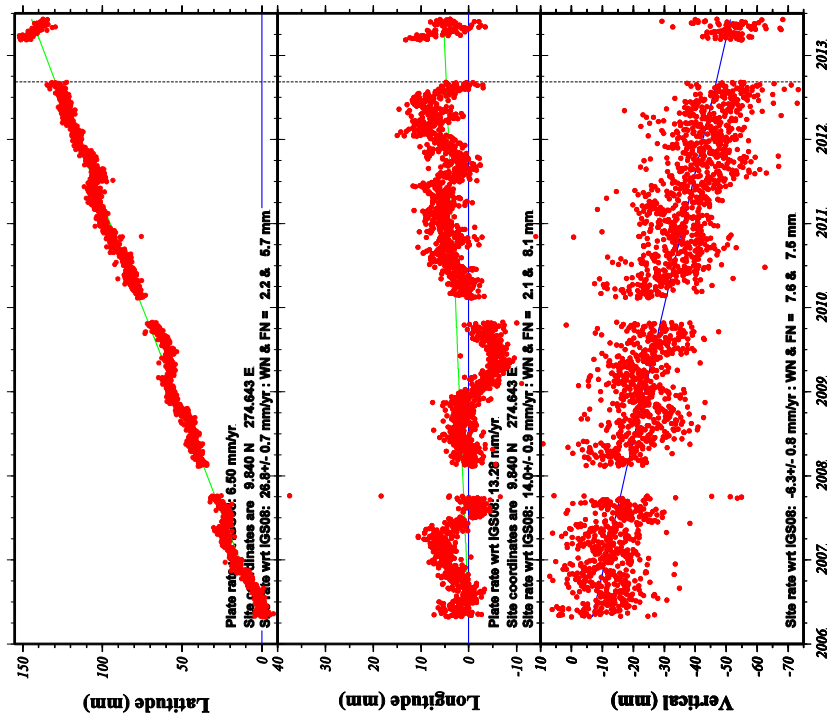
GM 2013 Sep 15 17:14:17 Hawaii/UTTA

VOIL Coordinate changes - CA is fixed stacovs used AMB



GM 2013 Jul 11 08:58:49 Hawaii/UTTA

QSEC Coordinate changes - CA is fixed stacovs used AMB



GNSS 2013 Sep 21 10:08:43 MATHAKUTA

Appendix C

Dominica site equipment history

Dominica campaign site equipment occupation history

	2001		2003		2004		2006		2007		2011/2012	
SITE	mount	antenna	receiver	mount	antenna	receiver	mount	antenna	receiver	mount	antenna	receiver
artu	not occupied	not occupied	not occupied	tripod	choke ring	Ashtech Z12	tripod	choke ring	Ashtech Z12	tripod	choke ring	Ashtech u-Z
belv	0.5 m spike	choke ring	Ashtech Z12	0.5 m spike	choke ring	Ashtech Z12	tripod	choke ring	Trimble R7	tripod	zephyr	Trimble R7
bolg	not occupied	not occupied	not occupied	not occupied	not occupied	not occupied	tripod	choke ring	Ashtech Z12	tripod	choke ring	Ashtech u-Z
brox	not occupied	not occupied	not occupied	0.5 m spike	choke ring	Ashtech Z12	0.5 m spike	choke ring	Ashtech Z12	0.5 m spike	choke ring	Ashtech u-Z
cabr	tripod	choke ring	Ashtech Z12	tripod	choke ring	Ashtech Z12	tripod	choke ring	Trimble R7	tripod	choke ring	Trimble R7
casr	0.5 m spike	choke ring	Ashtech Z12	0.5 m spike	choke ring	Ashtech Z12	0.5 m spike	choke ring	Trimble 4000SSI	0.5 m spike	choke ring	Ashtech u-Z
cncl	0.5 m spike	choke ring	Ashtech Z12	tripod	choke ring	Ashtech Z12	tripod	choke ring	Trimble 4000SSI	0.5 m spike	choke ring	Trimble R7
coht	not occupied	not occupied	not occupied	tripod	choke ring	Ashtech Z12	tripod	choke ring	Ashtech Z12	tripod	choke ring	Ashtech u-Z
corn	not occupied	not occupied	not occupied	not occupied	not occupied	not occupied	0.5 m spike	choke ring	Ashtech Z12	0.5 m spike	choke ring	Ashtech u-Z
fish	0.5 m spike	choke ring	Ashtech Z12	tripod	choke ring	Ashtech Z12	tripod	choke ring	Trimble R7	tripod	zephyr	Trimble R7
gorm	0.5 m spike	choke ring	Ashtech Z12	0.5 m spike	choke ring	Ashtech Z12	0.5 m spike	choke ring	Ashtech u-Z	0.5 m spike	choke ring	Ashtech u-Z
gsav	not occupied	not occupied	not occupied	0.5 m spike	choke ring	Ashtech Z12	0.5 m spike	choke ring	Ashtech Z12	0.5 m spike	choke ring	Ashtech u-Z
infrm	not occupied	not occupied	not occupied	not occupied	not occupied	not occupied	not occupied	not occupied	not occupied	not occupied	not occupied	not occupied
intv	not occupied	not occupied	not occupied	0.5 m spike	choke ring	Ashtech Z12	0.5 m spike	choke ring	Ashtech Z12	0.5 m spike	choke ring	Ashtech u-Z
newf	0.5 m spike	choke ring	Ashtech Z12	0.5 m spike	choke ring	Ashtech Z12	tripod	choke ring	Ashtech Z12	0.5 m spike	choke ring	Ashtech u-Z
nwen	not occupied	not occupied	not occupied	not occupied	not occupied	not occupied	0.5 m spike	choke ring	Ashtech Z12	0.5 m spike	choke ring	Ashtech u-Z
scft	0.5 m spike	choke ring	Ashtech Z12	tripod	choke ring	Ashtech Z12	0.5 m spike	choke ring	Ashtech Z12	0.5 m spike	choke ring	Ashtech u-Z
sole	0.5 m spike	choke ring	Ashtech Z12	0.5 m spike	choke ring	Ashtech Z12	0.5 m spike	choke ring	Ashtech Z12	0.5 m spike	choke ring	Ashtech u-Z
stg	not occupied	not occupied	not occupied	0.5 m spike	choke ring	Ashtech Z12	0.5 m spike	choke ring	Trimble 4000SSI	0.5 m spike	choke ring	Ashtech u-Z
tag	not occupied	not occupied	not occupied	tripod	choke ring	Ashtech Z12	tripod	choke ring	Ashtech Z12	tripod	choke ring	Ashtech u-Z
teat	not occupied	not occupied	not occupied	0.5 m spike	choke ring	Ashtech Z12	0.5 m spike	choke ring	Ashtech Z12	0.5 m spike	choke ring	Ashtech u-Z
wot	0.5 m spike	choke ring	Ashtech Z12	0.5 m spike	choke ring	Ashtech Z12	0.5 m spike	choke ring	Trimble R7	0.5 m spike	choke ring	Ashtech u-Z

Appendix D  
Inversion Input Files

DeMets, 2007 values, 1-plate, 15 sites, ITRF fixed

```

caribbean gps site velocities - IGS08
  0 0 0 0 0 0 0 0 0 0
it
ca 0.0 0.0 0.5 # Fixed plate
zz # Starting est of IGS08-CAR ca ang vel lat/long/omega
# End of plate list
ca it vn 15.67 296.38 1.42 0.132 AVES ITRF08 3.8740 yrs #= 28
ca it ve 15.67 296.38 1.13 0.231 AVES Start/stop times:1994.3740-1998.2479
ca it cv 15.67 296.38 0.00000 Corr. coeff. for AVES
ca it vn 13.09 300.39 1.71 0.186 BARB ITRF08 1.6164 yrs #= 333
ca it ve 13.09 300.39 0.81 0.104 BARB Start/stop times:1999.5000-2001.1164
ca it cv 13.09 300.39 -0.07188 Corr. coeff. for BARB
ca it vn 14.51 274.29 0.54 0.167 CMP1 ITRF08 5.2142 yrs #= 6
ca it ve 14.51 274.29 1.17 0.236 CMP1 Start/stop times:2000.1926-2005.4068
ca it cv 14.51 274.29 0.00000 Corr. coeff. for CMP1
ca it vn 17.76 295.42 1.30 0.039 CRO1 ITRF08 10.2164 yrs #= 3410
ca it ve 17.76 295.42 1.10 0.047 CRO1 Start/stop times:1995.7822-2005.9986
ca it cv 17.76 295.42 -0.09560 Corr. coeff. for CRO1
ca it vn 14.73 298.85 1.58 0.122 FSD0 ITRF08 5.4685 yrs #= 14
ca it ve 14.73 298.85 1.31 0.318 FSD0 Start/stop times:1994.3986-1999.8671
ca it cv 14.73 298.85 0.00000 Corr. coeff. for FSD0
ca it vn 14.73 298.85 1.63 0.167 FSD1 ITRF08 5.4575 yrs #= 9
ca it ve 14.73 298.85 1.33 0.214 FSD1 Start/stop times:1994.4096-1999.8671
ca it cv 14.73 298.85 0.00000 Corr. coeff. for FSD1
ca it vn 15.03 273.93 0.80 0.133 GLCO ITRF08 4.3579 yrs #= 7
ca it ve 15.03 273.93 0.99 0.321 GLCO Start/stop times:2000.1790-2004.5369
ca it cv 15.03 273.93 0.00000 Corr. coeff. for GLCO
ca it vn 14.92 273.62 0.69 0.134 MNTO ITRF08 4.3689 yrs #= 6
ca it ve 14.92 273.62 1.17 0.246 MNTO Start/stop times:2000.1680-2004.5369
ca it cv 14.92 273.62 0.00000 Corr. coeff. for MNTO
ca it vn 12.57 274.63 0.59 0.289 PORT ITRF08 2.5387 yrs #= 10
ca it ve 12.57 274.63 1.33 0.380 PORT Start/stop times:2000.6134-2003.1521
ca it cv 12.57 274.63 0.00000 Corr. coeff. for PORT
ca it vn 14.04 276.62 0.50 0.230 PUEC ITRF08 2.0986 yrs #= 9
ca it ve 14.04 276.62 1.30 0.441 PUEC Start/stop times:2001.0397-2003.1384
ca it cv 14.04 276.62 0.00000 Corr. coeff. for PUEC
ca it vn 12.92 274.78 0.67 0.250 RIOB ITRF08 2.5496 yrs #= 12
ca it ve 12.92 274.78 1.18 0.429 RIOB Start/stop times:2000.6025-2003.1521
ca it cv 12.92 274.78 0.00000 Corr. coeff. for RIOB
ca it vn 17.90 288.33 0.91 0.093 ROJO ITRF08 6.7507 yrs #= 16
ca it ve 17.90 288.33 0.91 0.161 ROJO Start/stop times:1994.3959-2001.1466
ca it cv 17.90 288.33 0.00000 Corr. coeff. for ROJO
ca it vn 12.52 278.27 0.72 0.066 SANA ITRF08 9.1616 yrs #= 22
ca it ve 12.52 278.27 1.31 0.115 SANA Start/stop times:1994.1082-2003.2699
ca it cv 12.52 278.27 0.00000 Corr. coeff. for SANA
ca it vn 14.97 273.76 0.66 0.138 SFDP ITRF08 4.3607 yrs #= 6
ca it ve 14.97 273.76 1.13 0.244 SFDP Start/stop times:2000.1762-2004.5369
ca it cv 14.97 273.76 0.00000 Corr. coeff. for SFDP
ca it vn 12.41 274.19 0.75 0.209 TEUS ITRF08 2.5523 yrs #= 15
ca it ve 12.41 274.19 1.04 0.362 TEUS Start/stop times:2000.5888-2003.1411
ca it cv 12.41 274.19 0.00000 Corr. coeff. for TEUS

```

DeMets et al., 2007 values-updated, 1-plate, 15 sites, ITRF fixed

```

caribbean gps site velocities - IGS08
  0 0 0 0 0 0 0 0 0 0
it                                     # Fixed plate
ca  0.0    0.0    0.5                 # Starting est of IGS08-CAR ca ang vel
lat/long/omega
zz                                     # End of plate list
ca it vn 15.67 296.38 1.42 0.132 AVES ITRF08 3.8740 yrs #= 28
ca it ve 15.67 296.38 1.13 0.231 AVES Start/stop times:1994.3740-1998.2479
ca it cv 15.67 296.38 0.00000 Corr. coeff. for AVES
ca it vn 13.09 300.39 1.71 0.186 BARB ITRF08 1.6164 yrs #= 333
ca it ve 13.09 300.39 0.81 0.104 BARB Start/stop times:1999.5000-2001.1164
ca it cv 13.09 300.39 -0.07188 Corr. coeff. for BARB
ca it vn 14.51 274.29 0.54 0.167 CMP1 ITRF08 5.2142 yrs #= 6
ca it ve 14.51 274.29 1.17 0.236 CMP1 Start/stop times:2000.1926-2005.4068
ca it cv 14.51 274.29 0.00000 Corr. coeff. for CMP1
ca it vn 17.76 295.42 1.36 0.029 CRO1 ITRF08 17.6438 yrs #=12070
ca it ve 17.76 295.42 1.10 0.033 CRO1 Start/stop times:1995.7822-2013.4260
ca it cv 17.76 295.42 0.00160 Corr. coeff. for CRO1
ca it vn 14.73 298.85 1.58 0.122 FSD0 ITRF08 5.4685 yrs #= 14
ca it ve 14.73 298.85 1.31 0.318 FSD0 Start/stop times:1994.3986-1999.8671
ca it cv 14.73 298.85 0.00000 Corr. coeff. for FSD0
ca it vn 14.73 298.85 1.63 0.167 FSD1 ITRF08 5.4575 yrs #= 9
ca it ve 14.73 298.85 1.33 0.214 FSD1 Start/stop times:1994.4096-1999.8671
ca it cv 14.73 298.85 0.00000 Corr. coeff. for FSD1
ca it vn 15.03 273.93 0.71 0.095 GLCO ITRF08 10.2882 yrs #= 13
ca it ve 15.03 273.93 1.08 0.184 GLCO Start/stop times:2000.1790-2010.4671
ca it cv 15.03 273.93 0.00000 Corr. coeff. for GLCO
ca it vn 14.92 273.62 0.67 0.062 MNTO ITRF08 10.2991 yrs #= 9
ca it ve 14.92 273.62 1.10 0.112 MNTO Start/stop times:2000.1680-2010.4671
ca it cv 14.92 273.62 0.00000 Corr. coeff. for MNTO
ca it vn 12.57 274.63 0.73 0.057 PORT ITRF08 11.9563 yrs #= 22
ca it ve 12.57 274.63 0.95 0.110 PORT Start/stop times:2000.6134-2012.5697
ca it cv 12.57 274.63 0.00000 Corr. coeff. for PORT
ca it vn 14.04 276.62 0.61 0.107 PUEC ITRF08 5.1233 yrs #= 13
ca it ve 14.04 276.62 1.10 0.197 PUEC Start/stop times:2001.0397-2006.1630
ca it cv 14.04 276.62 0.00000 Corr. coeff. for PUEC
ca it vn 12.92 274.78 0.67 0.250 RIOB ITRF08 2.5496 yrs #= 12
ca it ve 12.92 274.78 1.18 0.429 RIOB Start/stop times:2000.6025-2003.1521
ca it cv 12.92 274.78 0.00000 Corr. coeff. for RIOB
ca it vn 17.90 288.33 0.91 0.093 ROJO ITRF08 6.7507 yrs #= 16
ca it ve 17.90 288.33 0.91 0.161 ROJO Start/stop times:1994.3959-2001.1466
ca it cv 17.90 288.33 0.00000 Corr. coeff. for ROJO
ca it vn 12.52 278.27 0.72 0.066 SANA ITRF08 9.1616 yrs #= 22
ca it ve 12.52 278.27 1.31 0.115 SANA Start/stop times:1994.1082-2003.2699
ca it cv 12.52 278.27 0.00000 Corr. coeff. for SANA
ca it vn 14.97 273.76 0.66 0.138 SFDP ITRF08 4.3607 yrs #= 6
ca it ve 14.97 273.76 1.13 0.244 SFDP Start/stop times:2000.1762-2004.5369
ca it cv 14.97 273.76 0.00000 Corr. coeff. for SFDP
ca it vn 12.41 274.19 0.59 0.058 TEUS ITRF08 11.9836 yrs #= 23
ca it ve 12.41 274.19 0.97 0.090 TEUS Start/stop times:2000.5888-2012.5724
ca it cv 12.41 274.19 0.00000 Corr. coeff. for TEUS

```



## 2 plates, 24 sites, Caribbean (east) fixed

```

caribbean gps site velocities - IGS08
  0 0 0 0 0 0 0 0 0 0 0
ce                                     # Fixed plate
it  0.0    0.0    0.5                # Starting est of IGS08-CAR ca ang vel lat/long/omega
cw  0.0    0.0    0.5                #
zz                                     # End of plate list
ce it vn  16.26  298.47  1.44  0.082  ABMF ITRF08  2.8438 yrs  #=  977
ce it ve  16.26  298.47  1.20  0.089  ABMF Start/stop times:2010.6671-2013.5110
ce it cv  16.26  298.47 -0.03874  Corr. coeff. for ABMF
ce it vn  12.22  298.36  1.52  0.049  GRE0 ITRF08  5.9397 yrs  #=  4214
ce it ve  12.22  298.36  1.36  0.052  GRE0 Start/stop times:2007.4863-2013.4260
ce it cv  12.22  298.36 -0.11443  Corr. coeff. for GRE0
ce it vn  14.59  299.00  1.50  0.080  LMMF ITRF08  2.8438 yrs  #=  1023
ce it ve  14.59  299.00  1.25  0.091  LMMF Start/stop times:2010.6671-2013.5110
ce it cv  14.59  299.00  0.01081  Corr. coeff. for LMMF
ce it vn  14.73  298.85  1.58  0.122  FSD0 ITRF08  5.4685 yrs  #=   14
ce it ve  14.73  298.85  1.31  0.318  FSD0 Start/stop times:1994.3986-1999.8671
ce it cv  14.73  298.85  0.00000  Corr. coeff. for FSD0
ce it vn  14.73  298.85  1.63  0.167  FSD1 ITRF08  5.4575 yrs  #=   9
ce it ve  14.73  298.85  1.33  0.214  FSD1 Start/stop times:1994.4096-1999.8671
ce it cv  14.73  298.85  0.00000  Corr. coeff. for FSD1
ce it vn  15.24  298.71  1.40  0.063  CASS ITRF08  10.9879 yrs  #=   20
ce it ve  15.24  298.71  1.18  0.111  CASS Start/stop times:2001.4288-2012.4167
ce it cv  15.24  298.71  0.00000  Corr. coeff. for ceSS
ce it vn  15.34  298.69  1.51  0.084  FRSH ITRF08  10.9906 yrs  #=   21
ce it ve  15.34  298.69  1.07  0.117  FRSH Start/stop times:2001.4452-2012.4358
ce it cv  15.34  298.69  0.00000  Corr. coeff. for FRSH
ce it vn  15.51  298.72  1.42  0.071  CNCD ITRF08  10.0877 yrs  #=   25
ce it ve  15.51  298.72  1.18  0.109  CNCD Start/stop times:2001.4534-2011.5411
ce it cv  15.51  298.72  0.00000  Corr. coeff. for CNCD
ce it vn  15.67  296.38  1.42  0.132  AVES ITRF08  3.8740 yrs  #=   28
ce it ve  15.67  296.38  1.13  0.231  AVES Start/stop times:1994.3740-1998.2479
ce it cv  15.67  296.38  0.00000  Corr. coeff. for AVES
ce it vn  17.67  298.21  1.26  0.384  CN00 ITRF08  0.7689 yrs  #=  282
ce it ve  17.67  298.21  1.12  0.737  CN00 Start/stop times:2012.6407-2013.4096
ce it cv  17.67  298.21 -0.00308  Corr. coeff. for CN00
ce it vn  17.72  295.20  1.36  0.057  VIKH ITRF08  6.7644 yrs  #=  2170
ce it ve  17.72  295.20  1.08  0.044  VIKH Start/stop times:2006.6425-2013.4068
ce it cv  17.72  295.20 -0.00329  Corr. coeff. for VIKH
cw it vn  15.03  273.93  0.71  0.095  GLCO ITRF08  10.2882 yrs  #=   13
cw it ve  15.03  273.93  1.08  0.184  GLCO Start/stop times:2000.1790-2010.4671
cw it cv  15.03  273.93  0.00000  Corr. coeff. for GLCO
cw it vn  14.97  273.76  0.66  0.138  SFDP ITRF08  4.3607 yrs  #=   6
cw it ve  14.97  273.76  1.13  0.244  SFDP Start/stop times:2000.1762-2004.5369
cw it cv  14.97  273.76  0.00000  Corr. coeff. for SFDP
cw it vn  14.92  273.62  0.67  0.062  MNTO ITRF08  10.2991 yrs  #=   9
cw it ve  14.92  273.62  1.10  0.112  MNTO Start/stop times:2000.1680-2010.4671
cw it cv  14.92  273.62  0.00000  Corr. coeff. for MNTO
cw it vn  14.51  274.29  0.54  0.167  CMP1 ITRF08  5.2142 yrs  #=   6
cw it ve  14.51  274.29  1.17  0.236  CMP1 Start/stop times:2000.1926-2005.4068
cw it cv  14.51  274.29  0.00000  Corr. coeff. for CMP1
cw it vn  14.04  276.62  0.61  0.107  PUEC ITRF08  5.1233 yrs  #=   13
cw it ve  14.04  276.62  1.10  0.197  PUEC Start/stop times:2001.0397-2006.1630
cw it cv  14.04  276.62  0.00000  Corr. coeff. for PUEC
cw it vn  12.58  278.28  0.69  0.061  SAN0 ITRF08  5.4932 yrs  #=  1764
cw it ve  12.58  278.28  1.25  0.063  SAN0 Start/stop times:2007.9356-2013.4288
cw it cv  12.58  278.28  0.11575  Corr. coeff. for SAN0
cw it vn  12.57  274.63  0.73  0.057  PORT ITRF08  11.9563 yrs  #=   22
cw it ve  12.57  274.63  0.95  0.110  PORT Start/stop times:2000.6134-2012.5697
cw it cv  12.57  274.63  0.00000  Corr. coeff. for PORT
cw it vn  12.52  278.27  0.72  0.066  SANA ITRF08  9.1616 yrs  #=   22
cw it ve  12.52  278.27  1.31  0.115  SANA Start/stop times:1994.1082-2003.2699
cw it cv  12.52  278.27  0.00000  Corr. coeff. for SANA
cw it vn  12.41  274.19  0.59  0.058  TEUS ITRF08  11.9836 yrs  #=   23
cw it ve  12.41  274.19  0.97  0.090  TEUS Start/stop times:2000.5888-2012.5724
cw it cv  12.41  274.19  0.00000  Corr. coeff. for TEUS
cw it vn  12.92  274.78  0.67  0.250  RIOB ITRF08  2.5496 yrs  #=   12

```

	ce	it	ve	12.92	274.78	1.18	0.429	RIOB Start/stop times:2000.6025-2003.1521
	cw	it	cv	12.92	274.78	0.00000		Corr. coeff. for RIOB
	ce	it	vn	17.76	295.42	1.36	0.030	CRO1 ITRF08 17.6740 yrs # = 6018
	ce	it	ve	17.76	295.42	1.10	0.031	CRO1 Start/stop times:1995.7822-2013.4562
	ce	it	cv	17.76	295.42	-0.01438		Corr. coeff. for CRO1
	ce	it	vn	16.93	297.65	1.47	0.151	RDON ITRF08 1.2860 yrs # = 403
	ce	it	ve	16.93	297.65	1.04	0.129	RDON Start/stop times:2012.3975-2013.6836
	ce	it	cv	16.93	297.65	0.02801		Corr. coeff. for RDON
	cw	it	vn	13.38	278.64	0.30	0.400	CN35 ITRF08 0.7389 yrs # = 268
	cw	it	ve	13.38	278.64	0.92	0.767	CN35 Start/stop times:2012.6899-2013.4288
	cw	it	cv	13.38	278.64	-0.01010		Corr. coeff. for CN35
site	it	it	vn	16.26	298.47	1.44	0.082	ABMF ITRF08 2.8438 yrs # = 977
site	it	it	ve	16.26	298.47	1.20	0.089	ABMF Start/stop times:2010.6671-2013.5110
site	it	it	cv	16.26	298.47	-0.03874		Corr. coeff. for ABMF
site	it	it	vn	12.22	298.36	1.52	0.049	GRE0 ITRF08 5.9397 yrs # = 4214
site	it	it	ve	12.22	298.36	1.36	0.052	GRE0 Start/stop times:2007.4863-2013.4260
site	it	it	cv	12.22	298.36	-0.11443		Corr. coeff. for GRE0
site	it	it	vn	14.59	299.00	1.50	0.080	LMMF ITRF08 2.8438 yrs # = 1023
site	it	it	ve	14.59	299.00	1.25	0.091	LMMF Start/stop times:2010.6671-2013.5110
site	it	it	cv	14.59	299.00	0.01081		Corr. coeff. for LMMF
site	it	it	vn	14.73	298.85	1.58	0.122	FSD0 ITRF08 5.4685 yrs # = 14
site	it	it	ve	14.73	298.85	1.31	0.318	FSD0 Start/stop times:1994.3986-1999.8671
site	it	it	cv	14.73	298.85	0.00000		Corr. coeff. for FSD0
site	it	it	vn	14.73	298.85	1.63	0.167	FSD1 ITRF08 5.4575 yrs # = 9
site	it	it	ve	14.73	298.85	1.33	0.214	FSD1 Start/stop times:1994.4096-1999.8671
site	it	it	cv	14.73	298.85	0.00000		Corr. coeff. for FSD1
site	it	it	vn	15.24	298.71	1.40	0.063	CASS ITRF08 10.9879 yrs # = 20
site	it	it	ve	15.24	298.71	1.18	0.111	CASS Start/stop times:2001.4288-2012.4167
site	it	it	cv	15.24	298.71	0.00000		Corr. coeff. for ceSS
site	it	it	vn	15.34	298.69	1.51	0.084	FRSH ITRF08 10.9906 yrs # = 21
site	it	it	ve	15.34	298.69	1.07	0.117	FRSH Start/stop times:2001.4452-2012.4358
site	it	it	cv	15.34	298.69	0.00000		Corr. coeff. for FRSH
site	it	it	vn	15.51	298.72	1.42	0.071	CNCD ITRF08 10.0877 yrs # = 25
site	it	it	ve	15.51	298.72	1.18	0.109	CNCD Start/stop times:2001.4534-2011.5411
site	it	it	cv	15.51	298.72	0.00000		Corr. coeff. for CNCD
site	it	it	vn	15.67	296.38	1.42	0.132	AVES ITRF08 3.8740 yrs # = 28
site	it	it	ve	15.67	296.38	1.13	0.231	AVES Start/stop times:1994.3740-1998.2479
site	it	it	cv	15.67	296.38	0.00000		Corr. coeff. for AVES
site	it	it	vn	17.67	298.21	1.26	0.384	CN00 ITRF08 0.7689 yrs # = 282
site	it	it	ve	17.67	298.21	1.12	0.737	CN00 Start/stop times:2012.6407-2013.4096
site	it	it	cv	17.67	298.21	-0.00308		Corr. coeff. for CN00
site	it	it	vn	17.72	295.20	1.36	0.057	VIKH ITRF08 6.7644 yrs # = 2170
site	it	it	ve	17.72	295.20	1.08	0.044	VIKH Start/stop times:2006.6425-2013.4068
site	it	it	cv	17.72	295.20	-0.00329		Corr. coeff. for VIKH
site	it	it	vn	15.03	273.93	0.71	0.095	GLCO ITRF08 10.2882 yrs # = 13
site	it	it	ve	15.03	273.93	1.08	0.184	GLCO Start/stop times:2000.1790-2010.4671
site	it	it	cv	15.03	273.93	0.00000		Corr. coeff. for GLCO
site	it	it	vn	14.97	273.76	0.66	0.138	SFDP ITRF08 4.3607 yrs # = 6
site	it	it	ve	14.97	273.76	1.13	0.244	SFDP Start/stop times:2000.1762-2004.5369
site	it	it	cv	14.97	273.76	0.00000		Corr. coeff. for SFDP
site	it	it	vn	14.92	273.62	0.67	0.062	MNTO ITRF08 10.2991 yrs # = 9
site	it	it	ve	14.92	273.62	1.10	0.112	MNTO Start/stop times:2000.1680-2010.4671
site	it	it	cv	14.92	273.62	0.00000		Corr. coeff. for MNTO
site	it	it	vn	14.51	274.29	0.54	0.167	CMP1 ITRF08 5.2142 yrs # = 6
site	it	it	ve	14.51	274.29	1.17	0.236	CMP1 Start/stop times:2000.1926-2005.4068
site	it	it	cv	14.51	274.29	0.00000		Corr. coeff. for CMP1
site	it	it	vn	14.04	276.62	0.61	0.107	PUEC ITRF08 5.1233 yrs # = 13
site	it	it	ve	14.04	276.62	1.10	0.197	PUEC Start/stop times:2001.0397-2006.1630
site	it	it	cv	14.04	276.62	0.00000		Corr. coeff. for PUEC
site	it	it	vn	12.58	278.28	0.69	0.061	SANO ITRF08 5.4932 yrs # = 1764
site	it	it	ve	12.58	278.28	1.25	0.063	SANO Start/stop times:2007.9356-2013.4288
site	it	it	cv	12.58	278.28	0.11575		Corr. coeff. for SANO
site	it	it	vn	12.57	274.63	0.73	0.057	PORT ITRF08 11.9563 yrs # = 22
site	it	it	ve	12.57	274.63	0.95	0.110	PORT Start/stop times:2000.6134-2012.5697
site	it	it	cv	12.57	274.63	0.00000		Corr. coeff. for PORT
site	it	it	vn	12.52	278.27	0.72	0.066	SANA ITRF08 9.1616 yrs # = 22
site	it	it	ve	12.52	278.27	1.31	0.115	SANA Start/stop times:1994.1082-2003.2699
site	it	it	cv	12.52	278.27	0.00000		Corr. coeff. for SANA
site	it	it	vn	12.41	274.19	0.59	0.058	TEUS ITRF08 11.9836 yrs # = 23
site	it	it	ve	12.41	274.19	0.97	0.090	TEUS Start/stop times:2000.5888-2012.5724
site	it	it	cv	12.41	274.19	0.00000		Corr. coeff. for TEUS
site	it	it	vn	12.92	274.78	0.67	0.250	RIOB ITRF08 2.5496 yrs # = 12

site	it	it	ve	12.92	274.78	1.18	0.429	RIOB Start/stop times:2000.6025-2003.1521
site	it	it	cv	12.92	274.78	0.00000		Corr. coeff. for RIOB
site	it	it	vn	17.76	295.42	1.36	0.030	CRO1 ITRF08 17.6740 yrs #= 6018
site	it	it	ve	17.76	295.42	1.10	0.031	CRO1 Start/stop times:1995.7822-2013.4562
site	it	it	cv	17.76	295.42	-0.01438		Corr. coeff. for CRO1
site	it	it	vn	16.93	297.65	1.47	0.151	RDON ITRF08 1.2860 yrs #= 403
site	it	it	ve	16.93	297.65	1.04	0.129	RDON Start/stop times:2012.3975-2013.6836
site	it	it	cv	16.93	297.65	0.02801		Corr. coeff. for RDON
site	it	it	vn	13.38	278.64	0.30	0.400	CN35 ITRF08 0.7389 yrs #= 268
site	it	it	ve	13.38	278.64	0.92	0.767	CN35 Start/stop times:2012.6899-2013.4288
site	it	it	cv	13.38	278.64	-0.01010		Corr. coeff. for CN35

1 plate, 24 sites, ITRF2008 fixed

```

caribbean gps site velocities - IGS08
0 0 0 0 0 0 0 0 0 0
it
ca 0.0 0.0 0.5 # Fixed plate
zz 0.0 0.0 0.5 # Starting est of IGS08-CAR ca ang vel lat/long/omega
# end of plate list
ca it vn 16.26 298.47 1.44 0.082 ABMF ITRF08 2.8438 yrs #= 977
ca it ve 16.26 298.47 1.20 0.089 ABMF Start/stop times:2010.6671-2013.5110
ca it cv 16.26 298.47 -0.03874 Corr. coeff. for ABMF
ca it vn 12.22 298.36 1.52 0.049 GRE0 ITRF08 5.9397 yrs #= 4214
ca it ve 12.22 298.36 1.36 0.052 GRE0 Start/stop times:2007.4863-2013.4260
ca it cv 12.22 298.36 -0.11443 Corr. coeff. for GRE0
ca it vn 14.59 299.00 1.50 0.080 LMMF ITRF08 2.8438 yrs #= 1023
ca it ve 14.59 299.00 1.25 0.091 LMMF Start/stop times:2010.6671-2013.5110
ca it cv 14.59 299.00 0.01081 Corr. coeff. for LMMF
ca it vn 14.73 298.85 1.58 0.122 FSD0 ITRF08 5.4685 yrs #= 14
ca it ve 14.73 298.85 1.31 0.318 FSD0 Start/stop times:1994.3986-1999.8671
ca it cv 14.73 298.85 0.00000 Corr. coeff. for FSD0
ca it vn 14.73 298.85 1.63 0.167 FSD1 ITRF08 5.4575 yrs #= 9
ca it ve 14.73 298.85 1.33 0.214 FSD1 Start/stop times:1994.4096-1999.8671
ca it cv 14.73 298.85 0.00000 Corr. coeff. for FSD1
ca it vn 15.24 298.71 1.40 0.063 CASS ITRF08 10.9879 yrs #= 20
ca it ve 15.24 298.71 1.18 0.111 CASS Start/stop times:2001.4288-2012.4167
ca it cv 15.24 298.71 0.00000 Corr. coeff. for caSS
ca it vn 15.34 298.69 1.51 0.084 FRSH ITRF08 10.9906 yrs #= 21
ca it ve 15.34 298.69 1.07 0.117 FRSH Start/stop times:2001.4452-2012.4358
ca it cv 15.34 298.69 0.00000 Corr. coeff. for FRSH
ca it vn 15.51 298.72 1.42 0.071 CNCD ITRF08 10.0877 yrs #= 25
ca it ve 15.51 298.72 1.18 0.109 CNCD Start/stop times:2001.4534-2011.5411
ca it cv 15.51 298.72 0.00000 Corr. coeff. for CNCD
ca it vn 15.67 296.38 1.42 0.132 AVES ITRF08 3.8740 yrs #= 28
ca it ve 15.67 296.38 1.13 0.231 AVES Start/stop times:1994.3740-1998.2479
ca it cv 15.67 296.38 0.00000 Corr. coeff. for AVES
ca it vn 17.67 298.21 1.26 0.384 CN00 ITRF08 0.7689 yrs #= 282
ca it ve 17.67 298.21 1.12 0.737 CN00 Start/stop times:2012.6407-2013.4096
ca it cv 17.67 298.21 -0.00308 Corr. coeff. for CN00
ca it vn 17.72 295.20 1.36 0.057 VIKH ITRF08 6.7644 yrs #= 2170
ca it ve 17.72 295.20 1.08 0.044 VIKH Start/stop times:2006.6425-2013.4068
ca it cv 17.72 295.20 -0.00329 Corr. coeff. for VIKH
ca it vn 15.03 273.93 0.71 0.095 GLCO ITRF08 10.2882 yrs #= 13
ca it ve 15.03 273.93 1.08 0.184 GLCO Start/stop times:2000.1790-2010.4671
ca it cv 15.03 273.93 0.00000 Corr. coeff. for GLCO
ca it vn 14.97 273.76 0.66 0.138 SFDP ITRF08 4.3607 yrs #= 6
ca it ve 14.97 273.76 1.13 0.244 SFDP Start/stop times:2000.1762-2004.5369
ca it cv 14.97 273.76 0.00000 Corr. coeff. for SFDP
ca it vn 14.92 273.62 0.67 0.062 MNTO ITRF08 10.2991 yrs #= 9
ca it ve 14.92 273.62 1.10 0.112 MNTO Start/stop times:2000.1680-2010.4671
ca it cv 14.92 273.62 0.00000 Corr. coeff. for MNTO
ca it vn 14.51 274.29 0.54 0.167 CMP1 ITRF08 5.2142 yrs #= 6
ca it ve 14.51 274.29 1.17 0.236 CMP1 Start/stop times:2000.1926-2005.4068
ca it cv 14.51 274.29 0.00000 Corr. coeff. for CMP1
ca it vn 14.04 276.62 0.61 0.107 PUEC ITRF08 5.1233 yrs #= 13
ca it ve 14.04 276.62 1.10 0.197 PUEC Start/stop times:2001.0397-2006.1630
ca it cv 14.04 276.62 0.00000 Corr. coeff. for PUEC
ca it vn 12.58 278.28 0.69 0.061 SAN0 ITRF08 5.4932 yrs #= 1764
ca it ve 12.58 278.28 1.25 0.063 SAN0 Start/stop times:2007.9356-2013.4288
ca it cv 12.58 278.28 0.11575 Corr. coeff. for SAN0
ca it vn 12.57 274.63 0.73 0.057 PORT ITRF08 11.9563 yrs #= 22
ca it ve 12.57 274.63 0.95 0.110 PORT Start/stop times:2000.6134-2012.5697
ca it cv 12.57 274.63 0.00000 Corr. coeff. for PORT
ca it vn 12.52 278.27 0.72 0.066 SANA ITRF08 9.1616 yrs #= 22
ca it ve 12.52 278.27 1.31 0.115 SANA Start/stop times:1994.1082-2003.2699
ca it cv 12.52 278.27 0.00000 Corr. coeff. for SANA
ca it vn 12.41 274.19 0.59 0.058 TEUS ITRF08 11.9836 yrs #= 23
ca it ve 12.41 274.19 0.97 0.090 TEUS Start/stop times:2000.5888-2012.5724
ca it cv 12.41 274.19 0.00000 Corr. coeff. for TEUS
ca it vn 12.92 274.78 0.67 0.250 RIOB ITRF08 2.5496 yrs #= 12
ca it ve 12.92 274.78 1.18 0.429 RIOB Start/stop times:2000.6025-2003.1521

```

ca it cv	12.92	274.78	0.00000		Corr. coeff. for RIOB	
ca it vn	17.76	295.42	1.36	0.030	CRO1 ITRF08 17.6740 yrs	#= 6018
ca it ve	17.76	295.42	1.10	0.031	CRO1 Start/stop times:1995.7822-2013.4562	
ca it cv	17.76	295.42	-0.01438		Corr. coeff. for CRO1	
ca it vn	16.93	297.65	1.47	0.151	RDON ITRF08 1.2860 yrs	#= 403
ca it ve	16.93	297.65	1.04	0.129	RDON Start/stop times:2012.3975-2013.6836	
ca it cv	16.93	297.65	0.02801		Corr. coeff. for RDON	
ca it vn	13.38	278.64	0.30	0.400	CN35 ITRF08 0.7389 yrs	#= 268
ca it ve	13.38	278.64	0.92	0.767	CN35 Start/stop times:2012.6899-2013.4288	
ca it cv	13.38	278.64	-0.01010		Corr. coeff. for CN35	

## 2 plates, 24 sites, Caribbean (west) fixed

```

caribbean gps site velocities - IGS08
0 0 0 0 0 0 0 0 0 0
cw # Fixed plate
it 0.0 0.0 0.5 # Starting est of IGS08-CAR ca ang vel lat/long/omega
ce 0.0 0.0 0.5 #
zz # End of plate list
ce it vn 16.26 298.47 1.44 0.082 ABMF ITRF08 2.8438 yrs # = 977
ce it ve 16.26 298.47 1.20 0.089 ABMF Start/stop times:2010.6671-2013.5110
ce it cv 16.26 298.47 -0.03874 Corr. coeff. for ABMF
ce it vn 12.22 298.36 1.52 0.049 GRE0 ITRF08 5.9397 yrs # = 4214
ce it ve 12.22 298.36 1.36 0.052 GRE0 Start/stop times:2007.4863-2013.4260
ce it cv 12.22 298.36 -0.11443 Corr. coeff. for GRE0
ce it vn 14.59 299.00 1.50 0.080 LMMF ITRF08 2.8438 yrs # = 1023
ce it ve 14.59 299.00 1.25 0.091 LMMF Start/stop times:2010.6671-2013.5110
ce it cv 14.59 299.00 0.01081 Corr. coeff. for LMMF
ce it vn 14.73 298.85 1.58 0.122 FSD0 ITRF08 5.4685 yrs # = 14
ce it ve 14.73 298.85 1.31 0.318 FSD0 Start/stop times:1994.3986-1999.8671
ce it cv 14.73 298.85 0.00000 Corr. coeff. for FSD0
ce it vn 14.73 298.85 1.63 0.167 FSD1 ITRF08 5.4575 yrs # = 9
ce it ve 14.73 298.85 1.33 0.214 FSD1 Start/stop times:1994.4096-1999.8671
ce it cv 14.73 298.85 0.00000 Corr. coeff. for FSD1
ce it vn 15.24 298.71 1.40 0.063 CASS ITRF08 10.9879 yrs # = 20
ce it ve 15.24 298.71 1.18 0.111 CASS Start/stop times:2001.4288-2012.4167
ce it cv 15.24 298.71 0.00000 Corr. coeff. for ceSS
ce it vn 15.34 298.69 1.51 0.084 FRSH ITRF08 10.9906 yrs # = 21
ce it ve 15.34 298.69 1.07 0.117 FRSH Start/stop times:2001.4452-2012.4358
ce it cv 15.34 298.69 0.00000 Corr. coeff. for FRSH
ce it vn 15.51 298.72 1.42 0.071 CNCD ITRF08 10.0877 yrs # = 25
ce it ve 15.51 298.72 1.18 0.109 CNCD Start/stop times:2001.4534-2011.5411
ce it cv 15.51 298.72 0.00000 Corr. coeff. for CNCD
ce it vn 15.67 296.38 1.42 0.132 AVES ITRF08 3.8740 yrs # = 28
ce it ve 15.67 296.38 1.13 0.231 AVES Start/stop times:1994.3740-1998.2479
ce it cv 15.67 296.38 0.00000 Corr. coeff. for AVES
ce it vn 17.67 298.21 1.26 0.384 CN00 ITRF08 0.7689 yrs # = 282
ce it ve 17.67 298.21 1.12 0.737 CN00 Start/stop times:2012.6407-2013.4096
ce it cv 17.67 298.21 -0.00308 Corr. coeff. for CN00
ce it vn 17.72 295.20 1.36 0.057 VIKH ITRF08 6.7644 yrs # = 2170
ce it ve 17.72 295.20 1.08 0.044 VIKH Start/stop times:2006.6425-2013.4068
ce it cv 17.72 295.20 -0.00329 Corr. coeff. for VIKH
cw it vn 15.03 273.93 0.71 0.095 GLCO ITRF08 10.2882 yrs # = 13
cw it ve 15.03 273.93 1.08 0.184 GLCO Start/stop times:2000.1790-2010.4671
cw it cv 15.03 273.93 0.00000 Corr. coeff. for GLCO
cw it vn 14.97 273.76 0.66 0.138 SFDP ITRF08 4.3607 yrs # = 6
cw it ve 14.97 273.76 1.13 0.244 SFDP Start/stop times:2000.1762-2004.5369
cw it cv 14.97 273.76 0.00000 Corr. coeff. for SFDP
cw it vn 14.92 273.62 0.67 0.062 MNTO ITRF08 10.2991 yrs # = 9
cw it ve 14.92 273.62 1.10 0.112 MNTO Start/stop times:2000.1680-2010.4671
cw it cv 14.92 273.62 0.00000 Corr. coeff. for MNTO
cw it vn 14.51 274.29 0.54 0.167 CMP1 ITRF08 5.2142 yrs # = 6
cw it ve 14.51 274.29 1.17 0.236 CMP1 Start/stop times:2000.1926-2005.4068
cw it cv 14.51 274.29 0.00000 Corr. coeff. for CMP1
cw it vn 14.04 276.62 0.61 0.107 PUEC ITRF08 5.1233 yrs # = 13
cw it ve 14.04 276.62 1.10 0.197 PUEC Start/stop times:2001.0397-2006.1630
cw it cv 14.04 276.62 0.00000 Corr. coeff. for PUEC
cw it vn 12.58 278.28 0.69 0.061 SAN0 ITRF08 5.4932 yrs # = 1764
cw it ve 12.58 278.28 1.25 0.063 SAN0 Start/stop times:2007.9356-2013.4288
cw it cv 12.58 278.28 0.11575 Corr. coeff. for SAN0
cw it vn 12.57 274.63 0.73 0.057 PORT ITRF08 11.9563 yrs # = 22
cw it ve 12.57 274.63 0.95 0.110 PORT Start/stop times:2000.6134-2012.5697
cw it cv 12.57 274.63 0.00000 Corr. coeff. for PORT
cw it vn 12.52 278.27 0.72 0.066 SANA ITRF08 9.1616 yrs # = 22
cw it ve 12.52 278.27 1.31 0.115 SANA Start/stop times:1994.1082-2003.2699
cw it cv 12.52 278.27 0.00000 Corr. coeff. for SANA
cw it vn 12.41 274.19 0.59 0.058 TEUS ITRF08 11.9836 yrs # = 23
cw it ve 12.41 274.19 0.97 0.090 TEUS Start/stop times:2000.5888-2012.5724
cw it cv 12.41 274.19 0.00000 Corr. coeff. for TEUS
cw it vn 12.92 274.78 0.67 0.250 RIOB ITRF08 2.5496 yrs # = 12
cw it ve 12.92 274.78 1.18 0.429 RIOB Start/stop times:2000.6025-2003.1521
cw it cv 12.92 274.78 0.00000 Corr. coeff. for RIOB

```

	ce	it	vn	17.76	295.42	1.36	0.030	CRO1	ITRF08	17.6740	yrs	#=	6018
	ce	it	ve	17.76	295.42	1.10	0.031	CRO1	Start/stop times:	1995.7822-2013.4562			
	ce	it	cv	17.76	295.42	-0.01438			Corr. coeff. for	CRO1			
	ce	it	vn	16.93	297.65	1.47	0.151	RDON	ITRF08	1.2860	yrs	#=	403
	ce	it	ve	16.93	297.65	1.04	0.129	RDON	Start/stop times:	2012.3975-2013.6836			
	ce	it	cv	16.93	297.65	0.02801			Corr. coeff. for	RDON			
	cw	it	vn	13.38	278.64	0.30	0.400	CN35	ITRF08	0.7389	yrs	#=	268
	cw	it	ve	13.38	278.64	0.92	0.767	CN35	Start/stop times:	2012.6899-2013.4288			
	cw	it	cv	13.38	278.64	-0.01010			Corr. coeff. for	CN35			
site	it	it	vn	16.26	298.47	1.44	0.082	ABMF	ITRF08	2.8438	yrs	#=	977
site	it	it	ve	16.26	298.47	1.20	0.089	ABMF	Start/stop times:	2010.6671-2013.5110			
site	it	it	cv	16.26	298.47	-0.03874			Corr. coeff. for	ABMF			
site	it	it	vn	12.22	298.36	1.52	0.049	GRE0	ITRF08	5.9397	yrs	#=	4214
site	it	it	ve	12.22	298.36	1.36	0.052	GRE0	Start/stop times:	2007.4863-2013.4260			
site	it	it	cv	12.22	298.36	-0.11443			Corr. coeff. for	GRE0			
site	it	it	vn	14.59	299.00	1.50	0.080	LMMF	ITRF08	2.8438	yrs	#=	1023
site	it	it	ve	14.59	299.00	1.25	0.091	LMMF	Start/stop times:	2010.6671-2013.5110			
site	it	it	cv	14.59	299.00	0.01081			Corr. coeff. for	LMMF			
site	it	it	vn	14.73	298.85	1.58	0.122	FSD0	ITRF08	5.4685	yrs	#=	14
site	it	it	ve	14.73	298.85	1.31	0.318	FSD0	Start/stop times:	1994.3986-1999.8671			
site	it	it	cv	14.73	298.85	0.00000			Corr. coeff. for	FSD0			
site	it	it	vn	14.73	298.85	1.63	0.167	FSD1	ITRF08	5.4575	yrs	#=	9
site	it	it	ve	14.73	298.85	1.33	0.214	FSD1	Start/stop times:	1994.4096-1999.8671			
site	it	it	cv	14.73	298.85	0.00000			Corr. coeff. for	FSD1			
site	it	it	vn	15.24	298.71	1.40	0.063	CASS	ITRF08	10.9879	yrs	#=	20
site	it	it	ve	15.24	298.71	1.18	0.111	CASS	Start/stop times:	2001.4288-2012.4167			
site	it	it	cv	15.24	298.71	0.00000			Corr. coeff. for	ceSS			
site	it	it	vn	15.34	298.69	1.51	0.084	FRSH	ITRF08	10.9906	yrs	#=	21
site	it	it	ve	15.34	298.69	1.07	0.117	FRSH	Start/stop times:	2001.4452-2012.4358			
site	it	it	cv	15.34	298.69	0.00000			Corr. coeff. for	FRSH			
site	it	it	vn	15.51	298.72	1.42	0.071	CNCD	ITRF08	10.0877	yrs	#=	25
site	it	it	ve	15.51	298.72	1.18	0.109	CNCD	Start/stop times:	2001.4534-2011.5411			
site	it	it	cv	15.51	298.72	0.00000			Corr. coeff. for	CNCD			
site	it	it	vn	15.67	296.38	1.42	0.132	AVES	ITRF08	3.8740	yrs	#=	28
site	it	it	ve	15.67	296.38	1.13	0.231	AVES	Start/stop times:	1994.3740-1998.2479			
site	it	it	cv	15.67	296.38	0.00000			Corr. coeff. for	AVES			
site	it	it	vn	17.67	298.21	1.26	0.384	CN00	ITRF08	0.7689	yrs	#=	282
site	it	it	ve	17.67	298.21	1.12	0.737	CN00	Start/stop times:	2012.6407-2013.4096			
site	it	it	cv	17.67	298.21	-0.00308			Corr. coeff. for	CN00			
site	it	it	vn	17.72	295.20	1.36	0.057	VIKH	ITRF08	6.7644	yrs	#=	2170
site	it	it	ve	17.72	295.20	1.08	0.044	VIKH	Start/stop times:	2006.6425-2013.4068			
site	it	it	cv	17.72	295.20	-0.00329			Corr. coeff. for	VIKH			
site	it	it	vn	15.03	273.93	0.71	0.095	GLCO	ITRF08	10.2882	yrs	#=	13
site	it	it	ve	15.03	273.93	1.08	0.184	GLCO	Start/stop times:	2000.1790-2010.4671			
site	it	it	cv	15.03	273.93	0.00000			Corr. coeff. for	GLCO			
site	it	it	vn	14.97	273.76	0.66	0.138	SFDP	ITRF08	4.3607	yrs	#=	6
site	it	it	ve	14.97	273.76	1.13	0.244	SFDP	Start/stop times:	2000.1762-2004.5369			
site	it	it	cv	14.97	273.76	0.00000			Corr. coeff. for	SFDP			
site	it	it	vn	14.92	273.62	0.67	0.062	MNTO	ITRF08	10.2991	yrs	#=	9
site	it	it	ve	14.92	273.62	1.10	0.112	MNTO	Start/stop times:	2000.1680-2010.4671			
site	it	it	cv	14.92	273.62	0.00000			Corr. coeff. for	MNTO			
site	it	it	vn	14.51	274.29	0.54	0.167	CMP1	ITRF08	5.2142	yrs	#=	6
site	it	it	ve	14.51	274.29	1.17	0.236	CMP1	Start/stop times:	2000.1926-2005.4068			
site	it	it	cv	14.51	274.29	0.00000			Corr. coeff. for	CMP1			
site	it	it	vn	14.04	276.62	0.61	0.107	PUEC	ITRF08	5.1233	yrs	#=	13
site	it	it	ve	14.04	276.62	1.10	0.197	PUEC	Start/stop times:	2001.0397-2006.1630			
site	it	it	cv	14.04	276.62	0.00000			Corr. coeff. for	PUEC			
site	it	it	vn	12.58	278.28	0.69	0.061	SANO	ITRF08	5.4932	yrs	#=	1764
site	it	it	ve	12.58	278.28	1.25	0.063	SANO	Start/stop times:	2007.9356-2013.4288			
site	it	it	cv	12.58	278.28	0.11575			Corr. coeff. for	SANO			
site	it	it	vn	12.57	274.63	0.73	0.057	PORT	ITRF08	11.9563	yrs	#=	22
site	it	it	ve	12.57	274.63	0.95	0.110	PORT	Start/stop times:	2000.6134-2012.5697			
site	it	it	cv	12.57	274.63	0.00000			Corr. coeff. for	PORT			
site	it	it	vn	12.52	278.27	0.72	0.066	SANA	ITRF08	9.1616	yrs	#=	22
site	it	it	ve	12.52	278.27	1.31	0.115	SANA	Start/stop times:	1994.1082-2003.2699			
site	it	it	cv	12.52	278.27	0.00000			Corr. coeff. for	SANA			
site	it	it	vn	12.41	274.19	0.59	0.058	TEUS	ITRF08	11.9836	yrs	#=	23
site	it	it	ve	12.41	274.19	0.97	0.090	TEUS	Start/stop times:	2000.5888-2012.5724			
site	it	it	cv	12.41	274.19	0.00000			Corr. coeff. for	TEUS			
site	it	it	vn	12.92	274.78	0.67	0.250	RIOB	ITRF08	2.5496	yrs	#=	12
site	it	it	ve	12.92	274.78	1.18	0.429	RIOB	Start/stop times:	2000.6025-2003.1521			
site	it	it	cv	12.92	274.78	0.00000			Corr. coeff. for	RIOB			

site	it	it	vn	17.76	295.42	1.36	0.030	CRO1	ITRF08	17.6740	yrs	#=	6018
site	it	it	ve	17.76	295.42	1.10	0.031	CRO1	Start/stop times:	1995.7822-2013.4562			
site	it	it	cv	17.76	295.42	-0.01438		Corr.	coeff. for	CRO1			
site	it	it	vn	16.93	297.65	1.47	0.151	RDON	ITRF08	1.2860	yrs	#=	403
site	it	it	ve	16.93	297.65	1.04	0.129	RDON	Start/stop times:	2012.3975-2013.6836			
site	it	it	cv	16.93	297.65	0.02801		Corr.	coeff. for	RDON			
site	it	it	vn	13.38	278.64	0.30	0.400	CN35	ITRF08	0.7389	yrs	#=	268
site	it	it	ve	13.38	278.64	0.92	0.767	CN35	Start/stop times:	2012.6899-2013.4288			
site	it	it	cv	13.38	278.64	-0.01010		Corr.	coeff. for	CN35			



Appendix E  
Inversion Results

DeMets et al., 2007 values, 1 plate, 15 sites, ITRF fixed

```
*****INVERSION RESULTS - CDeMets *****
>> File header is
caribbean gps site velocities - IGS08

----- INPUT DATA STATISTICS -----

# PLATES: 2 # of DATA: 30 DOF: 27
Fixed plate is it
Optimal angular velocities are in file fort.7

----- BEGIN ITERATIVE SEARCH -----

Results from Iteration 0
-----
> Trial angular velocities
> ca 0.000 0.000 0.5000

> Chi**2 Reduced Chi**2
*****
> Convergence criteria are: 0.009459633 0.003273831
0.002573694

Results from Iteration 1
-----
> Trial angular velocities
> ca 37.494 -102.620 0.2423

> Chi**2 Reduced Chi**2
35.846 1.3276

> Convergence criteria are: 0.000000000 0.000000000
0.000000000

----- END ITERATIVE SEARCH -----

The best fitting angular velocities are:
plate id Lat Long W deg/Myr
-----
it 0.0 0.0 .00
ca 37.494-102.620 0.2423

Final chi**2 and reduced chi**2 are 35.846 and 1.3276
```

2D 1-sigma error ellipse and 1D 1-sigma angular velocity uncertainty

Plate id	Ellipse major	Ellipse minor	azimuth of major axis (CCW from east)	rot. rate uncert.
ca	2.91	0.97	149.43	0.0122

Data Type	# Data	Chi**2	Data Importance
Rates	0	0.00	0.00
Transforms	0	0.00	0.00
Slip vectors	0	0.00	0.00
Baselines	0	0.00	0.00
Vn/Ve pairs	30	35.85	3.03

Plate IDs	Data Type	Lat (N)	Long (E)	Datum	S.D.	Pred	Wt.	Res.	Imp.	Pred. az CCW of E	SITE
ca	it	vn	15.67	296.38	1.420	0.132	1.346	0.559	0.065	90.00	AVES
ca	it	ve	15.67	296.38	1.130	0.231	1.131	-0.005	0.024	0.00	AVES
ca	it	vn	13.09	300.39	1.710	0.186	1.459	1.348	0.159	90.00	BARB
ca	it	ve	13.09	300.39	0.810	0.104	1.244	-4.176	0.039	0.00	BARB
ca	it	vn	14.51	274.29	0.540	0.167	0.622	-0.493	0.079	90.00	CMP1
ca	it	ve	14.51	274.29	1.170	0.236	1.076	0.398	0.023	0.00	CMP1
ca	it	vn	17.76	295.42	1.300	0.039	1.318	-0.465	0.701	90.00	CRO1
ca	it	ve	17.76	295.42	1.100	0.047	1.049	1.087	0.564	0.00	CRO1
ca	it	vn	14.73	298.85	1.580	0.122	1.417	1.338	0.098	90.00	FSD0
ca	it	ve	14.73	298.85	1.310	0.318	1.180	0.410	0.013	0.00	FSD0
ca	it	vn	14.73	298.85	1.630	0.167	1.417	1.277	0.052	90.00	FSD1
ca	it	ve	14.73	298.85	1.330	0.214	1.180	0.703	0.028	0.00	FSD1
ca	it	vn	15.03	273.93	0.800	0.133	0.609	1.433	0.128	90.00	GLCO
ca	it	ve	15.03	273.93	0.990	0.321	1.053	-0.197	0.013	0.00	GLCO
ca	it	vn	14.92	273.62	0.690	0.134	0.598	0.684	0.130	90.00	MNTO
ca	it	ve	14.92	273.62	1.170	0.246	1.057	0.459	0.021	0.00	MNTO
ca	it	vn	12.57	274.63	0.590	0.289	0.634	-0.154	0.025	90.00	PORT
ca	it	ve	12.57	274.63	1.330	0.380	1.157	0.455	0.010	0.00	PORT
ca	it	vn	14.04	276.62	0.500	0.230	0.705	-0.891	0.033	90.00	PUEC
ca	it	ve	14.04	276.62	1.300	0.441	1.102	0.449	0.007	0.00	PUEC
ca	it	vn	12.92	274.78	0.670	0.250	0.640	0.121	0.034	90.00	RIOB
ca	it	ve	12.92	274.78	1.180	0.429	1.143	0.086	0.007	0.00	RIOB
ca	it	vn	17.90	288.33	0.910	0.093	1.100	-2.044	0.081	90.00	ROJO
ca	it	ve	17.90	288.33	0.910	0.161	0.998	-0.545	0.049	0.00	ROJO
ca	it	vn	12.52	278.27	0.720	0.066	0.763	-0.650	0.342	90.00	SANA
ca	it	ve	12.52	278.27	1.310	0.115	1.169	1.227	0.105	0.00	SANA
ca	it	vn	14.97	273.76	0.660	0.138	0.603	0.411	0.121	90.00	SFDP
ca	it	ve	14.97	273.76	1.130	0.244	1.055	0.306	0.022	0.00	SFDP
ca	it	vn	12.41	274.19	0.750	0.209	0.619	0.628	0.051	90.00	TEUS
ca	it	ve	12.41	274.19	1.040	0.362	1.163	-0.339	0.011	0.00	TEUS

DeMets et al., 2007 values-updated, 1 plate, 15 sites, ITRF fixed

```

*****INVERSION RESULTS - CDeMets *****
>> File header is
caribbean gps site velocities - IGS08

----- INPUT DATA STATISTICS -----

# PLATES: 2 # of DATA: 30 DOF: 27
Fixed plate is it
Optimal angular velocities are in file fort.7

----- BEGIN ITERATIVE SEARCH -----

Results from Iteration 0
-----
> Trial angular velocities
> ca 0.000 0.000 0.5000

> Chi**2 Reduced Chi**2
*****
> Convergence criteria are: 0.009501628 0.003308453 0.002562150

Results from Iteration 1
-----
> Trial angular velocities
> ca 37.017 -103.183 0.2438

> Chi**2 Reduced Chi**2
46.118 1.7081

> Convergence criteria are: 0.000000000 0.000000000 0.000000000

----- END ITERATIVE SEARCH -----

The best fitting angular velocities are:
plate id Lat Long W deg/Myr
-----
it 0.0 0.0 .00
ca 37.017-103.183 0.2438

Final chi**2 and reduced chi**2 are 46.118 and 1.7081

2D 1-sigma error ellipse and 1D 1-sigma angular velocity uncertainty
Plate Ellipse axes azimuth of major axis rot. rate
id major minor (CCW from east) uncert.
--
ca 1.79 0.67 146.77 0.0082

Data Type # Data Chi**2 Data Importance
-----

```

Rates	0	0.00	0.00
Transforms	0	0.00	0.00
Slip vectors	0	0.00	0.00
Baselines	0	0.00	0.00
Vn/Ve pairs	30	46.12	3.02

Plate IDs	Data Type	Lat (N)	Long (E)	Datum	S.D.	Pred	Wt.	Res.	Imp.	Pred. az CCW of E	SITE
---	----	---	----	-----	----	----	-----	-----	-----	-----	-----
ca	it	vn	15.67	296.38	1.420	0.132	1.380	0.302	0.042	90.00	AVES
ca	it	ve	15.67	296.38	1.130	0.231	1.122	0.035	0.012	0.00	AVES
ca	it	vn	13.09	300.39	1.710	0.186	1.494	1.163	0.096	90.00	BARB
ca	it	ve	13.09	300.39	0.810	0.104	1.236	-4.095	0.020	0.00	BARB
ca	it	vn	14.51	274.29	0.540	0.167	0.651	-0.662	0.026	90.00	CMP1
ca	it	ve	14.51	274.29	1.170	0.236	1.064	0.450	0.012	0.00	CMP1
ca	it	vn	17.76	295.42	1.360	0.029	1.352	0.283	0.788	90.00	CRO1
ca	it	ve	17.76	295.42	1.100	0.033	1.039	1.838	0.590	0.00	CRO1
ca	it	vn	14.73	298.85	1.580	0.122	1.451	1.059	0.061	90.00	FSD0
ca	it	ve	14.73	298.85	1.310	0.318	1.171	0.437	0.007	0.00	FSD0
ca	it	vn	14.73	298.85	1.630	0.167	1.451	1.073	0.032	90.00	FSD1
ca	it	ve	14.73	298.85	1.330	0.214	1.171	0.743	0.014	0.00	FSD1
ca	it	vn	15.03	273.93	0.710	0.095	0.638	0.762	0.084	90.00	GLCO
ca	it	ve	15.03	273.93	1.080	0.184	1.041	0.213	0.019	0.00	GLCO
ca	it	vn	14.92	273.62	0.670	0.062	0.626	0.703	0.203	90.00	MNTO
ca	it	ve	14.92	273.62	1.100	0.112	1.045	0.494	0.052	0.00	MNTO
ca	it	vn	12.57	274.63	0.730	0.057	0.663	1.177	0.219	90.00	PORT
ca	it	ve	12.57	274.63	0.950	0.110	1.146	-1.780	0.058	0.00	PORT
ca	it	vn	14.04	276.62	0.610	0.107	0.734	-1.160	0.052	90.00	PUEC
ca	it	ve	14.04	276.62	1.100	0.197	1.090	0.049	0.017	0.00	PUEC
ca	it	vn	12.92	274.78	0.670	0.250	0.668	0.007	0.011	90.00	RIOB
ca	it	ve	12.92	274.78	1.180	0.429	1.132	0.113	0.004	0.00	RIOB
ca	it	vn	17.90	288.33	0.910	0.093	1.132	-2.392	0.044	90.00	ROJO
ca	it	ve	17.90	288.33	0.910	0.161	0.987	-0.477	0.025	0.00	ROJO
ca	it	vn	12.52	278.27	0.720	0.066	0.793	-1.099	0.118	90.00	SANA
ca	it	ve	12.52	278.27	1.310	0.115	1.158	1.323	0.053	0.00	SANA
ca	it	vn	14.97	273.76	0.660	0.138	0.631	0.207	0.040	90.00	SFDP
ca	it	ve	14.97	273.76	1.130	0.244	1.043	0.357	0.011	0.00	SFDP
ca	it	vn	12.41	274.19	0.590	0.058	0.647	-0.984	0.220	90.00	TEUS
ca	it	ve	12.41	274.19	0.970	0.090	1.151	-2.014	0.088	0.00	TEUS

1 plate, 24 sites, ITRF08 fixed

\*\*\*\*\*INVERSION RESULTS - CDeMets \*\*\*\*\*

>> File header is  
caribbean gps site velocities - IGS08

----- INPUT DATA STATISTICS -----

# PLATES: 2 # of DATA: 48 DOF: 45  
Fixed plate is it  
Optimal angular velocities are in file fort.7

----- BEGIN ITERATIVE SEARCH -----

Results from Iteration 0

-----

> Trial angular velocities  
> ca 0.000 0.000 0.5000

> Chi\*\*2 Reduced Chi\*\*2  
\*\*\*\*\* \*\*\*\*\*

> Convergence criteria are: 0.009459468 0.003462410 0.002684867

Results from Iteration 1

-----

> Trial angular velocities  
> ca 37.185 -101.950 0.2545

> Chi\*\*2 Reduced Chi\*\*2  
34.020 0.7560

> Convergence criteria are: 0.000000000 0.000000000 0.000000000

----- END ITERATIVE SEARCH -----

The best fitting angular velocities are:

plate id Lat Long W deg/Myr

-----  
it 0.0 0.0 .00  
ca 37.185-101.950 0.2545

Final chi\*\*2 and reduced chi\*\*2 are 34.020 and 0.7560

2D 1-sigma error ellipse and 1D 1-sigma angular velocity uncertainty

Plate Ellipse axes azimuth of major axis rot. rate

id major minor (CCW from east) uncert.  
--  
ca 1.40 0.47 149.98 0.0061

Data Type # Data Chi\*\*2 Data Importance  
-----

Rates	0	0.00	0.00
Transforms	0	0.00	0.00
Slip vectors	0	0.00	0.00
Baselines	0	0.00	0.00
Vn/Ve pairs	48	34.02	2.99

Plate IDs	Data Type	Lat (N)	Long (E)	Datum	S.D.	Pred	Wt.	Res.	Imp.	Pred. az CCW of E	SITE
ca it vn		16.26	298.47	1.440	0.082	1.463	-0.283	0.057	90.00	ABMF	
ca it ve		16.26	298.47	1.200	0.089	1.162	0.422	0.039	0.00	ABMF	
ca it vn		12.22	298.36	1.520	0.049	1.460	1.223	0.168	90.00	GRE0	
ca it ve		12.22	298.36	1.360	0.052	1.309	0.979	0.117	0.00	GRE0	
ca it vn		14.59	299.00	1.500	0.080	1.479	0.261	0.062	90.00	LMMF	
ca it ve		14.59	299.00	1.250	0.091	1.227	0.247	0.038	0.00	LMMF	
ca it vn		14.73	298.85	1.580	0.122	1.475	0.864	0.026	90.00	FSD0	
ca it ve		14.73	298.85	1.310	0.318	1.221	0.279	0.003	0.00	FSD0	
ca it vn		14.73	298.85	1.630	0.167	1.475	0.930	0.014	90.00	FSD1	
ca it ve		14.73	298.85	1.330	0.214	1.221	0.507	0.007	0.00	FSD1	
ca it vn		15.24	298.71	1.400	0.063	1.470	-1.118	0.097	90.00	CASS	
ca it ve		15.24	298.71	1.180	0.111	1.202	-0.197	0.025	0.00	CASS	
ca it vn		15.34	298.69	1.510	0.084	1.470	0.478	0.054	90.00	FRSH	
ca it ve		15.34	298.69	1.070	0.117	1.198	-1.094	0.023	0.00	FRSH	
ca it vn		15.51	298.72	1.420	0.071	1.471	-0.715	0.076	90.00	CNCD	
ca it ve		15.51	298.72	1.180	0.109	1.192	-0.110	0.026	0.00	CNCD	
ca it vn		15.67	296.38	1.420	0.132	1.400	0.154	0.018	90.00	AVES	
ca it ve		15.67	296.38	1.130	0.231	1.170	-0.174	0.006	0.00	AVES	
ca it vn		17.67	298.21	1.260	0.384	1.455	-0.509	0.002	90.00	CN00	
ca it ve		17.67	298.21	1.120	0.737	1.108	0.017	0.001	0.00	CN00	
ca it vn		17.72	295.20	1.360	0.057	1.363	-0.049	0.148	90.00	VIKH	
ca it ve		17.72	295.20	1.080	0.044	1.083	-0.074	0.097	0.00	VIKH	
ca it vn		15.03	273.93	0.710	0.095	0.618	0.973	0.072	90.00	GLCO	
ca it ve		15.03	273.93	1.080	0.184	1.091	-0.057	0.009	0.00	GLCO	
ca it vn		14.97	273.76	0.660	0.138	0.611	0.355	0.035	90.00	SFDP	
ca it ve		14.97	273.76	1.130	0.244	1.093	0.153	0.005	0.00	SFDP	
ca it vn		14.92	273.62	0.670	0.062	0.606	1.036	0.173	90.00	MNTO	
ca it ve		14.92	273.62	1.100	0.112	1.095	0.048	0.025	0.00	MNTO	
ca it vn		14.51	274.29	0.540	0.167	0.631	-0.546	0.023	90.00	CMP1	
ca it ve		14.51	274.29	1.170	0.236	1.115	0.235	0.006	0.00	CMP1	
ca it vn		14.04	276.62	0.610	0.107	0.719	-1.016	0.045	90.00	PUEC	
ca it ve		14.04	276.62	1.100	0.197	1.142	-0.213	0.008	0.00	PUEC	
ca it vn		12.58	278.28	0.690	0.061	0.780	-1.482	0.132	90.00	SAN0	
ca it ve		12.58	278.28	1.250	0.063	1.210	0.638	0.078	0.00	SAN0	
ca it vn		12.57	274.63	0.730	0.057	0.644	1.508	0.189	90.00	PORT	
ca it ve		12.57	274.63	0.950	0.110	1.200	-2.276	0.028	0.00	PORT	
ca it vn		12.52	278.27	0.720	0.066	0.780	-0.910	0.102	90.00	SANA	
ca it ve		12.52	278.27	1.310	0.115	1.212	0.849	0.025	0.00	SANA	
ca it vn		12.41	274.19	0.590	0.058	0.627	-0.645	0.189	90.00	TEUS	
ca it ve		12.41	274.19	0.970	0.090	1.206	-2.625	0.042	0.00	TEUS	
ca it vn		12.92	274.78	0.670	0.250	0.650	0.081	0.010	90.00	RIOB	
ca it ve		12.92	274.78	1.180	0.429	1.186	-0.013	0.002	0.00	RIOB	
ca it vn		17.76	295.42	1.360	0.030	1.370	-0.322	0.325	90.00	CRO1	
ca it ve		17.76	295.42	1.100	0.031	1.083	0.539	0.326	0.00	CRO1	
ca it vn		16.93	297.65	1.470	0.151	1.438	0.209	0.021	90.00	RDON	
ca it ve		16.93	297.65	1.040	0.129	1.131	-0.709	0.014	0.00	RDON	
ca it vn		13.38	278.64	0.300	0.400	0.794	-1.234	0.003	90.00	CN35	
ca it ve		13.38	278.64	0.920	0.767	1.177	-0.335	0.001	0.00	CN35	

2 plates, 24 sites, ITRF08 fixed

\*\*\*\*\*INVERSION RESULTS - CDeMets \*\*\*\*\*

>> File header is  
caribbean gps site velocities - IGS08

----- INPUT DATA STATISTICS -----

# PLATES: 3 # of DATA: 48 DOF: 42  
Fixed plate is it  
Optimal angular velocities are in file fort.7

----- BEGIN ITERATIVE SEARCH -----

Results from Iteration 0

-----

> Trial angular velocities  
> ce 0.000 0.000 0.5000  
> cw 0.000 0.000 0.5000

> Chi\*\*2 Reduced Chi\*\*2  
\*\*\*\*\*

> Convergence criteria are: 0.009469778 0.002309885 0.002412420

Results from Iteration 1

-----

> Trial angular velocities  
> ce 35.789 -97.178 0.2802  
> cw 58.506 -145.355 0.1321

> Chi\*\*2 Reduced Chi\*\*2  
25.148 0.5988

> Convergence criteria are: 0.000000000 0.000000000 0.000000000

----- END ITERATIVE SEARCH -----

The best fitting angular velocities are:

plate id	Lat	Long	W deg/Myr
it	0.0	0.0	.00
ce	35.789	-97.178	0.2802
cw	58.506	-145.355	0.1321

Final chi\*\*2 and reduced chi\*\*2 are 25.148 and 0.5988

2D 1-sigma error ellipse and 1D 1-sigma angular velocity uncertainty

Plate id	Ellipse axes	azimuth of major axis (CCW from east)	rot. rate uncert.
ce	6.59 0.51	156.49	0.0313



cw 33.29 1.54 161.47 0.0285

Data Type	# Data	Chi**2	Data Importance
Rates	0	0.00	0.00
Transforms	0	0.00	0.00
Slip vectors	0	0.00	0.00
Baselines	0	0.00	0.00
Vn/Ve pairs	48	25.15	5.97

Plate IDs	Data Type	Lat (N)	Long (E)	Datum	S.D.	Pred	Wt.	Res.	Imp.	Pred. az CCW of E	SITE
ce	it vn	16.26	298.47	1.440	0.082	1.474	-0.414	0.066	90.00		ABMF
ce	it ve	16.26	298.47	1.200	0.089	1.175	0.282	0.050	0.00		ABMF
ce	it vn	12.22	298.36	1.520	0.049	1.470	1.017	0.192	90.00		GRE0
ce	it ve	12.22	298.36	1.360	0.052	1.347	0.259	0.480	0.00		GRE0
ce	it vn	14.59	299.00	1.500	0.080	1.493	0.088	0.083	90.00		LMMF
ce	it ve	14.59	299.00	1.250	0.091	1.250	-0.003	0.070	0.00		LMMF
ce	it vn	14.73	298.85	1.580	0.122	1.488	0.757	0.034	90.00		FSD0
ce	it ve	14.73	298.85	1.310	0.318	1.243	0.210	0.005	0.00		FSD0
ce	it vn	14.73	298.85	1.630	0.167	1.488	0.852	0.018	90.00		FSD1
ce	it ve	14.73	298.85	1.330	0.214	1.243	0.405	0.012	0.00		FSD1
ce	it vn	15.24	298.71	1.400	0.063	1.483	-1.311	0.121	90.00		CASS
ce	it ve	15.24	298.71	1.180	0.111	1.221	-0.366	0.038	0.00		CASS
ce	it vn	15.34	298.69	1.510	0.084	1.482	0.335	0.067	90.00		FRSH
ce	it ve	15.34	298.69	1.070	0.117	1.216	-1.249	0.034	0.00		FRSH
ce	it vn	15.51	298.72	1.420	0.071	1.483	-0.887	0.095	90.00		CNCD
ce	it ve	15.51	298.72	1.180	0.109	1.209	-0.267	0.037	0.00		CNCD
ce	it vn	15.67	296.38	1.420	0.132	1.398	0.166	0.021	90.00		AVES
ce	it ve	15.67	296.38	1.130	0.231	1.186	-0.244	0.008	0.00		AVES
ce	it vn	17.67	298.21	1.260	0.384	1.465	-0.533	0.003	90.00		CN00
ce	it ve	17.67	298.21	1.120	0.737	1.111	0.012	0.001	0.00		CN00
ce	it vn	17.72	295.20	1.360	0.057	1.354	0.100	0.269	90.00		VIKH
ce	it ve	17.72	295.20	1.080	0.044	1.087	-0.151	0.152	0.00		VIKH
cw	it vn	15.03	273.93	0.710	0.095	0.660	0.525	0.107	90.00		GLCO
cw	it ve	15.03	273.93	1.080	0.184	1.109	-0.156	0.056	0.00		GLCO
cw	it vn	14.97	273.76	0.660	0.138	0.659	0.007	0.055	90.00		SFDP
cw	it ve	14.97	273.76	1.130	0.244	1.109	0.086	0.032	0.00		SFDP
cw	it vn	14.92	273.62	0.670	0.062	0.658	0.193	0.293	90.00		MNTO
cw	it ve	14.92	273.62	1.100	0.112	1.109	-0.082	0.147	0.00		MNTO
cw	it vn	14.51	274.29	0.540	0.167	0.663	-0.734	0.029	90.00		CMP1
cw	it ve	14.51	274.29	1.170	0.236	1.116	0.228	0.030	0.00		CMP1
cw	it vn	14.04	276.62	0.610	0.107	0.678	-0.634	0.068	90.00		PUEC
cw	it ve	14.04	276.62	1.100	0.197	1.128	-0.144	0.039	0.00		PUEC
cw	it vn	12.58	278.28	0.690	0.061	0.688	0.032	0.508	90.00		SAN0
cw	it ve	12.58	278.28	1.250	0.063	1.149	1.603	0.340	0.00		SAN0
cw	it vn	12.57	274.63	0.730	0.057	0.665	1.142	0.220	90.00		PORT
cw	it ve	12.57	274.63	0.950	0.110	1.140	-1.725	0.121	0.00		PORT
cw	it vn	12.52	278.27	0.720	0.066	0.688	0.485	0.393	90.00		SANA
cw	it ve	12.52	278.27	1.310	0.115	1.150	1.395	0.112	0.00		SANA
cw	it vn	12.41	274.19	0.590	0.058	0.662	-1.241	0.255	90.00		TEUS
cw	it ve	12.41	274.19	0.970	0.090	1.140	-1.894	0.185	0.00		TEUS
cw	it vn	12.92	274.78	0.670	0.250	0.666	0.016	0.011	90.00		RIOB
cw	it ve	12.92	274.78	1.180	0.429	1.136	0.102	0.008	0.00		RIOB
ce	it vn	17.76	295.42	1.360	0.030	1.362	-0.082	0.536	90.00		CRO1
ce	it ve	17.76	295.42	1.100	0.031	1.086	0.438	0.518	0.00		CRO1
ce	it vn	16.93	297.65	1.470	0.151	1.444	0.170	0.022	90.00		RDON
ce	it ve	16.93	297.65	1.040	0.129	1.140	-0.773	0.018	0.00		RDON
cw	it vn	13.38	278.64	0.300	0.400	0.690	-0.975	0.013	90.00		CN35
cw	it ve	13.38	278.64	0.920	0.767	1.141	-0.289	0.002	0.00		CN35

2 plates, 24 sites, Caribbean (west) fixed

\*\*\*\*\*INVERSION RESULTS - CDeMets \*\*\*\*\*

>> File header is  
 caribbean gps site velocities - IGS08

----- INPUT DATA STATISTICS -----

# PLATES: 3 # of DATA: 48 DOF: 42  
 Fixed plate is cw  
 Optimal angular velocities are in file fort.7

----- BEGIN ITERATIVE SEARCH -----

Results from Iteration 0

-----

> Trial angular velocities  
 > it 0.000 0.000 0.5000  
 > ce 0.000 0.000 0.5000

> Chi\*\*2 Reduced Chi\*\*2  
 \*\*\*\*\* \*\*\*\*\*

> Convergence criteria are: 0.007983810 0.001967615 0.001429710

Results from Iteration 1

-----

> Trial angular velocities  
 > it -58.506 34.645 0.1321  
 > ce 15.210 -81.341 0.1952

> Chi\*\*2 Reduced Chi\*\*2  
 25.148 0.5988

> Convergence criteria are: 0.000000000 0.000000000 0.000000000

----- END ITERATIVE SEARCH -----

The best fitting angular velocities are:

plate id	Lat	Long	W deg/Myr
---	---	---	---
cw	0.0	0.0	.00
it	-58.506	34.645	0.1321
ce	15.210	-81.341	0.1952

Final chi\*\*2 and reduced chi\*\*2 are 25.148 and 0.5988

2D 1-sigma error ellipse and 1D 1-sigma angular velocity uncertainty

Plate id	Ellipse axes	azimuth of major axis	rot. rate
---	major minor	(CCW from east)	uncert.
---	---	-----	-----
it	33.29 1.54	18.53	0.0285

ce 5.25 1.73 9.29 0.0739

Data Type	# Data	Chi**2	Data Importance
Rates	0	0.00	0.00
Transforms	0	0.00	0.00
Slip vectors	0	0.00	0.00
Baselines	0	0.00	0.00
Vn/Ve pairs	48	25.15	5.97

Plate IDs	Data Type	Lat (N)	Long (E)	Datum	S.D.	Pred	Wt.	Res.	Imp.	Pred. az CCW of E	SITE
ce it vn		16.26	298.47	1.440	0.082	1.474	-0.414	0.066	90.00		ABMF
ce it ve		16.26	298.47	1.200	0.089	1.175	0.282	0.050	0.00		ABMF
ce it vn		12.22	298.36	1.520	0.049	1.470	1.017	0.192	90.00		GRE0
ce it ve		12.22	298.36	1.360	0.052	1.347	0.259	0.480	0.00		GRE0
ce it vn		14.59	299.00	1.500	0.080	1.493	0.088	0.083	90.00		LMMF
ce it ve		14.59	299.00	1.250	0.091	1.250	-0.003	0.070	0.00		LMMF
ce it vn		14.73	298.85	1.580	0.122	1.488	0.757	0.034	90.00		FSD0
ce it ve		14.73	298.85	1.310	0.318	1.243	0.210	0.005	0.00		FSD0
ce it vn		14.73	298.85	1.630	0.167	1.488	0.852	0.018	90.00		FSD1
ce it ve		14.73	298.85	1.330	0.214	1.243	0.405	0.012	0.00		FSD1
ce it vn		15.24	298.71	1.400	0.063	1.483	-1.311	0.121	90.00		CASS
ce it ve		15.24	298.71	1.180	0.111	1.221	-0.366	0.038	0.00		CASS
ce it vn		15.34	298.69	1.510	0.084	1.482	0.335	0.067	90.00		FRSH
ce it ve		15.34	298.69	1.070	0.117	1.216	-1.249	0.034	0.00		FRSH
ce it vn		15.51	298.72	1.420	0.071	1.483	-0.887	0.095	90.00		CNCD
ce it ve		15.51	298.72	1.180	0.109	1.209	-0.267	0.037	0.00		CNCD
ce it vn		15.67	296.38	1.420	0.132	1.398	0.166	0.021	90.00		AVES
ce it ve		15.67	296.38	1.130	0.231	1.186	-0.244	0.008	0.00		AVES
ce it vn		17.67	298.21	1.260	0.384	1.465	-0.533	0.003	90.00		CN00
ce it ve		17.67	298.21	1.120	0.737	1.111	0.012	0.001	0.00		CN00
ce it vn		17.72	295.20	1.360	0.057	1.354	0.100	0.269	90.00		VIKH
ce it ve		17.72	295.20	1.080	0.044	1.087	-0.151	0.152	0.00		VIKH
cw it vn		15.03	273.93	0.710	0.095	0.660	0.525	0.107	90.00		GLCO
cw it ve		15.03	273.93	1.080	0.184	1.109	-0.156	0.056	0.00		GLCO
cw it vn		14.97	273.76	0.660	0.138	0.659	0.007	0.055	90.00		SFDP
cw it ve		14.97	273.76	1.130	0.244	1.109	0.086	0.032	0.00		SFDP
cw it vn		14.92	273.62	0.670	0.062	0.658	0.193	0.293	90.00		MNTO
cw it ve		14.92	273.62	1.100	0.112	1.109	-0.082	0.147	0.00		MNTO
cw it vn		14.51	274.29	0.540	0.167	0.663	-0.734	0.029	90.00		CMP1
cw it ve		14.51	274.29	1.170	0.236	1.116	0.228	0.030	0.00		CMP1
cw it vn		14.04	276.62	0.610	0.107	0.678	-0.634	0.068	90.00		PUEC
cw it ve		14.04	276.62	1.100	0.197	1.128	-0.144	0.039	0.00		PUEC
cw it vn		12.58	278.28	0.690	0.061	0.688	0.032	0.508	90.00		SAN0
cw it ve		12.58	278.28	1.250	0.063	1.149	1.603	0.340	0.00		SAN0
cw it vn		12.57	274.63	0.730	0.057	0.665	1.142	0.220	90.00		PORT
cw it ve		12.57	274.63	0.950	0.110	1.140	-1.725	0.121	0.00		PORT
cw it vn		12.52	278.27	0.720	0.066	0.688	0.485	0.393	90.00		SANA
cw it ve		12.52	278.27	1.310	0.115	1.150	1.395	0.112	0.00		SANA
cw it vn		12.41	274.19	0.590	0.058	0.662	-1.241	0.255	90.00		TEUS
cw it ve		12.41	274.19	0.970	0.090	1.140	-1.894	0.185	0.00		TEUS
cw it vn		12.92	274.78	0.670	0.250	0.666	0.016	0.011	90.00		RIOB
cw it ve		12.92	274.78	1.180	0.429	1.136	0.102	0.008	0.00		RIOB
ce it vn		17.76	295.42	1.360	0.030	1.362	-0.082	0.536	90.00		CRO1
ce it ve		17.76	295.42	1.100	0.031	1.086	0.438	0.518	0.00		CRO1
ce it vn		16.93	297.65	1.470	0.151	1.444	0.170	0.022	90.00		RDON
ce it ve		16.93	297.65	1.040	0.129	1.140	-0.773	0.018	0.00		RDON
cw it vn		13.38	278.64	0.300	0.400	0.690	-0.975	0.013	90.00		CN35
cw it ve		13.38	278.64	0.920	0.767	1.141	-0.289	0.002	0.00		CN35

2 plates, 24 sites, Caribbean (east) fixed

\*\*\*\*\*INVERSION RESULTS - CDeMets \*\*\*\*\*

>> File header is  
 caribbean gps site velocities - IGS08

----- INPUT DATA STATISTICS -----

# PLATES: 3 # of DATA: 48 DOF: 42  
 Fixed plate is ce  
 Optimal angular velocities are in file fort.7

----- BEGIN ITERATIVE SEARCH -----

Results from Iteration 0

-----  
 > Trial angular velocities  
 > it 0.000 0.000 0.5000  
 > cw 0.000 0.000 0.5000

> Chi\*\*2 Reduced Chi\*\*2  
 \*\*\*\*\* \*\*\*\*\*

> Convergence criteria are: 0.008726351 0.003592960 0.001876711

Results from Iteration 1

-----  
 > Trial angular velocities  
 > it -35.789 82.822 0.2802  
 > cw -15.210 98.659 0.1952

> Chi\*\*2 Reduced Chi\*\*2  
 25.148 0.5988

> Convergence criteria are: 0.000000000 0.000000000 0.000000000

----- END ITERATIVE SEARCH -----

The best fitting angular velocities are:

plate id	Lat	Long	W deg/Myr
ce	0.0	0.0	.00
it	-35.789	82.822	0.2802
cw	-15.210	98.659	0.1952

Final chi\*\*2 and reduced chi\*\*2 are 25.148 and 0.5988

2D 1-sigma error ellipse and 1D 1-sigma angular velocity uncertainty

Plate id	Ellipse axes major	minor	azimuth of major axis (CCW from east)	rot. rate uncert.
it	6.59	0.51	23.51	0.0313

cw 5.25 1.73 170.71 0.0739

Data Type	# Data	Chi**2	Data Importance
Rates	0	0.00	0.00
Transforms	0	0.00	0.00
Slip vectors	0	0.00	0.00
Baselines	0	0.00	0.00
Vn/Ve pairs	48	25.15	5.97

Plate IDs	Data Type	Lat (N)	Long (E)	Datum	S.D.	Pred	Wt.	Res.	Imp.	Pred. az CCW of E	SITE
ce	it vn	16.26	298.47	1.440	0.082	1.474	-0.414	0.066	90.00		ABMF
ce	it ve	16.26	298.47	1.200	0.089	1.175	0.282	0.050	0.00		ABMF
ce	it vn	12.22	298.36	1.520	0.049	1.470	1.017	0.192	90.00		GRE0
ce	it ve	12.22	298.36	1.360	0.052	1.347	0.259	0.480	0.00		GRE0
ce	it vn	14.59	299.00	1.500	0.080	1.493	0.088	0.083	90.00		LMMF
ce	it ve	14.59	299.00	1.250	0.091	1.250	-0.003	0.070	0.00		LMMF
ce	it vn	14.73	298.85	1.580	0.122	1.488	0.757	0.034	90.00		FSD0
ce	it ve	14.73	298.85	1.310	0.318	1.243	0.210	0.005	0.00		FSD0
ce	it vn	14.73	298.85	1.630	0.167	1.488	0.852	0.018	90.00		FSD1
ce	it ve	14.73	298.85	1.330	0.214	1.243	0.405	0.012	0.00		FSD1
ce	it vn	15.24	298.71	1.400	0.063	1.483	-1.311	0.121	90.00		CASS
ce	it ve	15.24	298.71	1.180	0.111	1.221	-0.366	0.038	0.00		CASS
ce	it vn	15.34	298.69	1.510	0.084	1.482	0.335	0.067	90.00		FRSH
ce	it ve	15.34	298.69	1.070	0.117	1.216	-1.249	0.034	0.00		FRSH
ce	it vn	15.51	298.72	1.420	0.071	1.483	-0.887	0.095	90.00		CNCD
ce	it ve	15.51	298.72	1.180	0.109	1.209	-0.267	0.037	0.00		CNCD
ce	it vn	15.67	296.38	1.420	0.132	1.398	0.166	0.021	90.00		AVES
ce	it ve	15.67	296.38	1.130	0.231	1.186	-0.244	0.008	0.00		AVES
ce	it vn	17.67	298.21	1.260	0.384	1.465	-0.533	0.003	90.00		CN00
ce	it ve	17.67	298.21	1.120	0.737	1.111	0.012	0.001	0.00		CN00
ce	it vn	17.72	295.20	1.360	0.057	1.354	0.100	0.269	90.00		VIKH
ce	it ve	17.72	295.20	1.080	0.044	1.087	-0.151	0.152	0.00		VIKH
cw	it vn	15.03	273.93	0.710	0.095	0.660	0.525	0.107	90.00		GLCO
cw	it ve	15.03	273.93	1.080	0.184	1.109	-0.156	0.056	0.00		GLCO
cw	it vn	14.97	273.76	0.660	0.138	0.659	0.007	0.055	90.00		SFDP
cw	it ve	14.97	273.76	1.130	0.244	1.109	0.086	0.032	0.00		SFDP
cw	it vn	14.92	273.62	0.670	0.062	0.658	0.193	0.293	90.00		MNTO
cw	it ve	14.92	273.62	1.100	0.112	1.109	-0.082	0.147	0.00		MNTO
cw	it vn	14.51	274.29	0.540	0.167	0.663	-0.734	0.029	90.00		CMP1
cw	it ve	14.51	274.29	1.170	0.236	1.116	0.228	0.030	0.00		CMP1
cw	it vn	14.04	276.62	0.610	0.107	0.678	-0.634	0.068	90.00		PUEC
cw	it ve	14.04	276.62	1.100	0.197	1.128	-0.144	0.039	0.00		PUEC
cw	it vn	12.58	278.28	0.690	0.061	0.688	0.032	0.508	90.00		SAN0
cw	it ve	12.58	278.28	1.250	0.063	1.149	1.603	0.340	0.00		SAN0
cw	it vn	12.57	274.63	0.730	0.057	0.665	1.142	0.220	90.00		PORT
cw	it ve	12.57	274.63	0.950	0.110	1.140	-1.725	0.121	0.00		PORT
cw	it vn	12.52	278.27	0.720	0.066	0.688	0.485	0.393	90.00		SANA
cw	it ve	12.52	278.27	1.310	0.115	1.150	1.395	0.112	0.00		SANA
cw	it vn	12.41	274.19	0.590	0.058	0.662	-1.241	0.255	90.00		TEUS
cw	it ve	12.41	274.19	0.970	0.090	1.140	-1.894	0.185	0.00		TEUS
cw	it vn	12.92	274.78	0.670	0.250	0.666	0.016	0.011	90.00		RIOB
cw	it ve	12.92	274.78	1.180	0.429	1.136	0.102	0.008	0.00		RIOB
ce	it vn	17.76	295.42	1.360	0.030	1.362	-0.082	0.536	90.00		CRO1
ce	it ve	17.76	295.42	1.100	0.031	1.086	0.438	0.518	0.00		CRO1
ce	it vn	16.93	297.65	1.470	0.151	1.444	0.170	0.022	90.00		RDON
ce	it ve	16.93	297.65	1.040	0.129	1.140	-0.773	0.018	0.00		RDON
cw	it vn	13.38	278.64	0.300	0.400	0.690	-0.975	0.013	90.00		CN35
cw	it ve	13.38	278.64	0.920	0.767	1.141	-0.289	0.002	0.00		CN35

## References

- Altamimi, Z., Collilieux, X., & Métivier, L., 2011, ITRF2008: an improved solution of the international terrestrial reference frame: *Journal of Geodesy*, 85(8), p. 457-473.
- Argus, D.F., Gordon, R.G., DeMets, C., 2011, Geologically current motion of 56 plates relative to the no-net-rotation reference frame: *Geochem. Geophys. Geosyst.*, v. 12, n. 11, doi 10.1029/2011GC003751.
- Benford, B., DeMets, C, Calais, E., 2012, GPS estimates of microplate motions, northern Caribbean: evidence for a Hispaniola microplate and implications for earthquake hazard, *Geophys. J. Int.*, 191, p. 481-490, doi: 10.1111/j.1365-246X.2012.05662.x.
- Benford, B., DeMets, C., Tikoff, B., Williams, P., Brown, L., Wiggins-Grandison, M., 2012, Seismic hazard along the southern boundary of the Gonave microplate: block modelling of GPS velocities from Jamaica and nearby islands, northern Caribbean: *Geophys. J. Int.*, 190, p. 59-74, doi: 10.1111/j.1365-246X.2012.05493.x.
- Bertiger, W., Desai, S. D., Haines, B., Harvey, N., Moore, A. W., Owen, S., & Weiss, J. P., 2010, Single receiver phase ambiguity resolution with GPS data. *Journal of Geodesy*, 84(5), 327-337.
- Bevington, P. R., 1969: *Data Reduction and Error Analysis for the Physical Sciences*, McGraw Hill, Inc
- Bouysse, P., Westercamp, D., 1990, Subduction of Atlantic aseismic ridges and Late Cenozoic evolution of the Lesser Antilles island arc: *Tectonophysics*, 175, p. 349–380.
- Bouysse, P., Westercamp, D., Andreieff, P., 1990, The Lesser Antilles Island Arc: Proceedings of the Ocean Drilling Program, Scientific Results, V. 110.
- Burke, K., 1988, Tectonic Evolution of the Caribbean: *Annual Review of Earth and Planetary Sciences*, v. 16, p. 201-230.
- Bouysse, P., 1988, Opening of the Grenada back-arc basin and evolution of the Caribbean plate during the Mesozoic and Early Paleogene: *Tectonophysics*, 149, p. 121-143.
- Braun, J.J., Calais, E., Feaux, K.F., Mattioli, G., Miller, M., Wang, G., 2012, <http://nldr.library.ucar.edu/repository/collections/OSGC-000-000-009-040>
- Carey, S.N., and Sigurdsson, H., 1980, The Roseau ash: Deep sea tephra deposits from a major eruption on Dominica, Lesser Antilles arc: *Journal of Volcanology Geothermal Research*, v. 7, p. 67-86.
- Carmichael, I. S. E., 2002, The andesite aqueduct: perspectives on the evolution of intermediate magmatism in west-central (105-99°W) Mexico: *Contributions to Mineralogy and Petrology*, v. 143, p. 641-663.

- Christiansen, R. L., 1979, Cooling units and composite sheets in relation to caldera structure: Ash Flow Tufts, *Geological Society of America Special Paper 180*, p. 29-41.
- DeMets, C., Gordon, R. G., Argus, D. F., 2010, Geologically current plate motions, *Geophysical Journal International*, v. 181, no. 1, p. 1-80, doi: 10.1111/j.1365-246X.2009.04491.x
- DeMets, C., Jansma, P. E., Mattioli, G. S., Dixon, T. H., Farina, F., Bilham, R., Mann, P., 2000, GPS geodetic constraints on Caribbean-North America plate motion, *Geophysical Research Letters*, 27(3), p. 437-440.
- DeMets, C., Mattioli, G.S, Jansma, P. E., Rogers, R.D., Tenorio, C., Turner, H.L., 2007, Present motion and deformation of the Caribbean plate: Constraints from new GPS geodetic measurement from Honduras and Nicaragua: *Geological Society of America Special Paper 428*, p. 21-36.
- Deng, J., Sykes, L.R., 1995. Determination of the Euler pole for contemporary relative motion of Caribbean and North American plates using slip vectors of interplate earthquakes: *Tectonics*, 14 (1), p. 39–53.
- Dixon, T.H., Farina, F., DeMets, C., Jansma, P., Mann, P., Calais, E., 1998. Relative motion between the Caribbean and North American plates and related boundary zone deformation from a decade of GPS observations: *J. Geophys. Res.* 103 (B7), p. 15157–15183.
- Dow, J.M., Neilan, R. E., and Rizos, C., The International GNSS Service in a changing landscape of Global Navigation Satellite Systems, *Journal of Geodesy* (2009) 83:191–198, DOI: 10.1007/s00190-008-0300-3
- Estey, L.H., Meertens, C.M., 1999, TEQC: the multi-purpose toolkit for GPS/GLONASS data: *GPS solutions* 3.1, p. 42-49.
- Fowler, C. M. R., 1990, *The Solid Earth: An Introduction to Global Geophysics*. Cambridge University Press.
- Giunta, G. and Orioli, S., 2011, The Caribbean Plate Evolution: Trying to Resolve a Very Complicated Tectonic Puzzle, *New Frontiers in Tectonic Research - General Problems, Sedimentary Basins and Island Arcs*, Prof. Evgenii Sharkov (Ed.), ISBN: 978-953-307-595-2, InTech, DOI: 10.5772/18723.
- Gregorius, T., 1997, An Introduction to GIPSY-OASIS II, Jet Propulsion Laboratory User Manual: *JPL Technical Document D-11088*, California Institute of Technology.
- Gunn, B.M., Roobol, M.J., and Smith A.L., 1974, The petrochemistry of Pelean-type volcanoes of Martinique: *Geological Society of America Bulletin*, v. 85, p. 1023-1030.
- Hoernle, K., Hauff, F., van den Bogaard, P., 2004, 70 m.y. history (139-69 Ma) for the Caribbean large igneous province: *Geology*, v. 32, no. 8, p. 697-700, doi: 10.1130/G20574.1.

Hopp, H., Weinzierl, W., Becel, A., Charvis, P., Evain, M., Flueh, E.R., Gailler, A., Galve, A., Hirn, A., Kandilarov, A., Klaeschen, D., Laigle, M., Papenberg, C., Planert, L., Roux, E., Trail and Thales teams, 2011, Deep Structure of the Central Lesser Antilles Island Arc: Relevance for the formation of continental crust: *Earth and Planetary Science Letters*, v. 304, p. 121-134, doi:10.1016/j.epsl.2011.01.024.

Hughes, G., and Mahood, G., 2008, Tectonic controls of the nature of large silicic calderas in volcanic arcs: *Geology*, v. 36, p. 627-630.

James, S., 2008, Volcanic Processes Inferred from GPS Geodesy, Dominica, Lesser Antilles, M.S. August, 2008, University of Arkansas, 101 p.

Linde, A. T., Sacks, S., Hidayat, D., Voight, B., Clarke, A., Elsworth, D., Widiwijayanti, C., 2010, Vulcanian explosion at Soufrière Hills Volcano, Montserrat on March 2004 as revealed by strain data: *Geophysical Research Letters*, 37(19).

Manaker, D. M., Calais, E., Freed, A. M., Ali, S. T., Przybylski, P., Mattioli, G., De Chabaliér, J. B., 2008, Interseismic plate coupling and strain partitioning in the northeastern Caribbean: *Geophysical Journal International*, 174(3), p. 889-903.

Mann, P., Calais, E., Rugg, J., DeMets, C., Jansma, P., Mattioli, G., 2002, Oblique collision in the northeastern Caribbean from GPS measurements and geological observations, *Tectonics*, 21(6), 1057, doi: 10.1029/2001TC001304

Mann, P., Rogers, R., Gahagan, L., 2007, Overview of plate tectonic history and its unresolved tectonic problems: Central America: *Geology, resources and hazards*, v. 1, p. 201-237.

Mao, A., Harrison, C.G.A., Dixon, T.H., 1999, Noise in GPS coordinate time series: *Journal of Geophysical Research*, v. 104, p. 2797 – 2816, doi:10.1029/2001TC001304.

Mattioli, G. S., Dixon, T. H., Farina, F., Howell, E. S., Jansma, P. E., & Smith, A. L., 1998, GPS measurement of surface deformation around Soufrière Hills Volcano, Montserrat from October 1995 to July 1996: *Geophysical Research Letters*, 25(18), p. 3417-3420.

Maufrett, A., Leroy, S., 1999, Neogene intraplate deformation of the Caribbean plate at the Beata Ridge: *Caribbean Basins, Sedimentary Basins of the World, 4 edited by Mann*, p. 627-669.

Maufrett, A., Leroy, S., 1997, Seismic stratigraphy and structure of the Caribbean Igneous province: *Tectonophysics* v. 283, p. 61-104.

Minster, J. B., Jordan, T.H., Molnar, P., Haines, E., 1974, Numerical model of instantaneous plate tectonics: *Geophysical Journal of the Royal Astronomical Society*, v. 36, p. 541-576.

Poland, M., Hamburger, M., Newman, A., 2006, The changing shapes of active volcanoes: History, evolution and future challenges for volcano geodesy: *Journal of*



*Volcanology and Geothermal Research*, v. 150, 13 p. doi:  
10.1016/j.volgeores.2005.11.005

Roobol, J.M., and Smith, A.L., 2004, Geologic Map of Dominica, West Indies. Geology Department, University of Puerto Rico at Mayaguez.

Ross, M., and Scotese, C., 1998, A hierarchical tectonic model of the Gulf of Mexico and Caribbean region: *Tectonophysics*, v. 155, p. 139-168, doi: 2103/10.1016/0040-1951(88)90263-6.

Ruiz, M., Galve, A., Monfret, T. Sapin, M., Charvis, P., Laigle, M., Evain, M., Hirn, A., Fleuh, E., Gallart, J., Diaz, J., Lebrun, J.F., and The Lesser Antilles Thales Scientific Party, 2011, Seismic activity offshore Martinique and Dominica Islands (Central Lesser Antilles subduction zone) from temporary onshore and offshore seismic networks: *Tectonophysics*, article in press, doi:10.1016/j.tecto.2011.08.006.

Schmitt, A. K., Stockli, D. F., Lindsay, J. M., Robertson, R., Lovera, O. M., & Kislitsyn, R., 2010, Episodic growth and homogenization of plutonic roots in arc volcanoes from combined U–Th and (U–Th)/He zircon dating: *Earth and Planetary Science Letters*, 295(1), p. 91-103.

Smith, A.L., Roobol, M.J., Mattioli, G.S., et al., 2013, The Volcanic Geology of the Mid-Arc Island of Dominica, Lesser Antilles – The surface expression of an island-arc batholith: *Geological Society of America Special Papers*, 496, 1-2, doi:10.1130/2013.2496

Smith, A.L., and Roobol, M.J., 1990, Mt. Pelée, Martinique: A study of an active island arc volcano: *Geological Society of America Memoir 175*, 105p

Smith, A.L., Roobol, J.M., Rheubottom, A., Kirkley, J., Freeman, Z., Karnes, K., Hinojosa, I., Stultz, H., Harris, S., and Pacheco, O., 2003, The geology of Dominica, Lesser Antilles: *Geological Society of America*, v. 35, no. 6, p. 323-324.

Speed, R. C., and Larue, D. K., 1982, Barbados: Architecture and implications for accretion: *Journal of Geophysical Research: Solid Earth (1978–2012)*, 87(B5), p. 3633-3643.

Stein, S., and Gordon, R.G., 1984, Statistical tests of additional plate boundaries from plate motion: *Earth and Planetary Science Letters*, v. 69, p. 401-412, doi: 10.1016/0012-821X(84)9019805

Turner, H.L., 2003, Strain/Slip partitioning along the Middle America Trench in Nicaragua: Constrained by GPS Geodesy, M.S. Thesis. University of Arkansas.

Turner, H.L., 2010, Forearc kinematics in obliquely convergent margins: examples from Nicaragua and the Northern Lesser Antilles, PhD dissertation. University of Arkansas.

van Benthem, S. A. C., Plate dynamics, mantle structure and tectonic evolution of the Caribbean region, PhD dissertation. Utrecht University.

Wadge, G., and Shepherd, J. B., 1984, Segmentation of the Lesser Antilles subduction zone: *Earth Planet. Sci. Lett.*, v. 71, p. 297-304.

Webb, F., Zumberge, J., 1995, An introduction to GIPSY/OASIS II, JPLM D-11088. Jet Propulsion Laboratory, California Institute of Technology.

Zumberge, J., Heflin, M., Jefferson, D., Watkins, M., Webb, F., 1997, Precise point positioning for the efficient and robust analysis of GPS data from large networks: *Journal of Geophysical Research*, v. 102, no. B3, p. 5005-5017

### Biographical Information

Jamie Miller earned a B.S. in Geology and an M.S. in Environmental Science and Engineering from the University of Texas at Arlington. She is currently an Assistant Professor of Geology at Tarrant County College and plans to continue her career as a teaching professor. Jamie enjoys teaching students in the field and her research interests include volcanic processes, tectonics, and geodesy.